DYNAMICS OF CYCLIC NUCLEOTIDE SIGNALING IN NEURONS

EDITED BY: Pierre Vincent, Nicholas C. Spitzer
PUBLISHED IN: Frontiers in Cellular Neuroscience

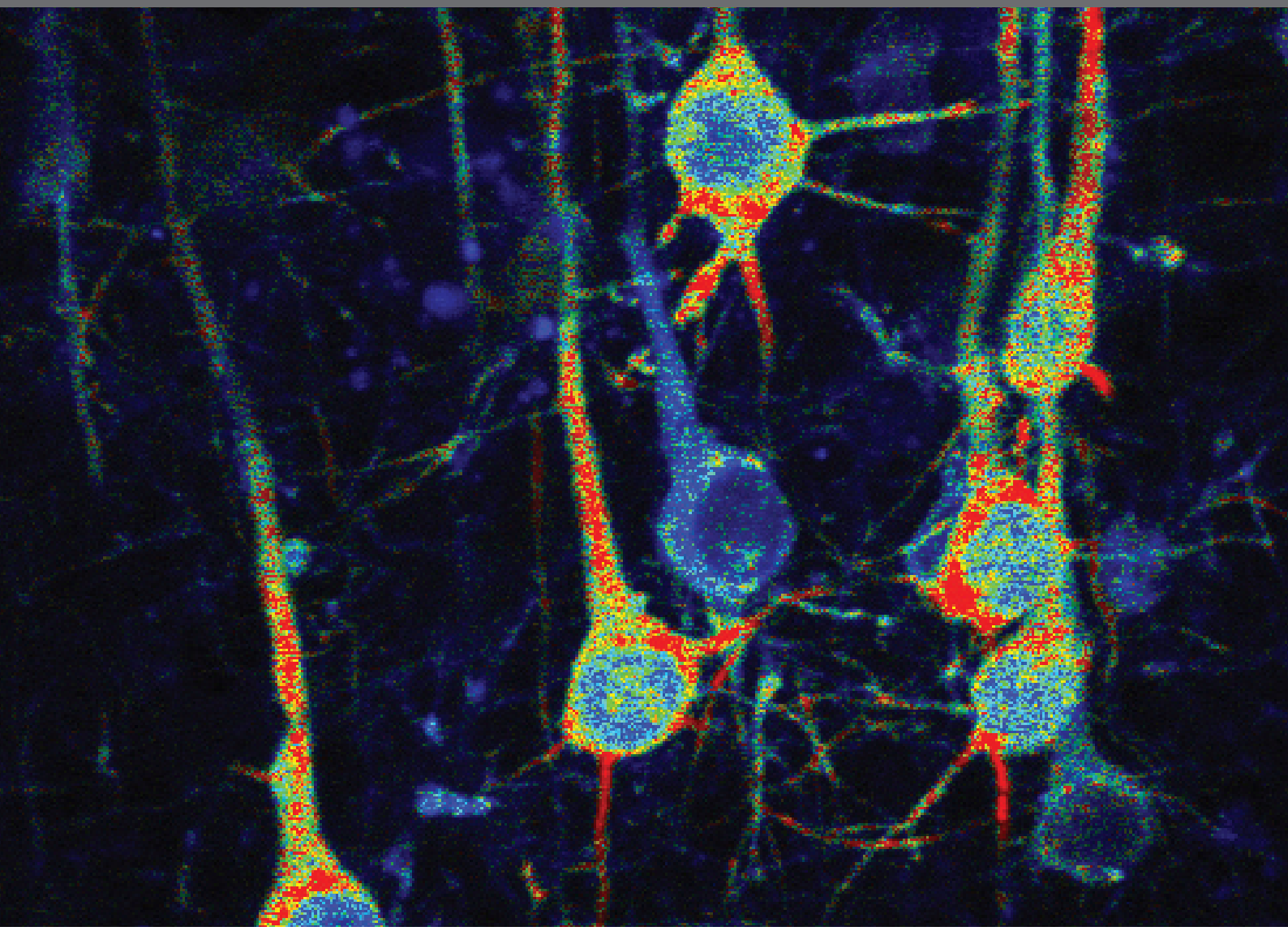

frontiers Research Topics

frontiers

ISSN 1664-8714
ISBN 978-2-88919-646-3
DOI 10.3389/978-2-88919-646-3

About Frontiers

Frontiers is more than just an open-access publisher of scholarly articles: it is a pioneering approach to the world of academia, radically improving the way scholarly research is managed. The grand vision of Frontiers is a world where all people have an equal opportunity to seek, share and generate knowledge. Frontiers provides immediate and permanent online open access to all its publications, but this alone is not enough to realize our grand goals.

Frontiers Journal Series

The Frontiers Journal Series is a multi-tier and interdisciplinary set of open-access, online journals, promising a paradigm shift from the current review, selection and dissemination processes in academic publishing. All Frontiers journals are driven by researchers for researchers; therefore, they constitute a service to the scholarly community. At the same time, the Frontiers Journal Series operates on a revolutionary invention, the tiered publishing system, initially addressing specific communities of scholars, and gradually climbing up to broader public understanding, thus serving the interests of the lay society, too.

Dedication to Quality

Each Frontiers article is a landmark of the highest quality, thanks to genuinely collaborative interactions between authors and review editors, who include some of the world's best academicians. Research must be certified by peers before entering a stream of knowledge that may eventually reach the public - and shape society; therefore, Frontiers only applies the most rigorous and unbiased reviews.
Frontiers revolutionizes research publishing by freely delivering the most outstanding research, evaluated with no bias from both the academic and social point of view.
By applying the most advanced information technologies, Frontiers is catapulting scholarly publishing into a new generation.

What are Frontiers Research Topics?

Frontiers Research Topics are very popular trademarks of the Frontiers Journals Series: they are collections of at least ten articles, all centered on a particular subject. With their unique mix of varied contributions from Original Research to Review Articles, Frontiers Research Topics unify the most influential researchers, the latest key findings and historical advances in a hot research area! Find out more on how to host your own Frontiers Research Topic or contribute to one as an author by contacting the Frontiers Editorial Office: **researchtopics@frontiersin.org**

DYNAMICS OF CYCLIC NUCLEOTIDE SIGNALING IN NEURONS

Topic Editors:
Pierre Vincent, CNRS, UMR8256 "Biological Adaptation and Ageing", Institut de Biologie Paris-Seine (IBPS), France and Université Pierre et Marie Curie (UPMC, Paris 6), France
Nicholas C. Spitzer, Neurobiology Section, Division of Biological Sciences & Kavli Institute for Brain and Mind, USA

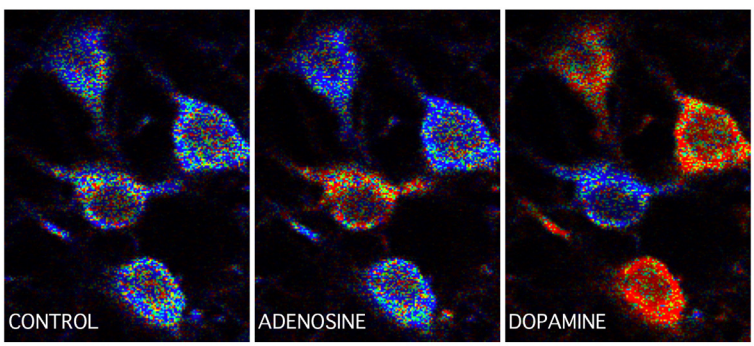

Cover figure:
Biosensor imaging reveals the sub-cellular compartmentation of signaling cascades, showing different activation levels of PKA in the cytosol and the nucleus as a result of the activation of Gs-coupled receptors. A cortical brain slice expressing the PKA biosensor AKAR3 is imaged with two-photon microscopy, and biosensor activation represented with pseudocolors. Here, the activation of D1-like dopamine receptors increases PKA-dependent phosphorylation in the cytosol within a few minutes (illustration) while the nucleus will respond after 10 min. Image by Elvire Guiot and Pierre Vincent.

Introductory page:
Real-time biosensor imaging reveals the sensitivity of neurons to specific neuromodulators. This striatal brain slice expressing the cAMP biosensor EpacS^{H150} is imaged with two-photon microscopy. Compared to control (left), the activation of adenosine A2A receptors (center) or dopamine D1-like receptors (right) selectively and reversibly increases cAMP concentration in medium spiny neurons of the indirect or direct pathway, respectively. Images by Cédric Yapo and Pierre Vincent.

Cyclic nucleotides control a number of neuronal properties including neuronal differentiation, pathfinding, regulation of excitability and synaptic transmission, and control of gene expression. Signaling events mediated by cAMP or cGMP are transient and take place within the complex 3-dimensional structure of the neuronal cell. Signaling events happen on the time scale of seconds to minutes and the biological significance of the temporal dimension remains poorly understood. Structural features of neurons (dendritic spines and branches, cell body, nucleus, axon…) as well as AKAPs and other scaffolding proteins that keep signaling enzymes together and form "signaling microdomains", are critical spatial determinants of signal integration. Finally,

the types of enzymes involved in signal integration, which are expressed as a number of different types and splice variants, yield another dimension that determines signal integration properties. Biosensor imaging provides direct temporal and spatial measurement of intracellular signals. This novel approach, together with more conventional methods such as biochemistry, electrophysiology, and modeling, now provide a better understanding of the spatial and temporal features of cyclic nucleotide signal integration in living neurons. This topic aims at providing a better understanding of how neurons are "making sense" of cyclic nucleotide signaling in living neurons.

Citation: Vincent, P., Spitzer, N. C., eds. (2015). Dynamics of Cyclic Nucleotide Signaling in Neurons. Lausanne: Frontiers Media. doi: 10.3389/978-2-88919-646-3

Table of Contents

frontiers in Cellular Neuroscience

EDITORIAL
published: 03 August 2015
doi: 10.3389/fncel.2015.00296

Editorial: Dynamics of cyclic nucleotide signaling in neurons

Pierre Vincent[1,2]* *and Nicholas C. Spitzer*[3]

[1] Biological Adaptation and Ageing, Centre National de la Recherche Scientifique, UMR 8256, Paris, France, [2] Université Pierre et Marie Curie, UMR 8256, Paris, France, [3] Neurobiology Section, Division of Biological Sciences & Kavli Institute for Brain and Mind, University of California San Diego, La Jolla, CA, USA

Keywords: cyclic GMP, cyclic AMP, G-protein coupled receptors, phosphodiesterases, biosensor imaging, sub-cellular compartmentation

The articles in this Frontiers Research Topic describe how neurons integrate the signals carried by cyclic nucleotide. Three articles present original research, two papers provide provocative opinions about aspects of cyclic nucleotides signaling and four reviews provide timely summary and analysis of the state of the field. The three original articles illustrate how biosensors can reveal the details of signaling cascades in "native" neurons, a major advance compared to the use of heterologous expression systems. Nomura et al. (2014) quantify responses at the level of individual neurons, revealing differences between different cortical regions in the sensitivity to dopamine or noradrenalin. As Polito et al. (2013) demonstrate, spatial resolution also allows analysis of the cAMP signaling cascade in specific neuronal types, a condition which is critical in brain regions where several neuronal types are intermingled, as in the striatum. At higher magnification, biosensor imaging reveals how different sub-cellular compartments differentially integrate the same extracellular signal. This is illustrated by Ladarre et al. who show different responsiveness of axonal and dendritic arbors to cannabinoid drugs (Ladarre et al., 2014). Biosensors have generally been used to study increases in cAMP, typically resulting from the activation of receptors coupled to $G_{s/olf}$, but this topic also reports effects mediated by G_i. Nomura et al. show that the positive cAMP/PKA response is moderated by the co-activation of G_i-coupled receptors coexpressed in the same neuron (Nomura et al., 2014). Ladarre et al. report the effect of CB_1 receptors that are tonically activated by the endogenous production of endocannabinoids (Ladarre et al., 2014). Finally, biosensor imaging opens the door to studies of the dynamics of signaling by analyzing the functional contribution of the enzymes that control the extent of the cAMP signal. Polito et al. show how phosphodiesterases determine the decay kinetics of transient cAMP responses and how modulation of phosphodiesterase allows for cross-regulation between the cGMP and cAMP pathways (Polito et al., 2013).

In an opinion piece, Iyengar proposes that spatially restricted elevation of cAMP levels and their action on downstream effectors may function as a scaling agent for computations by signaling networks (Iyengar, 2015). Goto, Kamioka, and Matsuda address the problem of control of the Rho-family GTPase, Rac, which controls actin dynamics and morphology, migration, and cytokinesis of neurons and regulates higher brain function (Goto et al., 2014). They suggest that progress in understanding this complex signaling requires simultaneous examination of PKA and Rac activities with FRET biosensors and implement this technology. Review articles address important and rapidly developing aspects of the signaling field. Averaimo and Nicol summarize advances in understanding cAMP signaling and its dynamic interaction with cGAMP and calcium to shape neuronal polarization, transmitter specification, axon guidance, and refinement of neuronal connectivity (Averaimo and Nicol, 2014). Gross, Pugh and Burns summarize the general principles of rod phototransduction and describe recent advances in understanding the dynamics of cGMP during single photon responses (Gross et al., 2015). Recognizing the growing body of evidence for the formation of cAMP gradients and microdomains near the sites of cAMP production, Calebiro and Maiellaro review the methods used for monitoring cAMP and protein kinase A (PKA) signaling

Edited and reviewed by:
Egidio D'Angelo, University of Pavia, Italy

***Correspondence:**
Pierre Vincent, pierre.vincent@upmc.fr

Received: *18 June 2015*
Accepted: *20 July 2015*
Published: *03 August 2015*

Citation:
Vincent P and Spitzer NC (2015) Editorial: Dynamics of cyclic nucleotide signaling in neurons. Front. Cell. Neurosci. 9:296. doi: 10.3389/fncel.2015.00296

in living cells and discuss the major hypotheses on the formation of cAMP/PKA microdomains (Calebiro and Maiellaro, 2014). Finally, Gorshkov and Zhang discuss the design of fluorescent biosensors and describe several of them in detail (Gorshkov and Zhang, 2014). They present examples of the use of cyclic nucleotide fluorescent biosensors to study regulation of neuronal function and consider recent advances in the field. Investigators already in the field as well as those newly attracted to it will find these compact presentations a useful source of new information, ideas, and summaries of the state of the art.

Funding

PV was supported by Labex Bio-Psy. NS was supported by NIH, the Ellison Medical Foundation and the W. M. Keck Foundation.

References

Averaimo, S., and Nicol, X. (2014). Intermingled cAMP, cGMP and calcium spatiotemporal dynamics in developing neuronal circuits. *Front. Cell Neurosci.* 8:376. doi: 10.3389/fncel.2014.00376

Calebiro, D., and Maiellaro, I. (2014). cAMP signaling microdomains and their observation by optical methods. *Front. Cell Neurosci.* 8:350. doi: 10.3389/fncel.2014.00350

Gorshkov, K., and Zhang, J. (2014). Visualization of cyclic nucleotide dynamics in neurons. *Front. Cell Neurosci.* 8:395. doi: 10.3389/fncel.2014.00395

Goto, A., Kamioka, Y., and Matsuda, M. (2014). PKA modulation of Rac in neuronal cells. *Front. Cell Neurosci.* 8:321. doi: 10.3389/fncel.2014.00321

Gross, O. P., Pugh, E. N. Jr., and Burns, M. E. (2015). cGMP in mouse rods: the spatiotemporal dynamics underlying single photon responses. *Front. Mol. Neurosci.* 8:6. doi: 10.3389/fnmol.2015.00006

Iyengar, R. (2015). Can intracellular cAMP dynamics enable scalable computation? *Front. Cell Neurosci.* 9:112. doi: 10.3389/fncel.2015.00112

Ladarre, D., Roland, A. B., Biedzinski, S., Ricobaraza, A., and Lenkei, Z. (2014). Polarized cellular patterns of endocannabinoid production and detection shape cannabinoid signaling in neurons. *Front. Cell Neurosci.* 8:426. doi: 10.3389/fncel.2014.00426

Nomura, S., Bouhadana, M., Morel, C., Faure, P., Cauli, B., Lambolez, B., et al. (2014). Noradrenalin and dopamine receptors both control cAMP-PKA signaling throughout the cerebral cortex. *Front. Cell Neurosci.* 8:247. doi: 10.3389/fncel.2014.00247

Polito, M., Klarenbeek, J., Jalink, K., Paupardin-Tritsch, D., Vincent, P., and Castro, L. R. (2013). The NO/cGMP pathway inhibits transient cAMP signals through the activation of PDE2 in striatal neurons. *Front. Cell Neurosci.* 7:211. doi: 10.3389/fncel.2013.00211

Conflict of Interest Statement: The authors declare that the research was conducted in the absence of any commercial or financial relationships that could be construed as a potential conflict of interest.

frontiers in
CELLULAR NEUROSCIENCE

ORIGINAL RESEARCH ARTICLE
published: 21 August 2014
doi: 10.3389/fncel.2014.00247

Noradrenalin and dopamine receptors both control cAMP-PKA signaling throughout the cerebral cortex

Shinobu Nomura[1,2,3], Maud Bouhadana[1,2,3], Carole Morel[1,2,3], Philippe Faure[1,2,3], Bruno Cauli[1,2,3], Bertrand Lambolez[1,2,3] and Régine Hepp[1,2,3]*

[1] Sorbonne Universités, UPMC Université Paris 06, UM CR 18, Neuroscience Paris Seine, Paris, France
[2] Centre National de la Recherche Scientifique (CNRS), UMR 8246, Paris, France
[3] Institut National de la Santé et de la Recherche Médicale (INSERM), U 1130, Paris, France

Edited by:
Nicholas C. Spitzer, University of California, San Diego, USA

Reviewed by:
Ursula Felderhoff-Müser, University of Duisburg-Essen, Germany
De-Lai Qiu, YanBian University, China

***Correspondence:**
Régine Hepp, Sorbonne Universités, UPMC Université Paris 06, UM CR 18, Neuroscience Paris Seine, 9 Quai Saint Bernard, Case Courrier 16, 75005 Paris, France
e-mail: regine.hepp@snv.jussieu.fr

Noradrenergic fibers innervate the entire cerebral cortex, whereas the cortical distribution of dopaminergic fibers is more restricted. However, the relative functional impact of noradrenalin and dopamine receptors in various cortical regions is largely unknown. Using a specific genetic label, we first confirmed that noradrenergic fibers innervate the entire cortex whereas dopaminergic fibers were present in all layers of restricted medial and lateral areas but only in deep layers of other areas. Imaging of a genetically encoded sensor revealed that noradrenalin and dopamine widely activate PKA in cortical pyramidal neurons of frontal, parietal and occipital regions with scarce dopaminergic fibers. Responses to noradrenalin had higher amplitude, velocity and occurred at more than 10-fold lower dose than those elicited by dopamine, whose amplitude and velocity increased along the antero-posterior axis. The pharmacology of these responses was consistent with the involvement of Gs-coupled beta1 adrenergic and D1/D5 dopaminergic receptors, but the inhibition of both noradrenalin and dopamine responses by beta adrenergic antagonists was suggestive of the existence of beta1-D1/D5 heteromeric receptors. Responses also involved Gi-coupled alpha2 adrenergic and D2-like dopaminergic receptors that markedly reduced their amplitude and velocity and contributed to their cell-to-cell heterogeneity. Our results reveal that noradrenalin and dopamine receptors both control cAMP-PKA signaling throughout the cerebral cortex with moderate regional and laminar differences. These receptors can thus mediate widespread effects of both catecholamines, which are reportedly co-released by cortical noradrenergic fibers beyond the territory of dopaminergic fibers.

Keywords: catecholamines, GPCR, protein kinase A, imaging, cerebral cortex

INTRODUCTION

The catecholamines dopamine (DA) and noradrenalin (NA) are neurotransmitters that widely modulate brain circuits and behaviors. NA is involved in arousal, attention, memory, and stress whereas DA is implicated in learning, reward, attention, and movement control. Likewise, catecholaminergic dysfunctions are associated with cognitive, emotional, and motor disorders and catecholaminergic transmission is the target of multiple drugs used in therapy of human brain disorders. Catecholamines are synthesized in discrete brainstem nuclei via a common pathway involving tyrosine hydroxylase (TH) that leads to DA production, which is converted to NA by DA beta hydroxylase (DBH). The effects of DA and NA are mediated by G protein-coupled receptors. The five DA receptors belong to the D1/D5 or D2-like classes, which activate or inhibit cAMP/protein kinase A (PKA) signaling via Gs or Gi proteins, respectively (Beaulieu and Gainetdinov, 2011). NA also regulates the cAMP/PKA pathway by activating Gs-coupled beta1–3 receptors or Gi-coupled alpha2 adrenoceptors. NA additionally activates the phospholipase C pathway through Gq-coupled alpha1 receptors (Bylund, 1992; Cotecchia, 2010; Evans et al., 2010).

Dopamine- and NA-containing fibers exhibit wide, but distinctive, distributions in the brain. Catecholaminergic projections to the cerebral cortex stem from DA neurons of the ventral tegmental area (VTA) and NA neurons of the locus coeruleus (LC). LC fibers innervate the entire cortical mantle, whereas VTA fibers distribute in all layers of medio-frontal and ventro-lateral cortices, but are restricted to deep layers in other areas of the rodent cortex (Morrison et al., 1978, 1979; Descarries et al., 1987; Berger et al., 1991; Latsari et al., 2002). The broad distribution of NA receptors in the rodent cortex is consistent with that of LC fibers (Nicholas et al., 1996; Venkatesan et al., 1996; Papay et al., 2006; Paschalis et al., 2009). In contrast, a mismatch exists between the widespread expression also reported for DA receptors (Ariano and Sibley, 1994; Khan et al., 1998; Luedtke et al., 1999; Lemberger et al., 2007; Rivera et al., 2008; Oda et al., 2010), and the restricted distribution of VTA fibers in the rodent cortex. While LC fibers are a plausible source of cortical DA outside the VTA projection areas (Devoto et al., 2005, 2008), the question of the relative functional impact of DA and NA receptors in various cortical regions has not been addressed.

In the present study, we first examined the distribution of LC and VTA fibers in the rodent cortex using site and cell-type-specific labeling of catecholaminergic neurons with green fluorescent protein (GFP) via conditional viral transfer. We then characterized the functional impact of Gs- and Gi-coupled DA

and NA receptors on cAMP/PKA signaling in layers II/III and V of the frontal, parietal, and occipital cortex using 2-photon imaging of a genetically encoded PKA sensor in rat brain slices (Bonnot et al., 2014). Our results confirm the differential distribution of LC and VTA fibers in the cortex and reveal that both NA and DA receptors control cAMP-PKA signaling throughout the cerebral cortex with moderate regional and laminar differences.

MATERIALS AND METHODS

ANIMALS

All the experiments were performed according to the guidelines of the French Ministry of Agriculture, Food Processing Industry and Forestry for handling animals (decree 2013-118). Transgenic DBH-Cre mice (DBH-cre) were a gift from Bruno Giros [McGill University, Canada, MMRRC line: Tg(Dbh-cre) KH212Gsat/Mmucd, stock number 032081-UCD (Gong et al., 2007)]. DA transporter-Cre mice (DAT-cre) were a gift from Uwe Maskos [Institut Pasteur, France, (Tg)BAC-DATiCrefto (Turiault et al., 2007)]. Male Wistar rats (12–15 days old) were obtained from Janvier Labs. Animals were maintained in a 12 h light–12 h dark cycle, in stable conditions of temperature (22°C), with food and water available *ad libitum*.

AAV PRODUCTION AND STEREOTACTIC INJECTION

Site- and cell-type-specific labeling of NA or DA neurons was achieved by stereotactic injection of a viral vector into the LC of DBH-Cre or the VTA of DAT-Cre mice (1–3 month-old). The viral vector was a recombinant adeno-associated virus (AAV) driving Cre-dependent expression of a fusion protein containing channelrhodopsin 2 (ChR2) and a yellow variant (YFP) of the GFP from *Aequorea victoria*. The Cre-inducible vector AAV2/1-EF1a-DIO-hChR2(H134R)-EYFP-WPRE-HGHpA (titer: 3×10^{11} gc/ml) was produced from Addgene plasmid #20298 at the vector core facility of Nantes University (UMR 1089 IRT1, France). Aliquots of the pseudovirion were stored at −80°C before stereotactic injection. Mice (six DAT-Cre and six DBH-Cre) were anesthetized with isoflurane and placed on a small animal stereotactic frame. For transduction of LC NA neurons, AAV-EF1α-DIO-ChR2-YFP pseudovirion was bilaterally injected adjacent to the LC at coordinates from bregma: antero-posterior (AP), −5.45 mm; medio-lateral (ML), ±1 mm; dorso-ventral (DV) −3.65 mm). For DA neuron transduction, pseudovirion was bilaterally injected into the VTA (AP: −3.4 mm, ML: ±0.5 mm, DV: −4.4 mm). Injections were performed through an internal canula at a rate of 0.1 μl/min for 10 min (total 1 μl per site). The canula was held in place for 15 min before retraction out of the brain.

IMMUNOHISTOCHEMISTRY

Eight weeks after injection, mice were deeply anesthetized with 10 mg/ml ketamine and 0.1% xylazine before transcardiac perfusion with 50 ml of 4% paraformaldehyde in 0.12 mM phosphate buffer (pH 7.4). Brains were removed and post-fixed with the same solution for 2 h, cryoprotected with 30% sucrose and cut with a freezing microtome (Leica) at a thickness of 40 μm. Slices were washed overnight with PBS, then blocked and permeabilized with PBS complemented with 0.2% fish skin gelatin, 0.25% triton X-100 (PBS-GT) for 2 h at room temperature. Brain slices were incubated overnight at 4°C with primary antibody diluted in PBS-GT (monoclonal mouse anti TH: MAB318 (Clone LNC1), Millipore, 1/2000; polyclonal chicken anti-GFP: GFP-1020 (Aves Labs, 1/2000). After 6 ×10 min washes in PBS-GT, slices were incubated for 3 h at room temperature with fluorescently labeled secondary antibody diluted at 1/1000 in PBS-GT (goat anti chicken alexa488, Invitrogen A11039; goat anti mouse Alexa555, Invitrogen A21422). Slices were mounted in fluoromount (Clinisciences) after extensive washes in PBS-GT followed by PBS. Images were obtained using an AXIO Zoom.V16 macroscope (Zeiss). Labeled fibers were drawn in black (value of the pixel: 255) on white background (value of the pixel: 0) using Image J and Photoshop Cs2 (Adobe). The density of fibers was obtained from drawings using the line plot profile tool of ImageJ on lanes of 200 pixels (260 μm) width covering the vertical extent of the cortex from pia to white matter. The fiber density corresponds to the averaged value of black and white pixels in a 200 pixel line projected on the vertical axis along the lane.

BRAIN SLICE PREPARATION AND VIRAL TRANSDUCTION FOR IMAGING PKA ACTIVITY

Rats were killed by decapitation. Brains were quickly removed and immersed in ice-cold artificial cerebrospinal fluid (ACSF) containing (in mM): 126 NaCl, 2.5 KCl, 1.25 NaH_2PO_4, 2 $CaCl_2$, 1 $MgCl_2$, 26 $NaHCO_3$, 20 D-glucose, 5 Na pyruvate, 1 kynurenic acid, and saturated with 5% CO_2/95% O_2. Parasagittal slices (300 μm thick) of cortex were cut at an angle of 10° using a Leica VT 1000S Vibratome (Leica). Slices were kept at room temperature for 30 min in the same solution. Brain slices were placed onto a millicell-CM membrane (Millipore) with culture medium (50% minimum essential medium, 50% Hanks' balanced salt solution, 6.5 g/L glucose, and 100 U/ml penicillin/100 μg/ml streptomycin; Invitrogen). Transduction was performed by adding $\sim 5 \times 10^5$ particles per slice of sindbis virus encoding the GAkdYmut sensor that reports PKA activation through a reversible increase of fluorescence intensity (Bonnot et al., 2014). Slices were incubated overnight at 35°C in 5% CO_2. The next morning, brain slices were equilibrated in ACSF for 1 h and then placed into the recording chamber and perfused continuously at 2 ml/min with ACSF at 32°C. Under these conditions, sindbis viral transduction efficiently and selectively targets cortical pyramidal neurons, and leaves their functional properties essentially unaffected (Drobac et al., 2010; Hu et al., 2011).

OPTICAL RECORDINGS

Two-photon images were obtained with a custom-built 2-photon laser scanning microscope as described (Bonnot et al., 2014), based on an Olympus BX51WI upright microscope (Olympus, Tokyo, Japan) with ×40 (0.8 NA) or ×60 (0.9 NA) water-immersion objectives and a titanium:sapphire laser (MaiTai HP; Spectra Physics, Ellicot City, MD, USA). Two-photon excitation was performed at 920 nm for GFP. Images were acquired as z stacks and analyzed using ImageJ (U.S. National Institutes of Health, Bethesda, MD, USA; http://rsbweb.nih.gov/ij/). Occasional *x*, *y*, and *z* drifts were corrected using custom macros

developed from ImageJ plugins TurboReg, StackReg (Thevenaz et al., 1998), MultiStackReg, and Image CorrelationJ (Chinga and Syverud, 2007). Fluorescence variations were measured at the soma of pyramidal neurons. Fluorescence intensity of regions of interest (ROIs) was calculated for each time point from average intensity projection of 3–5 frames by averaging pixel intensity. Variations of fluorescence intensity in a given ROI were expressed as the ratio $\Delta F/F0$ and calculated according to the formula $(F - F0)/F0$. F corresponds to the fluorescence intensity in the ROI at a given time point, and $F0$ corresponds to the mean fluorescence intensity in the same ROI during control baseline prior to drug application. Pseudocolor hue saturation value (HSV) encoding of fluorescence intensity was performed using IGOR Pro (WaveMetrics) custom procedures. Pseudocolor images were obtained by dividing, pixel-by-pixel a raw fluorescence image F by the $F0$ image averaged over several time points prior to drug application. Color coding displays the ratio $F/F0$ (in hue) and the fluorescence F (in value). The EC_{50} for NA and DA were obtained by fitting the values with the Hill equation using IgorPro6. The same equation was used to determine the 10–90% rise time of the agonist induced PKA activation.

DRUGS

All drugs were bath applied. SKF38393, SCH23390; Propranolol, Yohimbin, CGP20712, and forskolin were purchased from Tocris. NA, DA, haloperidol, and isoproterenol were from Sigma-Aldrich.

STATISTICS

In this report, N represents the number of animals or brain slices tested while n represents the number of cells on which measurements were performed. Values are expressed as mean ± SEM. Statistical significance was assessed with Student's t-test. p value < 0.05 was considered statistically significant.

RESULTS

DISTRIBUTION OF LC AND VTA FIBERS IN THE CEREBRAL CORTEX

In order to compare LC and VTA projections to the rodent cortex, we selectively expressed GFP in DA or NA neurons using Cre-dependent viral transduction (see Materials and Methods). DBH-Cre mice ($N = 6$) and DAT-Cre mice ($N = 6$) were injected in the LC or in the VTA, respectively, with a recombinant pseudovirion driving GFP expression at the membrane of Cre-positive neurons. Anti-GFP and anti-TH immunohistochemistry showed that GFP was widely expressed in the LC of DBH-Cre mice and in the VTA and substantia nigra of DAT-Cre mice following viral transduction (**Figure 1A**). In LC-injected DBH-Cre mice, 83.9 ± 2.7% ($n = 227$; $N = 5$) of TH-positive neurons in the LC expressed GFP. Similarly, 86.1 ± 1.2% ($n = 158$; $N = 3$) of TH-positive neurons in the VTA co-expressed GFP. Conversely, LC neurons of VTA-injected DAT-Cre mice and VTA neurons of LC-injected DBH-Cre mice were GFP-negative (**Figure 1A**). These results show that the present protocol of conditional viral transduction enabled efficient site- and cell-type-specific GFP expression in LC NA neurons or VTA DA neurons. We next examined the distribution of NA and DA fibers in the cerebral cortex. GFP labeling revealed a high density of NA fibers throughout all cortical regions and layers examined (**Figures 1B,C**). Quantification of NA fibers (see Materials and Methods) revealed moderate laminar and regional differences, such as an overall lower density in frontal than other regions and a higher density in upper layers in cingulate, somatosensory, rhinal, and visual than in other layers of these regions (**Figure 2**). Similar results were obtained on six LC-injected DBH-Cre mice. DA fibers had a more contrasted distribution. The highest density of fibers was observed in a medial rostro-caudal band that comprised all layers of the prelimbic cortex and extended caudally to the cingulated cortex, but did not reach the retrosplenial occipital area (**Figures 1D** and **2**). A lateral rostro-caudal band of lower fiber density comprised all layers of the lateral part of the frontal association cortex, of the agranular insular cortex and of the rhinal occipital area. Between these two bands, DA fibers were restricted to deep layers in a large region extending from the medial part of the frontal association to the visual cortex through the somatosensory area (**Figures 1D** and **2**). Similar results were obtained on six VTA-injected DAT-Cre mice. The striatum contained a dense network of DA fibers but was sparsely innervated by NA fibers (**Figures 1C,D**), as expected from their known distributions (Aston-Jones, 2004; Gerfen, 2004). These data confirm that NA fibers widely innervate the cortical mantle, whereas the distribution of DA fibers is more restricted and exhibits area and layer specificity.

NA AND DA RECEPTORS ARE CO-EXPRESSED AND MEDIATE PKA ACTIVATION IN CORTICAL PYRAMIDAL NEURONS

We examined responses of cortical neurons to NA, DA or specific receptor agonists in frontal, parietal, and occipital areas where DA fibers are restricted to deep layers (i.e., lateral frontal, somato-sensory, and visual cortices; see above). We used 2-photon imaging to monitor responses of layers II/III and V pyramidal neurons expressing the PKA sensor GAkdYmut (Bonnot et al., 2014) following sindbis viral transfer in acute rat brain slices (see Materials and Methods and Drobac et al., 2010; Hu et al., 2011). Response amplitudes measured at the soma were normalized to those elicited by a maximally effective concentration of the adenylate cyclase activator forskolin (FSK, 12 μM; Gervasi et al., 2007). As illustrated in **Figure 3**, successive bath application of DA (10 μM) and NA (10 μM) triggered PKA activation in most pyramidal neurons of the parietal cortex, showing that DA and NA receptors can be co-expressed in individual neurons. To estimate the proportion of responsive cells, we arbitrarily defined a threshold at 5% of the maximal fluorescence variation obtained with FSK. Using this criterion, we found that virtually all pyramidal neurons responded to NA ($n = 45$, $N = 2$) and among those, 83 ± 4% responded to DA (39 out of 45 cells). These effects were mimicked by bath application of the D1/D5 agonist SKF38393 (1 μM) or the beta adrenoceptor agonist isoproterenol (1 μM; **Figure 3**). We found that 97% of the cells (57 out of 59) responded to isoproterenol and 75% to SKF (44 out of 59), suggesting that most pyramidal neurons co-express D1/D5 and beta-adrenergic receptors. Dose–response relationships of normalized NA and DA effects showed that NA was more potent than DA in activating PKA (**Figure 3**). Indeed, the EC_{50} of NA responses was estimated at 25 ± 2 nM and that of DA at 460 ± 30 nM from the fit of their dose–response curves

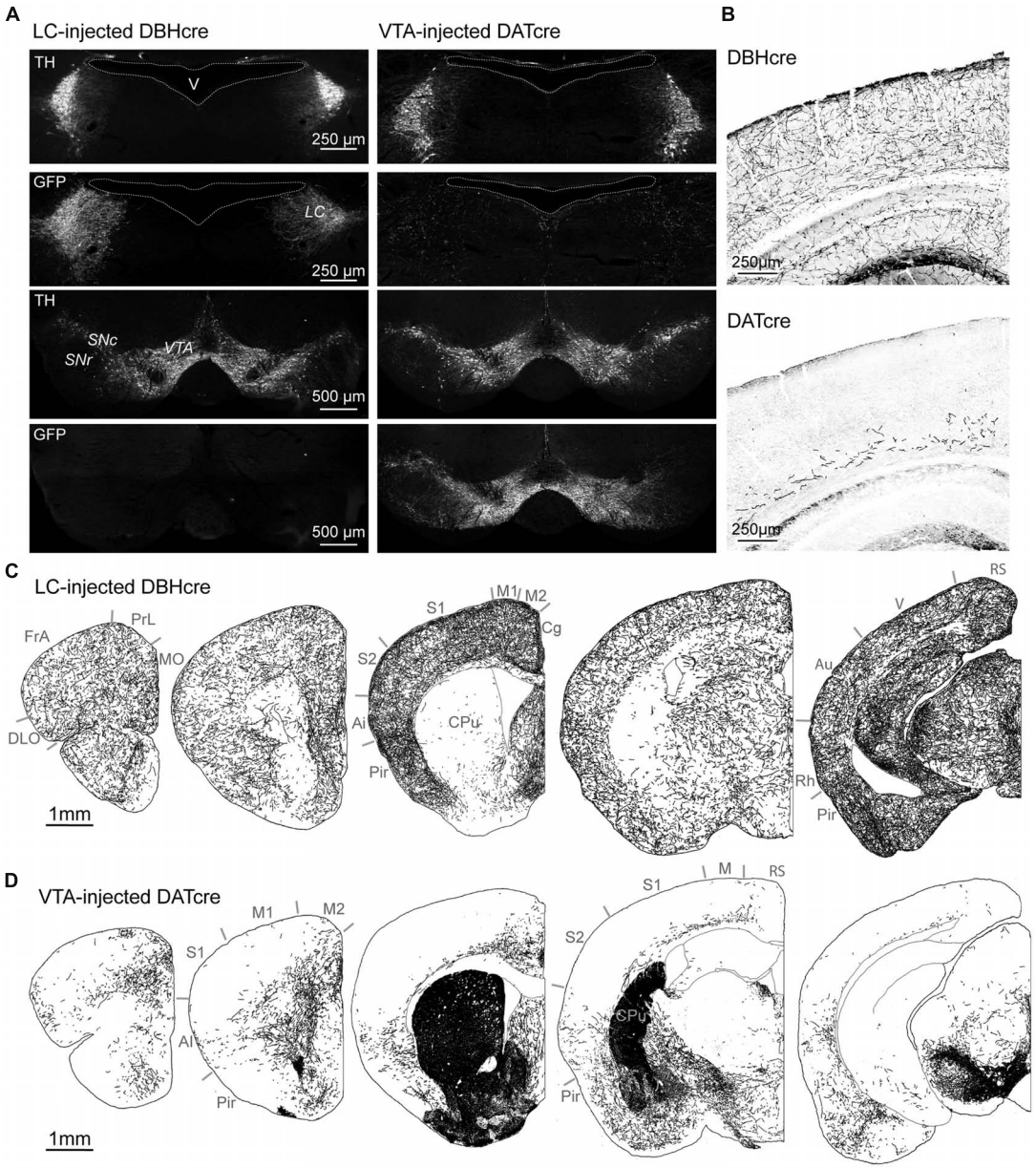

FIGURE 1 | Catecholaminergic projections to the cortex. (A) Immunolabeling against TH and GFP in the LC and VTA 8 weeks after bilateral injection of a Cre-dependent AAV expressing GFP in the LC of DBH-Cre mice or the VTA of DAT-Cre mice. Note that GFP labeling in VTA-injected DAT-Cre mice extends to neighbor DA neurons of the substantia nigra pars compacta (SNc) but is absent from NA neurons of the LC. **(B)** Immunolabeling of GFP-expressing fibers in the somato-sensory parietal cortex of DBH-Cre and DAT-Cre mice. **(C,D)** Drawings of NA or DA fibers obtained from immunolabeling of GFP positive fibers in coronal brain sections of LC-injected DBH-Cre and VTA-injected DAT-Cre mice (antero-posterior from left to right). Note the different distribution of NA and DA fibers in cortical areas and caudate-putamen (CPu). Ai: agranular insular cortex; Au: auditory cortex; Cg: cingulate cortex; DLO: dorso-lateral orbital cortex; FrA: frontal association cortex; M1-M2-M: primary or secondary motor cortex; MO: medial orbital cortex; Pir: piriform cortex; PrL: prelimbic cortex; Rh: rhinal cortex; RS: retrosplenial cortex; S1: primary somatosensory cortex; V: visual cortex.

(see Materials and Methods). Furthermore, maximal responses to NA and DA were 60 ± 1% and 47 ± 2% of the FSK response, respectively.

NA AND DA ACTIVATE PKA ACROSS CORTICAL REGIONS AND LAYERS

We next compared PKA activation elicited by DA, NA, SKF38393, and isoproterenol in layers II/III and V of frontal, parietal, and occipital cortices (**Figure 4** and **Table 1**). The mean amplitude of NA responses varied between 54 ± 4% in occipital layer V ($n = 43$; $N = 4$) and 75 ± 4% of the FSK effect in frontal layer II/III ($n = 37$, $N = 2$). Isoproterenol-induced responses varied similarly between 44 ± 3% in frontal layer V ($n = 50$, $N = 4$) and 56 ± 2% of the FSK effect in frontal layer II/III ($n = 76$, $N = 4$). DA and SKF38393 both caused PKA activation in all

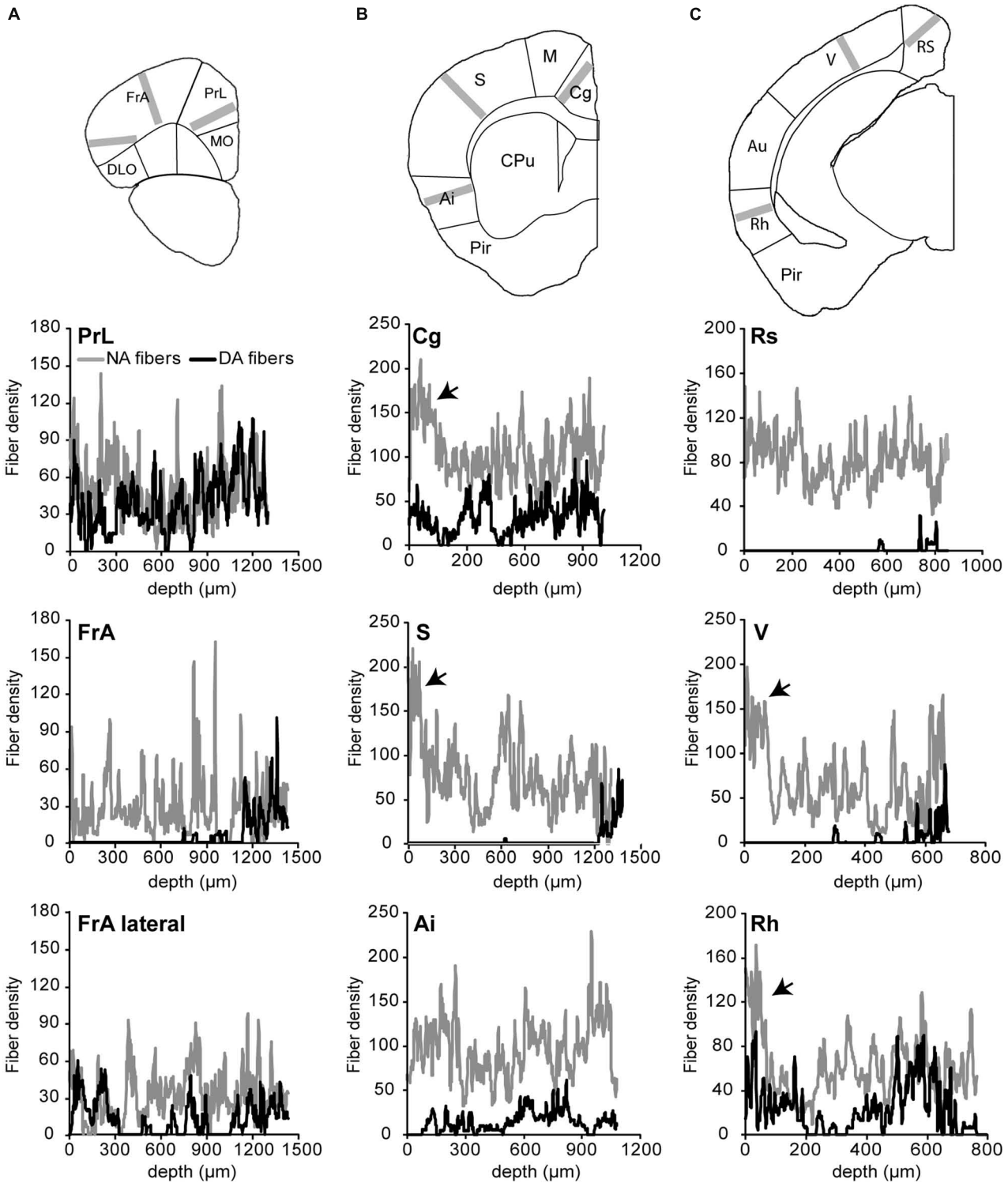

FIGURE 2 | Density of noradrenergic and dopaminergic fibers in various areas of the cortex. The density of fibers was obtained from the drawings shown in **Figure 1** on lanes of 200 pixels (260 μm) width orthogonal to the pial surface, as depicted in images of the upper panel (gray bars). The fiber density, measured in three regions of anterior **(A)**, intermediate **(B)**, and posterieor **(C)** coronal brain sections, corresponds to the averaged pixel value along the lane plotted on the x-axis of the graphs from the pial surface to indicated depths. NA fibers are widespread in the cortex and are enriched (arrows) in upper layers of cingulated (Cg), somato-sensory (S), visual (V), and rhinal (Rh) cortices. Note that DA fibers are absent from most layers of a rostro-caudal band comprising the medio-lateral part of the frontal association (FrA), S and V cortices, except for a thin lamina in deep layers.

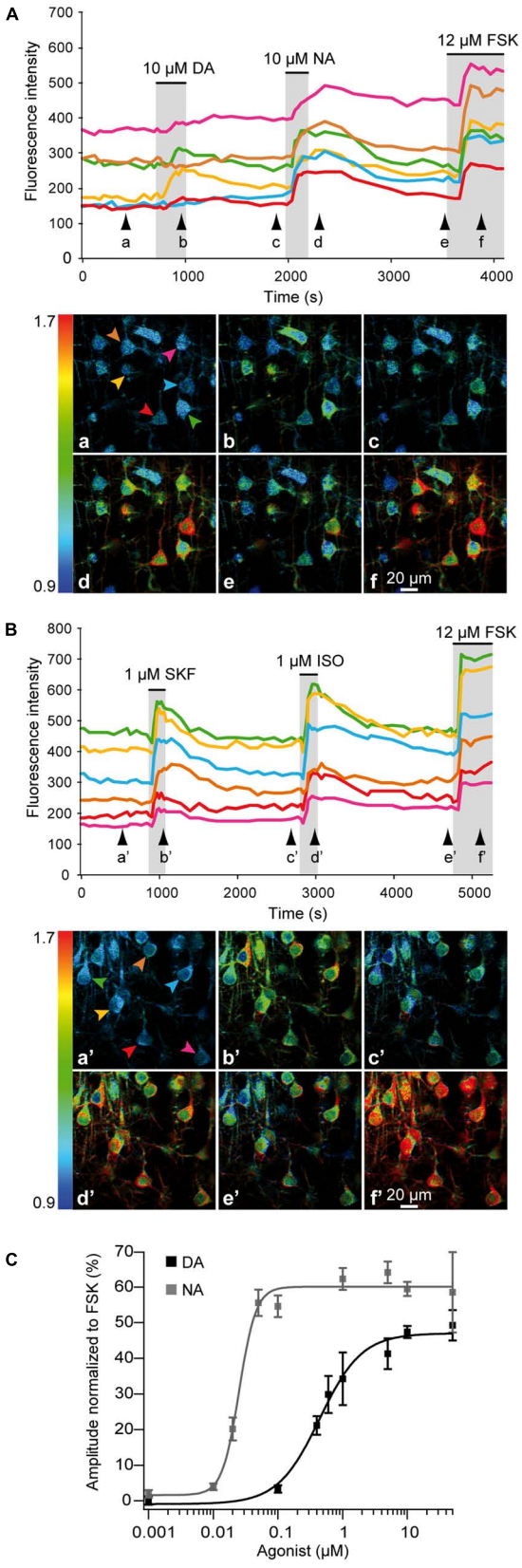

FIGURE 3 | Continued

FIGURE 3 | Continued
NA and DA activate the cAMP/PKA pathway in pyramidal neurons. 2-photon imaging of pyramidal neurons expressing the GAkdYmut fluorescent PKA sensor in parietal cortical slices. **(A)** Responses to bath application of DA, NA, and the adenylate cyclase activator FSK. Traces show the variation of fluorescence intensity measured at the soma of individual neurons indicated by arrows on pseudocolor images below. Black arrowheads indicate time points corresponding to pseudocolor images. **(B)** Responses to the D1/D5 agonist SKF38393 and the non-specific beta adrenergic agonist isoproterenol. **(C)** Dose–response curves of PKA activation by NA and DA. Each data point corresponds to the mean response measured in 10–140 individual neurons from 2 to 10 different brain slices. Curves were obtained by fitting the values with the Hill equation. NA was more potent than DA in activating PKA.

areas examined but responses were smaller than those elicited by NA or isoproterenol (**Figure 4A** and **Table 1**). DA responses were significantly smaller in both layers of the frontal cortex than in more caudal regions. Indeed, DA responses in layer II/III were 46 ± 4% in occipital ($n = 38$, $N = 2$) and 33 ± 3% of the FSK effect in the frontal cortex ($n = 39$, $N = 3$, $p = 0.006$). Similarly, DA responses in layer V were 44 ± 4% in occipital ($n = 37$, $N = 3$) and 29 ± 2% of the FSK effect in the frontal cortex ($n = 44$, $N = 3$, $p = 0.01$). Similar results were obtained with the D1/D5 agonist SKF38393, although amplitudes were smaller than those obtained with DA (**Figure 4A** and **Table 1**, $p = 0.04$ in layer II/III and $p = 0.02$ in layer V). We also observed that less than 5% of the recorded pyramidal neurons were unresponsive to NA or isoproterenol, regardless of the layer or cortical region examined. For DA, a similar result was obtained in layer II/III. However, the proportion of unresponsive cells was higher in layer V and reached 12% in the parietal cortex. For SFK38393, the proportion of unresponsive cells was above 5% in all cases with more unresponsive cells in layer V than in layer II/III. The highest value was observed in layer V of the parietal cortex with 27% of recorded neurons not responding to SFK38393. These results indicate that NA and isoproterenol induce overall larger and more homogeneous cortical responses than DA and SKF38393, whose effects increased along the antero-posterior axis.

We also examined the onset kinetics of PKA responses by determining their 10–90% rise time (**Figure 4B** and **Table 1**). Kinetics of NA and isoproterenol responses exhibited moderate regional differences. Conversely, DA and SKF38393 response onsets were faster in occipital than in frontal regions with intermediate values in the parietal cortex. This was observed in both layers II/III and V ($0.01 < p \leq 0.003$ for DA, $p < 0.001$ for SKF). As a consequence of these regional variations, the onset kinetics of DA-receptor mediated responses were markedly slower than those of NA-receptor mediated responses in the frontal cortex, but were comparable in the occipital cortex. These results confirm that NA and isoproterenol induce overall more homogeneous cortical responses and indicate that DA and SKF38393 effects increase in amplitude and velocity along the antero-posterior axis.

CORTICAL EFFECTS OF NA AND DA INVOLVE BOTH Gs- AND Gi-COUPLED RECEPTORS

Gs-coupled NA and DA receptors involved in PKA activation were characterized in parieto-cortical layer II/III pyramidal neurons

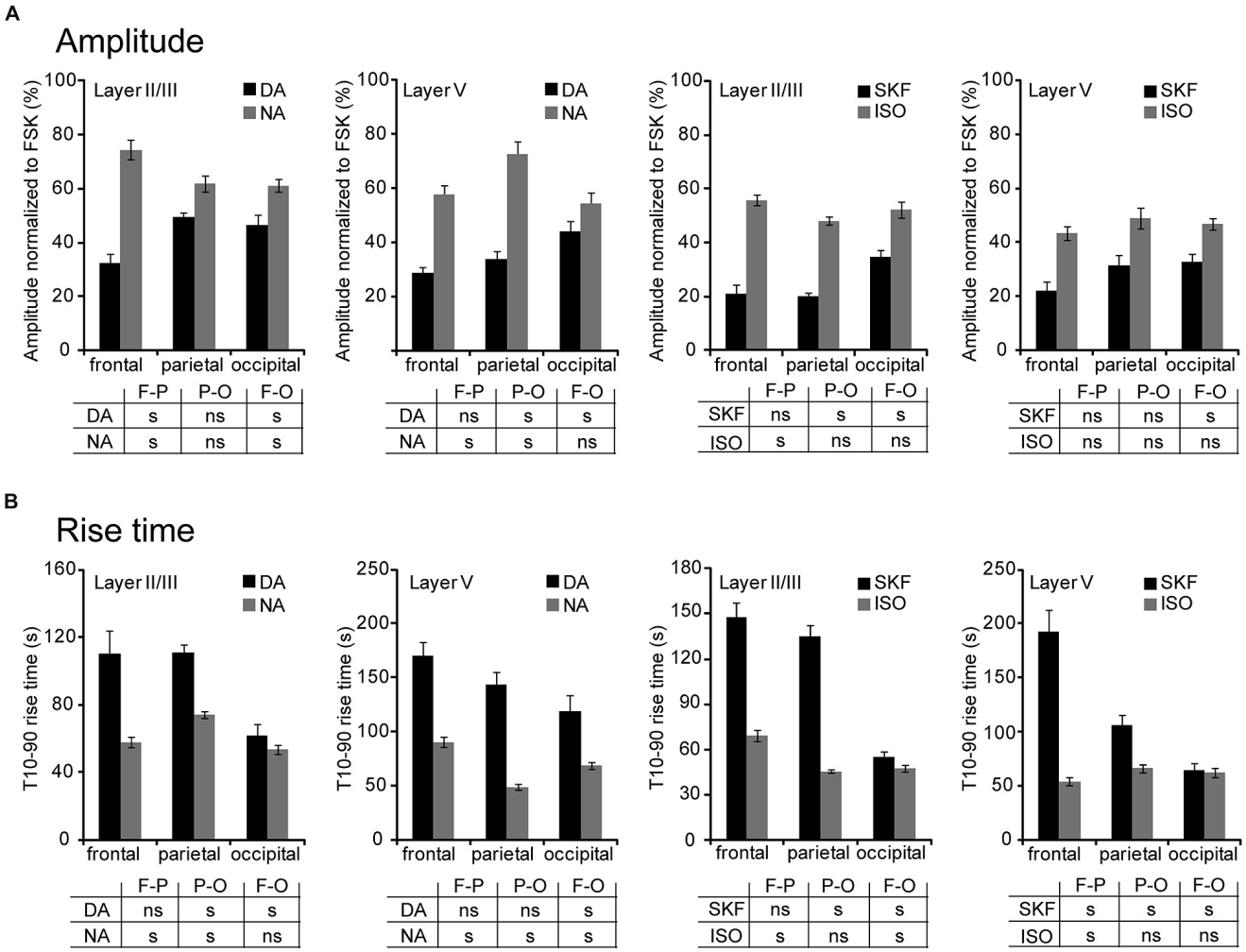

FIGURE 4 | NA and DA activate PKA across cortical regions and layers. Data were obtained by 2-photon imaging of PKA activity in pyramidal neurons as illustrated in **Figure 3**. Imaging was performed in frontal, parietal, and occipital regions of parasagittal slices of the medio-lateral cortex that exhibits scarce DA fibers restricted to deep layers. **(A)** Amplitude of fluorescence variations normalized to the response to FSK. **(B)** Onset kinetics of responses was analyzed by calculating the 10–90% rise time. Tables indicate significant (s) or non-significant (ns) differences between values measured in the areas (F-P: frontal vs. parietal; P-O: parietal vs. occipital; F-O: frontal vs. occipital). Note the antero-posterior gradient of DA responses amplitude and velocity.

Table 1 | NA and DA activate PKA across cortical region and layers.

		Frontal		Parietal		Occipital	
Drugs (n/N)	**Layer**	**Amplitude (% FSK)**	**T10–90% (s)**	**Amplitude (% FSK)**	**T10–90% (s)**	**Amplitude (% FSK)**	**T10–90% (s)**
DA	II/III	32.5 ± 3.3 (39/3)	109.9 ± 14.1 (22/3)	49.5 ± 1.8 (242/12)	110.5 ± 4.8 (181/12)	46.4 ± 3.9 (38/2)	61.7 ± 7.1 (27/2)
	V	28.5 ± 2.4 (44/3)	170.0 ± 13.1 (30/3)	33.7 ± 3.1 (105/6)	143.4 ± 11.9 (53/6)	44.1 ± 3.8 (37/3)	119.3 ± 14.0 (37/3)
NA	II/III	74.5 ± 3.7 (37/2)	57.8 ± 3.0 (32/2)	61.9 ± 2.9 (114/7)	74.3 ± 2.0 (84/7)	61.3 ± 2.5 (77/2)	53.3 ± 2.8 (62/2)
	V	57.6 ± 3.5 (26/3)	90.2 ± 4.9 (21/3)	72.5 ± 5.0 (29/2)	48.8 ± 2.8 (26/2)	53.9 ± 3.5 (43/4)	68.4 ± 3.2 (35/4)
SKF	II/III	21.1 ± 3.4 (31/4)	147.4 ± 9.9 (39/4)	19.9 ± 1.4 (196/10)	134.9 ± 7.9 (81/10)	34.5 ± 2.6 (40/4)	55.2 ± 3.4 (31/3)
	V	22.0 ± 3.6 (36/4)	192.4 ± 20.2 (24/3)	31.4 ± 3.8 (60/4)	106.3 ± 8.9 (32/4)	32.9 ± 2.8 (69/5)	64.6 ± 5.9 (28/3)
ISO	II/III	55.8 ± 2.0 (76/4)	69.2 ± 3.5 (70/4)	48.1 ± 1.5 (172/7)	45.7 ± 1.2 (98/7)	52.3 ± 3.1 (40/3)	47.5 ± 2.5 (32/3)
	V	43.5 ± 2.5 (50/4)	54.0 ± 3.8 (46/4)	48.9 ± 3.8 (60/4)	65.9 ± 4.1 (47/4)	46.8 ± 2.1 (135/5)	62.7 ± 4.3 (50/5)

using specific antagonists (**Figure 5** and **Table 2**). The non-selective beta-adrenergic receptor antagonist propranolol (50 μM, $N = 2$, $n = 22$) and the specific beta1 antagonist CGP20712 (100 nM, $N = 3$, $n = 40$) reduced PKA activation by NA (10 μM) by more than 90% (**Figure 5**). Responses to isoproterenol (1 μM) were also reduced by propranolol to a similar extent (**Table 2**). These results indicate that NA-induced PKA activation in cortical pyramidal neurons is primarily mediated by beta1-adrenergic receptors. Responses to DA (10 μM) and to SKF38393 (1 μM) were almost abolished in the presence of the D1/D5 receptor antagonist SCH23390 (1 μM; **Table 2**). These results indicate that DA-induced PKA activation in cortical pyramidal neurons is mediated by D1/D5 receptors. NA and isoproterenol responses were not significantly altered by the D1/D5 antagonist SCH23390 (1 μM), showing that NA effects did not involve DA receptors. Surprisingly, we found that responses to DA and SKF38393 were

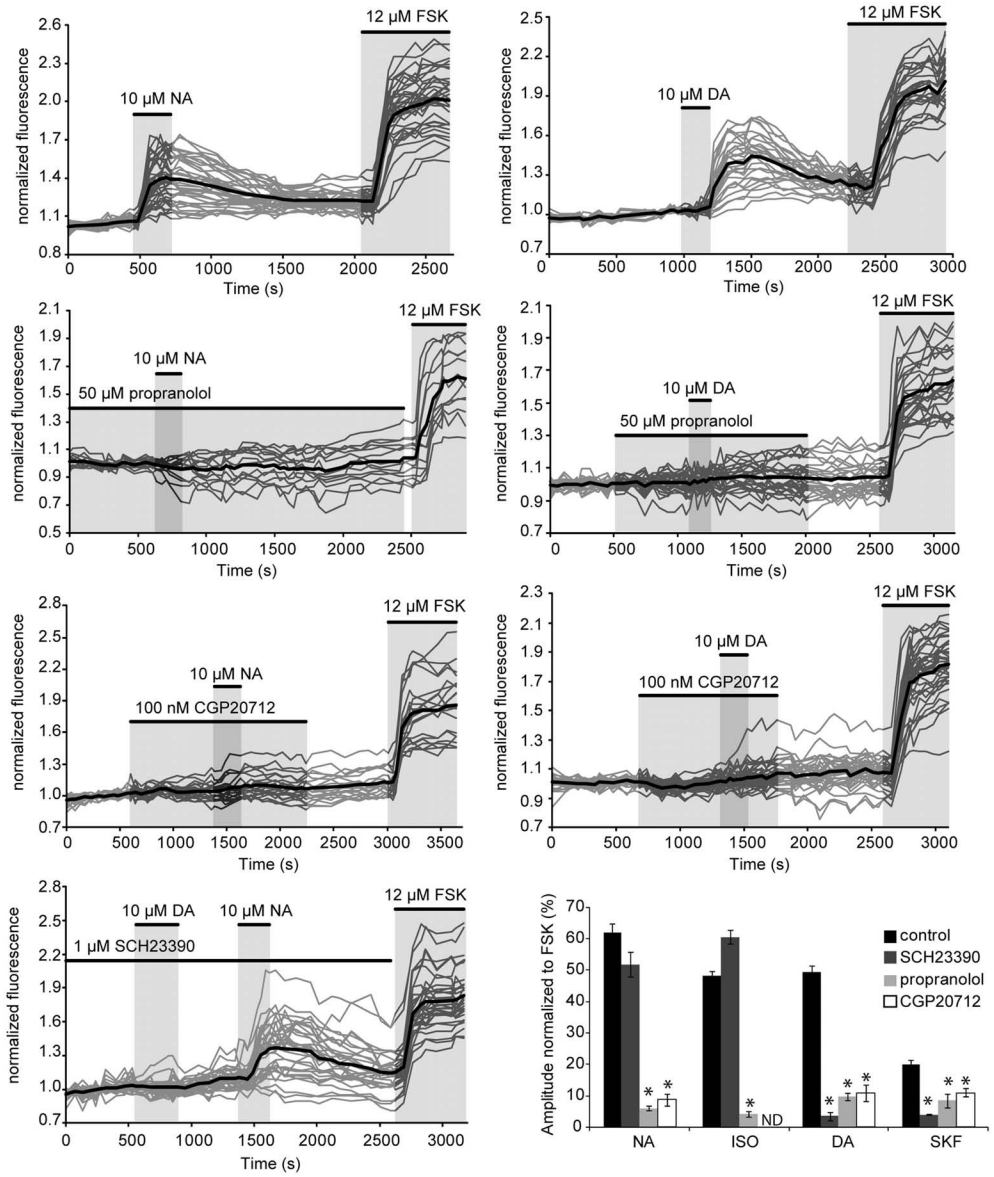

FIGURE 5 | NA and DA receptors involved in PKA activation. Graphs show the effects of antagonists propranolol (beta adrenergic), CGP20712 (beta1-specific) and SCH23390 (D1/D5) on responses to NA and DA of layer II/III pyramidal neurons of the parietal cortex. Gray traces correspond to the fluorescence intensity normalized to the baseline value measured on individual neurons expressing the PKA sensor in parietal cortical slices (averaged traces are in black). Histograms summarize the effects of these antagonists on responses to NA, DA, the beta adrenergic agonist isoproterenol and the D1/D5 agonist SKF38393. ND: not determined; but Castro et al. (2010) reported inhibition of isoproterenol responses in cortical pyramidal neurons by CGP20712 in similar experimental conditions. Values represent the mean response of 20–200 neurons recorded in 2–12 different brain slices. Statistical significance relative to control responses is indicated by an asterisk. Note that DA responses were prevented by both beta adrenergic antagonists whereas NA responses were insensitive to the D1/D5 antagonist.

Table 2 | PKA stimulation involves beta1 adrenergic and D1/D5 dopaminergic receptors.

	NA Amplitude (% FSK)	ISO Amplitude (% FSK)	DA Amplitude (% FSK)	SKF Amplitude (% FSK)
Control (n/N)	61.9 ± 2.9 (114/7)	48.1 ± 1.5 (172/7)	49.5 ± 1.8 (242/12)	19.9 ± 1.4 (196/10)
SCH23390 (n/N)	51.8 ± 3.9 (56/2)	60.5 ± 2.3 (66/2)	3.5 ± 1.4 (56/2)	4.0 ± 0.1(49/4)
Propranolol (n/N)	6.0 ± 0.7 (22/2)	4.1 ± 0.8 (21/2)	9.7 ± 1.3 (57/2)	8.5 ± 2.1(24/2)
CGP20712 (n/N)	8.8 ± 1.9 (40/3)	ND	11.0 ± 2.7 (54/2)	11.3 ± 1.2 (101/3)

inhibited by beta adrenergic antagonists. Indeed, propranolol and CGP20712 similarly reduced responses to DA (10 μM) by ∼80% and responses to SKF38393 (1 μM) by ∼50% (**Figure 4** and **Table 2**), suggesting that DA effects may involve beta1-D1/D5 heteromeric receptors.

We next examined the contribution of Gi-coupled receptors in the response of parieto-cortical layer II/III pyramidal neurons to NA and DA (**Figure 6** and **Table 3**). Inhibition of the alpha2 adrenoceptor by yohimbin (1 μM) significantly increased the mean amplitude of the NA response by 17% ($p = 0.007$). Similarly, the D2-like receptors antagonist haloperidol (1 μM) significantly increased the DA response by 30% ($p < 0.001$). Haloperidol and yohimbin also increased the velocity of DA and NA responses. Indeed, in the presence of haloperidol, the 10–90% rise time of DA responses decreased significantly from 111 ± 5 s ($n = 181$, $N = 12$) to 76 ± 3 s ($n = 84$, $N = 4$, $p < 0.001$). Yohimbin application similarly resulted in a decreased rise time of NA responses from 74 ± 2 ($n = 84$, $N = 7$) to 47 ± 2 s ($n = 119$, $N = 5$; $p < 0.001$; **Figure 6** and **Table 3**). We previously noted a large heterogeneity in the amplitudes of DA responses (**Figures 3** and **5**). We thus examined whether antagonists of Gi-coupled receptors could modify the distribution of DA and NA response amplitudes (**Figures 6B,C**). The plot of DA response amplitudes in control condition had a broad distribution, with almost half of the cells exhibiting responses below 40% of the FSK effect, and only 6% responding above 90%. The distribution of DA response amplitudes was shifted to higher values in the presence of haloperidol, with only 10% of the cells responding below 40% of the FSK effect, and 22% responding above 90%. Although NA response amplitudes were less variable, yohimbine also markedly shifted their distribution toward higher values. These results indicate that Gi-coupled receptors are co-activated with Gs-coupled receptors by DA and NA, and significantly limit DA- and NA-induced PKA activation in cortical pyramidal neurons.

DISCUSSION

Genetic labeling confirmed that NA neurons innervate the entire cortex whereas DA fibers were present in all layers of restricted medial and lateral cortical areas but only in deep layers of other areas. Imaging of PKA activity in frontal, parietal, and occipital regions with scarce DA fibers revealed that layers II/III and V pyramidal neurons widely respond to NA and DA. The EC50 of NA response was more than 10-fold lower than for DA. Responses to NA and isoproterenol had higher amplitude, velocity and were more homogeneous than those elicited by DA and SKF38393, whose amplitude and velocity increased along the antero-posterior axis. NA- and DA-induced PKA activation was mediated by Gs-coupled beta1 and D1/D5 receptors. Beta adrenergic antagonists inhibited both NA and DA responses whereas the effect of a D1/D5 antagonist was selective of DA responses. NA and DA responses also involved Gi-coupled alpha2 adrenergic and D2-like dopaminergic receptors that markedly reduced the amplitude and velocity of responses and contributed to their cell-to-cell heterogeneity.

DISTRIBUTION OF CATECHOLAMINERGIC FIBERS IN THE CORTEX

The overall distribution of GFP-labeled DA and NA fibers in the cortex we describe is largely congruent with previous maps obtained using histochemistry, radiolabeling or immunohistochemical approaches (Morrison et al., 1978, 1979; Descarries et al., 1987; Berger et al., 1991; Nicholas et al., 1996; Venkatesan et al., 1996; Latsari et al., 2002; Papay et al., 2006; Paschalis et al., 2009). NA fibers were present in all layers and areas of the cortex, although their density exhibited regional and laminar variations. Conversely, DA fibers were present in all layers of two medial and lateral rostro-caudal bands comprising frontal, cingulated, rhinal cortices as well as the agranular area of the insular cortex but were confined to deep layers of other cortical areas. The present study shows that DA receptors are functionally expressed in areas with scarce or no DA fibers, consistent with the presence of their cognate mRNAs and proteins (Ariano and Sibley, 1994; Khan et al., 1998; Luedtke et al., 1999; Lemberger et al., 2007; Rivera et al., 2008; Oda et al., 2010). The source and nature of the endogenous ligand activating these DA receptors is still unclear but several studies indicate that DA can be co-released from NA fibers where it is present as the biosynthetic precursor of NA. Indeed,

Table 3 | NA and DA effects involve alpha2 adrenergic and D2-like dopaminergic receptors.

	DA	DA + Haloperidol	NA	NA + Yohimbin
Amplitude (% FSK) (n/N)	49.5 ± 1.8 (242/12)	69.7 ± 1.9 (143/6)	61.9 ± 2.9 (114/7)	72.3 ± 1.7 (133/6)
T10−90% (s) (n/N)	110.5 ± 4.8 (181/12)	75.9 ± 3.0 (84/4)	74.3 ± 2.0 (84/7)	46.8 ± 1.9 (119/5)

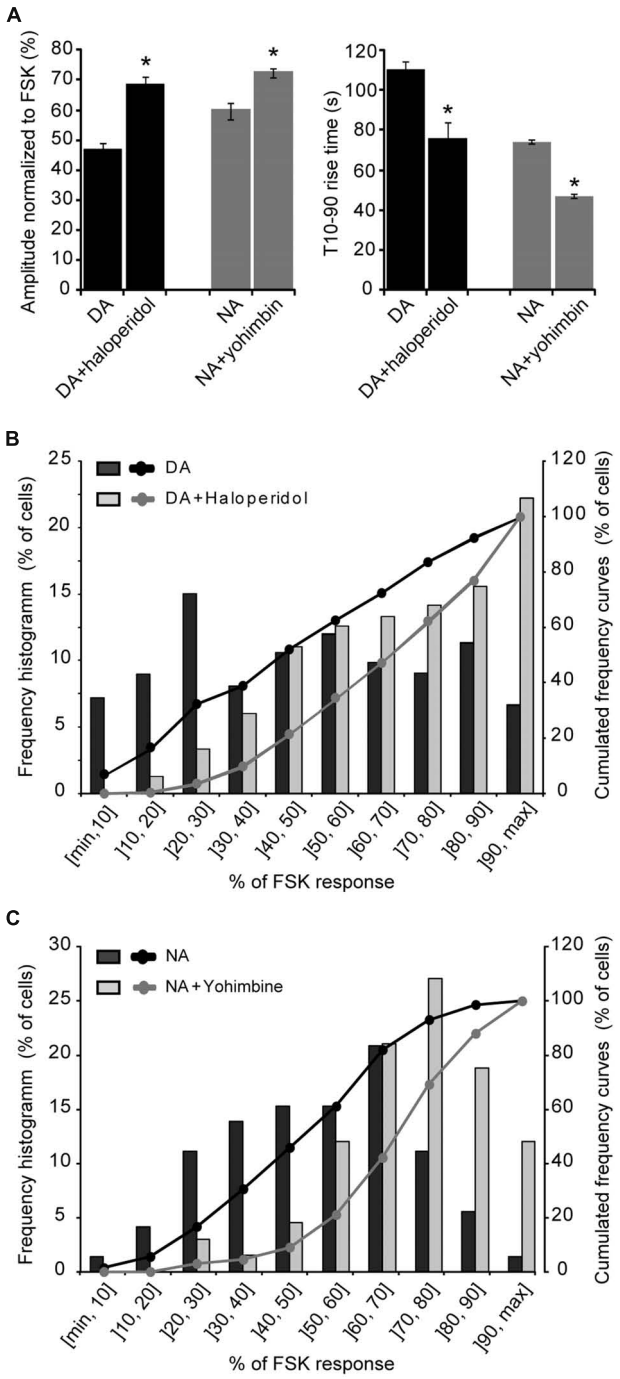

FIGURE 6 | Gi-coupled receptors dampen NA- and DA-induced PKA activation. (A) Mean amplitude and rise time of NA- and DA-induced (10 μM each) PKA activation measured on layer II/III pyramidal neurons of the parietal cortex in the absence or presence of the D2-like antagonist haloperidol (1 μM) or the alpha2 adrenergic antagonist yohimbin (1 μM). **(B,C)** Distribution of FSK-normalized DA or NA response amplitudes measured in the same sample of neurons as in **(A)** in absence or presence of haloperidol or yohimbin. The left axis corresponds to the histogram of the proportion of cells for each amplitude interval and the right axis to the curve of cumulated frequency over the amplitude intervals. Note the shift of NA and DA response amplitude distributions toward higher amplitudes in the presence of antagonists of Gi-coupled receptors.

Devoto et al. (2005, 2008) showed that electrical stimulation of the LC results in VTA-independent NA and DA increases in the frontal cortex but also in cortices devoid of DA fibers. Similar conclusions were drawn from a study of amphetamine-induced DA release in the dorsal hippocampus, which is prevented by TH knock-down using siRNAs in the LC but not in the VTA (Smith and Greene, 2012). Hence, LC fibers are a plausible source of endogenous DA that provides a rationale for the widespread functional expression of Gs- and Gi-coupled DA receptors in the cortex.

NA AND DA RECEPTORS WIDELY ACTIVATE cAMP/PKA IN THE CORTEX

Our results indicate that NA and DA receptors mediate activation of the cAMP/PKA pathway in pyramidal neurons throughout the cortex, even in areas with scarce or no DA fibers. Indeed, we observed robust PKA activation by NA and DA in layer II/III of fronto-lateral, parietal and occipital regions of the cortex where DA fibers are restricted to deep layers. These results indicate that NA released by LC fibers widely influences the function of neural networks in the entire cortical mantle. The same conclusion applies to DA, regardless of its source. We found that NA responses were generally larger, with faster onsets and exhibited less regional variability than DA responses. NA-induced PKA activation was mimicked by the beta agonist isoproterenol and primarily mediated by beta 1 receptors, as shown by the powerful inhibitory effect of the specific antagonist CGP20712 on NA responses. These results are consistent with the predominant expression of beta1 over beta2–3 receptors in the cortex and with the widespread expression of beta1 receptors in layers and areas of the rodent cortex (Nicholas et al., 1996; Paschalis et al., 2009). DA-induced PKA activation exhibited similar properties in layer II/III and layer V, but both the amplitude and velocity of DA responses increased from rostral to caudal regions. DA responses were mimicked by the D1/D5 agonist SKF38393 and prevented by the D1/D5 receptor antagonist SCH23390, pointing to the involvement of D1 and/or D5 receptors in DA-induced PKA activation and its rostrocaudal variations. Regional and laminar differences of D1 and D5 expression levels have been reported in the rodent cortex (Ariano and Sibley, 1994; Ciliax et al., 2000). However, the lack of specific pharmacological tools differentiating these receptors makes it difficult to assign the present functional variations to the regional levels of these receptors. The possibility that D1/D5 receptors forms heteromers with beta1 adrenoceptors further complicates the interpretation of DA response regional variations.

We found that the beta blocker propranolol and the beta1 antagonist CGP20712 inhibited NA responses. Surprisingly, these antagonists also prevented DA responses and largely reduced SKF38393 responses suggesting that DA-induced PKA activation in the cortex may involve beta1 adrenergic receptors. Previous studies established that DA effects can occur through the activation of adrenergic receptors (Aguayo and Grossie, 1994; Rey et al., 2001; Cornil et al., 2002). The present observations that DA effects were mimicked by SKF38393 and that response to these agonists were prevented by the D1/D5 antagonist SCH23390 imply a direct effect of DA through D1/D5,

but not beta adrenergic receptors. DA receptors are known to form heteromers with a variety of receptors including beta adrenoceptors (Rebois et al., 2012; Fuxe et al., 2014). Moreover, cross antagonism by specific antagonist has been demonstrated for the beta1-D4 receptor heteromer (Gonzalez et al., 2012). Hence, these reports substantiate the hypothesis that D1/D5 receptors exist as heteromers with beta1 adrenoceptors in the cortex, thus exhibiting the specific pharmacological pattern we observed.

NA AND DA CONTROL CORTICAL cAMP/PKA SIGNALING VIA Gs- and Gi-COUPLED RECEPTORS

Our results indicate that DA and NA exert a balanced control on cortical cAMP/PKA signaling by activating both Gs- and Gi-coupled receptors. We found that Gs-coupled beta1 and D1/D5 receptors are co-expressed in virtually all layers II/III and V pyramidal neurons throughout the antero-posterior axis of the cortex. The effects of yohimbin and haloperidol on NA and DA response in pyramidal neurons of parietal layer II/III suggest that alpha2 adrenoceptors and D2-like receptors are also broadly expressed in the cortex. This is in agreement with previous reports showing widespread immunoreactivity for alpha2 and D4 receptors in the cortex (Venkatesan et al., 1996; Khan et al., 1998; Rivera et al., 2008) and for D2 receptors in pyramidal cells of the medial prefrontal cortex (Zhang et al., 2010).

We showed that kinetics and amplitudes of catecholaminergic signals vary between cortical areas. It was previously shown in pyramidal neurons of the prefrontal cortex that intracellular elements of the cAMP/PKA cascade, such as phosphodiesterases, phosphatases, or the coupling between receptor and adenylate cyclases are essential in controlling the kinetics and shape of D1-like responses (Castro et al., 2013).

We found that block of alpha2 adrenoreceptors and D2-like receptors by yohimbin and haloperidol increased the amplitude and velocity of NA and DA responses. This is consistent with an inhibitory effect of these receptors on cAMP/PKA signaling that limits DA- and NA-induced PKA activation in cortical pyramidal neurons. In the case of DA, the balance of Gs- and Gi-coupled receptors effects was such that many cells were not responsive to a saturating DA concentration. Hence, regulation of the balance between Gs- and Gi-coupled receptor activities can largely influence the net effect of catecholamines on cortical neurons and networks. Interestingly, DA levels in basal conditions or upon LC stimulation are comparable to those of NA in various cortical regions, but markedly lower than DA levels in basal ganglia (Devoto et al., 2005, 2008). Our measurements of EC50 values are indicative of a ∼20-fold lower affinity of DA for D1/D5 receptors than of NA for beta1 receptors, while NA and DA Gi-coupled receptors exhibit higher affinities than their cognate Gs-coupled receptors (for a detailed comparison of pharmacological properties of receptors, see the International Union of Basic and Clinical Pharmacology database: http://www.guidetopharmacology.org/). This suggests that, at low catecholamine concentration, DA may essentially trigger cAMP/PKA inhibition whereas NA effects may be more balanced. Conversely, large catecholamine increases may be required for a significant contribution of DA to cAMP/PKA stimulation. Assuming co-release of NA and DA from LC fibers in the cortex, DA may thus expand the dynamic range of LC effects on cortical cAMP/PKA signaling.

ACKNOWLEDGMENTS

The authors thank Bruno Giros, Uwe Maskos, Julie Catteau, Ludovic Tricoire, Elvire Guiot, and the IFR83 Cell Imaging Facility for their valuable help. Shinobu Nomura is recipient of a Nakajima Foundation fellowship. This work was supported by Centre National de la Recherche Scientifique, Université Pierre et Marie Curie-P6 and by grants from Ecole des Neurosciences de Paris ("Network for Viral Transfer") and Fondation pour la Recherche sur le Cerveau/Rotary Club de France.

REFERENCES

Aguayo, L. G., and Grossie, J. (1994). Dopamine inhibits a sustained calcium current through activation of alpha adrenergic receptors and a GTP-binding protein in adult rat sympathetic neurons. *J. Pharmacol. Exp. Ther.* 269, 503–508.

Ariano, M. A., and Sibley, D. R. (1994). Dopamine receptor distribution in the rat CNS: elucidation using anti-peptide antisera directed against D1A and D3 subtypes. *Brain Res.* 649, 95–110. doi: 10.1016/0006-8993(94)91052-9

Aston-Jones, G. (2004). "Locus coeruleus, A5 and A7 noradrenergic cell groups," in *The Rat Nervous System*, 3rd Edn, Chap. 11, ed. G. Paxinos (San Diego, CA: Elsevier Academic Press), 259–294.

Beaulieu, J. M., and Gainetdinov, R. R. (2011). The physiology, signaling, and pharmacology of dopamine receptors. *Pharmacol. Rev.* 63, 182–217. doi: 10.1124/pr.110.002642

Berger, B., Gaspar, P., and Verney, C. (1991). Dopaminergic innervation of the cerebral cortex: unexpected differences between rodents and primates. *Trends Neurosci.* 14, 21–27. doi: 10.1016/0166-2236(91)90179-X

Bonnot, A., Guiot, E., Hepp, R., Cavellini, L., Tricoire, L., and Lambolez, B. (2014). Single-fluorophore biosensors based on conformation-sensitive GFP variants. *FASEB J.* 28, 1375–1385. doi: 10.1096/fj.13-240507

Bylund, D. B. (1992). Subtypes of alpha 1- and alpha 2-adrenergic receptors. *FASEB J.* 6, 832–839.

Castro, L. R., Brito, M., Guiot, E., Polito, M., Korn, C. W., Hervé, D., et al. (2013). Striatal neurones have a specific ability to respond to phasic dopamine release. *J. Physiol.* 591(Pt 13), 3197–3214. doi: 10.1113/jphysiol.2013.252197

Castro, L. R., Gervasi, N., Guiot, E., Cavellini, L., Nikolaev, V. O., Paupardin-Tritsch, D., et al. (2010). Type 4 phosphodiesterase plays different integrating roles in different cellular domains in pyramidal cortical neurons. *J. Neurosci.* 30, 6143–6151. doi: 10.1523/JNEUROSCI.5851-09.2010

Chinga, G., and Syverud, K. (2007). Quantification of paper mass distributions within local picking areas. *Nordic Pulp Paper Res. J.* 22, 441–446. doi: 10.3183/NPPRJ-2007-22-04-p441-446

Ciliax, B. J., Nash, N., Heilman, C., Sunahara, R., Hartney, A., Tiberi, M., et al. (2000). Dopamine D(5) receptor immunolocalization in rat and monkey brain. *Synapse* 37, 125–145. doi: 10.1002/1098-2396(200008)37:2<125::AID-SYN7>3.0.CO;2-7

Cornil, C. A., Balthazart, J., Motte, P., Massotte, L., and Seutin, V. (2002). Dopamine activates noradrenergic receptors in the preoptic area. *J. Neurosci.* 22, 9320–9330.

Cotecchia, S. (2010). The alpha1-adrenergic receptors: diversity of signaling networks and regulation. *J. Recept. Signal Transduct. Res.* 30, 410–419. doi: 10.3109/10799893.2010.518152

Descarries, L., Lemay, B., Doucet, G., and Berger, B. (1987). Regional and laminar density of the dopamine innervation in adult rat cerebral cortex. *Neuroscience* 21, 807–824. doi: 10.1016/0306-4522(87)90038-8

Devoto, P., Flore, G., Saba, P., Fa, M., and Gessa, G. L. (2005). Stimulation of the locus coeruleus elicits noradrenaline and dopamine release in the medial prefrontal and parietal cortex. *J. Neurochem.* 92, 368–374. doi: 10.1111/j.1471-4159.2004.02866.x

Devoto, P., Flore, G., Saba, P., Castelli, M. P., Piras, A. P., Luesu, W., et al. (2008). 6-Hydroxydopamine lesion in the ventral tegmental area fails to reduce extracellular dopamine in the cerebral cortex. *J. Neurosci. Res.* 86, 1647–1658. doi: 10.1002/jnr.21611

Drobac, E., Tricoire, L., Chaffotte, A. F., Guiot, E., and Lambolez, B. (2010). Calcium imaging in single neurons from brain slices using bioluminescent reporters. *J. Neurosci. Res.* 88, 695–711. doi: 10.1002/jnr.22249

Evans, B. A., Sato, M., Sarwar, M., Hutchinson, D. S., and Summers, R. J. (2010). Ligand-directed signalling at beta-adrenoceptors. *Br. J. Pharmacol.* 159, 1022–1038. doi: 10.1111/j.1476-5381.2009.00602.x

Fuxe, K., Tarakanov, A., Romero, F. W., Ferraro, L., Tanganelli, S., Filip, M., et al. (2014). Diversity and bias through receptor-receptor interactions in GPCR heteroreceptor complexes. Focus on examples from dopamine D2 receptor heteromerization. *Front. Endocrinol. (Lausanne)* 5:71. doi: 10.3389/fendo.2014.00071

Gerfen, C. R. (2004). "Basal ganglia," in *The Rat Nervous System*, 3rd Edn, Chap. 18, ed. G. Paxinos (San Diego, CA: Elsevier Academic Press), 455–508.

Gervasi, N., Hepp, R., Tricoire, L., Zhang, J., Lambolez, B., Paupardin-Tritsch, D., et al. (2007). Dynamics of protein kinase a signaling at the membrane, in the cytosol, and in the nucleus of neurons in mouse brain slices. *J. Neurosci.* 27, 2744–2750. doi: 10.1523/JNEUROSCI.5352-06.2007

Gong, S., Doughty, M., Harbaugh, C. R., Cummins, A., Hatten, M. E., Heintz, N., et al. (2007). Targeting Cre recombinase to specific neuron populations with bacterial artificial chromosome constructs. *J. Neurosci.* 27, 9817–9823. doi: 10.1523/JNEUROSCI.2707-07.2007

Gonzalez, S., Moreno-Delgado, D., Moreno, E., Perez-Capote, K., Franco, R., Mallol, J., et al. (2012). Circadian-related heteromerization of adrenergic and dopamine D_4 receptors modulates melatonin synthesis and release in the pineal gland. *PLoS Biol.* 10:e1001347. doi: 10.1371/journal.pbio.1001347

Hu, E., Demmou, L., Cauli, B., Gallopin, T., Geoffroy, H., Harris-Warrick, R. M., et al. (2011). VIP, CRF, and PACAP act at distinct receptors to elicit different cAMP/PKA dynamics in the neocortex. *Cereb. Cortex* 21, 708–718. doi: 10.1093/cercor/bhq143

Khan, Z. U., Gutierrez, A., Martin, R., Penafiel, A., Rivera, A., and De La, C. A. (1998). Differential regional and cellular distribution of dopamine D2-like receptors: an immunocytochemical study of subtype-specific antibodies in rat and human brain. *J. Comp. Neurol.* 402, 353–371. doi: 10.1002/(SICI)1096-9861(19981221)402:3<353::AID-CNE5>3.0.CO;2-4

Latsari, M., Dori, I., Antonopoulos, J., Chiotelli, M., and Dinopoulos, A. (2002). Noradrenergic innervation of the developing and mature visual and motor cortex of the rat brain: a light and electron microscopic immunocytochemical analysis. *J. Comp. Neurol.* 445, 145–158. doi: 10.1002/cne.10156

Lemberger, T., Parlato, R., Dassesse, D., Westphal, M., Casanova, E., Turiault, M., et al. (2007). Expression of Cre recombinase in dopaminoceptive neurons. *BMC Neurosci.* 8:4. doi: 10.1186/1471-2202-8-4

Luedtke, R. R., Griffin, S. A., Conroy, S. S., Jin, X., Pinto, A., and Sesack, S. R. (1999). Immunoblot and immunohistochemical comparison of murine monoclonal antibodies specific for the rat D1a and D1b dopamine receptor subtypes. *J. Neuroimmunol.* 101, 170–187. doi: 10.1016/S0165-5728(99)00142-3

Morrison, J. H., Grzanna, R., Molliver, M. E., and Coyle, J. T. (1978). The distribution and orientation of noradrenergic fibers in neocortex of the rat: an immunofluorescence study. *J. Comp. Neurol.* 181, 17–39. doi: 10.1002/cne.901810103

Morrison, J. H., Molliver, M. E., and Grzanna, R. (1979). Noradrenergic innervation of cerebral cortex: widespread effects of local cortical lesions. *Science* 205, 313–316. doi: 10.1126/science.451605

Nicholas, A. P., Hokfelt, T., and Pieribone, V. A. (1996). The distribution and significance of CNS adrenoceptors examined with in situ hybridization. *Trends Pharmacol. Sci.* 17, 245–255. doi: 10.1016/0165-6147(96)10022-5

Oda, S., Funato, H., Adachi-Akahane, S., Ito, M., Okada, A., Igarashi, H., et al. (2010). Dopamine D5 receptor immunoreactivity is differentially distributed in GABAergic interneurons and pyramidal cells in the rat medial prefrontal cortex. *Brain Res.* 1329, 89–102. doi: 10.1016/j.brainres.2010.03.011

Papay, R., Gaivin, R., Jha, A., McCune, D. F., McGrath, J. C., Rodrigo, M. C., et al. (2006). Localization of the mouse alpha1A-adrenergic receptor (AR) in the brain: alpha1AAR is expressed in neurons, GABAergic interneurons, and NG2 oligodendrocyte progenitors. *J. Comp. Neurol.* 497, 209–222. doi: 10.1002/cne.20992

Paschalis, A., Churchill, L., Marina, N., Kasymov, V., Gourine, A., and Ackland, G. (2009). Beta1-adrenoceptor distribution in the rat brain: an immunohistochemical study. *Neurosci. Lett.* 458, 84–88. doi: 10.1016/j.neulet.2009.04.023

Rebois, R. V., Maki, K., Meeks, J. A., Fishman, P. H., Hebert, T. E., and Northup, J. K. (2012). D2-like dopamine and beta-adrenergic receptors form a signaling complex that integrates Gs- and Gi-mediated regulation of adenylyl cyclase. *Cell. Signal.* 24, 2051–2060. doi: 10.1016/j.cellsig.2012.06.011

Rey, E., Hernandez-Diaz, F. J., Abreu, P., Alonso, R., and Tabares, L. (2001). Dopamine induces intracellular Ca^{2+} signals mediated by alpha1B-adrenoceptors in rat pineal cells. *Eur. J. Pharmacol.* 430, 9–17. doi: 10.1016/S0014-2999(01)01250-X

Rivera, A., Penafiel, A., Megias, M., Agnati, L. F., Lopez-Tellez, J. F., Gago, B., et al. (2008). Cellular localization and distribution of dopamine D(4) receptors in the rat cerebral cortex and their relationship with the cortical dopaminergic and noradrenergic nerve terminal networks. *Neuroscience* 155, 997–1010. doi: 10.1016/j.neuroscience.2008.05.060

Smith, C. C., and Greene, R. W. (2012). CNS dopamine transmission mediated by noradrenergic innervation. *J. Neurosci.* 32, 6072–6080. doi: 10.1523/JNEUROSCI.6486-11.2012

Thevenaz, P., Ruttimann, U. E., and Unser, M. (1998). A pyramid approach to subpixel registration based on intensity. *IEEE Trans. Image Process* 7, 27–41. doi: 10.1109/83.650848

Turiault, M., Parnaudeau, S., Milet, A., Parlato, R., Rouzeau, J. D., Lazar, M., et al. (2007). Analysis of dopamine transporter gene expression pattern – generation of DAT-iCre transgenic mice. *FEBS J.* 274, 3568–3577. doi: 10.1111/j.1742-4658.2007.05886.x

Venkatesan, C., Song, X. Z., Go, C. G., Kurose, H., and Aoki, C. (1996). Cellular and subcellular distribution of alpha 2A-adrenergic receptors in the visual cortex of neonatal and adult rats. *J. Comp. Neurol.* 365, 79–95. doi: 10.1002/(SICI)1096-9861(19960129)365:1<79::AID-CNE7>3.0.CO;2-G

Zhang, Z. W., Burke, M. W., Calakos, N., Beaulieu, J. M., and Vaucher, E. (2010). Confocal analysis of cholinergic and dopaminergic inputs onto pyramidal cells in the prefrontal cortex of rodents. *Front. Neuroanat.* 4:21. doi: 10.3389/fnana.2010.00021

Conflict of Interest Statement: The authors declare that the research was conducted in the absence of any commercial or financial relationships that could be construed as a potential conflict of interest.

Received: 19 June 2014; paper pending published: 15 July 2014; accepted: 05 August 2014; published online: 21 August 2014.

Citation: Nomura S, Bouhadana M, Morel C, Faure P, Cauli B, Lambolez B and Hepp R (2014) Noradrenalin and dopamine receptors both control cAMP-PKA signaling throughout the cerebral cortex. Front. Cell. Neurosci. ***8****:247. doi: 10.3389/fncel.2014.00247*

This article was submitted to the journal Frontiers in Cellular Neuroscience.

frontiers in
CELLULAR NEUROSCIENCE

ORIGINAL RESEARCH ARTICLE
published: 18 November 2013
doi: 10.3389/fncel.2013.00211

The NO/cGMP pathway inhibits transient cAMP signals through the activation of PDE2 in striatal neurons

***Marina Polito*[1,2], *Jeffrey Klarenbeek*[3], *Kees Jalink*[3], *Danièle Paupardin-Tritsch*[1,2], *Pierre Vincent*[1,2]*† *and Liliana R.V. Castro*[1,2†]**

[1] *UMR7102, Centre National de la Recherche Scientifique, Paris, France*
[2] *UMR7102, Neurobiology of Adaptive Processes, Université Pierre et Marie Curie, Paris, France*
[3] *Cellbiophysics Group, The Netherlands Cancer Institute, Amsterdam, Netherlands*

Edited by:
Arianna Maffei, SUNY Stony Brook, USA

Reviewed by:
John Garthwaite, University College London, UK
Gang Wang, Weill Cornell Medical College, USA

***Correspondence:**
Pierre Vincent, Centre National de la Recherche Scientifique, UMR7102, 9 quai St Bernard F-75005, Paris, France
e-mail: pierre.vincent@upmc.fr
† These authors have contributed equally to this work.

The NO-cGMP signaling plays an important role in the regulation of striatal function although the mechanisms of action of cGMP specifically in medium spiny neurons (MSNs) remain unclear. Using genetically encoded fluorescent biosensors, including a novel Epac-based sensor (EPAC-S^{H150}) with increased sensitivity for cAMP, we analyze the cGMP response to NO and whether it affected cAMP/PKA signaling in MSNs. The Cygnet2 sensor for cGMP reported large responses to NO donors in both striatonigral and striatopallidal MSNs, this cGMP signal was controlled partially by PDE2. At the level of cAMP brief forskolin stimulations produced transient cAMP signals which differed between D_1 and D_2 MSNs. NO inhibited these cAMP transients through cGMP-dependent PDE2 activation, an effect that was translated and magnified downstream of cAMP, at the level of PKA. PDE2 thus appears as a critical effector of NO which modulates the post-synaptic response of MSNs to dopaminergic transmission.

Keywords: cyclic AMP, cyclic GMP, phosphodiesterase, biosensor imaging, nitric oxide, striatum, dopamine

INTRODUCTION

Cyclic nucleotides control a range of cellular processes, particularly in neurons where they transduce extracellular signals carried by neuromodulators. The striatum is involved in reward, motor control and action selection, and cyclic nucleotide signaling plays a critical role in the normal function of this brain structure. While the involvement of cAMP in striatal physiology is widely acknowledged, much less is known on cGMP, although this signaling cascade also plays a critical role in the regulation of striatal function (West and Tseng, 2011). Medium spiny neurons (MSNs) in the striatum constitute 95% of the neuronal types, approximately half of which are anatomically defined as the "direct pathway" and express dopamine type 1 receptors (D_1). This receptor is positively coupled to cAMP production. The other half of MSNs, defined as the "indirect pathway," express high levels of dopamine type 2 receptors (D_2) and adenosine A_{2A} receptors (Le Moine and Bloch, 1995; Bateup et al., 2008; Bertran-Gonzalez et al., 2008). D_2 receptors are negatively coupled to adenylyl cyclases (AC) and therefore inhibit cAMP production while the A_{2A} receptors are positively coupled to AC and increase cAMP levels. The segregation between D_1 and A_{2A} expressing neurons is clearly visualized using cAMP/PKA biosensors (Castro et al., 2013). The functional effects of the cAMP signaling cascade has been widely documented in the striatum (Hervé and Girault, 2005) but much less is know about the cGMP signaling. cGMP is produced by the NO receptor, aka soluble guanylyl cyclase (sGC), in response to nitric oxide (NO), and NO/cGMP signaling regulates a number of neurobiological processes (Garthwaite, 2008). sGC is highly expressed in the striatum (Ariano et al., 1982; Matsuoka et al., 1992; Ding et al., 2004) while the NO producing enzyme nNOS is highly expressed by a fraction of striatal interneurons (Vincent and Kimura, 1992; Rushlow et al., 1995; Kawaguchi, 1997; Vincent, 2000). It is commonly accepted that NO produced by NOS interneurons diffuses throughout the striatal complex and increases corticostriatal and dopaminergic synaptic transmission via a sGC-cGMP dependent mechanism (West et al., 2002; West and Grace, 2004; West and Tseng, 2011). In addition, NO diffuses into the dendrites of MSNs modulating corticostriatal synaptic plasticity *in vitro* (Calabresi et al., 1999, 2000) and *in vivo* (West and Grace, 2004). While these effects are clearly mediated by cGMP, the downstream effectors of cGMP, often assumed to be the cGMP-dependent protein kinase (PKG), remain uncertain, since only moderate levels of expression have been reported in the striatum (el-Husseini et al., 1995; El-Husseini et al., 1999; de Vente et al., 2001) and CNG expression has not been reported in the striatum (Wei et al., 1998).

An important part of the signal transduction process is the rapid degradation of the cyclic nucleotides by cyclic nucleotide phosphodiesterases (PDEs). PDE2 mRNA and protein are present at high levels in the striatum (Repaske et al., 1993; Van Staveren et al., 2003) and functionally active (Wykes et al., 2002; Lin et al., 2010). PDE2 has dual enzymatic activity allowing to hydrolyze both cAMP and cGMP (Erneux et al., 1981; Martins et al., 1982). A characteristic feature of PDE2 is the positive cooperativity of the substrate cGMP: in the absence of cGMP, PDE2 activity is low, and the binding of sub-micromolar cGMP to the regulatory GAF-B domain of the amino-terminus of PDE2 results in a 5-fold increase in cAMP hydrolysis rate (Martins et al., 1982; Martinez et al., 2002). The interplay between cAMP and cGMP signals through PDE2 has been well characterized

mainly in the cardiovascular system (Maurice, 2005; Nikolaev et al., 2005), where cGMP-mediated regulation of cAMP occurs in a spatially confined cellular compartment and depends on the source of cGMP (Castro et al., 2006; Stangherlin et al., 2011). Regulation of cyclic nucleotides by PDE2 has already been shown in thalamic (Hepp et al., 2007) and striatal neurons (Lin et al., 2010), although in the striatum the role of PDE2 at the cellular level remained to be analyzed. Here, we improved the $^{T}Epac^{VV}$ cAMP sensor (Klarenbeek et al., 2011) which allowed us to analyze the dynamics of cAMP regulation in striatal neurons and to determine the functional effect of cGMP on this signal.

Our data reveal that NO/cGMP signaling reduces the cAMP signals in both striatonigral and striatopallidal MSNs through the activation of PDE2. This inhibitory effect propagates downstream to PKA, leading to an inhibition of the PKA response to D_1 stimulation. In addition, we found that the dynamics of the cAMP responses are not identical in MSNs, with striatopallidal neurons displaying larger and longer lasting cAMP transients than striatonigral MSNs.

MATERIALS AND METHODS

BIOSENSOR CONSTRUCT AND VALIDATION

From the starting material TEpacVV (Klarenbeek et al., 2011), numbered Epac-SH74 in our database, we first exchanged mTurquoise for mTurqouise2 using the same protocol as in Klarenbeek et al., creating Epac-SH126. Second the Q270E mutation was introduced by cutting the Epac-SH126 with PshAI en BstEII inserting annealed oligo's forward primer: GTGACCCA TGGCAAGGGGCTGGTGACCACCCTGCATGAGGGAGATGAT TTTGGAGAGCTGGCTCTGGTCAATGATGCACCCCGGGCAG CCACCATCATCCTGCGAGAAGACAA and reverse primer: TTGTCTTCTCGCAGGATGATGGTGGCTGCCCGGGGTGCAT CATTGACCAGAGCCAGCTCTCCAAAATCATCTCCCTCATGC AGGGTGGTCACCAGCCCCTTGCCATGG, yielding Epac-SH134. Third the acceptor was inserted as a PCR-product of cp174Citrine using forward primer: GGGGCTAGCGAGCTCAT GGACGGCGGCGTGCA and reverse primer: CGAATTCGG CTCGATGTTGTGGCGGAT digested with NheI and EcoRI, yielding Epac-SH150. All constructs were checked by sequence analysis. Hek293 embryonal kidney cells (American Type Culture Collection crl-1573) were cultured in DMEM supplemented with 10% FCS and antibiotics. Cells were seeded in six 15 cm^2 plates and transfected with 10 μg DNA per plate using calcium phosphate or fugene transfection agent. After overnight expression, cells were resuspended in 1 ml hypotonic buffer (PBS: H_2O 1: 2) and homogenized with a Downs piston. The homogenate was centrifuged for 10 min at 4°. The supernatant was corrected toward isotonic conditions using a concentrated stock of PBS. The supernatant was diluted 10 times in buffer containing (in mM) 150 KCl, 5 NaCl, 1 $MgCl_2$ 10 HEPES pH 7.2, with a total volume of 2 ml in a stirred cuvette of a PTI Quantamaster dual channel spectrofluorimeter (Lawrenceville, NJ). Small volumes of cAMP from concentrated stocks were added repeatedly to titrate in cAMP, total added volume 40 μl. The response to cAMP was quantified as the ratio between YFP (530 $\pm$ 10 nm) and CFP (490 $\pm$ 10 nm), when excited with 420 $\pm$ 3 nm.

BRAIN SLICE PREPARATION

Wild-type C57Bl/6J mice were obtained from Janvier (Le Genest Saint Isle, France). Mice were maintained in a 12 h light–12 h dark cycle, in stable conditions of temperature (22°C), with food and water available *ad libitum*. All the experiments were performed according to French Ministry of Agriculture and Forestry guidelines for handling animals (87–848°).

Brain slices were prepared from male mice aged from 9 to 13 days, as previously described (Castro et al., 2013). Coronal brain slices of 300 μm thickness were cut with a VT1200S microtome (Leica, Germany). Slices were prepared in an ice-cold solution of the following composition: 125 mM NaCl, 0.4 mM $CaCl_2$, 1 mM $MgCl_2$, 1.25 mM NaH_2PO_4, 26 mM $NaHCO_3$, 25 mM glucose and 1 mM kynurenic acid, saturated with 5% CO_2 and 95% O_2. The slices were incubated in this solution for 30 min and then placed on a Millicell-CM membrane (Millipore) in culture medium (50% Minimum Essential Medium, 50% Hanks' Balanced Salt Solution, 6.5 g/l glucose, penicillin-streptomycin, Invitrogen). We used the Sindbis virus as a vector to induce expression of the various probes (Ehrengruber et al., 1999).

The sindbis viral vector for AKAR3 and Cygnet2 was prepared as as previously described (Gervasi et al., 2007; Hepp et al., 2007). Similarly, the Epac-S^{H150} digested with HindIII was inserted into pSinRep5 (Invitrogen, San Diego, CA) digested with StuI and made blunt by Klenow and HpaI.

Compared to our previous work (Castro et al., 2013), the viral vector was diluted to decrease the number of infected neurons and thus facilitate individual cell measurement. Slices were incubated overnight at 35°C under an atmosphere containing 5% CO_2. Before the experiment, slices were incubated for 30 min in the recording solution (identical to the solution used for cutting, except that the calcium concentration was 2 mM and kynurenic acid was omitted). During recordings, brain slices were continuously perfused with this solution saturated with 5% CO_2/95% O_2, at a rate of 2 ml/min, in a recording chamber of ~1 ml volume maintained at 32°C. The viability of the neurons in these experimental conditions have been checked by patch-clamp recording, which showed electrical activity to be normal (Gervasi et al., 2007; Castro et al., 2010).

OPTICAL RECORDINGS ON BRAIN SLICES

Recordings were made on MSNs, that constitute 95% of neurons in the striatum. Large neurons, presumably cholinergic interneurones, were excluded (i.e., diameter larger than 14 μm). Wide-field images were obtained with an Olympus BX50WI or BX51WI upright microscope with a 20×0.5 NA or a 40 × 0.8 NA water-immersion objective and an ORCA-AG camera (Hamamatsu). Images were acquired with iVision (Biovision, Exton, PA, USA). The excitation and dichroic filters were D436/20 and 455dcxt. Signals were acquired by alternating the emission filters, HQ480/40 for CFP, and D535/40 for YFP, with a filter wheel (Sutter Instruments, Novato, CA, USA). All filters were obtained from Chroma Technology (Brattleboro, VT, USA). Image acquisition was triggered manually, except for kinetics measurement where images were acquired automatically with 3–5 s intervals.

Images were analyzed with custom routines written in the IGOR Pro environment (Wavemetrics, Lake Oswego, OR, USA).

The emission ratio was calculated for each pixel: F535/F480 for AKAR3 and F480/F535 for Epac-S^{H150}. Pseudocolor images display the ratio value coded in hue and the fluorescence intensity coded in intensity. A calibration square indicates the intensity values from left to right and the ratio values from bottom to top. The size of the square indicates the scale of the image in microns. No correction for bleed-through or direct excitation of the acceptor was applied and the ratio changes in our conditions therefore appear smaller than those reported by other studies in which such corrections were applied.

FAST DRUG APPLICATION

A fast focal application system was previously used for kinetic studies (Gervasi et al., 2007; Castro et al., 2013). A glass pipette (100–150 μm tip diameter) was placed 300 μm to the side of and 200 μm above the brain slice and ejected the drug contained in the same solution as the bath. Dopamine uncaging was performed with UV light at 360 nm applied in wide-field mode (UVILED, Rapp OptoElectronic, Hamburg, Germany). Image acquisition in these fast wide-field recordings was automatic at a frequency ranging from 0.2 to 0.3 Hz. Image acquisition was otherwise triggered manually by the user.

DATA ANALYSIS AND STATISTICS

Ratiometric quantification was performed with a ratio value between the Rmin and Rmax values, which correspond to the minimal ratio value (no biological signal) and maximal response (saturated biosensor) (Grynkiewicz et al., 1985; Börner et al., 2011). The baseline ratio in control conditions was considered to be equal to Rmin because adenylyl cyclase inhibition with 50 μM SQ22536 and guanylyl cyclase inhibition with 10 μM ODQ yielded no ratio decrease with Cygnet2 biosensor. The maximal response (Rmax, corresponding to biosensor saturation) was determined for each neuron at the end of the recording. This level was determined by applying 13 μM forskolin (for cAMP) or SNAP (for cGMP) in the presence of the broad-spectrum phosphodiesterase inhibitor IBMX (200 μM). Absolute ratio values differed between cells [as shown with the mutant biosensor in Castro et al. (2013)], so the amplitude of the response to receptor stimulation was quantified for each neuron as the fractional change in ratio from its own baseline (Rmin) and maximal final ratio response (Rmax).

Measurements were performed on regions of interest and some of the signal measured on a region of interest comes from out-of-focus neurons. Regions of interest which displayed clear responses to both SKF38393 and CGS21680 and which therefore contained fluorescence signal from out of focus cells were discarded from our analysis.

Kinetic parameters (amplitude, t_{max} and $t_{1/2off}$) were determined using IGOR Pro environment (Wavemetrics, Lake Oswego, OR, USA). t_{max} values were determined as the time to reach the peak of the response and the $t_{1/2off}$ represents the time to reach a half of the recovery of the response.

We analyzed at least four neurons per brain slice, with n indicating the number of independent neurons tested. Unpaired two-tailed student's *t*-tests were used for statistical comparisons. Differences were considered significant when $P < 0.001$.

DRUGS

SKF38393 hydrobromide, CGS21680 hydrochloride, 3-isobutyl-1-methylxanthine (IBMX), rolipram, NPEC-caged dopamine [(N)-1-(2-nitrophenyl) ethylcarboxy-3, 4-dihydroxyphenethyl amine], and forskolin were obtained from Tocris Cookson (Bristol, UK); 1H-[1,2,4]oxadiazolo[4,3-a]quinoxalin-1-one (ODQ), S-nitroso-N-acetyl-D,L-penicillamine (SNAP), diethylamine NO (DEANO), erythro-9-(2-hydroxy-3-nonyl)-adenine (EHNA), BAY-60–7550 were obtained from Sigma-Aldrich (St Quentin Fallavier, France); BAY60–7550 was obtained from Cayman (Teaduspargi, Estonia).

RESULTS

NO ACTIVATES THE sGC/cGMP SIGNALING CASCADE IN MSNs

We used the cGMP sensor Cygnet2 (Honda et al., 2001) to determine whether NO donors increase cGMP concentration in MSNs. The NO donor S-nitroso-N-acetyl-D,L-penicillamine (SNAP, 100 μM) induced a large increase in the F480/F535 emission ratio of all the cygnet-expressing MSNs (**Figure 1A**). This signal reversed with the washout of the drug and a second cGMP response could be elicited from the same cells, showing that the NO-cGMP signaling pathway can be activated repeatedly over the time-course of our recordings.

The steady-state cGMP level upon sGC stimulation depends on the relative activities of sGC and cGMP degradation mediated by PDEs. In the presence of the NO donor, the non-specific PDE inhibitor IBMX (200 μM) increased the ratio to a higher steady-state level, showing that PDE activities determine the steady-state cGMP level reached upon NO-mediated sGC stimulation. SNAP alone increased the emission ratio to 67 ± 8% ($n = 332$) of this maximal response. Similar responses (71 ± 20%; $n = 145$) were obtained with the NO donor diethylamine NO (DEANO, 100 μM). As expected, sGC inhibition by ODQ (10 μM) prevented the response to SNAP and SNAP plus IBMX (**Figure 1B**).

Previous studies performed with dissociated striatal neurons demonstrated that PDE2 regulates the cGMP responses to NO donors (Wykes et al., 2002; Lin et al., 2010). We tested the effect of PDE2 inhibition in our brain slice preparation and in all tested MSNs, the application of the PDE2 inhibitor EHNA (10 μM), added on top of the SNAP response, induced a further increase of the cGMP signal, rising from 67 ± 8% ($n = 332$) to 90 ± 5% ($n = 151$) of the maximal response obtained in the presence of IBMX (**Figures 1C,D**). Like IBMX, EHNA alone had no effect on basal cGMP levels.

These results confirm that PDE2 is critical in the regulation of the cGMP signals in MSNs of the dorsal striatum upon sGC stimulation.

A NEW BIOSENSOR TO MEASURE cAMP SIGNALS IN THE STRIATUM

Since cGMP increases PDE2 activity which also hydrolyzes cAMP, we wanted to precisely monitor whether PDE2 controlled cAMP levels in striatopallidal and striatonigral MSN. The recently published $^{T}Epac^{VV}$ (Epac-S^{H126}) exhibits one of the largest ratio changes known to date for a genetically-encoded biosensors (Klarenbeek et al., 2011) but we considered that its relatively low sensitivity for cAMP may be limiting. We have prepared a

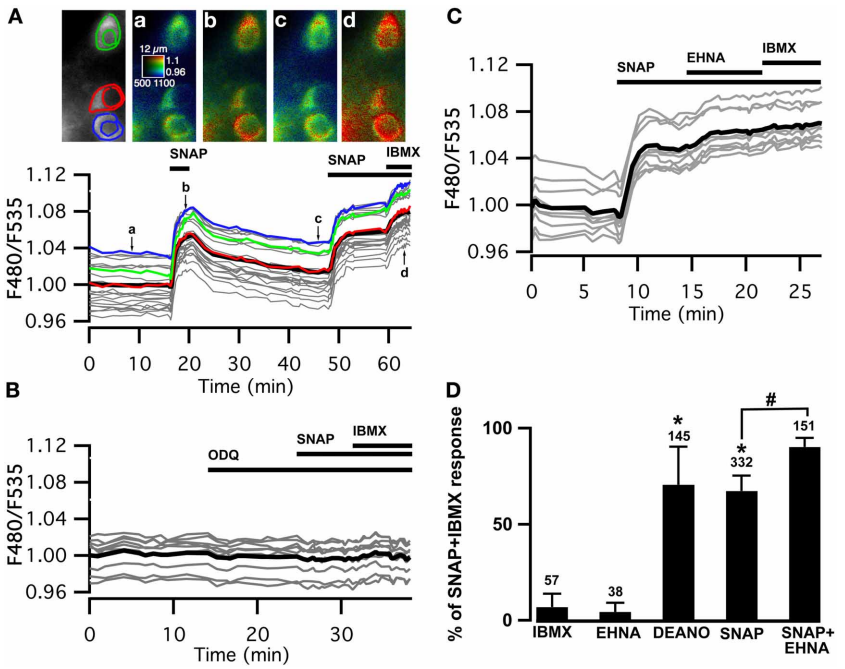

FIGURE 1 | Cygnet reports increases in cyclic GMP concentration in all medium spiny neurons of the striatum in response to soluble guanylyl cyclase activation. (A–C) Striatal neurons in a mouse brain slice expressing Cygnet2 sensor and imaged by wide-field microscopy. **(A)** Images show the raw fluorescence at 535 nm (left in gray scale) and the ratio (in pseudocolor), indicating the ratiometric change of Cygnet2 reporting the binding of cGMP, at the times indicated by the corresponding arrows on the graph below. Each trace on the graph indicates the F480/F535 emission ratio measurement on regions indicated by the color contour drawn on the raw image; the thick black line represents the average of all the traces. The NO donor SNAP (100 µM) induced a strong increase in the ratio in all MSNs visible in the field. SNAP + IBMX (200 µM) induced a maximal increase in the ratio response. **(B)** The responses to SNAP and SNAP + IBMX were completely blocked by the soluble guanylyl cyclase blocker ODQ (10 µM). **(C)** After the activation of sGC with SNAP, the PDE2 inhibitor EHNA (10 µM) increased the cGMP signal to a level that corresponded to the maximal response. **(D)** The amplitude measured with the Cygnet2 biosensor was normalized with respect to the maximal SNAP + IBMX response and plotted as a histogram. Error bars indicate s.e.m.; the numbers of tested neurons are indicated above each bar. Unpaired two-tailed *t*-tests were carried out for comparisons with control conditions (*) and with SNAP alone (#), and differences were considered significant when $P < 0.05$.

series of new Epac-based cAMP biosensors in which the donor was replaced by mTurquoise2, which has a higher quantum yield, longer lifetime and is more photo stable than mTurquoise (Goedhart et al., 2012). The Q270E mutation (Dao et al., 2006) was introduced in the cAMP binding site of the cAMP-binding domain of Epac1 to increase its affinity for cAMP. This sensor, called Epac-S^{H134} showed increased sensitivity to cAMP as compared to the previous version (EC_{50} was 4.4 ± 0.3 vs. 10.7 ± 0.8 µM, $n = 5$, $p < 0.01$, two-tailed paired *t*-test; **Figure 2A**). This sensor was further improved by replacing the acceptor cpVenus-Venus with a single circular permutation of Citrine (cp174Citrine), chosen for optimal resistance to pH changes and brightness. This sensor called Epac-S^{H150} showed a large change in emission spectrum upon cAMP binding (**Figure 2B**) and proved suitable to directly address the dynamics of cAMP in MSNs in the striatum (**Figure 2C**). A detailed characterization of this and other new cAMP sensors will be published elsewhere.

As shown previously with PKA and cAMP biosensors with two-photon microscopy (Castro et al., 2013), activation of the D_1 receptors with a saturating (1 µM) dose of SKF38393 strongly increased the F480/F535 emission ratio in one population of MSNs called hereafter D_1 neurons. In addition, the activation of the A_{2A} receptors with a saturating (1 µM) dose of CGS21680 increased the emission ratio in the remaining neuronal population, the D_2 neurons (**Figure 2C**). With low viral infection levels, wide-field imaging thus allowed a sufficient cell separation to distinguish between the D_1 and D_2 neurons. The D_1 response decreased with prolonged exposure to the agonist, probably a consequence of D_1 receptor desensitization. In contrast, the response to CGS21680 reached a stable steady-state level. Both responses were not maximal, as the addition of the adenylyl cyclase activator forskolin (FSK, 13 µM) further increased the ratio response, consistent with the wide cAMP sensitivity range of this new biosensor. Addition of 200 µM IBMX to forskolin produced a small additional response, considered as the maximal ratio response R_{max} (see methods). On average, SKF38393, CGS21680, and FSK increased the emission ration to 51 ± 2 % ($n = 32$), 27 ± 1 % ($n = 29$) and 95 ± 1% ($n = 48$) of the maximal response to forskolin and IBMX (**Figure 2D**).

BRIEF ADENYLYL CYCLASE ACTIVATION IN D_1 AND D_2 NEURONS

This imaging method thus allowed us to analyze the cAMP signal in identified D_1 or D_2 MSNs and we set up a protocol for transient adenylyl cyclase stimulation to analyze the onset, which mostly reflect cAMP synthesis, and the decay, which is mostly

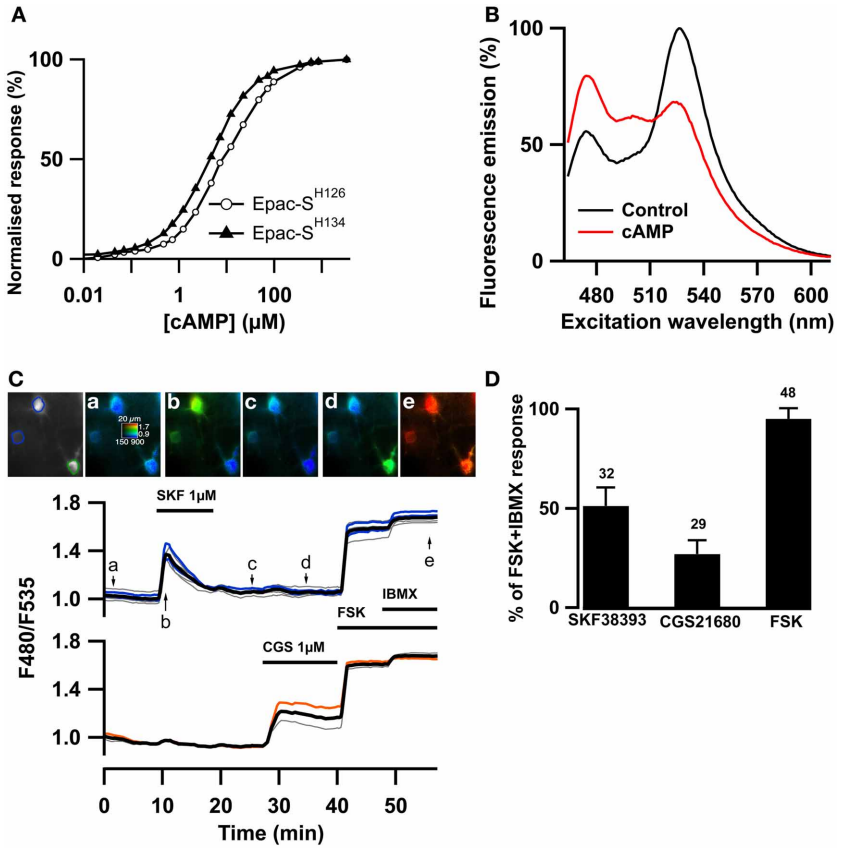

FIGURE 2 | The Epac-S^{H150} sensor reported large cAMP signals in D_1 and D_2 MSNs. The ^{T}Epac^{VV} sensor (labeled Epac-S^{H126}) was mutated to increase its sensitivity for cAMP, yielding Epac-S^{H134}; representative dose-response curves for both sensors are presented in **(A)**. The acceptor was then changed for a cp174Citrine, yielding Epac-S^{H150}. The emission spectrum of Epac-S^{H150} in the absence and in the presence of saturating (100 µM) cAMP is presented in **(B)**. **(C)** Medium spiny neurons (MSNs) in a mouse brain slice were transfected for expression of Epac-S^{H150} and imaged with wide field microscopy. Images show the raw fluorescence at 535 nm (left, in gray scale) and the ratio (in pseudocolor) indicating the ratiometric change of Epac-S^{H150} reporting the binding of cAMP, at the times indicated by the arrows on the graph below. Each trace on the graph indicates the F480/F535 emission ratio measurement on regions indicated by the color contour drawn on the raw image; the thick black line represents the average of all the traces in the two different groups. The D_1 receptor activator, SKF38393 (1 µM), induced a transient ratio increase in neurons thereby identified as D_1 MSNs; activation of the A_{2A} receptor with CGS21680 (1 µM) induced a sustained cAMP response in neurons thereby identified as D_2 MSNs. FSK + IBMX induced a ratio increase used as 100% value in normalization. **(D)** The amplitude of the responses to SKF38393 and CGS21680 was measured with the Epac-S^{H150} biosensor, normalized with respect to the maximal FSK + IBMX response and plotted as a histogram. The cAMP response to D_1 receptor stimulation (SKF38393) was significantly stronger than the response to D_2 receptor stimulation. Error bars indicate the s.e.m.; the number of tested neurons is indicated above each bar.

governed by PDEs activities. Because the activation of D_1 or A_{2A} receptors induced cAMP signals that differed in amplitude and kinetics, we examined the responses to direct stimulation of AC by forskolin, thereby analyzing the cAMP signal independently of receptors. We used a fast focal application system to apply 10-s pulses of forskolin (FSK) while monitoring the cAMP response, and bath application of SKF38393 and CGS21680 at the end of the recording to identify D_1 and D_2 neurons (**Figure 3A**). For both D_1 and D_2 MSNs, brief forskolin stimulation resulted in a transient increase in Epac-S^{H150} signal, which could be reproduced several times with no significant change in amplitude or kinetics. These forskolin-induced cAMP transients differed between the two types of MSNs in their amplitude and decay kinetics (**Figure 3B**): D_1 MSNs generated a cAMP transient that reached 67 ± 10% of R_{max} and had a $t_{1/2off}$ of 2.5 ± 0.4 min ($n = 112$; see method for $t_{1/2off}$ definition); D_2 neurons displayed a larger cAMP signal that reached 79 ± 9% of R_{max} and lasted two times longer than the response in D_1 neurons with a $t_{1/2off}$ of 4.3 ± 0.8 min ($n = 122$); both amplitude and $t_{1/2off}$ were statistically different from D_1 (unpaired two-tailed t-test, $P < 0.0001$; see **Table 1**).

We thought that this difference might result from regulation of cAMP levels by PDEs, including PDE2. We observed that inhibition of PDE2 with EHNA increased the amplitude and prolonged the decay of the forskolin-induced cAMP transients exclusively in D_2 MSNs (**Figure 3C**). No effect was observed in D_1 MSNs, despite the expression of PDE2 in these neurons (**Figure 3D**) (Lin et al., 2010). Because PDE2 inhibition exacerbates the differences between D_1 and D_2 MSNs, we hypothesized that other PDE activities differently regulate the cAMP signals in these neurons. We

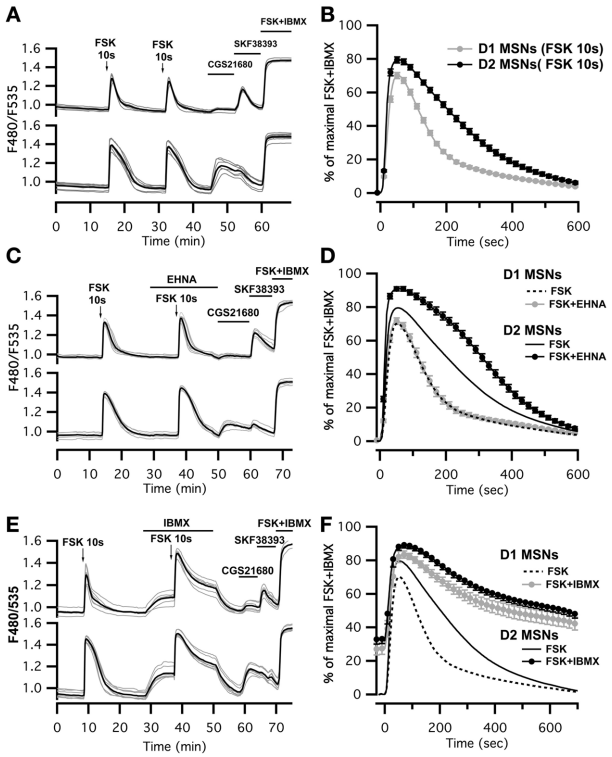

FIGURE 3 | Brief (10 s) application of FSK (13 μM) produced stronger and longer lasting cAMP responses in D_2 MSNs than in D_1 MSNs. **(A,C,E)** cAMP signals were measured in wide-field imaging with Epac-S^{H150} biosensor during the application of a 10 s pulse of FSK alone **(A)**, in the presence of EHNA **(C)** or IBMX **(E)**. Each trace on the graph indicate the Epac-S^{H150} emission ratio of an individual neuron. Traces were separated on the basis of their response to the A_{2A} agonist CGS21680 (1 μM) or D_1 agonist SKF38393 (1 μM). **(B)** Mean responses in D_1 ($n = 112$) and D_2 ($n = 122$) MSNs to brief FSK stimulation. **(D,F)** Mean responses in D_1 and D_2 to brief FSK stimulation in the presence of EHNA (10 μM) or IBMX (200 μM). Thin dashed and solid lines represent the mean responses in D_1 and D_2 MSNs to brief FSK alone, for comparison. IBMX strongly attenuated the differences between D_1 ($n = 17$) and D_2 ($n = 21$) MSNs. EHNA increased the cAMP signaling in D_2 MSNs ($n = 19$), but had no effect in D_1 cells ($n = 19$). Markers are plotted sparsely for clarity; error bars represent *SD*.

tested this hypothesis by inhibiting most of PDE activities with IBMX (**Figures 3E,F**). Application of IBMX alone increased basal cAMP levels in both type of cells [28 ± 3% ($n = 17$) for D1 MSNs and 33 ± 3% ($n = 21$) for D2 MSNs], showing that adenylyl cyclase constitutively active. When most PDEs were blocked, the cAMP transient induced with 10 s FSK was larger in amplitude and its duration was considerably prolonged. The difference in kinetics between D_1 and D_2 was almost obliterated, demonstrating that phosphodiesterase activities differ between D_1 and D_2 neurons. The slope of the 10–80% onset of the cAMP transient in the presence of IBMX was measured and showed no statistical difference between D_1 and D_2 neurons (0.020 ± 0.005, $n = 17$ for D_1 MSNs vs. 0.023 ± 0.007, $n = 20$ for D_2 MSNs, expressed in ratio units per second, $p = 0.199$). This suggests that the rate of cAMP synthesis is similar in both cell types. Further work is needed to identify the specific contribution of each PDEs in determining the shape of transient cAMP signals in D_1 and D_2 MSNs.

PDE2 ACTIVATION BY cGMP LIMITS cAMP ACCUMULATION IN BOTH D_1 AND D_2 MSNs

We then tested whether increasing PDE2 activity with cGMP affected cAMP signaling in MSNs: we compared the cAMP transients in the absence and in the presence of the NO donor SNAP (100 μM). Application of SNAP in the bath had no effect *per se* on basal cAMP signals (**Figure 4A**). However, the cAMP transient was reduced in amplitude by about 20–30% in both striatonigral and striatopallidal MSNs (**Figure 4B**; **Table 1**). The decay time-course, however, did not change significantly from the respective control (**Figure 4B**; **Table 1**).

This negative control exerted by NO was abolished when the PDE2 inhibitor EHNA (10 μM) was applied simultaneously with the NO donor SNAP (100 μM) (**Figures 4C,D**; **Table 1**). The application of EHNA alone or in the presence of SNAP had no effect on basal cAMP signal (**Figure 4C**). Since EHNA also inhibits adenosine deaminase, we also tested the specific PDE2 inhibitor BAY60-7550 at 100 nM (**Figures 4E,F**): this drug also blocked the inhibitory effect of NO donors on cAMP transients. These results show that the inhibitory crosstalk exerted by cGMP on cAMP transients is mediated by PDE2.

Table 1 | Kinetic parameters of the cAMP responses to FSK in MSNs.

	D1				D2			
	Amplitude (%)	**$t_{1/2off}$ (min)**	**t_{max} (s)**	***n***	**Amplitude (%)**	**$t_{1/2off}$ (min)**	**t_{max} (s)**	***n***
FSK	67 ± 10	2.6 ± 0.4	52 ± 10	112	79 ± 9	4.3 ± 0.8	51 ± 8	122
FSK + SNAP	41 ± 8	2.9 ± 0.6	54 ± 9	45	62 ± 7	4.0 ± 0.5	53 ± 7	48
FSK + EHNA	72 ± 8	2.5 ± 0.6	49 ± 7	19	91 ± 5	5.4 ± 0.8	55 ± 9	19
FSK + SNAP + EHNA	66 ± 9	2.6 ± 0.7	58 ± 13	46	84 ± 6	5.2 ± 1.1	54 ± 7	44
FSK + SNAP + Bay 607,550	60 ± 12	2.0 ± 0.3	46 ± 10	38	84 ± 12	5.3 ± 2.2	59 ± 9	25

cAMP signals were measure in wide-field imaging with Epac-S^{H150} biosensor during the application of a 10 s pulse of Forskoline (FSK, 13 μM) alone or in the presence of SNAP (100 μM), EHNA (10 μM), SNAP + EHNA and SNAP + Bay 607,550. The table shows the means (±SD) of the amplitudes, the t_{max} and $t_{1/2off}$ in each experimental condition. n indicate the number of tested neurons.

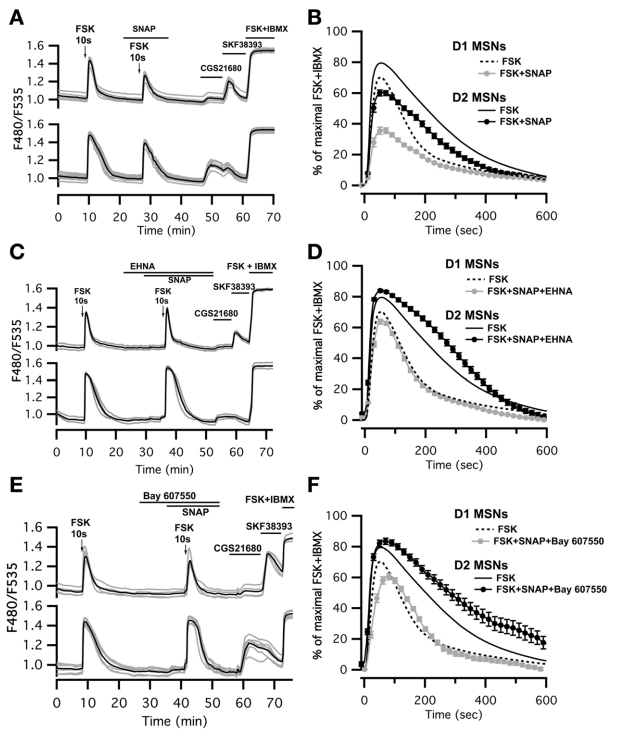

FIGURE 4 | SNAP reduces the cAMP/PKA signal in both D_1 and D_2 MSNs. cAMP signals were measure in wide-field imaging with Epac-S^{H150} biosensor during the application of a 10 s pulse of Forskolin (FSK, 13 μM). **(A)** Activation of soluble guanylyl cyclase with SNAP (100 μM) strongly reduced the amplitude of the cAMP response induced by brief (10 s) FSK application in both D_1 and D_2 MSNs. Inhibition of PDE2 with EHNA (10 μM) **(C)** or Bay 607,550 (100 nM) **(E)** abolished the effect of SNAP on the cAMP response. **(B)** Mean responses in D_1 ($n = 45$) and D_2 ($n = 48$) MSNs to brief FSK stimulation in the presence of SNAP. **(D)** Mean responses in D_1 ($n = 46$) and D_2 ($n = 44$) MSNs to brief FSK stimulation in the presence of SNAP plus EHNA; **(F)** Mean responses in D_1 ($n = 38$) and D_2 ($n = 25$) MSNs to brief FSK stimulation in the presence of SNAP plus Bay 607,550. **(B,D,F)** dashed and solid lines represent the average response to brief FSK alone in D_1 and D_2 MSNs, respectively. Markers are plotted sparsely for clarity; error bars represent *SD*.

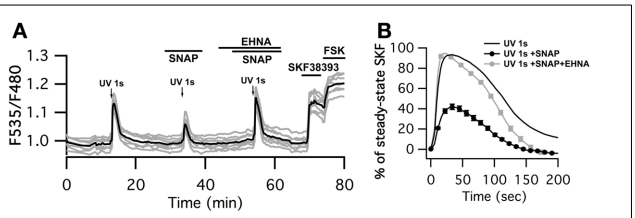

FIGURE 5 | SNAP inhibits the PKA response to brief (1 s) dopamine uncaging in D_1 MSNs. (A) MSNs expressing AKAR3 were imaged in wide-field microscopy to measure the PKA response to dopamine. Arrows indicate the UV flash. Flash photolysis of caged dopamine (NPEC-dopamine, 5 μM in the bath) induced a transient ratio increase. SNAP decreased this response, and the PDE2 inhibitor EHNA (10 μM) restored the response to caged dopamine to its initial level. **(B)** Mean responses in D_1 to 1s UV flash alone ($n = 84$), in the presence of SNAP ($n = 80$) and SNAP + EHNA ($n = 74$). For each flash, responses were normalized with respect to the steady-state response to SKF38393. Markers are plotted sparsely for clarity; error bars represent *SD*.

THE NO/cGMP/PDE2 PATHWAY LIMITS PKA ACTIVATION UPON A SUB-SECOND DOPAMINE SIGNAL

Finally, we checked whether the negative regulation exerted by cGMP on the cAMP signal was sufficient to down-regulate PKA activity. Physiological activation of D_1-like receptors is associated with phasic dopamine release related to a reward or novelty (Garris and Wightman, 1994; Gonon, 1997; Schultz and Dickinson, 2000). We mimicked phasic dopamine signals by uncaging NPEC-dopamine with a flash of UV light of 1 s duration while monitoring PKA activity with AKAR3. At the end of the experiment, bath application of SKF38393 allowed for the identification of D_1 neurons (**Figure 5A**). D_2 neurons, which did not respond to dopamine uncaging or SKF38393, were ignored. As already described (Castro et al., 2013), D_1 MSNs displayed a large and transient response to 1 s dopamine uncaging that reached 90 ± 2% $n = 84$ of the maximal steady-state response to SKF38393 response (**Figure 5B**). In the presence of the NO donor SNAP, the amplitude of the PKA signal was decreased by 45% (42 ± 3% $n = 80$). PDE2 inhibition by 10 μM EHNA reverted the inhibitory effect of SNAP (93 ± 4% $n = 74$) showing that PDE2 is indeed the mediator of this inhibitory effect.

Interestingly, the inhibitory effect of SNAP appeared larger at the level of PKA than at the level of cAMP, showing that a moderate change in cAMP dynamics is amplified at the PKA level.

DISCUSSION

Previous studies have clearly highlighted NO/cGMP as a key player in detecting and reinforcing corticostriatal glutamatergic and dopaminergic neurotransmission (Calabresi et al., 2007; West and Tseng, 2011). In this report, we highlight the importance of the post-synaptic level where NO affects the integrative properties of MSNs. Our data demonstrate the functional importance of PDE2 as a target of the NO/cGMP pathway, and its importance in the regulation of transient cAMP responses. With the high resolution provided by our improved biosensor, we also highlight significant differences between D_1 and D_2 MSNs in their response to transient AC stimulation, a difference that results from differences in phosphodiesterase activities.

PDE2 AS A MAJOR TARGET OF cGMP IN THE STRIATUM

The physiological effects of the NO/cGMP pathway largely depend on its targets which include cGMP-gated ion channels, cGMP-dependent kinase protein (PKG) and cGMP-regulated PDEs. Interestingly, brain regions such as the hippocampus and the striatum which express high levels of sGC (Matsuoka et al., 1992; Ding et al., 2004), do not express much PKG protein (el-Husseini et al., 1995; El-Husseini et al., 1999) but very high levels of PDE2 (Repaske et al., 1993; Van Staveren et al., 2003). This suggests that the major role of cGMP may be to regulate cAMP levels via PDE2 activation, rather than to directly activate PKG. This hypothesis is clearly supported by our experiments which show that one major functional effect of NO-triggered cGMP production is the activation of PDE2 which then strongly reduce the cAMP response in both D_1 and D_2 neurons.

The inhibitory effect of NO on the transient response was much more pronounced when considering the effect at the PKA level than at the cAMP level. This results appears counterintuitive as one might expect PKA to smooth-out small variations in cAMP concentration. This non-linearity in signal transduction from cAMP level to PKA level may result from positive feedback controls such as that mediated by DARPP-32: DARPP-32 was shown to prolong the PKA response once it was activated (Le Novere et al., 2008; Castro et al., 2013); in our experiments, a cAMP response that has been lowered by the NO-cGMP pathway may be insufficient to phosphorylate DARPP-32, while a larger cAMP signal may phosphorylate more DARPP-32, therefore inhibit Phosphatase 1 more efficiently and thus potentiate the net PKA effect. Such non-linear effects certainly determine the integrative properties of striatal neurons and further modeling studies are needed to understand how this parameter comes into play in the current learning theories.

DICHOTOMOUS cAMP RESPONSES IN MSNs

While the characteristic segregation of MSNs in two different cell types is notoriously difficult to study on dissociated neurons, biosensor imaging provides a measurement at the level of individual mature neurons which can be identified on the basis of their response to an agonist of either dopamine D_1 or adenosine A_{2A} receptor (Castro et al., 2013). In this study, the $^{T}Epac^{VV}$ cAMP sensor was improved to increase its affinity for cAMP and decrease it size, yielding a biosensor which proved highly efficient to monitor cAMP signals in striatal neurons. This new biosensor revealed the larger and desensitizing profile of the D_1 response which differed from the smaller and steady A_{2A} response in D_2 MSNs. These differences may be related to different regulations at the level of receptor transduction and remain to be explored in more details.

Our experiments also revealed a clear differences between these two types of MSNs that lie downstream of the receptors, which appeared when AC was transiently stimulated with forskolin: the cAMP signals were stronger and lasted longer in D2 MSNs than in D1 neurons. The AC activities do not explain the differences observed in these cells because the rate of cAMP production upon forskolin stimulation was similar in D1 and D2 MSNs as indicated by a similar onset slope. This dichotomy depends on differences in PDE activity since the broad-spectrum PDE inhibitor, IBMX, suppressed the differences between MSNs. Specific inhibition of PDE2 increased the cAMP signal exclusively in D2 neurons, despite the expression of PDE2 in both D1 and D2 neurons (Lin et al., 2010): this suggests that PDE2 is at the forefront in the degradation of cAMP in D2 neurons. Transient cAMP responses recover faster in D1 neurons than in D2 neurons, and this recovery is not affected by PDE2 inhibition suggesting that another PDE takes over PDE2 in D1 neurons. Based on these results, we consider that amplitude and decay of the cAMP signal are governed by a complex and non-linear network, which may include subcellular compartmentation, in which PDE2 appears as one critical element. Which PDE (or combination) is at the forefront in D1 neurons remains to be determined, possibly PDE1A (Polli and Kincaid, 1994) and/or PDE10A (Xie et al., 2006).

NO INCREASES cGMP LEVELS IN BOTH TYPES OF MSNs

This clear-cut segregation of MSNs into two populations with different pharmacological profiles and PDE activities that was observed for the cAMP/PKA signaling cascade was not seen at the level of cGMP with the cGMP biosensor Cygnet: sGC stimulation with NO donors produced a large and homogeneous increase in cGMP levels in all MSNs, which is consistent with the high levels of sGC present in both neuron types (Ding et al., 2004).

A tonic production of cGMP in response to the spontaneous release of NO was reported in the hippocampus, optic nerve, thalamus (Garthwaite et al., 2006; Hopper and Garthwaite, 2006; Hepp et al., 2007), as well as in the striatum (Calabresi et al., 1999; Galati et al., 2008). Our experiments in MSNs contrast with these observations as no changes in cGMP concentration was obtained upon bath application of ODQ or IBMX (**Figure 1**). However, data in the striatum were obtained in quite different experimental conditions: either the glutamatergic corticostriatal afferent fibers were repeatedly stimulated which should activate NOS interneurons (Calabresi et al., 1999), or the recordings were performed *in vivo* where a number of other parameters can directly or indirectly contribute to a tonic activation of these NO-synthesizing cells (West and Grace, 2000, 2004; Galati et al., 2008). This suggests that, *in vivo*, NOergic interneurons tonically release NO which downregulate the dopamine-induced PKA response of MSNs. Integrating this cellular mechanism into the whole animal would be of paramount importance to elucidate the clinical influence of compounds interfering with NO/cGMP pathway in disabling disorders associated with the striatum.

AUTHOR CONTRIBUTIONS

Liliana R. V. Castro and Pierre Vincent contributed equally to this work (co-last authors). Danièle Paupardin-Tritsch, Kees Jalink, Pierre Vincent, and Liliana R. V. Castro supervised the project. Liliana R. V. Castro, Marina Polito, and Jeffrey Klarenbeek performed the experiments. Liliana R. V. Castro, Marina Polito, Danièle Paupardin-Tritsch, and Pierre Vincent wrote the manuscript.

ACKNOWLEDGMENTS

This work was supported by Centre National de la Recherche Scientifique. The team of Marina Polito, Danièle Paupardin-Tritsch, Pierre Vincent, and Liliana R. V. Castro is part of the École des Neurosciences de Paris Ile-de-France and Labex BioPsy networks. We thank Regine Hepp for producing the sindbis virus. Initial characterization of novel Epac sensors was carried out during a visit of Pierre Vincent and Marina Polito to the Jalink lab in the context of the Proof-of-Concept phase of EuroBioImaging.

REFERENCES

Ariano, M. A., Lewicki, J. A., Brandwein, H. J., and Murad, F. (1982). Immunohistochemical localization of guanylate cyclase within neurons of rat brain. *Proc. Natl. Acad. Sci. U.S.A.* 79, 1316–1320. doi: 10.1073/pnas.79.4.1316

Bateup, H. S., Svenningsson, P., Kuroiwa, M., Gong, S., Nishi, A., Heintz, N., et al. (2008). Cell type-specific regulation of DARPP-32 phosphorylation by psychostimulant and antipsychotic drugs. *Nat. Neurosci.* 11, 932–939. doi: 10.1038/nn.2153

Bertran-Gonzalez, J., Bosch, C., Maroteaux, M., Matamales, M., Herve, D., Valjent, E., et al. (2008). Opposing patterns of signaling activation in dopamine D1 and D2 receptor-expressing striatal neurons in response to cocaine and haloperidol. *J. Neurosci.* 28, 5671–5685. doi: 10.1523/JNEUROSCI.1039-08.2008

Börner, S., Schwede, F., Schlipp, A., Berisha, F., Calebiro, D., Lohse, M. J., et al. (2011). FRET measurements of intracellular cAMP concentrations and cAMP analog permeability in intact cells. *Nat. Protoc.* 6, 427–438. doi: 10.1038/nprot.2010.198

Calabresi, P., Centonze, D., Gubellini, P., Marfia, G. A., Pisani, A., Sancesario, G., et al. (2000). Synaptic transmission in the striatum: from plasticity to neurodegeneration. *Prog. Neurobiol.* 61, 231–265. doi: 10.1016/S0301-0082(99)00030-1

Calabresi, P., Gubellini, P., Centonze, D., Sancesario, G., Morello, M., Giorgi, M., et al. (1999). A critical role of the nitric oxide/cGMP pathway in corticostriatal long-term depression. *J. Neurosci.* 19, 2489–2499.

Calabresi, P., Picconi, B., Tozzi, A., and Di Filippo, M. (2007). Dopamine-mediated regulation of corticostriatal synaptic plasticity. *Trends Neurosci.* 30, 211–219. doi: 10.1016/j.tins.2007.03.001

Castro, L. R., Brito, M., Guiot, E., Polito, M., Korn, C. W., Herve, D., et al. (2013). Striatal neurones have a specific ability to respond to phasic dopamine release. *J. Physiol.* 591, 3197–3214. doi: 10.1113/jphysiol.2013.252197

Castro, L. R., Gervasi, N., Guiot, E., Cavellini, L., Nikolaev, V. O., Paupardin-Tritsch, D., et al. (2010). Type 4 phosphodiesterase plays different integrating roles in different cellular domains in pyramidal cortical neurons. *J. Neurosci.* 30, 6143–6151. doi: 10.1523/JNEUROSCI.5851-09.2010

Castro, L. R., Verde, I., Cooper, D. M., and Fischmeister, R. (2006). Cyclic guanosine monophosphate compartmentation in rat cardiac myocytes. *Circulation* 113, 2221–2228. doi: 10.1161/CIRCULATIONAHA.105.599241

Dao, K. K., Teigen, K., Kopperud, R., Hodneland, E., Schwede, F., Christensen, A. E., et al. (2006). Epac1 and cAMP-dependent protein kinase holoenzyme have similar cAMP affinity, but their cAMP domains have distinct structural features and cyclic nucleotide recognition. *J. Biol. Chem.* 281, 21500–21511. doi: 10.1074/jbc.M603116200

de Vente, J., Asan, E., Gambaryan, S., Markerink-van Ittersum, M., Axer, H., Gallatz, K., et al. (2001). Localization of cGMP-dependent protein kinase type II in rat brain. *Neuroscience* 108, 27–49. doi: 10.1016/S0306-4522(01)00401-8

Ding, J. D., Burette, A., Nedvetsky, P. I., Schmidt, H. H., and Weinberg, R. J. (2004). Distribution of soluble guanylyl cyclase in the rat brain. *J. Comp. Neurol.* 472, 437–448. doi: 10.1002/cne.20054

Ehrengruber, M. U., Lundstrom, K., Schweitzer, C., Heuss, C., Schlesinger, S., and Gahwiler, B. H. (1999). Recombinant Semliki Forest virus and Sindbis virus efficiently infect neurons in hippocampal slice cultures. *Proc. Natl. Acad. Sci. U.S.A.* 96, 7041–7046. doi: 10.1073/pnas.96.12.7041

el-Husseini, A. E., Bladen, C., and Vincent, S. R. (1995). Molecular characterization of a type II cyclic GMP-dependent protein kinase expressed in the rat brain. *J. Neurochem.* 64, 2814–2817. doi: 10.1046/j.1471-4159.1995.64062814.x

El-Husseini, A. E., Williams, J., Reiner, P. B., Pelech, S., and Vincent, S. R. (1999). Localization of the cGMP-dependent protein kinases in relation to nitric oxide synthase in the brain. *J. Chem. Neuroanat.* 17, 45–55. doi: 10.1016/S0891-0618(99)00023-X

Erneux, C., Couchie, D., Dumont, J. E., Baraniak, J., Stec, W. J., Abbad, E. G., et al. (1981). Specificity of cyclic GMP activation of a multi-substrate cyclic nucleotide phosphodiesterase from rat liver. *Eur. J. Biochem.* 115, 503–510. doi: 10.1111/j.1432-1033.1981.tb0b231.x

Galati, S., D'angelo, V., Scarnati, E., Stanzione, P., Martorana, A., Procopio, T., et al. (2008). *In vivo* electrophysiology of dopamine-denervated striatum: focus on the nitric oxide/cGMP signaling pathway. *Synapse* 62, 409–420. doi: 10.1002/syn.20510

Garris, P. A., and Wightman, R. M. (1994). Different kinetics govern dopaminergic transmission in the amygdala, prefrontal cortex, and striatum: an *in vivo* voltammetric study. *J. Neurosci.* 14, 442–450.

Garthwaite, G., Bartus, K., Malcolm, D., Goodwin, D., Kollb-Sielecka, M., Dooldeniya, C., et al. (2006). Signaling from blood vessels to CNS axons through nitric oxide. *J. Neurosci.* 26, 7730–7740. doi: 10.1523/JNEUROSCI.1528-06.2006

Garthwaite, J. (2008). Concepts of neural nitric oxide-mediated transmission. *Eur. J. Neurosci.* 27, 2783–2802. doi: 10.1111/j.1460-9568.2008.06285.x

Gervasi, N., Hepp, R., Tricoire, L., Zhang, J., Lambolez, B., Paupardin-Tritsch, D., et al. (2007). Dynamics of protein kinase A signaling at the membrane, in the cytosol, and in the nucleus of neurons in mouse brain slices. *J. Neurosci.* 27, 2744–2750. doi: 10.1523/JNEUROSCI.5352-06.2007

Goedhart, J., von Stetten, D., Noirclerc-Savoye, M., Lelimousin, M., Joosen, L., Hink, M. A., et al. (2012). Structure-guided evolution of cyan fluorescent proteins towards a quantum yield of 93%. *Nat. Commun.* 3, 751. doi: 10.1038/ncomms1738

Gonon, F. (1997). Prolonged and extrasynaptic excitatory action of dopamine mediated by D1 receptors in the rat striatum *in vivo*. *J. Neurosci.* 17, 5972–5978.

Grynkiewicz, G., Poenie, M., and Tsien, R. Y. (1985). A new generation of Ca2+ indicators with greatly improved fluorescence properties. *J. Biol. Chem.* 260, 3440–3450.

Hepp, R., Tricoire, L., Hu, E., Gervasi, N., Paupardin-Tritsch, D., Lambolez, B., et al. (2007). Phosphodiesterase type 2 and the homeostasis of cyclic GMP in living thalamic neurons. *J. Neurochem.* 102, 1875–1886. doi: 10.1111/j.1471-4159.2007.04657.x

Hervé, D., and Girault, J.-A. (2005). "Chapter II Signal transduction of dopamine receptors," in *Handbook of Chemical Neuroanatomy*, Vol. 21, eds S. B. Dunnett, M. Bentivoglio, A. Björklund and T. Hökfelt, (Elsevier), 109–151. doi: 10.1016/S0924-8196(05)80006-5. Available online at: http://www.sciencedirect.com/science/article/pii/S0924819605800065

Honda, A., Adams, S. R., Sawyer, C. L., Lev-Ram, V., Tsien, R. Y., and Dostmann, W. R. G. (2001). Spatiotemporal dynamics of guanosine 3′,5′-cyclic monophosphate revealed by a genetically encoded, fluorescent indicator. *Proc. Natl. Acad. Sci. U.S.A.* 98, 2437–2442. doi: 10.1073/pnas.051631298

Hopper, R. A., and Garthwaite, J. (2006). Tonic and phasic nitric oxide signals in hippocampal long-term potentiation. *J. Neurosci.* 26, 11513–11521. doi: 10.1523/JNEUROSCI.2259-06.2006

Kawaguchi, Y. (1997). Neostriatal cell subtypes and their functional roles. *Neurosci. Res.* 27, 1–8. doi: 10.1016/S0168-0102(96)01134-0

Klarenbeek, J. B., Goedhart, J., Hink, M. A., Gadella, T. W., and Jalink, K. (2011). A mTurquoise-based cAMP sensor for both FLIM and ratiometric read-out has improved dynamic range. *PLoS ONE* 6:e19170. doi: 10.1371/journal.pone.0019170

Le Moine, C., and Bloch, B. (1995). D1 and D2 dopamine receptor gene expression in the rat striatum: sensitive cRNA probes demonstrate prominent segregation of D1 and D2 mRNAs in distinct neuronal populations of the dorsal and ventral striatum. *J. Comp. Neurol.* 355, 418–426. doi: 10.1002/cne.903550308

Le Novere, N., Li, L., and Girault, J. A. (2008). DARPP-32: molecular integration of phosphorylation potential. *Cell. Mol. Life Sci.* 65, 2125–2127. doi: 10.1007/s00018-008-8150-y

Lin, D. T., Fretier, P., Jiang, C., and Vincent, S. R. (2010). Nitric oxide signaling via cGMP-stimulated phosphodiesterase in striatal neurons. *Synapse* 64, 460–466. doi: 10.1002/syn.20750

Martinez, S. E., Wu, A. Y., Glavas, N. A., Tang, X. B., Turley, S., Hol, W. G., et al. (2002). The two GAF domains in phosphodiesterase 2A have distinct roles in dimerization and in cGMP binding. *Proc. Natl. Acad. Sci. U.S.A.* 99, 13260–13265. doi: 10.1073/pnas.192374899

Martins, T. J., Mumby, M. C., and Beavo, J. A. (1982). Purification and characterization of a cyclic GMP-stimulated cyclic nucleotide phosphodiesterase from bovine tissues. *J. Biol. Chem.* 257, 1973–1979.

Matsuoka, I., Giuili, G., Poyard, M., Stengel, D., Parma, J., Guellaen, G., et al. (1992). Localization of adenylyl and guanylyl cyclase in rat brain by *in situ* hybridization: comparison with calmodulin mRNA distribution. *J. Neurosci.* 12, 3350–3360.

Maurice, D. H. (2005). Cyclic nucleotide phosphodiesterase-mediated integration of cGMP and cAMP signaling in cells of the cardiovascular system. *Front. Biosci.* 10:1221–1228. doi: 10.2741/1614

Nikolaev, V. O., Gambaryan, S., Engelhardt, S., Walter, U., and Lohse, M. J. (2005). Real-time monitoring of the PDE2 activity of live cells: hormone-stimulated cAMP hydrolysis is faster than hormone-stimulated cAMP synthesis. *J. Biol. Chem.* 280, 1716–1719. doi: 10.1074/jbc.c400505200

Polli, J. W., and Kincaid, R. L. (1994). Expression of a calmodulin-dependent phosphodiesterase isoform (PDE1B1) correlates with brain regions having extensive dopaminergic innervation. *J. Neurosci.* 14, 1251–1261.

Repaske, D. R., Corbin, J. G., Conti, M., and Goy, M. F. (1993). A cyclic GMP-stimulated cyclic nucleotide phosphodiesterase gene is highly expressed in the limbic system of the rat brain. *Neuroscience* 56, 673–686. doi: 10.1016/0306-4522(93)90364-L

Rushlow, W., Flumerfelt, B. A., and Naus, C. C. (1995). Colocalization of somatostatin, neuropeptide Y, and NADPH-diaphorase in the caudate-putamen of the rat. *J. Comp. Neurol.* 351, 499–508. doi: 10.1002/cne.903510403

Schultz, W., and Dickinson, A. (2000). Neuronal coding of prediction errors. *Annu. Rev. Neurosci.* 23, 473–500. doi: 10.1146/annurev.neuro.23.1.473

Stangherlin, A., Gesellchen, F., Zoccarato, A., Terrin, A., Fields, L. A, Berrera, M., et al. (2011). cGMP signals modulate cAMP levels in a compartment-specific manner to regulate catecholamine-dependent signaling in cardiac myocytes. *Circ. Res.* 108, 929–939. doi: 10.1161/CIRCRESAHA.110.230698

Van Staveren, W. C., Steinbusch, H. W., Markerink-Van Ittersum, M., Repaske, D. R., Goy, M. F., Kotera, J., et al. (2003). mRNA expression patterns of the cGMP-hydrolyzing phosphodiesterases types 2, 5, and 9 during development of the rat brain. *J. Comp. Neurol.* 467, 566–580. doi: 10.1002/cne.10955

Vincent, S. R. (2000). "Chapter II Histochemistry of nitric oxide synthase in the central nervous system," in *Handbook of Chemical Neuroanatomy*, Vol. 17, eds H. W. M. Steinbusch, J. De Vente, and S. R. Vincent (Elsevier), 19–49. doi: 10.1016/S0924-8196(00)80056-1

Vincent, S. R., and Kimura, H. (1992). Histochemical mapping of nitric oxide synthase in the rat brain. *Neuroscience* 46, 755–784. doi: 10.1016/0306-4522(92)90184-4

Wei, J. Y., Roy, D. S., Leconte, L., and Barnstable, C. J. (1998). Molecular and pharmacological analysis of cyclic nucleotide-gated channel function in the central nervous system. *Prog. Neurobiol.* 56, 37–64. doi: 10.1016/S0301-0082(98)00029-X

West, A. R., Galloway, M. P., and Grace, A. A. (2002). Regulation of striatal dopamine neurotransmission by nitric oxide: effector pathways and signaling mechanisms. *Synapse* 44, 227–245. doi: 10.1002/syn.10076

West, A. R., and Grace, A. A. (2000). Striatal nitric oxide signaling regulates the neuronal activity of midbrain dopamine neurons *in vivo*. *J. Neurophysiol.* 83, 1796–1808.

West, A. R., and Grace, A. A. (2004). The nitric oxide-guanylyl cyclase signaling pathway modulates membrane activity states and electrophysiological properties of striatal medium spiny neurons recorded *in vivo*. *J. Neurosci.* 24, 1924–1935. doi: 10.1523/JNEUROSCI.4470-03.2004

West, A. R., and Tseng, K. Y. (2011). Nitric oxide-soluble guanylyl cyclase-cyclic GMP signaling in the striatum: new targets for the treatment of Parkinson's disease? *Front. Syst. Neurosci.* 5:55. doi: 10.3389/fnsys.2011.00055

Wykes, V., Bellamy, T. C., and Garthwaite, J. (2002). Kinetics of nitric oxide-cyclic GMP signalling in CNS cells and its possible regulation by cyclic GMP. *J. Neurochem.* 83, 37–47. doi: 10.1046/j.1471-4159.2002.01106.x

Xie, Z., Adamowicz, W. O., Eldred, W. D., Jakowski, A. B., Kleiman, R. J., Morton, D. G., et al. (2006). Cellular and subcellular localization of PDE10A, a striatum-enriched phosphodiesterase. *Neuroscience* 139, 597–607. doi: 10.1016/j.neuroscience.2005.12.042

Conflict of Interest Statement: The authors declare that the research was conducted in the absence of any commercial or financial relationships that could be construed as a potential conflict of interest.

Received: 23 July 2013; accepted: 25 October 2013; published online: 18 November 2013.

Citation: Polito M, Klarenbeek J, Jalink K, Paupardin-Tritsch D, Vincent P and Castro LRV (2013) The NO/cGMP pathway inhibits transient cAMP signals through the activation of PDE2 in striatal neurons. Front. Cell. Neurosci. 7:211. doi: 10.3389/fncel.2013.00211

This article was submitted to the journal Frontiers in Cellular Neuroscience.

frontiers in
CELLULAR NEUROSCIENCE

ORIGINAL RESEARCH ARTICLE
published: 06 January 2015
doi: 10.3389/fncel.2014.00426

Polarized cellular patterns of endocannabinoid production and detection shape cannabinoid signaling in neurons

Delphine Ladarre[1,2], Alexandre B. Roland[1,2†], Stefan Biedzinski[1,2], Ana Ricobaraza[1,2] and Zsolt Lenkei[1,2]*

[1] *Brain Plasticity Unit, ESPCI-ParisTech, Paris, France*
[2] *Centre National de la Recherche Scientifique UMR 8249, Paris, France*

Edited by:
Pierre Vincent, Centre National de la Recherche Scientifique, France

Reviewed by:
Thomas Launey, RIKEN, Japan
Xiang Yu, The Chinese Academy of Sciences, China

***Correspondence:**
Zsolt Lenkei, Brain Plasticity Unit, ESPCI-ParisTech, 10, rue Vauquelin, 75005 Paris, France
e-mail: zsolt.lenkei@espci.fr

†Present address:
Alexandre B. Roland, FAS Center for Systems Biology, Harvard University, Cambridge, MA, USA

Neurons display important differences in plasma membrane composition between somatodendritic and axonal compartments, potentially leading to currently unexplored consequences in G-protein-coupled-receptor signaling. Here, by using highly-resolved biosensor imaging to measure local changes in basal levels of key signaling components, we explored features of type-1 cannabinoid receptor (CB1R) signaling in individual axons and dendrites of cultured rat hippocampal neurons. Activation of endogenous CB1Rs led to rapid, $G_{i/o}$-protein- and cAMP-mediated decrease of cyclic-AMP-dependent protein kinase (PKA) activity in the somatodendritic compartment. In axons, PKA inhibition was significantly stronger, in line with axonally-polarized distribution of CB1Rs. Conversely, inverse agonist AM281 produced marked rapid increase of basal PKA activation in somata and dendrites, but not in axons, removing constitutive activation of CB1Rs generated by local production of the endocannabinoid 2-arachidonoylglycerol (2-AG). Interestingly, somatodendritic 2-AG levels differently modified signaling responses to CB1R activation by Δ^9-THC, the psychoactive compound of marijuana, and by the synthetic cannabinoids WIN55,212-2 and CP55,940. These highly contrasted differences in sub-neuronal signaling responses warrant caution in extrapolating pharmacological profiles, which are typically obtained in non-polarized cells, to predict *in vivo* responses of axonal (i.e., presynaptic) GPCRs. Therefore, our results suggest that enhanced comprehension of GPCR signaling constraints imposed by neuronal cell biology may improve the understanding of neuropharmacological action.

Keywords: CB1, DAGL, endocannabinoid, cyclic nucleotide, allosteric, biased agonism, lipid, FRET

INTRODUCTION

Polarized neuronal architecture maintains the directionality of information flow through neuronal networks. Accordingly, protein and lipid composition of the plasma membrane greatly differs between axons and the somatodendritic compartment (Horton and Ehlers, 2003). Local interaction between cell membrane components is increasingly considered as a key dynamic component in sensory and signaling pathways. Notably, the highly regulated lipid environment may control the structure, conformation and function of embedded proteins (Phillips et al., 2009). A major brain G-protein coupled receptor (GPCR) that may be particularly sensitive to the lipid composition of the plasma membrane is the type-1 cannabinoid receptor (CB1R). Predominantly localized in axons and specific presynaptic nerve terminals, CB1R is the neuronal target of endocannabinoid lipids (eCBs) and of Δ^9-tetrahydrocannabinol (THC), the major psychoactive substance of marijuana. CB1Rs may show elevated tonic (constitutive) activation in neurons (Pertwee, 2005), potentially resulting from a combined effect of conformational instability (D'Antona et al., 2006) and ubiquitously present membrane-borne eCBs, such as 2-arachidonoylglycerol (2-AG), which is the most prominent brain eCB (Alger and Kim, 2011; Howlett et al., 2011) as well as an important intermediate in the production of several other bioactive lipids (Nomura et al., 2011). 2-AG is released from cell membrane phospholipids by the action of phospholipase C and diacylglycerol lipases (DAGLα and DAGLβ). eCBs are generally considered to be retrograde signals, being produced in the postsynaptic cell and traveling "backwards" across the synaptic cleft to activate CB1Rs on presynaptic nerve terminals (Freund et al., 2003; Kano et al., 2009). However, in addition to this retrograde synaptic signaling effect, eCBs synthetized in the somatodendritic membrane may also have cell-autonomous effects on local CB1Rs, such as endocannabinoid-mediated somatodendritic slow self-inhibition (SSI) (Bacci et al., 2004; Marinelli et al., 2009) or somatodendritic endocytosis-driven transcytotic targeting (Leterrier et al., 2006; Simon et al., 2013). These findings suggest that locally produced 2-AG may activate somatodendritic CB1Rs, although such CB1R-induced somatodendritic signaling has not yet been shown directly.

CB1R activation, through coupling to $G_{i/o}$ heterotrimeric proteins, leads to inhibition of cyclic adenosine monophosphate (cAMP) production and inhibition of cyclic-AMP-dependent protein kinase (PKA) activity (Howlett, 2005). cAMP and PKA regulate essential biological functions in neurons such

as excitability, efficacy of synaptic transmission and axonal growth/pathfinding. Therefore, CB1R coupling to this major signaling pathway may have important consequences on neuronal function. However, in absence of direct measurement of somatodendritic and axonal CB1R signaling, whether and how differences in local CB1R density and local 2-AG content regulate signaling responses to cannabinoids remain unknown.

More generally, it is currently not known how the highly-polarized neuronal membrane environment may shape GPCR signaling. This information may be important to better understand neuronal effects of therapeutic or abused drugs. Indeed, pharmacological response profiles are usually established in non-polarized heterologous expression systems, such as immortalized cell lines, but results derived from these experimental setups may not precisely indicate the pharmacological response that the studied ligand will elicit in polarized neuronal environments, for instance in the extremely thin axons. Therefore, here we used a highly-resolved and sensitive Förster Resonance Energy Transfer (FRET) approach to measure *in vitro* ligand-induced modulation of basal cAMP/PKA levels downstream of endogenous CB1Rs, in individual axons, dendrites, and somata of well-differentiated hippocampal neurons.

MATERIALS AND METHODS

ANIMALS

All experiments were performed in agreement with the European Community Council Directive of 22nd September 2010 (010/63/UE) and the local ethics committee (*Comité d'éthique en matière d'expérimentation animale n°59, C2EA – 59, 'Paris Centre et Sud'*) were used for dissociated cell culture experiments.

CHEMICALS, ANTIBODIES AND DNA CONSTRUCTS

CB1R agonists WIN55,212,2 (WIN), CP55,940 (CP) and 2-arachydonoylglycerol (2-AG), CB1R inverse agonist AM281 (AM) and DAGL inhibitor RHC80267 (RHC) were obtained from R&D Systems Europe. Dimethyl Sulfoxide (DMSO), Tetrahydrolipstatin (THL), Δ^9-Tetrahydrocannabinol solution (THC), Pertussis Toxin (PTX), Forskolin (Fsk), monoclonal mouse anti-Tau antibody, monoclonal mouse anti-microtubule-associated protein 2 (anti-MAP2) antibody, Bovine Serum Albumin (BSA) and Poly-D-Lysine were obtained from SIGMA-ALDRICH. Polyclonal anti-DAGLα antibody was obtained from Frontier Institute co., ltd (JAPAN). B27, Lipofectamine 2000 and Neurobasal were obtained from Life Technologies.

AKAR4, Lyn-AKAR4 and AKAR4-Kras probes were provided by Dr. Jin Zhang's laboratory (Baltimore, USA). ^{T}Epac^{VV} probe provided by Dr. Kees Jalink laboratory (Amsterdam, Netherlands).

HIPPOCAMPAL NEURONAL CULTURES

Hippocampal neuronal cultures were performed essentially as described previously (Leterrier et al., 2006). Briefly, hippocampi of Sprague–Dawley rat (Janvier) embryos were dissected at embryonic day 18. After trypsinization, dissociation was achieved with a fire-polished Pasteur pipette. Cells were counted and plated on poly-D-lysine-coated 18-mm diameter glass coverslips, at a density of 300–400 cells/mm^2. The plating medium was Neurobasal supplemented with 2% B27 and containing Stabilized Glutamine (0.5 mM) and penicillin G (10 U/ml)/streptomycin (10 g/ml). Four hours after plating, the coverslips were transferred into Petri dishes containing supplemented Neurobasal medium that had been conditioned for 24 h on a 80% confluent glia layer. Neurons were transfected after 6 days *in vitro* (DIV6) using Lipofectamine 2000, following the manufacturer's instructions.

FRET IMAGING

Neurons transfected either with ^{T}Epac^{VV} or AKAR4-Kras probes were imaged by videomicroscopy between DIV7 and DIV11 on a motorized Nikon Eclipse Ti-E/B inverted microscope with the Perfect Focus System (PFS) in a 37°C thermostated chamber, using an oil immersion CFI Plan APO VC 60X, NA 1.4 objective (Nikon).

Acquisitions were carried out at the excitation wavelength of the CFP (434 ± 15 nm) using an Intensilight (Nikon). Emitted light passed through an Optosplit II beam-splitter (Cairn Research) equipped with a FF509-FDi01 dichroïc mirror, a FF01-483/32-25 CFP filter and a FF01-542/27-25 YFP filter and was collected by an EM-CCD camera (Evolve 512, Photometrics), mounted behind a 2× magnification lens. Acquisitions were performed by piloting the set-up with Metamorph 7.7 (Molecular Devices). All filter sets were purchased from Semrock.

Cultured neurons on 18-mm coverslips were placed in a closed imaging chamber containing an imaging medium: 120 mM NaCl, 3 mM KCl, 10 mM HEPES, 2 mM $CaCl_2$, 2 mM $MgCl_2$, 10 mM D-glucose, 2% B27, 0.001% BSA.

We have previously characterized axons and dendrites in our cultures by using immunolabeling for Tau and MAP2 proteins, respectively, that allowed to establish the characteristic morphology of these neurites in cultured hippocampal neurons. Here we have used this morphological criteria to identify axons and dendrites. The acquisition lasted 90 min, recording one image each 2 min, by imaging in parallel 25–30 [10 à15 neurones mais pour chaque neurone: 1 champs sur soma, 1 champ sur l'axone et une champ sur dendrites distales (facultatif)] fields-of view on the same coverslip. 30 min after the beginning of the acquisition, pharmacological treatment was applied then 60 min after the beginning of the acquisition, Forskolin 10 μM was applied.

FRET DATA ANALYSIS

All imaged neurons were analyzed and included in the final result, except the neurons that matched at least one of the three predefined exclusion criteria: (1) lack of response to the terminal Fsk stimulation, (2) loss of focus during the time-lapse sequence, or (3) the impossibility to realign artifactual lateral movement. All key analysis results were obtained by an experimenter blind to the treatment condition.

Images were divided in two parts in ImageJ to separate the CFP channel from the YFP channel. Stacks were realigned to correct for artifactual lateral movement. Data were then analyzed on Matlab by calculating the FRET ratio at each time point for one or several Regions Of Interest (ROIs). The user defined ROIs for each position. For each image, the value of the FRET ratio corresponds to $\frac{IC-BC}{IY-BY}$ for ^{T}Epac^{VV} probe and to $\frac{IY-BY}{IC-BC}$ for AKAR4-Kras probe

IY: Mean Intensity of ROI in YFP channel;
BY: Mean Intensity of the background in YFP channel;
IC: Mean Intensity of ROI in CFP channel;
BC: Mean intensity of the background in CFP channel

For each ROI, the FRET ratio was then normalized by the baseline mean, defined as the 7 time points before first treatment application.

FRET Ratio normalized to baseline$= 100 * \frac{Rc-Ro}{Ro}$
Rc: Value of raw FRET ratio
Ro: Mean of the baseline

The quantitative results obtained for each neuronal compartment were grouped together and, for each time point, the mean FRET ratio normalized to baseline and S.E.M. were calculated. Due to CFP photobleaching, FRET ratio tends to increase slowly during the acquisition. This deviation was corrected for somata and dendrites on Matlab. Mean slope was calculated for all neurons in somata and dendrites, respectively, for the last 7 time points before addition of treatment and substracted from all FRET ratio time points. In the axon, precise execution of this correction is not possible. Indeed, as the signal-to-noise ratio is lower in the extremely thin axons as compared to somata and dendrites, the bleaching is "hidden" in the noise, hindering the precise establishment of the correction slope. Thus, we did not correct for CFP photobleaching in the axon.

FRET STATISTICAL ANALYSIS

FRET Response was obtained by calculating the mean FRET ratio in Matlab for 6 time points after treatment, from +4 to +14 min (Response).

Groups were compared using GraphPad Prism. Significance of differences between various conditions was calculated using unpaired *t*-tests or one-way ANOVA with Newman-Keuls post-tests for computing p estimates. NS $p > 0.05$, $^{*}p < 0.05$, $^{**}p < 0.01$ and $^{***}p < 0.001$.

IMMUNOCYTOCHEMISTRY

DIV9 hippocampal cultured neurons were briefly rinsed with Dulbecco's PBS (DPBS; PAA laboratories) and fixed in DPBS containing 4% paraformaldehyde and 4% sucrose. After permeabilization with a 5 min incubation in DPBS containing 0.1% Triton X-100 and blocking for 30 min in antibody buffer (DPBS supplemented with 2% BSA and 3% normal goat serum), neurons were incubated with primary antibodies diluted 1:200 (DAGLα) or 1:250 (MAP2 and Tau) in antibody buffer for 1 h at room temperature. After DPBS rinses, neurons were labeled with secondary antibodies 1:400 in antibody buffer for 30 min at room temperature. Coverslips were fixed with Mowiol containing Hoechst. Images were obtained using a dry 40× objective lens on Zeiss Axio Imager M1. Excitation wavelengths of 488 nm (DAGLα) and 568 nm (MAP2 or Tau) were used.

CONFOCAL MICROSCOPY

Hippocampal cultured neurons were cotransfected at DIV6 with DsRed2 and various FRET probes ($^{T}Epac^{VV}$, AKAR4, AKAR4-Kras, Lyn-AKAR4) and fixed in DPBS containing 4% paraformaldehyde and 4% sucrose at DIV7. Images were obtained using an oil immersion objective lens (Plan-Apochromat 60X, NA 1.4) on a Nikon A1 confocal microscope. Excitation wavelengths of 488 nm (FRET probes) and 568 nm (DsRed2) were used. Stacks were obtained with one image per optical section and 300 nm between each section.

RESULTS

ENDOGENOUS CB1Rs MODULATE BASAL PKA ACTIVATION LEVELS IN NEURONS

The characteristic inhibition of cyclic AMP production and PKA activity by $G_{i/o}$-protein coupled GPCRs is usually detected in pharmacological assays after GPCR over-expression and forskolin-induced artificial activation of adenylyl cyclases. Here we aimed to directly measure cannabinoid-induced changes in basal levels of neuronal PKA signaling, downstream of endogenous CB1Rs in cultured hippocampal neurons. Pilot experiments indicated that by using a sensitive EM-CCD camera and hardware-based focus stabilization (see Materials and Methods) we are able to measure cannabinoid-induced inhibition of cyclic AMP production and PKA activity in relatively large cytoplasmic volumes such as neuronal somata by using the soluble $^{T}Epac^{VV}$ probe (Klarenbeek et al., 2011) (**Figure 1A**) and AKAR4 (Depry et al., 2011) (**Figure 1B**), respectively. However, smaller diameter neurites such as distal dendrites and axons gave weak (low amplitude) and highly variable responses, leading to a low signal-to-noise ratio, which impeded the reliable measure of the relatively small amplitude cannabinoid-induced changes in the FRET ratio with the AKAR4 probe. To overcome this experimental limitation, we hypothesized that, since the PKA activator cAMP is produced by membrane-bound adenylyl cyclases at the plasma membrane and PKA deactivator phosphodiesterases are cytosolic (Neves et al., 2008), targeting a PKA probe to the plasma membrane may strongly increase experimental sensitivity. Indeed, results of a previous report show both higher FRET responses and higher PKA-sensitive potassium current responses downstream of G_s-protein activation in dendrites that have a high surface-to-volume ratio as compared to the soma (Castro et al., 2010). Therefore, we expressed separately two membrane-targeted PKA biosensors: AKAR4-Kras (Depry et al., 2011), which is targeted to the non-raft domains of the plasma membrane (**Figure 1C**), and Lyn-AKAR4 (Depry et al., 2011), which is targeted to the raft regions of the plasma membrane (**Figure 1D**) in well-differentiated hippocampal neurons. In our experimental conditions, AKAR4-Kras showed a more homogenous distribution that segregated well with the plasma membrane at different optical sections of the somatodendritic domain, while Lyn-AKAR4 was more strongly localized to relatively small membrane microdomains and intracellular structures (**Figures 1C,D**). In order to focus on plasma-membrane localized endogenous CB1Rs, further experiments were therefore performed using AKAR4-Kras.

Does the membrane-targeted AKAR4-Kras probe permit the measurement of cannabinoid-induced modulation of basal PKA levels downstream of endogenous CB1Rs in all neuronal subcompartments? We tested the sensitivity of our experimental setup by determining the minimal amount of cytoplasmic volume necessary to the detection of cannabinoid-induced modulation of basal PKA levels, in individual thin (mean diameter =

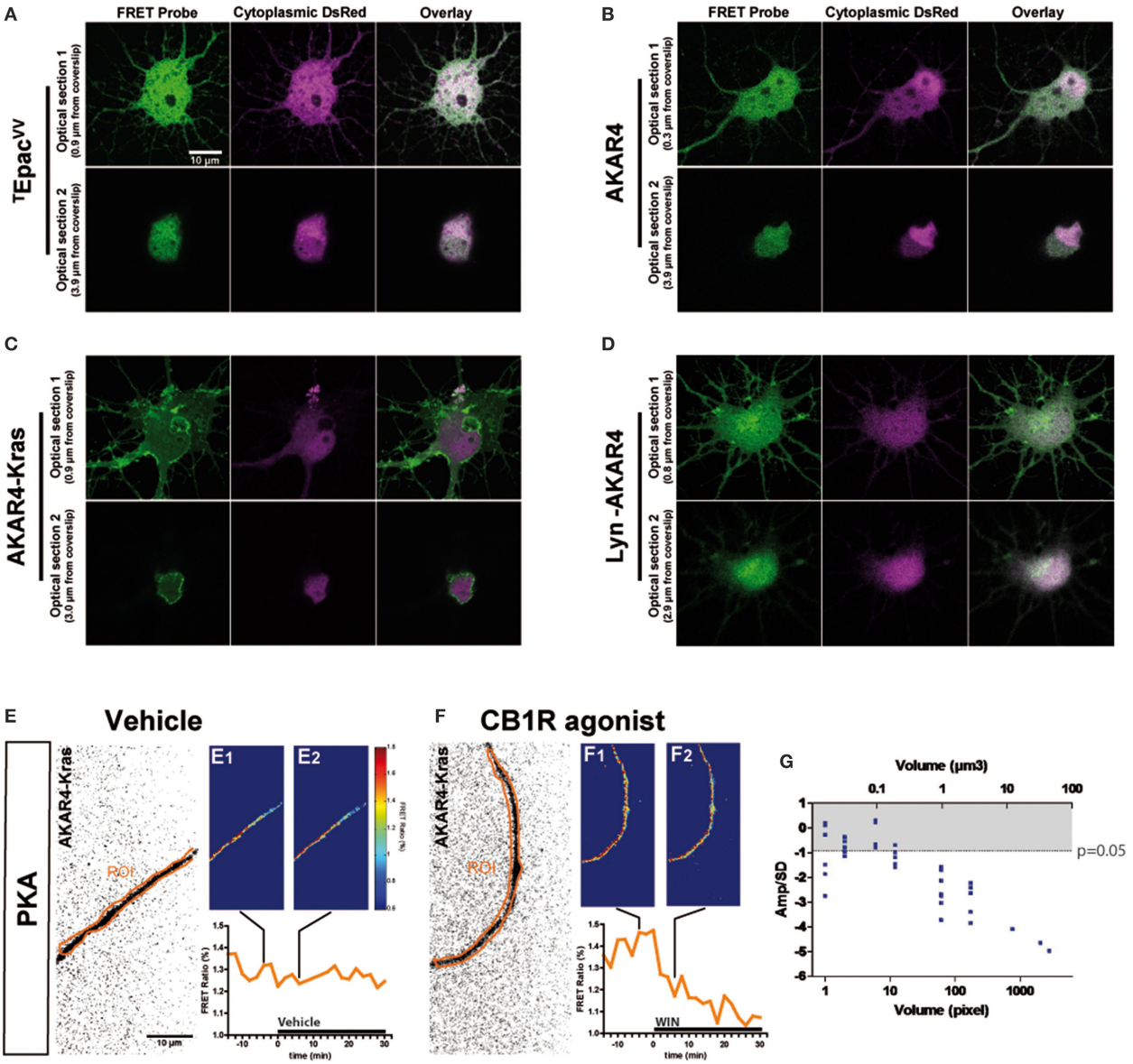

FIGURE 1 | Quantitative measure of basal cAMP/PKA pathway modulation downstream of endogenous neuronal CB1Rs in small cytoplasmic volumes. (A–D) Cultured hippocampal neurons expressing soluble (cytoplasmic) DsRed2 and various FRET probes designed to measure cAMP concentration or PKA activity: ^{T}Epac^{VV} **(A)**, AKAR4 **(B)**, AKAR4-Kras **(C)**, LYN-AKAR4 **(D)**. After fixation, confocal imaging at two different optical sections shows sub-cellular localization of the probes. AKAR4-Kras probes are well-localized to the plasma membrane in the somatodendritic region. **(E,F)** Modulation of basal PKA activity downstream of endogenous CB1Rs in axonal Regions of Interest (ROI) in AKAR4-Kras expressing neurons. The first image of the acquisition on YFP channel, inverted and with enhanced contrast for better visibility, is shown with the ROI (orange) **(E,F)**. The mean FRET ratio is shown at 4 min (-t4) before **(E_1,F_1)** and at 6 min (t6) after **(E_2,F_2)** the addition of treatment at t0. Incubation with vehicle does not change the FRET ratio **(E_2)** compared to baseline **(E_1)** but addition of agonist WIN 55-212,2 (WIN) 100 nM induces a rapid FRET-ratio decrease **(F_2)**, as compared to baseline **(F_1)**. **(G)** Test of FRET imaging sensitivity by determining the smallest axonal cytoplasmic volume allowing the measurement of significant PKA activity decrease after WIN-induced activation of endogenous CB1Rs. We calculated the mean value of the FRET response amplitude normalized to baseline (Amp) and its standard deviation (*SD*), in different axonal ROIs, between t4 (4 min after drug treatment) and t14. The ratio of the FRET response amplitude to its standard deviation (Amp/SD) is represented in function of the volume (see text). The WIN effect is significantly different from control (modeled as an effect of Amp = 0 with the same standard deviation than the corresponding WIN-stimulated response) at the Amp/SD ratio equal to −0.91 (in gray, $p < 0.05$, Student's *t*-test, $N = 10$), which is reached starting from ∼1 µm^3 axonal volume. Data information: Scale bar: 10 µm **(A–F)**.

0.7 µm, see **Figure 3C**) and mature (day *in vitro* 9—DIV9) axons of AKAR4-Kras expressing neurons. By using a large region of interest (ROI) to measure the FRET ratio change, treatment with the synthetic CB1R agonist, WIN55,212-2 (WIN) at 100 nM (**Figure 1F**), but not with vehicle (**Figure 1E**), induced a important change of the FRET ratio within 2 min, indicating that CB1R activation induces a decrease of basal PKA activity downstream of endogenous CB1Rs. Measuring the FRET

responses in a single axon by gradually decreasing the size of the ROI, we determined the minimum cytoplasmic volume necessary for reliable measurement of the WIN-induced FRET signal change. ROI volumes have been determined as described in "Supplementary Materials and Methods." We found that a significant decrease of WIN-induced basal PKA activity downstream of endogenous CB1Rs could be measured in volumes as small as 1 μm^3, which corresponds to 1 femtoliter of axonal cytoplasm (**Figure 1G**), by using a membrane targeted biosensor, such as AKAR4-Kras, possibly because of the high surface-to-volume ratio of extremely thin neurites.

In conclusion, this experimental approach enables the measurement of modulation of basal neuronal PKA activation levels, downstream of an endogenous $G_{i/o}$ protein coupled receptor, in extremely small cellular volumes, such as the cytoplasm of mature axons.

TRANSIENT SOMATODENDRITIC CB1Rs CONSTITUTIVELY INHIBIT THE cAMP/PKA PATHWAY

Previous ultrastructural analysis of hippocampal neurons has shown that in the somatodendritic region, the steady-state presence of endogenous CB1Rs at the plasma membrane is very low both *in vitro* (Leterrier et al., 2006) and *in vivo* (Katona et al., 1999; Thibault et al., 2013). However, previous studies have also reported that most axonally targeted CB1Rs accomplish a transient passage on the somatodendritic plasma membrane (Leterrier et al., 2006; McDonald et al., 2007; Simon et al., 2013). Currently, it remains unknown whether somatodendritic CB1Rs are able to inhibit cAMP/PKA signaling in this neuronal compartment. Therefore, we measured modulation of basal somatodendritic PKA activity downstream of endogenous CB1Rs and found that treatment with WIN at 100 nM, but not with vehicle, induced a moderate decrease of the FRET ratio in individual neurons within a few minutes (**Figures 2A,B**). To precisely analyze this WIN-induced response, we compared PKA activity in two groups of neurons treated either with vehicle or WIN (100 nM) during 30 min, followed by treatment with the adenylyl cyclase activator Forskolin (Fsk, 10 μM) (**Figures 2C,D**), to induce a saturating level of AKAR phosporylation, as reported previously (Gervasi et al., 2007). Fsk induced strong somatodendritic PKA activation with a raw baseline-normalized FRET-ratio increase between 20 and 30%. This increase is in the expected range, since activation of AKAR4-Kras in HEK293 cells by addition of 50 μM Fsk induced an increase of 8% of the raw FRET Ratio (Depry et al., 2011). Conversely, activation of CB1Rs with WIN induced a rapid decrease of basal PKA activity in somata ($-2.5 \pm 0.4\%$) and dendrites ($-3.2 \pm 0.5\%$), which was significant as compared to vehicle (somata: $0.1 \pm 0.3\%$, dendrites: $-0.2 \pm 0.4\%$) (**Figures 2C$_1$,C$_2$,D$_1$,D$_2$**). Please note that the measured 2–4% changes of the raw baseline-normalized FRET ratio correspond to 10–20% of the maximal response, which equals typically to 20–25% elevation of the raw baseline-normalized FRET ratio, as established by the terminal saturating Fsk treatment. Given that endogenous CB1Rs are not the only $G\alpha_{i/o}$-coupled GPCRs in hippocampal neurons, mobilization of the cAMP/PKA pathway in the 10–20% range of the maximal response suggests physiological relevance. Moreover, FRET responses showed Gaussian distribution pattern (as verified by the normality test), indicating that hippocampal neurons did not segregate into subpopulations regarding the effects of CB1R agonist/antagonist application (Supplementary Figures 1A–C). This is in contrast to a previous *ex-vivo* report that studied somatic slow self-inhibition in cortical neurons, where only a subpopulation of neurons was responsive to cannabinoid treatment (Marinelli et al., 2009). The effect of WIN was blocked after overnight treatment with 100 ng/mL of the $G_{i/o}$-protein specific inhibitor pertussis toxin (PTX) (somata: $-0.3 \pm 0.2\%$, dendrites: $-1.5 \pm 0.3\%$) as well as after 3 h pre-treatment with 1 μM of the CB1R-specific antagonist/inverse-agonist AM281 (somata: $0.3 \pm 0.3\%$, dendrites: $-1.1 \pm 0.5\%$). Therefore, endogenous CB1Rs, transiently present on the somatodendritic plasma membrane, can be activated by exogenous cannabinoids and are able to subsequently inhibit basal PKA signaling through their coupling to $G_{i/o}$ proteins both in somata and dendrites.

We have previously reported that somatodendritic CB1Rs are constitutively endocytosed because of constitutive receptor activation, which can be inhibited by pharmacological or genetic tools (Leterrier et al., 2006; Simon et al., 2013). To investigate whether CB1Rs also constitutively inhibit cAMP/PKA signaling in the somatodendritic compartment, we applied the CB1R inverse agonist, AM281 at 100 nM, to neurons expressing AKAR4-Kras. This treatment led to a rapid and significant increase of the FRET ratio both in somata and dendrites (somata: $1.3 \pm 0.2\%$, dendrites: $2.0 \pm 0.4\%$) (**Figures 2C$_1$,C$_2$,D$_1$,D$_2$**). Therefore, somatodendritic CB1Rs exert a constitutive inhibition on PKA activity that is removed by inverse agonist treatment.

Taken together these results indicate that somatodendritic CB1Rs constitutively inhibit PKA activity through the mobilization of $G_{i/o}$ proteins, which is likely due to the inhibition of adenylate cyclase and subsequent decrease of cAMP production. To confirm this mechanism, we directly measured the modulation of basal somatodendritic cAMP concentration, downstream of CB1Rs, by using the $^{T}Epac^{VV}$ probe (Klarenbeek et al., 2011). The activation of endogenous CB1Rs with WIN (100 nM) induced a rapid and significant decrease of cAMP concentration in somata ($-1.5 \pm 0.3\%$) and dendrites ($-2.6 \pm 0.6\%$), while application of the inverse agonist AM281 at 100 nM led to a rapid and significant increase of cAMP concentration both in somata ($1.7 \pm 0.3\%$) and dendrites ($2.6 \pm 0.5\%$) (**Figures 2E,E$_1$,E$_2$,F,F$_1$,F$_2$**). Responses to the final 10 μM Fsk treatment are also a slightly different. However, accurate measure of ligand-induced modifications of artificial adenylyl cyclase stimulation by Fsk was not the scope of the present study, where we focused on endogenous CB1R-induced modification of basal PKA activation levels.

These results show that endogenous CB1Rs exert a constitutive inhibition on the cAMP/PKA signaling pathway both in somata and dendrites. In addition, somatodendritic CB1Rs can be further activated by exogenous cannabinoids leading to a rapid decrease of cAMP concentration and PKA activity through activation of $G_{i/o}$ proteins.

AXONAL CB1R SIGNALING IS DIFFERENT FROM DENDRITIC SIGNALING

Previous studies have found a polarized accumulation of transcytosed CB1Rs on the axonal plasma membrane due to reduced

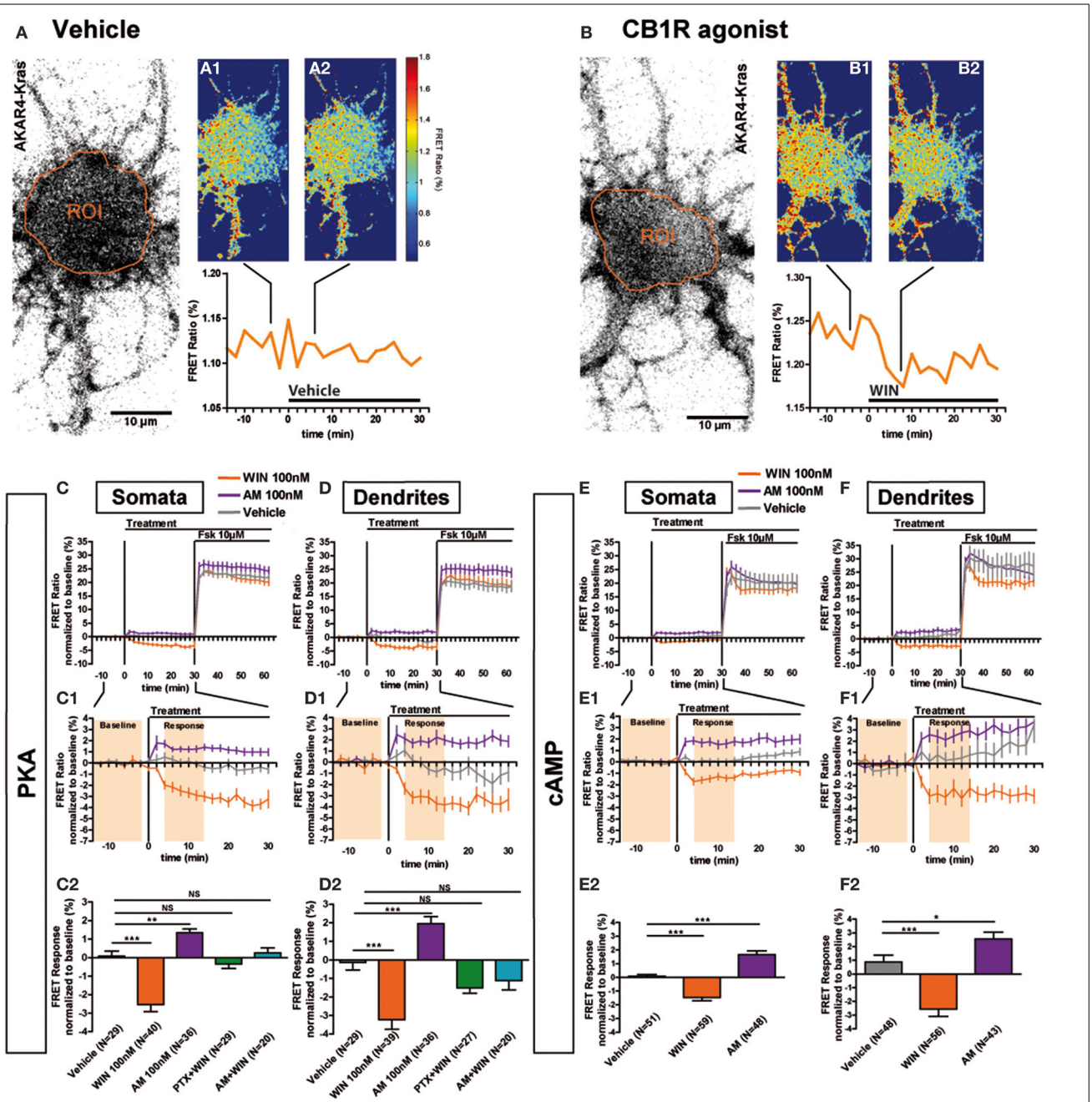

FIGURE 2 | Somatodendritic CB1Rs constitutively inhibit the cAMP/PKA pathway. (A,B) Two representative neurons expressing the membrane-targeted PKA sensor AKAR4-Kras. The first image of the acquisition on YFP channel with the ROI is shown **(A,B)**. The mean FRET ratio in somatic ROIs (orange) is shown at 4 min (-t4) before **(A_1, B_1)** and at 6 min (t6) after the addition of treatment at t0: Vehicle **(A_2)** or agonist WIN55-212,2 (WIN) 100 nM **(B_2)**. **(C–F)** Averaged responses of AKAR4-Kras **(C,D)** or the cAMP sensor $^{T}Epac^{VV}$ expressing neurons **(E,F)**. The FRET ratio normalized to baseline was calculated for each neuron with a time-resolution of 2 min, separately in somata and dendrites. The curves represent mean ± S.E.M. of the FRET ratio for all imaged neurons at each time point. Addition of agonist WIN 100 nM but not of vehicle at t0 results in rapid FRET ratio decrease while inverse-agonist AM281 100 nM (AM) treatment results in increased PKA-activation. At 30 min, adenylyl-cyclase activator Forskolin (Fsk) was added at 10 µM, inducing a saturating increase of the FRET ratio. **C_1,D_1,E_1,F_1:** Zoom between -t14 and t30 of **C,D,E,F**, respectively, shows significant modulation of basal PKA activity after activation or blockade of CB1Rs. **C_2,D_2,E_2,F_2:** FRET responses were calculated as the mean response between t4 and t14 min (shaded zone labeled "Response" on **C_1,D_1,E_1,F_1**), using data normalized to the baseline (shaded zone between -t14 and -t2, labeled "Baseline" on **C_1,D_1,E_1,F_1**), as described in the Materials and Methods Section. Implication of $G_{i/o}$-proteins was shown by the specific inhibitor pertussis toxin (PTX), applied overnight at 100 ng/mL before the beginning of the experiment. The WIN effect was CB1R-induced as shown by pre-treatment with the CB1R-specific antagonist AM281 (1 µM 3 h before the beginning of the experiment). Data information: Data are expressed as mean ± S.E.M.; Statistical analysis was realized with one-way ANOVA followed by Newmann-Keuls post-test; NS $p > 0.05$, $^{*}p < 0.05$, $^{**}p < 0.01$, $^{***}p < 0.001$. Scale bar: 10 µm **(A,B)**.

internalization levels as compared to dendrites (Leterrier et al., 2006; McDonald et al., 2007; Simon et al., 2013). We asked whether the recruitment of signaling pathways downstream of CB1Rs in axons also differ from somata and dendrites. Application of 100 nM WIN led to a rapid and significant decrease of basal PKA activity in axons ($-14.6 \pm 1.4\%$) compared to vehicle ($-1.8 \pm 0.6\%$) (**Figures 3A,A$_1$,A$_2$**). This effect was blocked by pre-treatment with AM281 1 μM ($-2.6 \pm 1.0\%$) and PTX 100 ng/mL ($-5.5 \pm 1.1\%$), showing that PKA inhibition is specifically mediated by CB1Rs acting through $G_{i/o}$ proteins. In addition, CB1R activation decreased PKA activity more strongly in the axon than in dendrites (dendrite response normalized to vehicle: $-3.1 \pm 0.5\%$, axonal response normalized to vehicle: -12.8 ± 1.4) (**Figure 3B**). Interestingly, in contrast to dendrites, application of the inverse agonist AM281 at 100 nM did not induce a detectable change of PKA activity in the axon ($0.1 \pm 0.8\%$), suggesting that axonal CB1Rs are not constitutively activated (**Figures 3A,A$_1$,A$_2$**).

Why does axonal CB1R activation lead to a significantly higher amplitude of PKA inhibition in axons than in dendrites and somata? First, similarly to their distribution *in vivo* (Katona et al., 2001; Bodor et al., 2005; Thibault et al., 2013), CB1Rs display an axonally polarized distribution in cultured neurons (Coutts et al., 2001; Leterrier et al., 2006; McDonald et al., 2007; Simon et al., 2013). Second, theoretical models predict, and experiments show that, for signaling molecules produced at the plasma membrane and degraded in the cytoplasm, such as cAMP, the ratio of the surface area of the plasma membrane to the cytoplasmic volume [surface/volume ratio (S/V)] becomes important (Neves et al., 2008). As such, we asked whether the strong decrease of PKA activity observed after CB1R activation in the axon is related to the high S/V ratio of this compartment. However, for both axons and distal dendrites, we found no correlation between neurite diameter and FRET response amplitude after CB1R activation (Pearson's correlation coefficient: $r_{\text{distal dendrites}} = -0.065$ and $r_{\text{axons}} = 0.03649$) (**Figure 3C**). Moreover, a sub-population of distal dendrites has the same diameter range as axons. In these thin dendritic segments, the amplitude of the FRET response after CB1R activation was again significantly different from the axonal response (dendrites normalized to vehicle: $-4.0 \pm 0.8\%$, axons normalized to vehicle: -12.8 ± 1.4) (**Figure 3D**). Therefore, morphological differences between axons and dendrites do not explain the observed signaling disparity among these two compartments, suggesting that the polarized distribution of neuronal CB1Rs is the main reason for the enhanced agonist response in axons.

CONSTITUTIVE ACTIVATION OF SOMATODENDRITIC CB1Rs REQUIRES LOCAL SYNTHESIS OF ENDOCANNABINOIDS

Next we investigated why CB1Rs are constitutively activated in the somatodendritic compartment but not in the axon, by focusing on the contribution of endocannabinoids, which play an important role in basal CB1R activation in several experimental systems (Turu et al., 2007; Howlett et al., 2011). The major endocannabinoid 2-arachidonoylglycerol (2-AG) is a lipid molecule present in the cell plasma membrane and is synthesized by DAG Lipases (DAGL). DAGLα, the major DAGL in the postnatal brain, is segregated to axonal tracts during embryonic development but was shown to accumulate after birth in the somatodendritic plasma membrane in several brain areas, such as the cerebellum (Bisogno et al., 2003), striatum (Uchigashima et al., 2007), hippocampus (Katona et al., 2006; Yoshida et al., 2006) and amygdala (Yoshida et al., 2011). Similarly, we found a somatodendritic segregation of DAGLα in fully-polarized (DIV9) cultured hippocampal neurons, while no labeling was found in the axon (**Figures 4A,A$_1$**). This indicates local production of 2-AG in the plasma membrane of the somatodendritic compartment but not in the axonal counterpart. To investigate whether such polarized 2-AG production may explain the aforementioned differences in constitutive CB1R activation between dendrites and axons, we pre-treated neurons expressing the AKAR4-Kras probe with the DAGL inhibitors, Tetrahydrolipstatin (THL) or RHC80267 (RHC), during 3 h before treatment with the inverse agonist AM281 100 nM (**Figures 4B,B$_1$,C,C$_1$**). The FRET ratio did not increase in these neurons after adding AM281, neither in somata (AM281: $1.6 \pm 0.3\%$, vehicle: $0.2 \pm 0.3\%$, AM281 after THL 1 μM: $0.4 \pm 0.3\%$, AM281 after RHC 25 μM: $0.1 \pm 0.3\%$) nor in dendrites (AM281: $2.0 \pm 0.5\%$, vehicle: $0.4 \pm 0.4\%$, AM281 after THL 1 μM: $0.4 \pm 0.3\%$, AM281 after RHC 25 μM: $-0.1 \pm 0.5\%$). Thus, the constitutive inhibition on PKA activity was removed by DAGL blockade, demonstrating that constitutive activation of somatodendritic CB1Rs requires locally produced 2-AG.

SIGNALING RESPONSES TO EXOGENOUS LIGANDS WIN, CP55,940 AND Δ^9-THC ARE DIFFERENTIALLY SHAPED BY LOCAL PRODUCTION OF 2-AG IN THE SOMATODENDRITIC COMPARTMENT

Previous results show that, after DAGL inhibition, the amount of CB1Rs increase on the plasma membrane, both in the somatodendritic compartments of neurons and in CHO cells (Turu et al., 2007). In CHO cells, the elevated CB1R levels at the plasma membrane yield enhanced G-protein activation following WIN administration (Turu et al., 2007). We asked whether the THL-induced accumulation of CB1Rs on the somatodendritic membrane is able to produce similar enhanced inhibition of PKA activity after WIN administration, as compared to basal conditions. Therefore, we pre-treated neurons with THL (1 μM) during 3 h before acquisition and applied WIN during the FRET acquisition (**Figure 5A**). Surprisingly, DAGL inhibition blocked the effect of 100 nM WIN in the somatodendritic compartment instead of signaling enhancement (somatic response to WIN 100nM: $-2.4 \pm 0.4\%$, $P < 0.01$ compared to vehicle ($0.1 \pm 0.2\%$) and $P < 0.01$ compared to response to WIN 100 nM after 3 h THL 1 μM ($-0.2 \pm 0.6\%$), one-way ANOVA followed by Newman-Keuls post-test; dendrite response to WIN 100 nM: $-2.8 \pm 0.4\%$, $P < 0.01$ compared to vehicle ($-0.4 \pm 0.4\%$) and $P < 0.01$ compared to response to WIN 100 nM after 3 h THL 1 μM ($-0.6 \pm 0.6\%$), one-way ANOVA followed by Newman-Keuls post-test) (**Figures 5A,A$_1$,C,C$_1$**), while it did not change the FRET response in the axon (response to WIN 100 nM: $-14.6 \pm 1.1\%$, $P < 0.001$ compared to vehicle ($-1.9 \pm 0.9\%$) and $P > 0.05$ compared to WIN 100 nM after 3 h THL 1 μM ($-12.4 \pm 1.2\%$), one-way ANOVA followed by Newman-Keuls post-test) (**Figures 5A$_2$,C$_2$**). This suggests that a local 2-AG production drop, caused by THL pre-treatment, was

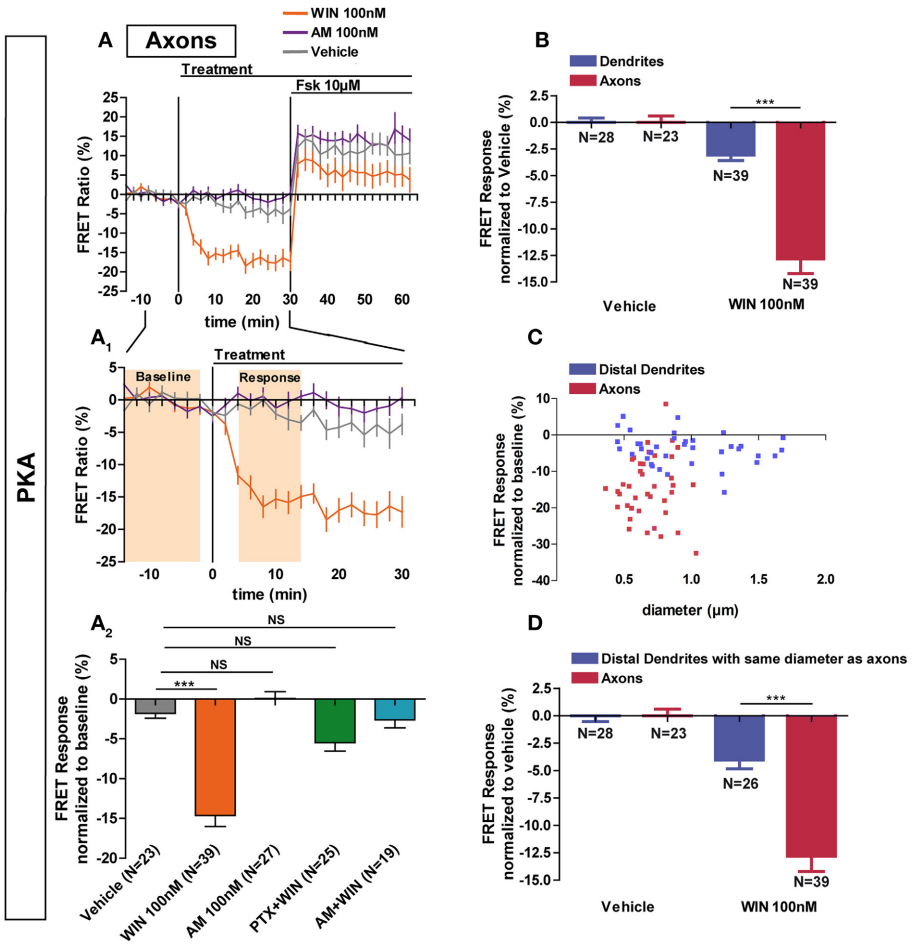

FIGURE 3 | Axonal CB1R signaling differs from dendritic signaling. (A) Averaged axonal responses of AKAR4-Kras expressing neurons, as shown on **Figures 1E,F**. The FRET ratio normalized to baseline was calculated for each neuron with a time-resolution of 2 min. The curves represent mean ± S.E.M. of the FRET ratio for all imaged neurons at each time point. Addition of agonist WIN 100 nM but not of vehicle or inverse-agonist AM281 100 nM (AM) at t0 results in rapid high-amplitude FRET ratio decrease. At 30 min, adenylyl-cyclase activator Forskolin (Fsk) was added at 10 µM, inducing a saturating increase of the FRET ratio. **A_1:** Zoom between −t14 and t30 of **A** shows significant modulation of basal PKA activity after activation of CB1Rs. **A2:** FRET responses were calculated as the mean response between t4 and t14 min (shaded zone labeled "Response" on **A_1**), using data normalized to the baseline (shaded zone between −t14 and −t2, labeled "Baseline" on **A_1**). Implication of $G_{i/o}$-proteins was shown by the specific inhibitor pertussis toxin (PTX), applied overnight at 100 ng/mL before the beginning of the experiment. The WIN effect was CB1R-induced as shown by pre-treatment with the CB1R-specific antagonist AM281 (1 µM, 3 h before the beginning of the experiment). **(B)** Vehicle-normalized FRET response to WIN is significantly stronger in axons than in dendrites. **(C)** Individual FRET responses in axons and distal dendrites are represented in function of their respective diameter. For each group (distal dendrites and axons), a Pearson correlation test was calculated showing no correlation between FRET response and diameter ($r_{\text{distal dendrites}} = -0.065$ and $r_{\text{axons}} = 0.03649$). **(D)** Distal dendrites having the similar diameter than axons still display significantly weaker vehicle-normalized FRET responses to WIN compared to axons. Data information: Data are expressed as means ± S.E.M.; Statistical analysis was realized with one-way ANOVA followed by Newmann-Keuls post-test **(A_2)** or unpaired *t*-test **(B,D)**; NS $p > 0.05$, $^{***}p < 0.001$.

responsible for the somatodendritic signaling decrease, which indeed could be rescued by 2-AG (100 nM), applied for 10 min before WIN treatment (somata: −3.3 ± 1.0%, dendrites: −3.7 ± 1.2%, axons: −11.8 ± 1.6%; WIN responses were compared to vehicle) (**Figures 5B,B_1,C,C_1,C_2**). By itself, 2-AG used at 1 µM is able to decrease PKA activity in all neuronal compartments, with a stronger effect in axons as compared to the somatodendritic compartment (somata: −2.6 ± 0.7%, dendrites: −5.5 ± 0.5%, axons: −17.7 ± 1.5%) (**Figures 5C,C_1,C_2**). To verify if the presence of local 2-AG is a general requirement for somatodendritic CB1R activation, we tested two other, structurally different, CB1R agonists: CP55,940 (CP) and Δ^9-THC (THC), the psychoactive compound of marijuana. In control neurons, the effect of CB1R activation with 100 nM CP was comparable to WIN, with a decrease of PKA activity in both dendrites and axons as well as a stronger amplitude in the axonal response compared to dendrites (somata: −1.0 ± 0.4%; dendrites: −2.1 ± 0.7%; axons: −18.4 ± 1.6%) (**Figures 5C,C_1,C_2**). However, blockade of DAGL by THL pretreatment did not decrease the effect of CP (100 nM) in the somatodendritic compartment. On the contrary, and according to our previous expectations for WIN, this response was enhanced as compared to control neurons

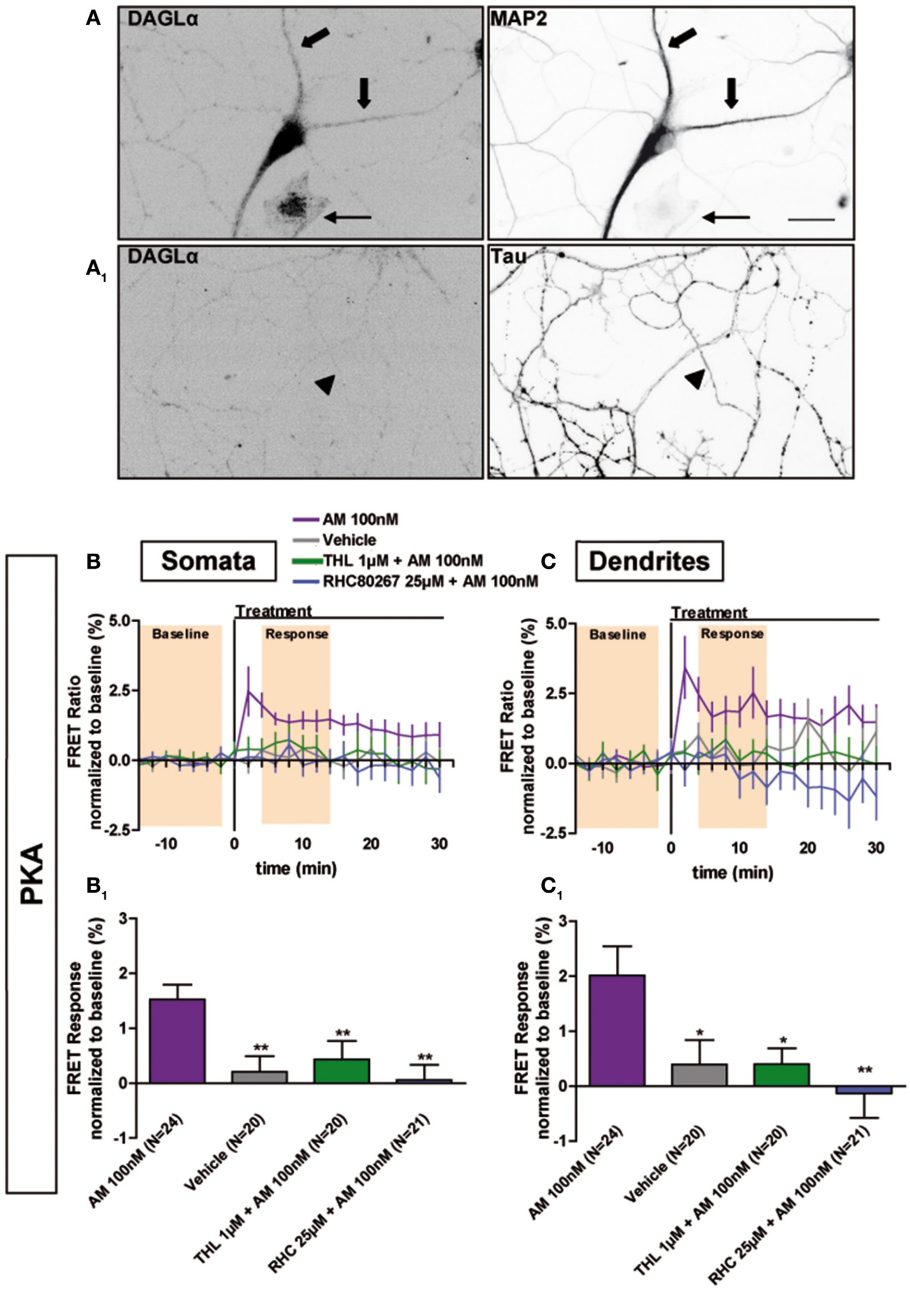

FIGURE 4 | Constitutive activation of somatodendritic CB1Rs requires locally synthesized endocannabinoids. (A) Simultaneous immunolabeling of fully-polarized (DIV9) neurons with anti-DAGLα antibody and either anti-MAP2 **(A)** or anti-Tau **(A_1)** antibodies. Large arrows indicate dendrites, arrow-heads indicate axon and the thin arrow shows an astrocyte. **(B,C)** Averaged somatic and dendritic responses of AKAR4-Kras expressing neurons to inverse-agonist AM281 (AM), with or without inhibiting DAGL activity. The FRET ratio normalized to baseline was calculated for each neuron with a time-resolution of 2 min. The curves represent mean ± S.E.M. of the FRET ratio for all imaged neurons at each time point. Addition of 100 nM AM but not of vehicle at t0 results in elevated PKA activity, revealing constitutive CB1R activation, which is significantly decreased after DAGL inhibition either by tetrahydrolipstatin (THL) 1 μM or RHC80267 25 μM. Data information: Data are expressed as mean ± S.E.M.; Statistical analysis was realized with one-way ANOVA followed by Newmann-Keuls post-test; $^{*}p < 0.05$, $^{**}p < 0.01$. Scale bar: 20 μm **(A,A1)**.

(somata: −5.0 ± 1.2%, dendrites: −5.7 ± 1.3%, axons: −19.2 ± 1.4%; responses to CP 100 nM after 3 h THL 1 μM were compared to CP 100 nM alone). Finally, treatment with THC (1 μM) also decreased PKA activity in all neuronal compartments, with a stronger effect in the axon compared to the somatodendritic compartment (somata: −1.5 ± 0.4%, dendrites: −2.8 ± 0.5%, axons: −15.8 ± 2.1%) (**Figures 5C,C_1,C_2**). However, the somatodendritic effect of 1 μM THC was suppressed by THL pretreatment while it did not affect the axonal response (somata: −0.3 ± 0.7%, dendrites: 0.1 ± 1.0%, axons: −14.2 ± 2.5%; responses to THC 1 μM after 3 h THL 1 μM were compared to THC 1 μM alone) (**Figures 5C,C_1,C_2**). Thus, THC and WIN

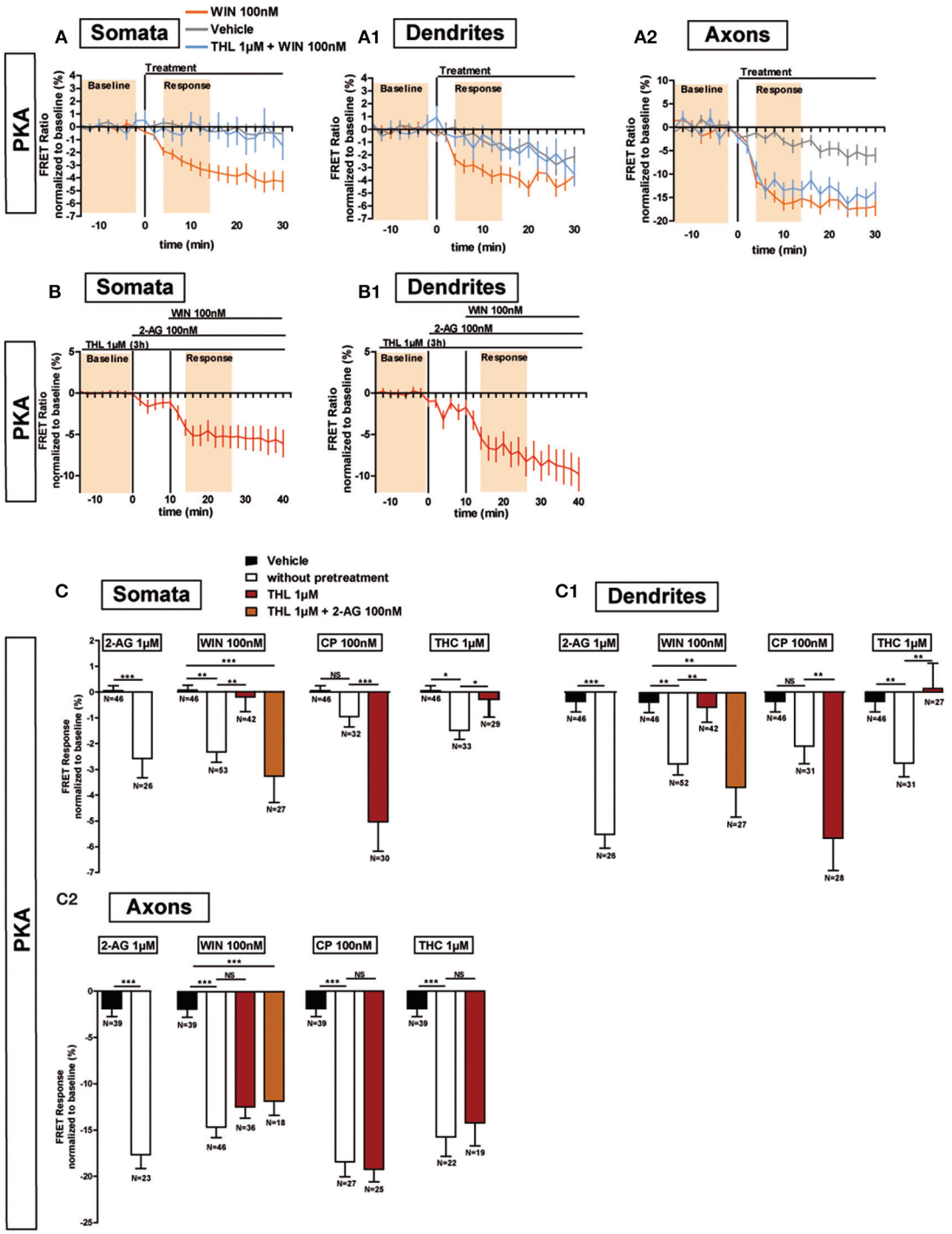

FIGURE 5 | Endogenous 2-AG significantly modifies CB1R responses to exogenous cannabinoids. (A,B) Averaged somatic, dendritic and axonal responses of AKAR4-Kras expressing neurons to agonist WIN 55-212,2 (WIN). The FRET ratio normalized to baseline was calculated for each neuron with a time-resolution of 2 min. The curves represent mean ± S.E.M. of the FRET ratio for all imaged neurons at each time point. Addition of WIN 100 nM but not of vehicle at t0 results in decreased PKA activity, which effect is significantly inhibited after DAGL inhibition by tetrahydrolipstatin (THL) 1 µM in somata **(A)** and dendrites **(A_1)** but not in axons **(A_2)**. The effect of THL pre-treatment on the WIN effect in somata **(B)** and dendrites **(B1)** can be rescued by applying 2-AG at 100 nM 10 min before WIN. **(C)** Variation of neuronal 2-AG levels (similarly to **A,B**) modifies the FRET responses to exocannabinoids WIN55-212,2 100 nM (WIN), CP55,940 100 nM (CP) and Δ^9-THC 1 µM (THC), shown as the mean response between t4 and t14 min (shaded zone labeled "Response" on **A,B**), using data normalized to the baseline (shaded zone between −t14 and −t2, labeled "Baseline" on **A,B**) in somata **(C)**, dendrites **(C_1)** or axons **(C_2)**. 2-AG levels were reduced by THL 1 µM, applied 3 h before the beginning of the experiment and rescued by 2-AG 100 nM at 10 min before agonist treatment. Data information: Data are expressed as mean ± S.E.M.; Statistical analysis was realized with unpaired *t*-test (2-AG) or one-way ANOVA followed by Newmann-Keuls post-test (WIN, CP, and THC); NS $p > 0.05$, $*p < 0.05$, $**p < 0.01$ and $***p < 0.001$.

require local presence of 2-AG to activate somatodendritic CB1Rs.

In conclusion, activation of CB1Rs by exogenous cannabinoids can have contrasted effects on the mobilization of somatodendritic signaling pathways: these effects are highly shaped by local presence of 2-AG which is necessary for the effects of both WIN and THC, but not of CP, in this neuronal compartment.

DISCUSSION

We developed a highly sensitive quantitative *in vitro* method to evaluate, for the first time to our knowledge, the modulation of the cAMP/PKA signaling pathway downstream of an endogenous $G_{i/o}$ protein coupled receptor with sub-neuronal resolution. We measured modulation of basal cAMP/PKA signaling, after activation or blockade of endogenous CB1Rs, in somata, dendrites and axons of well-differentiated cultured rat hippocampal neurons. Our results show that polarized distribution of two neuronal proteins, the endocannabinoid synthesizing DAGLα enzyme and the CB1R, leads to previously unappreciated quantitative subdomain dependent differences in intraneuronal GPCR signaling. In axons, the combined effect of high CB1R density and absence of DAGLα activity leads both to elevated response amplitude following agonist stimulation, as well as to a lack of constitutive activation. In the somatodendritic compartment, relatively low CB1R density and high DAGLα activity, locally producing the membrane component endocannabinoid 2-AG, results in constitutive activation of CB1R-activated signaling which is accompanied by significant but relatively low amplitude agonist-induced signaling responses.

In addition, we show that the 2-AG content of the somatodendritic plasma membrane has contrasted effects on CB1R activation by various exogenous cannabinoid ligands: at the ligand concentrations used in the present study, CP acts as a classical agonist while both WIN and THC require the presence of endogenous 2-AG to efficiently activate CB1Rs.

CB1Rs CONSTITUTIVELY INHIBIT cAMP/PKA SIGNALING IN THE SOMATODENDRITIC COMPARTMENT BUT NOT IN THE AXON

Several studies reported that CB1Rs display constitutive activity in neurons (Pan et al., 1998; Hillard et al., 1999) and notably, these receptors are constitutively endocytosed in the somatodendritic compartment, but not in axons, due to basal activation (Leterrier et al., 2006; Simon et al., 2013). Here we show that application of the inverse agonist AM281 leads to a rapid increase in both somatodendritic cAMP concentration and PKA activity, suggesting constitutive CB1R activation in the somatodendritic compartment but not in the axon. In non-polarized cells, constitutive CB1R activity is highly diminished in the absence of endocannabinoid 2-AG (Turu et al., 2007). We found here that DAGLα is segregated in the somatodendritic compartment and its inhibition removes the effect of AM281. Therefore, somatodendritic CB1Rs are constitutively activated by a high-tone of locally produced 2-AG, and the lack of constitutive activity in the axon is due to the absence of 2-AG.

Our results show important somatodendritic effects on cAMP/PKA regulation for an axonal (i.e., presynaptic) receptor. Previously, CB1R-mediated somatodendritic slow self-inhibition (SSI) was reported in neocortical interneurons (Bacci et al., 2004) and pyramidal neurons (Marinelli et al., 2009). During SSI, activation-induced post-synaptic increase of calcium stimulates somatodendritic DAGL, leading to local 2-AG production and cell-autonomous activation of somatodendritic CB1Rs and G protein inwardly rectifying K^+ (GIRK) channels (Marinelli et al., 2008). Our results are coherent with these observations and extend the mechanical understanding of the phenomenon. βγ subunits of $G_{i/o}$ proteins may directly activate GIRK channels (Lujan et al., 2009). Here we directly demonstrate that such $G_{i/o}$ proteins can be activated by CB1Rs in the somatodendritic region and we show that this activation impacts on local cAMP and PKA activation levels. Therefore, it is likely that SSI-inducing activation leads to a parallel decrease of somatodendritic cAMP levels and to PKA inhibition. Interestingly, while cortical neurons are segregated into sub-populations that respond differently to CB1R activation *ex vivo* (Marinelli et al., 2009), our results, which show a Gaussian distribution in responses (Supplementary Figure 1), suggest that either such sub-populations are not present in hippocampal neurons or that our technique is not sensitive enough to detect such differences. We also report that basal production of 2-AG is both necessary and sufficient to activate $G_{i/o}$ proteins through CB1Rs to achieve measurable constitutive inhibition of somatodendritic cAMP/PKA signaling. GPCRs may also display constitutive activity due to conformational instability (Kenakin, 2004) and several studies reported that CB1Rs may display constitutive activity in systems apparently free of endocannabinoids (review in Pertwee, 2005). However, it is difficult to formally exclude the presence of endocannabinoids, since these lipid molecules may be present in cell plasma membrane at high levels even in non-stimulated neurons (Alger and Kim, 2011).

Here, our results indicate the complete elimination of measurable constitutive somatodendritic CB1R activation after pharmacological inhibition of DAGL and the lack of constitutive activation in the mature axon, where the absence of DAGL suggests low levels of membrane-borne 2-AG. However, a certain level of conformational instability may be necessary to enable constitutive activation of CB1R by 2-AG. Alanine substitution of the T210 residue, which is located in the 3rd transmembrane helix and is well-conserved in the cannabinoid receptor family but absent in other class A GPCRs (D'Antona et al., 2006), results in change of the CB1R conformational state (Simon et al., 2013) and yields a hypoactive receptor form, which displays significantly lower constitutive activity but preserves responsiveness to agonists (D'Antona et al., 2006). Overexpressed T210A mutant CB1Rs accumulate on the somatodendritic surface because of reduced steady-state endocytosis and this accumulation leads to elevated somatodendritic responses to WIN treatment (Simon et al., 2013). To further understand the effect of conformational instability induced by T210 on CB1R signaling, it would be useful in the future to induce the T210A mutation in the endogenous CB1R through a genetic editing approach, in order to avoid the putative effects of receptor overexpression on the signaling response.

CB1R ACTIVATION BY EXOGENOUS CANNABINOIDS IN AXONS DIFFERS FROM THAT IN DENDRITES, WHERE LOCAL 2-AG MODULATES THE RESPONSE TO AGONISTS

Activation of endogenous CB1Rs leads to a stronger decrease of PKA activity in axons compared to dendrites. This difference is not due to the shape of neurites. CB1Rs are enriched in the axonal plasma membrane, leading to approximately 10-fold more endogenous CB1Rs receptors at the plasma membrane in axons as compared to dendrites (McDonald et al., 2007). Here, we observed that the decrease of PKA activity after CB1R activation is about 3-fold stronger in the axon than in dendrites. Thus, differences in sub-neuronal signaling and receptor density are in the same range, suggesting that the main cause of the polarized signaling response is polarized CB1R distribution. Our previous results have shown that polarized spatial distribution of CB1Rs is precisely regulated by steady-state somatodendritic activation and endocytosis coupled to trans-cytotic targeting (Simon et al., 2013), so it is likely that polarized distribution (i.e., somatodendritic segregation) of DAGLα is the principal cause of the polarized distribution of CB1Rs. However, this model is based on previous data obtained by using a highly-sensitive quantitative experimental approach employing overexpressed epitope-tagged CB1Rs and exogenous cannabinoids (Simon et al., 2013). In future studies, it would be interesting to verify this hypothesis with sensitive detection of endogenous CB1R localization and well-controlled modification of cell-autonomous endocannabinoid levels.

Our results also indicate that inhibition of 2-AG synthesis prevents WIN-induced activation of CB1Rs in the somatodendritic compartment, whereas, in the axon, absence of 2-AG leads to a lack of constitutive activity but does not prevent activation by WIN. Presently, possible interactions between 2-AG and WIN on CB1R activation are not clearly understood. CB1R intramembrane loops were proposed to shape a "binding pocket" that 2-AG could reach through a gap allowing lipidic ligands to enter from membrane bilayer, without need of extracellular access (Hurst et al., 2013). Aminoalkylindole cannabinoids such as WIN bind at a different site (McAllister et al., 2003; Hurst et al., 2013), so WIN could act as a positive allosteric modulator for 2-AG, by increasing 2-AG-induced constitutive CB1R activation, leading to enhanced inhibition of cAMP/PKA signaling in the somatodendritic compartment. Interestingly, the agonist CP55,940 binds at a different site than WIN (Kapur et al., 2007) and dissimilarly to WIN, CP55,940-mediated inhibition of somatodendritic PKA activity is significantly stronger after DAGL inhibition. After DAGL inhibition, CB1R levels increase at the somatodendritic plasma membrane because of reduced endocytic elimination (Turu et al., 2007) possibly explaining the enhanced CP effect in the somatodendritic compartment. In the axon, CP-induced PKA activity decrease is not modified by THL, as DAGL is absent in this compartment. Finally, the phytocannabinoid THC induces a decrease of PKA activity in the somatodendritic compartment that is removed after DAGL inhibition. Therefore, neuronal pharmacology of THC is similar to WIN but not to CP, suggesting that THC may also act as an exogenous positive allosteric modulator, that amplifies the CB1R-activating effect of locally produced 2-AG in the somatodendritic compartment. These surprising interactions between 2-AG and exogenous cannabinoid ligands may result from changes in CB1R levels on the somatodendritic surface but also from different, potentially overlapping and to date not completely understood mechanisms, such as conformation-induced changes in ligand affinity and efficiency and competition for ligand binding sites. Full comprehension of these effects requires further technical development that, through enhancing the sensitivity of the experimental approach presented here, may allow detailed pharmacological characterization in the future, such as precise measurement of ligand affinity and efficacy, of endogenous GPCR signaling in neuronal sub-domains.

In conclusion, our results show that pharmacological responses to activation of a major neuronal GPCR are different in axons and dendrites. In the somatodendritic compartment, CB1Rs are constitutively activated by locally produced 2-AG, constitutively inhibit the cAMP/PKA pathway and can be further activated, significantly albeit moderately, by exogenous cannabinoids. A similar activation profile was reported in non-polarized cells (Turu et al., 2007). However, the pharmacological profile of axonal CB1Rs is different: their activation leads to a strong decrease of PKA activity and no significant constitutive activation is observed. This highly contrasted difference in sub-neuronal signaling responses warrants caution in extrapolating pharmacological profiles, which are typically obtained in non-polarized cells, to predict *in vivo* responses of axonal (i.e., presynaptic) GPCRs. Therefore, the *in situ* pharmacological approach presented in our study may also be useful for a better understanding of the physiology of other neuronal GPCRs.

AUTHOR CONTRIBUTIONS

Delphine Ladarre and Zsolt Lenkei designed the experiments, Delphine Ladarre, Alexandre B. Roland, Stefan Biedzinski and Ana Ricobaraza performed the experiments, Delphine Ladarre, and Stefan Biedzinski analyzed the data and Delphine Ladarre and Zsolt Lenkei wrote the paper.

ACKNOWLEDGMENTS

This work was supported by a grant from the ANR (L' Agence Nationale de la Recherche) to Zsolt Lenkei (ANR-09-MNPS-004-01). Ana Ricobaraza was supported by a postdoctoral fellowship from the Basque Country Government. We thank Dr. Christophe Leterrier (Marseille) for discussions and advice and Maureen McFadden for the help with the English syntax.

SUPPLEMENTARY MATERIAL

The Supplementary Material for this article can be found online at: http://www.frontiersin.org/journal/10.3389/fncel.2014.00426/abstract

REFERENCES

Alger, B. E., and Kim, J. (2011). Supply and demand for endocannabinoids. *Trends Neurosci.* 34, 304–315. doi: 10.1016/j.tins.2011.03.003

Bacci, A., Huguenard, J. R., and Prince, D. A. (2004). Long-lasting self-inhibition of neocortical interneurons mediated by endocannabinoids. *Nature* 431, 312–316. doi: 10.1038/nature02913

Bisogno, T., Howell, F., Williams, G., Minassi, A., Cascio, M. G., Ligresti, A., et al. (2003). Cloning of the first sn1-DAG lipases points to the spatial and temporal regulation of endocannabinoid signaling in the brain. *J. Cell Biol.* 163, 463–468. doi: 10.1083/jcb.200305129

Bodor, A. L., Katona, I., Nyiri, G., Mackie, K., Ledent, C., Hajos, N., et al. (2005). Endocannabinoid signaling in rat somatosensory cortex: laminar differences and involvement of specific interneuron types. *J. Neurosci.* 25, 6845–6856. doi: 10.1523/JNEUROSCI.0442-05.2005

Castro, L. R., Gervasi, N., Guiot, E., Cavellini, L., Nikolaev, V. O., Paupardin-Tritsch, D., et al. (2010). Type 4 phosphodiesterase plays different integrating roles in different cellular domains in pyramidal cortical neurons. *J. Neurosci.* 30, 6143–6151. doi: 10.1523/JNEUROSCI.5851-09.2010

Coutts, A. A., Anavi-Goffer, S., Ross, R. A., MacEwan, D. J., Mackie, K., Pertwee, R. G., et al. (2001). Agonist-induced internalization and trafficking of cannabinoid CB1 receptors in hippocampal neurons. *J. Neurosci.* 21, 2425–2433.

D'Antona, A. M., Ahn, K. H., and Kendall, D. A. (2006). Mutations of CB1 T210 produce active and inactive receptor forms: correlations with ligand affinity, receptor stability, and cellular localization. *Biochemistry* 45, 5606–5617. doi: 10.1021/bi060067k

Depry, C., Allen, M. D., and Zhang, J. (2011). Visualization of PKA activity in plasma membrane microdomains. *Mol. Biosyst.* 7, 52–58. doi: 10.1039/c0mb00079e

Freund, T. F., Katona, I., and Piomelli, D. (2003). Role of endogenous cannabinoids in synaptic signaling. *Physiol. Rev.* 83, 1017–1066. doi: 10.1152/physrev.00004.2003

Gervasi, N., Hepp, R., Tricoire, L., Zhang, J., Lambolez, B., Paupardin-Tritsch, D., et al. (2007). Dynamics of PKA signaling at the membrane, in the cytosol, and in the nucleus of neurons in mouse brain slices. *J. Neurosci.* 27, 2744–2750. doi: 10.1523/JNEUROSCI.5352-06.2007

Hillard, C. J., Muthian, S., and Kearn, C. S. (1999). Effects of CB(1) cannabinoid receptor activation on cerebellar granule cell nitric oxide synthase activity. *FEBS Lett.* 459, 277–281. doi: 10.1016/S0014-5793(99)01253-3

Horton, A. C., and Ehlers, M. D. (2003). Neuronal polarity and trafficking. *Neuron* 40, 277–295. doi: 10.1016/S0896-6273(03)00629-9

Howlett, A. C. (2005). Cannabinoid receptor signaling. *Handb. Exp. Pharmacol.* 168, 53–79. doi: 10.1007/3-540-26573-2_2

Howlett, A. C., Reggio, P. H., Childers, S. R., Hampson, R. E., Ulloa, N. M., and Deutsch, D. G. (2011). Endocannabinoid tone versus constitutive activity of cannabinoid receptors. *Br. J. Pharmacol.* 163, 1329–1343. doi: 10.1111/j.1476-5381.2011.01364.x

Hurst, D. P., Schmeisser, M., and Reggio, P. H. (2013). Endogenous lipid activated G protein-coupled receptors: emerging structural features from crystallography and molecular dynamics simulations. *Chem. Phys. Lipids* 169, 46–56. doi: 10.1016/j.chemphyslip.2013.01.009

Kano, M., Ohno-Shosaku, T., Hashimotodani, Y., Uchigashima, M., and Watanabe, M. (2009). Endocannabinoid-mediated control of synaptic transmission. *Physiol. Rev.* 89, 309–380. doi: 10.1152/physrev.00019.2008

Kapur, A., Hurst, D. P., Fleischer, D., Whitnell, R., Thakur, G. A., Makriyannis, A., et al. (2007). Mutation studies of Ser7.39 and Ser2.60 in the human CB1 cannabinoid receptor: evidence for a serine-induced bend in CB1 transmembrane helix 7. *Mol. Pharmacol.* 71, 1512–1524. doi: 10.1124/mol.107.034645

Katona, I., Rancz, E. A., Acsady, L., Ledent, C., Mackie, K., Hajos, N., et al. (2001). Distribution of CB1 cannabinoid receptors in the amygdala and their role in the control of GABAergic transmission. *J. Neurosci.* 21, 9506–9518.

Katona, I., Sperlagh, B., Sik, A., Kafalvi, A., Vizi, E. S., Mackie, K., et al. (1999). Presynaptically located CB1 cannabinoid receptors regulate GABA release from axon terminals of specific hippocampal interneurons. *J. Neurosci.* 19, 4544–4558.

Katona, I., Urban, G. M., Wallace, M., Ledent, C., Jung, K. M., Piomelli, D., et al. (2006). Molecular composition of the endocannabinoid system at glutamatergic synapses. *J. Neurosci.* 26, 5628–5637. doi: 10.1523/JNEUROSCI.0309-06.2006

Kenakin, T. (2004). Principles: receptor theory in pharmacology. *Trends Pharmacol. Sci.* 25, 186–192. doi: 10.1016/j.tips.2004.02.012

Klarenbeek, J. B., Goedhart, J., Hink, M. A., Gadella, T. W., and Jalink, K. (2011). A mTurquoise-based cAMP sensor for both FLIM and ratiometric read-out has improved dynamic range. *PLoS ONE* 6:e19170. doi: 10.1371/journal.pone.0019170

Leterrier, C., Laine, J., Darmon, M., Boudin, H., Rossier, J., and Lenkei, Z. (2006). Constitutive activation drives compartment-selective endocytosis and axonal targeting of type 1 cannabinoid receptors. *J. Neurosci.* 26, 3141–3153. doi: 10.1523/JNEUROSCI.5437-05.2006

Lujan, R., Maylie, J., and Adelman, J. P. (2009). New sites of action for GIRK and SK channels. *Nat. Rev. Neurosci.* 10, 475–480. doi: 10.1038/nrn2668

Marinelli, S., Pacioni, S., Bisogno, T., Di Marzo, V., Prince, D. A., Huguenard, J. R., et al. (2008). The endocannabinoid 2-arachidonoylglycerol is responsible for the slow self-inhibition in neocortical interneurons. *J. Neurosci.* 28, 13532–13541. doi: 10.1523/JNEUROSCI.0847-08.2008

Marinelli, S., Pacioni, S., Cannich, A., Marsicano, G., and Bacci, A. (2009). Self-modulation of neocortical pyramidal neurons by endocannabinoids. *Nat. Neurosci.* 12, 1488–1490. doi: 10.1038/nn.2430

McAllister, S. D., Rizvi, G., Anavi-Goffer, S., Hurst, D. P., Barnett-Norris, J., Lynch, D. L., et al. (2003). An aromatic microdomain at the cannabinoid CB(1) receptor constitutes an agonist/inverse agonist binding region. *J. Med. Chem.* 46, 5139–5152. doi: 10.1021/jm0302647

McDonald, N. A., Henstridge, C. M., Connolly, C. N., and Irving, A. J. (2007). An essential role for constitutive endocytosis, but not activity, in the axonal targeting of the CB1 cannabinoid receptor. *Mol. Pharmacol.* 71, 976–984. doi: 10.1124/mol.106.029348

Neves, S. R., Tsokas, P., Sarkar, A., Grace, E. A., Rangamani, P., Taubenfeld, S. M., et al. (2008). Cell shape and negative links in regulatory motifs together control spatial information flow in signaling networks. *Cell* 133, 666–680. doi: 10.1016/j.cell.2008.04.025

Nomura, D. K., Morrison, B. E., Blankman, J. L., Long, J. Z., Kinsey, S. G., Marcondes, M. C., et al. (2011). Endocannabinoid hydrolysis generates brain prostaglandins that promote neuroinflammation. *Science* 334, 809–813. doi: 10.1126/science.1209200

Pan, X., Ikeda, S. R., and Lewis, D. L. (1998). SR 141716A acts as an inverse agonist to increase neuronal voltage-dependent Ca2+ currents by reversal of tonic CB1 cannabinoid receptor activity. *Mol. Pharmacol.* 54, 1064–1072.

Pertwee, R. G. (2005). Inverse agonism and neutral antagonism at cannabinoid CB1 receptors. *Life Sci.* 76, 1307–1324. doi: 10.1016/j.lfs.2004.10.025

Phillips, R., Ursell, T., Wiggins, P., and Sens, P. (2009). Emerging roles for lipids in shaping membrane-protein function. *Nature* 459, 379–385. doi: 10.1038/nature08147

Simon, A. C., Loverdo, C., Gaffuri, A. L., Urbanski, M., Ladarre, D., Carrel, D., et al. (2013). Activation-dependent plasticity of polarized GPCR distribution on the neuronal surface. *J. Mol. Cell Biol.* 5, 250–265. doi: 10.1093/jmcb/mjt014

Thibault, K., Carrel, D., Bonnard, D., Gallatz, K., Simon, A., Biard, M., et al. (2013). Activation-dependent subcellular distribution patterns of CB1 cannabinoid receptors in the rat forebrain. *Cereb. Cortex* 23, 2581–2591. doi: 10.1093/cercor/bhs240

Turu, G., Simon, A., Gyombolai, P., Szidonya, L., Bagdy, G., Lenkei, Z., et al. (2007). The role of diacylglycerol lipase in constitutive and angiotensin AT1 receptor-stimulated cannabinoid CB1 receptor activity. *J. Biol. Chem.* 282, 7753–7757. doi: 10.1074/jbc.C600318200

Uchigashima, M., Narushima, M., Fukaya, M., Katona, I., Kano, M., and Watanabe, M. (2007). Subcellular arrangement of molecules for 2-arachidonoylglycerol-mediated retrograde signaling and its physiological contribution to synaptic modulation in the striatum. *J. Neurosci.* 27, 3663–3676. doi: 10.1523/JNEUROSCI.0448-07.2007

Yoshida, T., Fukaya, M., Uchigashima, M., Miura, E., Kamiya, H., Kano, M., et al. (2006). Localization of diacylglycerol lipase-alpha around postsynaptic spine suggests close proximity between production site of an endocannabinoid, 2-arachidonoyl-glycerol, and presynaptic cannabinoid CB1 receptor. *J. Neurosci.* 26, 4740–4751. doi: 10.1523/JNEUROSCI.0054-06.2006

Yoshida, T., Uchigashima, M., Yamasaki, M., Katona, I., Yamazaki, M., Sakimura, K., et al. (2011). Unique inhibitory synapse with particularly rich endocannabinoid signaling machinery on pyramidal neurons in basal amygdaloid nucleus. *Proc. Natl. Acad. Sci. U.S.A.* 108, 3059–3064. doi: 10.1073/pnas.1012875108

Conflict of Interest Statement: The authors declare that the research was conducted in the absence of any commercial or financial relationships that could be construed as a potential conflict of interest.

Received: 13 August 2014; accepted: 26 November 2014; published online: 06 January 2015.

Citation: Ladarre D, Roland AB, Biedzinski S, Ricobaraza A and Lenkei Z (2015) Polarized cellular patterns of endocannabinoid production and detection shape cannabinoid signaling in neurons. Front. Cell. Neurosci. ***8****:426. doi: 10.3389/fncel.2014.00426*

This article was submitted to the journal Frontiers in Cellular Neuroscience.

frontiers in Cellular Neuroscience

OPINION
published: 27 March 2015
doi: 10.3389/fncel.2015.00112

Can intracellular cAMP dynamics enable scalable computation?

Ravi Iyengar *

Department of Pharmacology and Systems Therapeutics, Systems Biology Center, Icahn School of Medicine at Mount Sinai, New York, NY, USA

Keywords: cAMP, circuit, networks, adenylyl cyclases, computational modeling

cAMP, an important neuronal intracellular messenger, is produced in a spatially specified manner within neurons such that distinct patterns of elevated cAMP levels can be observed in dendrites. The spatial information encoded in local elevation of cAMP can be transmitted to downstream components such as MAP-kinases (Neves et al., 2008). Such spatially restricted changes in cAMP levels and information flow from cAMP to downstream effectors may enable it to function as a scaling agent for computation by signaling networks Computation within signaling networks may enable integration as well as sorting of signals from multiple receptors and channels. The output of signaling network computation can define thresholds for switching between states, temporal resolution of responses as well as other alterations to signal/response relationships. An intriguing question is whether such computation within signaling networks can be manifested in changes of electrical activity patterns of neuronal circuits.

The ability of cAMP to serve as an agent of scalability whereby computation within signaling networks can be manifested as altered patterns of circuit activity arising from two other major factors: (a) The production of cAMP is controlled by the expression of multiple adenylyl cyclases within a neuron that integrate signals from different receptor types and channels in a mix and match format (Pieroni et al., 1993). (b) cAMP has its effects through multiple effectors. These include protein kinase A, the cAMP-dependent GEFs and the cyclic nucleotide gated channels (HCN channels). The multiplicity of adenylyl cyclases provides (Pieroni et al., 1993; Jordan et al., 2000) for a rich capability to compute relationships between different input signals and have this computation reflected in net changes in local cAMP levels. (**Figure 1A** upper part) The multiplicity of effectors ensures that cAMP dynamics can be captured across different time scales from acute electrophysiological effects mediated by the HCN channels to medium term effects mediated by regulation of phosphorylation of other channels and longer term effects such as changes in gene expression mediated by PKA or by cAMP GEFs that can through Rap regulate the activity of MAP-kinases (**Figure 1A** lower). Regulation of gene expression by both PKA and MAP-kinases enables cells to alter the levels of numerous components within these signaling networks and thus can further enhance the computational capability of the cAMP signaling network in different regions of the neurons.

The role of the direct binding of cAMP to HCNs and regulating the activity of these channels is particularly relevant for its ability to act as a scaling agent. HCN channels are hyperpolarizing and are activated by a combination of membrane depolarization and cAMP binding. Local changes in cAMP levels in dendrites coupled with differential distribution of HCNs that are localized in the distal dendrites in pyramidal neurons (Magee, 1998) can regulate excitability in the hippocampus. In other types of neurons the HCN channels are localized to other regions within the neurons (Magee, 1998) and can thus regulate differing types of electrophysiological responses. In addition to directly controlling the HCN channels, cAMP, through protein kinase A regulates the insertion of AMPA channels into the postsynaptic region thus regulating synaptic excitability. This regulation is controlled by a dense network involving both phosphodiesterases as well as MAP-kinases (Song et al., 2013) thus allowing for additional computational

Edited by:
Nicholas C. Spitzer, University of California, San Diego, USA

Reviewed by:
Panagiota T. Foteinou, The Johns Hopkins University, USA

***Correspondence:**
Ravi Iyengar, ravi.iyengar@mssm.edu

Received: *12 November 2014*
Paper pending published: *24 December 2014*
Accepted: *11 March 2015*
Published: *27 March 2015*

Citation:
Iyengar R (2015) Can intracellular cAMP dynamics enable scalable computation? Front. Cell. Neurosci. 9:112. doi: 10.3389/fncel.2015.00112

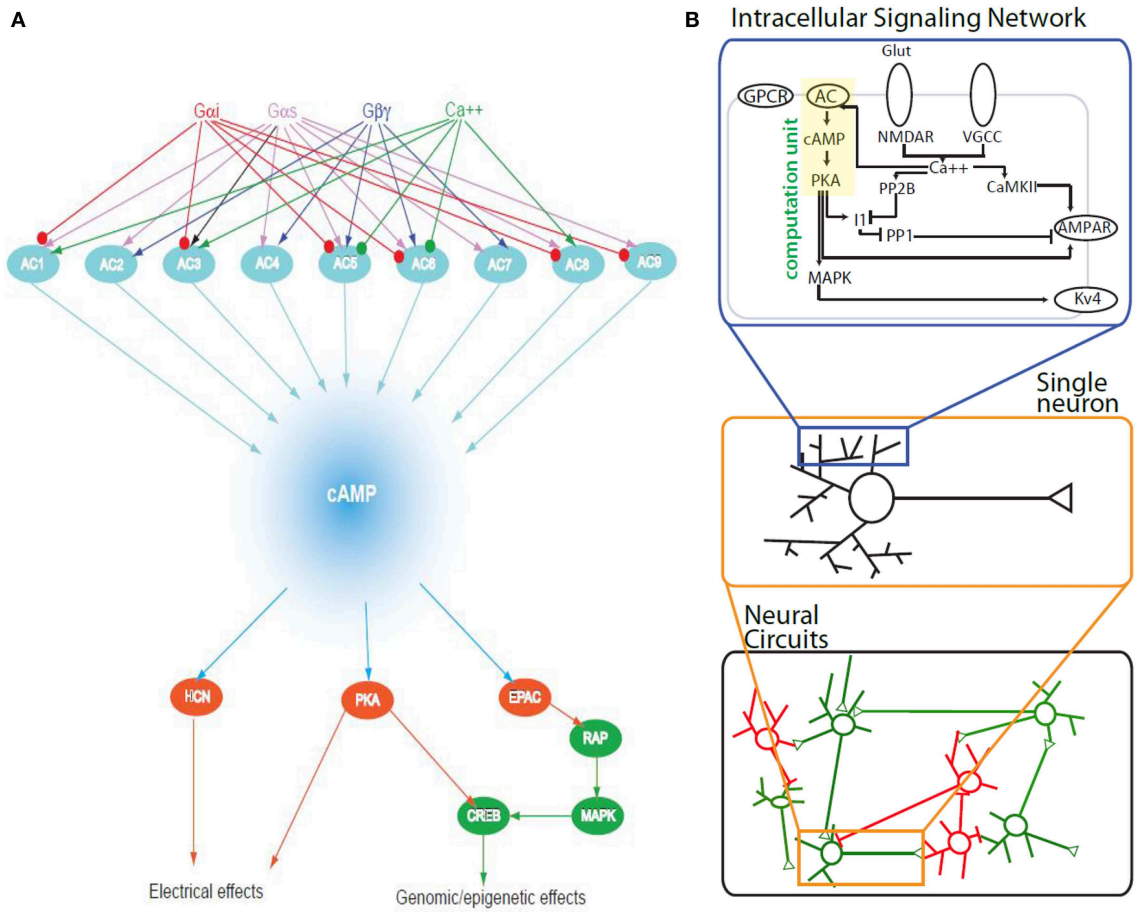

FIGURE 1 | (A) The cAMP signaling network organized for computing. In this simplified bow-tie diagram the ability of different adenylyl cyclases to receive signals from different G proteins that couple to different types of receptors as well as from calcium is shown as the upper half. Integration of these signals can be reflected in the levels of cAMP which may represent different types of computation such as addition, subtraction or multiplication. The bottom half of the bowtie shows effectors of cAMP that include ion channels, protein kinases and guanine nucleotide exchange factors such as EPAC that respond to changes in cAMP levels and thus change cellular responses at different time spaces. **(B)** A schematic representation of the scaling of computation within the cAMP signaling network. Upper panel represents the cAMP cell signaling network within spines and dendrites. Computation within such a single network can alter the ability of a neuron to display a firing pattern (middle panel). When such a neuron is part of a circuit it can alter the electrical activity of the circuit that in turn can result in change in organismal behavior.

capability depending on both transcriptional and translational control. PKA also controls NMDA-type channels and voltage gated calcium channels by phosphorylation (Gray et al., 1998). Taken together, cAMP regulation of all these channels allows for a varied expression of electrophysiological responses of individual neurons in response to changes in cAMP levels in different subdomains. Since the specialized shape of the neuron can effectively restrict changes in cAMP levels to different regions the information from cell shape such as dendritic arborization can be coupled to electrophysiological activity through the local levels of cAMP. Further since the net level of cAMP is reflective of the computation that occurs due to the presence of multiple adenylyl cyclase isoforms and their differential regulation it can be readily seen how computation within signaling networks can be expressed as altered electrophysiological responses in individual neurons.

For the relationship between local cAMP levels and the overall electrophysiological response of the neuron to be scalable, the altered excitability of the individual neuron needs to be reflected in the overall electrical behavior of the circuit of which the neuron is a part. At this level there is little experimental data that would allow us to build specific conjectures that one can turn into experimental or computationally testable hypothesis. For this, two classes of data are needed anatomical/physiological connectivity between neurons and biochemical activity in individual cells as part of a functional tissue.

The first class of data that is part anatomical and part electrophysiological is being called connectomics. We need to get a first–pass description of the organization of the circuit at the level of individual neurons and their connections. So far this is only known in the worm (Jarrell et al., 2012), which has only 302 neurons (White et al., 1986). We need to identify how the excitatory neurons, inhibitory interneurons and glial cells are connected to one another within a functional circuit, and determine that the anatomically observed synapses are electrically active. We also

need to know how the modulatory inputs into the circuit are organized since modulatory regulation, such as those by adrenergic receptors, play a major role in tuning neuronal function at a cellular level. Furthermore, we need to identify the regulatory network motifs such as both feedfoward paths through interneurons as well as short and long range feedback loops if they exist. Even for an extensively studied region such as the CA3-CA1 region of the hippocampus detailed circuit topology is not yet available for rodents or humans. Hopefully as the ambitious BRAIN project takes shape newer technologies will help gain such knowledge.

The second class of data we need is measurements of biochemical activities in individual cells when cells are part of functional circuitries and how such biochemical activity is related to cellular electrophysiology. Initially such cell-based measurements within tissue may be conducted *in vitro* such as in brain slices but eventually we are going to need information regarding biochemical activities at the cellular level *in vivo*. The cAMP network can serve as a prototype for such studies since the cAMP live cell imaging probes that are used in cultured neuron experiments also work in the tissues (Castro et al., 2010). Studies of cAMP levels in hippocampal slices (Castro et al., 2010) are in agreement with computational predictions developed using kinetic parameters estimated from purified proteins (Neves et al., 2008). This type of quantitative convergence indicates that we should be able to develop computational models that can make useful predictions regarding regulation of signal flow within intracellular signaling networks controlling electrical output. A recent study using live cell imaging of cAMP dynamics in mouse tissue nicely demonstrates the potential for pathway analysis and study of physiological responses (Castro et al., 2013).

If the experimental technologies are developed to get connectomics data in the various brain regions and imaging advances allow us to follow biochemical activities of one or a few neurons as they function within tissue, in combination with multielectrode recording of circuits, then we should be able to obtain scalable information of how and when computation within signaling networks are manifested in changes in circuit behavior. Such studies beyond providing fundamental understanding of information processing in the brain may help us understanding ageing as well as pathophysiology induced cognitive decline. A number of components of the cAMP signaling pathways and cAMP regulated genes such as BDNF change with age and such changes are associated with cognitive deficits both in normal ageing and pathophysiology such as Alzheimer's disease (Hansen and Zhang, 2013). One hypothesis could be that reduced capability of biochemical computations when transmitted to circuit level functions results in observed cognitive deficit. Alternatively, damage to circuit connectivity could result in inability of the circuit to convert biochemical computation in into altered organismal behaviors. So from both basic knowledge and disease mechanism viewpoints a question of particular interest for me is what circuit configurations at the multicellular level (i.e., connectivity between neurons) enable explicit manifestation of biochemical computation within signaling networks as functionally altered electrophysiological responses of neuronal circuits that in turn evoke different behaviors in the intact animals. Some circuit configurations may enable computations within signaling networks to be manifested as organismal behaviors while with other circuit configurations computation at the circuit level may drive behavioral responses. Current efforts such as the BRAIN project indicate that we should be able to design and conduct such experiments and build computational models to understand such multiscale functions. (**Figure 1B**) Here too studies on the cAMP systems could lead the way as it did when we started to move from pathways to networks (Pieroni et al., 1993; Iyengar, 1996).

Acknowledgments

I thank Dr. Susana Neves for comments on the manuscript and drawing the figures. Research in my laboratory is supported by GM54508 and GM 072853 and computational resources provided by the Systems Biology Center grant P50- GM071558.

References

Castro, L. R., Brito, M., Guiot, E., Polito, M., Korn, C. W., Hervé, D. et al. (2013). Striatal neurones have a specific ability to respond to phasic dopamine release. *J. Physiol.* 591, 3197–3214. doi: 10.1113/jphysiol.2013.252197

Castro, L. R., Gervasi, N., Guiot, E., Cavellini, L., Nikolaev, V. O., Paupardin-Tritsch, D., et al. (2010). Type 4 phosphodiesterase plays different integrating roles in different cellular domains in pyramidal cortical neurons. *J. Neurosci.* 30, 6143–6151. doi: 10.1523/JNEUROSCI.5851-09.2010

Gray, P. C., Scott, J. D., and Catterall, W. A. (1998). Regulation of ion channels by cAMP-dependent protein kinase and A-kinase anchoring proteins. *Curr. Opin. Neurobiol.* 8, 330–334. doi: 10.1016/S0959-4388(98)80057-3

Hansen, R. T. III., and Zhang, H.-T. (2013). Senescent–induced dysregulation of cAMP/CREB signaling and correlations with cognitive declines. *Brain Res.* 1516, 93–109. doi: 10.1016/j.brainres.2013.04.033

Iyengar, R. (1996). Gating by cyclic AMP: expanded role for an old signaling pathway. *Science* 271, 461–463. doi: 10.1126/science.271.5248.461

Jarrell, T. A., Wang, Y., Bloniarz, A. E., Brittin, C. A., Xu, M., Thomson, J. N., et al. (2012). The connectome of a decision-making neural network. *Science* 337, 437–444. doi: 10.1126/science.1221762

Jordan, J. D., Landau, E. M., and Iyengar, R. (2000). Signaling networks: the origins of cellular multitasking. *Cell* 103, 193–200. doi: 10.1016/S0092-8674(00)00112-4

Magee, J. C. (1998). Dendritic hyperpolarization-activated currents modify the integrative properties of hippocampal CA1 pyramidal neurons. *J. Neurosci.* 18, 7613–7624.

Neves, S. R., Tsokas, P., Sarkar, A., Grace, E. A., Rangamani, P., Taubenfeld, S.M., et al. (2008). Cell shape and negative links in regulatory motifs together control spatial information flow in signaling networks. *Cell* 133, 666–680. doi: 10.1016/j.cell.2008.04.025

Pieroni, J. P., Jacobowitz, O., Chen, J., and Iyengar, R. (1993). Signal recognition and integration by Gs-stimulated adenylyl cyclases. *Curr. Opin. Neurobiol.* 3, 345–345. doi: 10.1016/0959-4388(93)90127-K

Song, R. S., Massenburg, B., Wenderski, W., Jayaraman, V., Thompson, L., and Neves, S.R. (2013). ERK regulation of phosphodiesterase 4 enhances dopamine-stimulated AMPA receptor membrane insertion. *Proc. Natl. Acad. Sci. U.S.A.* 110, 15437–15434. doi: 10.1073/pnas.1311783110

White, J. G., Southgate, E., Thomson, J. N., and Brenner, S. (1986). The structure of the nervous system of the nematode *Caenorhadtis elegans*.

Philos. Trans. R. Soc. Lond B Biol. Sci. 314, 1–340. doi: 10.1098/rstb.1986.0056

Conflict of Interest Statement: The authors declare that the research was conducted in the absence of any commercial or financial relationships that could be construed as a potential conflict of interest.

frontiers in
CELLULAR NEUROSCIENCE

OPINION ARTICLE
published: 14 October 2014
doi: 10.3389/fncel.2014.00321

PKA modulation of Rac in neuronal cells

Akihiro Goto, Yuji Kamioka and Michiyuki Matsuda*

Department of Pathology and Biology of Diseases, Graduate School of Medicine, Kyoto University, Kyoto, Japan
**Correspondence: matsuda.michiyuki.2c@kyoto-u.ac.jp*

Edited by:
Pierre Vincent, Centre National de la Recherche Scientifique, France

Reviewed by:
Olivier C. G. Gavet, Institut Gustave Roussy, France
Jean-vianney Barnier, Centre National de la Recherche Scientifique, France

Keywords: PKA, Rac, guanine nucleotide exchange factor, migration

The Rho-family GTPase, Rac, is a molecular switch that controls actin dynamics and thereby the morphology, migration, and cytokinesis of most, if not all, cell types (Heasman and Ridley, 2008). Neuronal cells are not an exception, although Rac-regulated replication and migration are limited mostly to the embryonic stages (Luo, 2000; Tashiro and Yuste, 2004; Fuchs et al., 2009; Govek et al., 2011). Recently, it has also been shown that Rac is required for proliferative production and retention of new neurons generated during learning, indicating that Rac also regulates higher brain function (Haditsch et al., 2013). This small molecular switch is able to bring about so many different outcomes because it is embedded in many circuits, each of which comprises of a number of signaling molecules. Therefore, the function and regulation of Rac are inevitably cell context-dependent.

Protein kinase A (PKA), a canonical signal transducer of cAMP, plays pivotal roles in neuronal outgrowth, survival and regeneration (Qiu et al., 2002) and in axonal guidance (Song et al., 1998; Tojima et al., 2011). PKA activity is also required for the migration of enteric neural crest-derived cells during development of the enteric nervous system (Barlow et al., 2003; Asai et al., 2006). These observations suggest that PKA may regulate Rac to induce s a number of morphological changes. Here, we focus on the regulation of Rac by PKA in neuronal cells.

The direct upstream input to Rac comes from guanine nucleotide exchange factors (GEFs) and GTPase-activating proteins (**Figure 1A**). Among Ras-superfamily small GTPases, Rac, and Cdc42, a close relative of Rac1, are unique in that they are activated by two structurally unrelated families of GEFs, the classical Dbl homology-pleckstrin homology domain-containing GEFs (Cook et al., 2014) and the DOCK180-related atypical GEFs (Laurin and Cote, 2014). Among the more than 60 Dbl-family GEFs, Tiam1, STEF/Tiam2, P-Rex1, and Vav3 have been shown to regulate the migration of neuronal progenitor cells and neurite extension of neurons (Govek et al., 2011). On the other hand, studies with knockout mice or gene silencing of DOCK-family genes have revealed that DOCK3/MOCA deficiency leads to axonal degeneration and sensorimotor impairments (Chen et al., 2009), that DOCK6 is required for axon extension in dorsal root ganglion neurons (Miyamoto et al., 2013), and that DOCK7 regulates the interkinetic nuclear migration of radial glial progenitor cells (Yang et al., 2012).

At one level above GEF are various serine/threonine kinases, which phosphorylate GEFs and thereby activate or inactivate them. PKA is a good candidate for such a serine/threonine kinase; however, there have been no direct demonstrations of PKA regulation of GEFs for Rac, except for a few examples, in neuronal cells. In PC12D cells, PKA phosphorylates and activates a Rac GEF, STEF/Tiam2, and induces neurite extension (Goto et al., 2011). On the other hand, phosphorylation of P-Rex1, another GEF, has been shown to suppress GEF activity in HEK293T cells (Mayeenuddin and Garrison, 2006; Barber et al., 2012). Although knockout mice of P-Rex1 exhibit cerebellar dysfunction (Donald et al., 2008), it is unknown whether the PKA-P-Rex1 axis operates in neuronal cells. Less is known about the direct link between PKA and DOCK-family GEFs. Only recently it has been shown that, in glioblastoma cells, PKA phosphorylates and stimulates DOCK180 and thereby promotes growth and invasion (Feng et al., 2014).

Additional complexity comes from the regulation by phosphoinositides and phosphatidic acid. Although the Dbl-family GEFs and the DOCK-family GEFs are structurally unrelated, both GEFs are regulated by phosphoinositides or phosphatidic acid, which are bound to the PH domain in the Dbl-family GEFs or the DHR-2 domain in the DOCK-family GEFs (Cook et al., 2014; Laurin and Cote, 2014). Considering the pleiotropic effects of PKA, it is likely that PKA regulates Rac by controlling the levels of phosphoinositides and phosphatidic acid. For example, PKA has been shown to activate phosphatidylinositol 3-kinase (PI3K) via p85 subunit phosphorylation (Cosentino et al., 2006). In another report, however, PKA was shown to inhibit PI3K via p110 subunit phosphorylation (Perino et al., 2011). Therefore, the effect of PKA on PI3K is cell context-dependent. The development of probes for phosphoinositides and phosphatidic acid will help to resolve this issue (Nishioka et al., 2010). Finally, PKA can directly inhibit Rac1 by phosphorylating at Ser 71 during bacterial infection (Brandt et al., 2009).

Furthermore, Bachmann et al. have reported a direct binding of Rac1 with PKA by GFP complementation assay (Bachmann et al., 2013). The PKA-Rac1 axis functions to activate ERK MAP kinase and thereby regulates cell proliferation. It should be studied further whether the

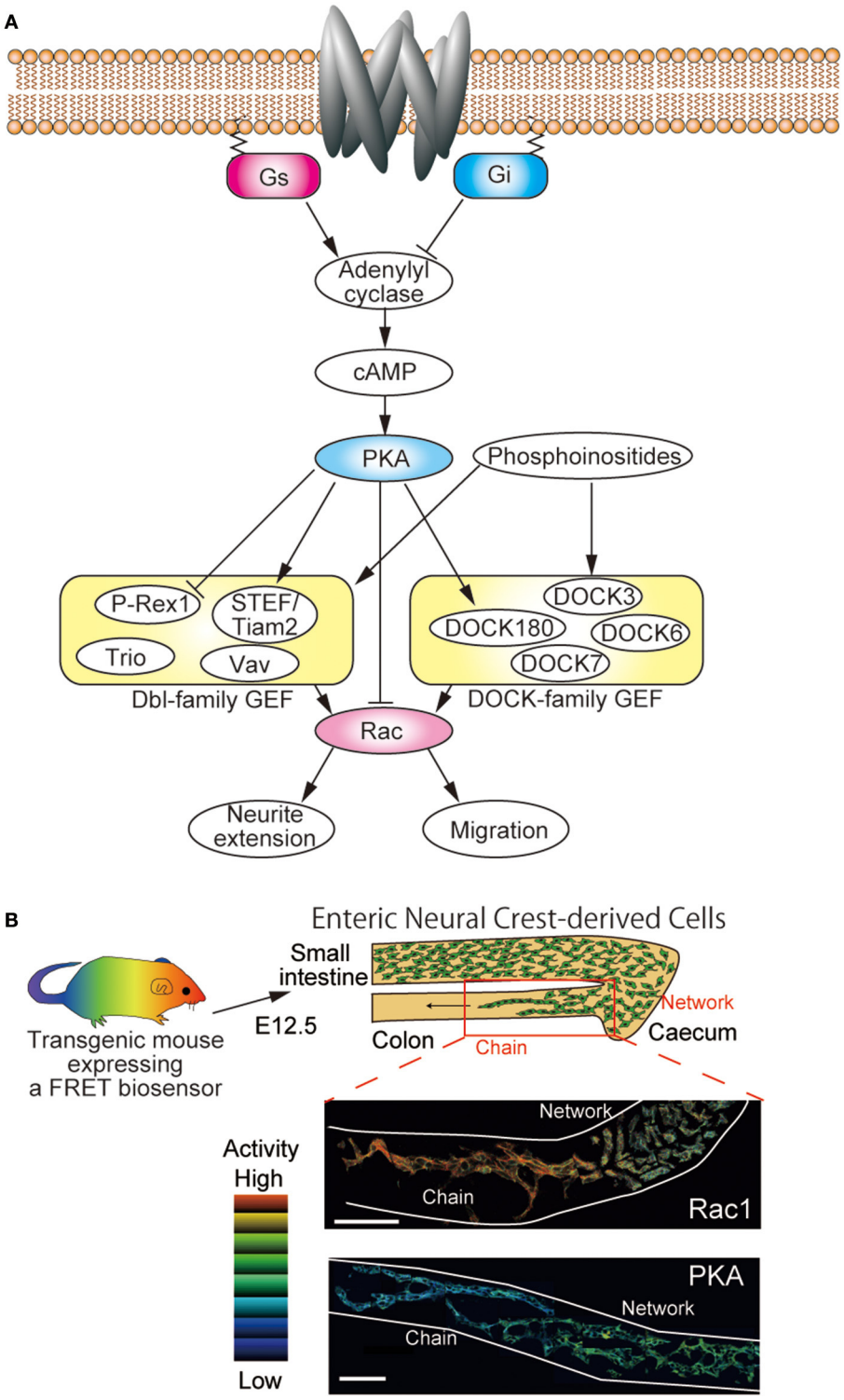

FIGURE 1 | Regulation of Rac by PKA in neuronal cells. (A) Schematic view of the regulatory network of Rac in neuronal cells. Neuronal cells express both Dbl-family and DOCK-family GEFs. Among them, P-Rex1, STEF/Tiam2, and DOCK180 have been shown to be phosphorylated by PKA. Rac activity is required for neurite extension, migration, and so on. **(B)** Transgenic mice expressing FRET biosensors can be used to examine the *in vivo* activities of Rac1 and PKA. Embryonic intestines of E12.5 derived from transgenic mice expressing a FRET biosensor for either Rac1 or PKA were observed under two-photon microscopes. FRET images were prepared to show the activity of Rac1 and PKA. Enteric neural crest cells (ENCCs) migrate from the stomach to the colon during development. The ENCCs that migrate rapidly in chains exhibit higher Rac1 activity and lower PKA activity than the ENCCs that form a neural network.

PKA-Rac1 axis functions also in neuronal cells.

Due to the complexity and cell context-dependency of the regulatory networks where PKA and Rac are embedded, the role played by PKA in the regulation of Rac and the resulting morphological changes are almost entirely unpredictable *in vivo*. Thus, the activities of PKA and Rac should be examined together with biological outputs such as migration and neurite extension. To accomplish such comprehensive investigation, transgenic mice expressing biosensors based on the principle of Förster resonance energy transfer (FRET) were developed recently (Kamioka et al., 2012; Johnsson et al., 2014). By observing the embryonic intestines of transgenic mice expressing FRET biosensors for PKA and Rac1, clear reciprocal activation of PKA and Rac1 has been demonstrated in migrating enteric neural crest-derived cells (**Figure 1B**) (Goto et al., 2013). Currently, simultaneous observation of two FRET biosensors is a difficult task, but recent advent of bright infrared fluorescence will open a way to use two different FRET biosensors to visualize the interplay by two different signaling molecules in a single cell.

Further insight into the role played by PKA and Rac1 will be obtained by modulating the activity of Rac1 or PKA. Inhibitors against Rac1 and PKA are available; however, there is a critical problem for *in vivo* or *ex vivo* experiment. By the conventional bath application of reagents, we cannot tell whether the reagent affected the neuronal cells directly or indirectly via surrounding cells. Application of caged cAMP analogs or optogenetic tools such as light-activatable Rac1 (Wu et al., 2009) to the FRET biosensor-expressing mice will overcome this problem and help us to untangle the complex signaling networks that regulate the morphological changes of neuronal cells.

ACKNOWLEDGMENTS

Michiyuki Matsuda was supported by the Platform for Dynamic Approaches to Living System and by a Grant-in-Aid for Scientific Research on the Innovative Area "Fluorescence Live Imaging" (No. 22113002) from the Ministry of Education, Culture, Sports, Science, and Technology (MEXT). The authors have no conflicting financial interests.

REFERENCES

Asai, N., Fukuda, T., Wu, Z., Enomoto, A., Pachnis, V., Takahashi, M., et al. (2006). Targeted mutation of serine 697 in the Ret tyrosine kinase causes migration defect of enteric neural crest cells. *Development* 133, 4507–4516. doi: 10.1242/dev.02616

Bachmann, V. A., Riml, A., Huber, R. G., Baillie, G. S., Liedl, K. R., Valovka, T., et al. (2013). Reciprocal regulation of PKA and Rac signaling. *Proc. Natl. Acad. Sci. U.S.A.* 110, 8531–8536. doi: 10.1073/pnas.1215902110

Barber, M. A., Hendrickx, A., Beullens, M., Ceulemans, H., Oxley, D., Thelen, S., et al. (2012). The guanine-nucleotide-exchange factor P-Rex1 is activated by protein phosphatase 1alpha. *Biochem. J.* 443, 173–183. doi: 10.1042/bj20112078

Barlow, A., de Graaff, E., and Pachnis, V. (2003). Enteric nervous system progenitors are coordinately controlled by the G protein-coupled receptor EDNRB and the receptor tyrosine kinase RET. *Neuron* 40, 905–916. doi: 10.1016/S0896-6273(03)00730-X

Brandt, S., Kenny, B., Rohde, M., Martinez-Quiles, N., and Backert, S. (2009). Dual infection system identifies a crucial role for PKA-mediated serine phosphorylation of the EPEC-Tir-injected effector protein in regulating Rac1 function. *Cell. Microbiol.* 11, 1254–1271. doi: 10.1111/j.1462-5822.2009.01330.x

Chen, Q., Peto, C. A., Shelton, G. D., Mizisin, A., Sawchenko, P. E., and Schubert, D. (2009). Loss of modifier of cell adhesion reveals a pathway leading to axonal degeneration. *J. Neurosci.* 29, 118–130. doi: 10.1523/jneurosci.3985-08.2009

Cook, D. R., Rossman, K. L., and Der, C. J. (2014). Rho guanine nucleotide exchange factors: regulators of Rho GTPase activity in development and disease. *Oncogene* 33, 4021–4035. doi: 10.1038/onc.2013.362

Cosentino, C., Di Domenico, M., Porcellini, A., Cuozzo, C., De Gregorio, G., Santillo, M. R., et al. (2006). p85 regulatory subunit of PI3K mediates cAMP-PKA and estrogens biological effects on growth and survival. *Oncogene* 26, 2095–2103. doi: 10.1038/sj.onc.1210027

Donald, S., Humby, T., Fyfe, I., Segonds-Pichon, A., Walker, S. A., Andrews, S. R., et al. (2008). P-Rex2 regulates Purkinje cell dendrite morphology and motor coordination. *Proc. Natl. Acad. Sci. U.S.A.* 105, 4483–4488. doi: 10.1073/pnas.0712324105

Feng, H., Hu, B., Vuori, K., Sarkaria, J. N., Furnari, F. B., Cavenee, W. K., et al. (2014). EGFRvIII stimulates glioma growth and invasion through PKA-dependent serine phosphorylation of Dock180. *Oncogene* 33, 2504–2512. doi: 10.1038/onc.2013.198

Fuchs, S., Herzog, D., Sumara, G., Buchmann-Moller, S., Civenni, G., Wu, X., et al. (2009). Stage-specific control of neural crest stem cell proliferation by the small rho GTPases Cdc42 and Rac1. *Cell Stem Cell* 4, 236–247. doi: 10.1016/j.stem.2009.01.017

Goto, A., Hoshino, M., Matsuda, M., and Nakamura, T. (2011). Phosphorylation of STEF/Tiam2 by protein kinase A is critical for Rac1 activation and neurite outgrowth in dibutyryl cAMP-treated PC12D cells. *Mol. Biol. Cell* 22, 1780–1790. doi: 10.1091/mbc.E10-09-0783

Goto, A., Sumiyama, K., Kamioka, Y., Nakasyo, E., Ito, K., Iwasaki, M., et al. (2013). GDNF and endothelin 3 regulate migration of enteric neural crest-derived cells via protein kinase A and Rac1. *J. Neurosci.* 33, 4901–4912. doi: 10.1523/JNEUROSCI.4828-12.2013

Govek, E. E., Hatten, M. E., and Van Aelst, L. (2011). The role of Rho GTPase proteins in CNS neuronal migration. *Dev. Neurobiol.* 71, 528–553. doi: 10.1002/dneu.20850

Haditsch, U., Anderson, M. P., Freewoman, J., Cord, B., Babu, H., Brakebusch, C., et al. (2013). Neuronal Rac1 is required for learning-evoked neurogenesis. *J. Neurosci.* 33, 12229–12241. doi: 10.1523/jneurosci.2939-12.2013

Heasman, S. J., and Ridley, A. J. (2008). Mammalian Rho GTPases: new insights into their functions from *in vivo* studies. *Nat. Rev. Mol. Cell Biol.* 9, 690–701. doi: 10.1038/nrm2476

Johnsson, A. K., Dai, Y., Nobis, M., Baker, M. J., McGhee, E. J., Walker, S., et al. (2014). The Rac-FRET mouse reveals tight spatiotemporal control of rac activity in primary cells and tissues. *Cell Rep.* 6, 1153–1164. doi: 10.1016/j.celrep.2014.02.024

Kamioka, Y., Sumiyama, K., Mizuno, R., Sakai, Y., Hirata, E., Kiyokawa, E., et al. (2012). Live imaging of protein kinase activities in transgenic mice expressing FRET biosensors. *Cell Struct. Funct.* 37, 65–73. doi: 10.1247/csf.11045

Laurin, M., and Cote, J. F. (2014). Insights into the biological functions of Dock family guanine nucleotide exchange factors. *Genes Dev.* 28, 533–547. doi: 10.1101/gad.236349.113

Luo, L. (2000). Rho GTPases in neuronal morphogenesis. *Nat. Rev. Neurosci.* 1, 173–180. doi: 10.1038/35044547

Mayeenuddin, L. H., and Garrison, J. C. (2006). Phosphorylation of P-Rex1 by the cyclic AMP-dependent protein kinase inhibits the phosphatidylinositiol (3,4,5)-trisphosphate and Gbetagamma-mediated regulation of its activity. *J. Biol. Chem.* 281, 1921–1928. doi: 10.1074/jbc.M506035200

Miyamoto, Y., Torii, T., Yamamori, N., Ogata, T., Tanoue, A., and Yamauchi, J. (2013). Akt and PP2A reciprocally regulate the guanine nucleotide exchange factor Dock6 to control axon growth of sensory neurons. *Sci. Signal.* 6, ra15. doi: 10.1126/scisignal.2003661

Nishioka, T., Frohman, M. A., Matsuda, M., and Kiyokawa, E. (2010). Heterogeneity of phosphatidic acid levels and distribution at the plasma membrane in living cells as visualized by a Foerster resonance energy transfer (FRET) biosensor. *J. Biol. Chem.* 285, 35979–35987. doi: 10.1074/jbc.M110.153007

Perino, A., Ghigo, A., Ferrero, E., Morello, F., Santulli, G., Baillie, G. S., et al. (2011). Integrating cardiac PIP3 and cAMP signaling through a PKA anchoring function of p110gamma. *Mol. Cell* 42, 84–95. doi: 10.1016/j.molcel.2011.01.030

Qiu, J., Cai, D., Dai, H., McAtee, M., Hoffman, P. N., Bregman, B. S., et al. (2002). Spinal axon regeneration induced by elevation of cyclic AMP. *Neuron* 34, 895–903. doi: 10.1016/S0896-6273(02)00730-4

Song, H., Ming, G., He, Z., Lehmann, M., McKerracher, L., Tessier-Lavigne, M., et al. (1998). Conversion of neuronal growth cone responses from repulsion to attraction by cyclic nucleotides. *Science* 281, 1515–1518. doi: 10.1126/science.281.5382.1515

Tashiro, A., and Yuste, R. (2004). Regulation of dendritic spine motility and stability by Rac1 and Rho kinase: evidence for two forms of spine motility. *Mol. Cell. Neurosci.* 26, 429–440. doi: 10.1016/j.mcn.2004.04.001

Tojima, T., Hines, J. H., Henley, J. R., and Kamiguchi, H. (2011). Second messengers and membrane trafficking direct and organize growth cone steering. *Nat. Rev. Neurosci.* 12, 191–203. doi: 10.1038/nrn2996

Wu, Y. I., Frey, D., Lungu, O. I., Jaehrig, A., Schlichting, I., Kuhlman, B., et al. (2009). A genetically encoded photoactivatable Rac controls the motility of living cells. *Nature* 461, 104–108. doi: 10.1038/nature08241

Yang, Y. T., Wang, C. L., and Van Aelst, L. (2012). DOCK7 interacts with TACC3 to regulate interkinetic nuclear migration and cortical neurogenesis. *Nat. Neurosci.* 15, 1201–1210. doi: 10.1038/nn.3171

Conflict of Interest Statement: The authors declare that the research was conducted in the absence of any commercial or financial relationships that could be construed as a potential conflict of interest.

Received: 30 June 2014; accepted: 24 September 2014; published online: 14 October 2014.

Citation: Goto A, Kamioka Y and Matsuda M (2014) PKA modulation of Rac in neuronal cells. Front. Cell. Neurosci. ***8****:321. doi: 10.3389/fncel.2014.00321*

This article was submitted to the journal Frontiers in Cellular Neuroscience.

frontiers in
CELLULAR NEUROSCIENCE

REVIEW ARTICLE
published: 13 November 2014
doi: 10.3389/fncel.2014.00376

Intermingled cAMP, cGMP and calcium spatiotemporal dynamics in developing neuronal circuits

Stefania Averaimo [1,2,3] ***and Xavier Nicol*** [1,2,3] *******

[1] *UMR_7210, Centre National de la Recherche Scientifique, Paris, France*
[2] *UMR_S 968, Institut de la Vision, Sorbonne Universités, UPMC Univ Paris 06, Paris, France*
[3] *U968, Institut National de la Santé et de la Recherche Médicale, Paris, France*

Edited by:
Nicholas C. Spitzer, University of California, San Diego, USA

Reviewed by:
Claudia Lodovichi, Venetian Institute of Molecular Medicine, Italy
Alberto Pereda, Albert Einstein College of Medicine, USA

****Correspondence:***
Xavier Nicol, UMR_S 968, Institut de la Vision, Sorbonne Universités, UPMC Univ Paris 06, 17 Rue Moreau, Paris F-75012, France
e-mail: xavier.nicol@inserm.fr

cAMP critically modulates the development of neuronal connectivity. It is involved in a wide range of cellular processes that require independent regulation. However, our understanding of how this single second messenger achieves specific modulation of the signaling pathways involved remains incomplete. The subcellular compartmentalization and temporal regulation of cAMP signals have recently been identified as important coding strategies leading to specificity. Dynamic interactions of this cyclic nucleotide with other second messenger including calcium and cGMP are critically involved in the regulation of spatiotemporal control of cAMP. Recent technical improvements of fluorescent sensors facilitate cAMP monitoring, whereas optogenetic tools permit spatial and temporal control of cAMP manipulations, all of which enabled the direct investigation of spatiotemporal characteristics of cAMP modulation in developing neurons. Focusing on neuronal polarization, neurotransmitter specification, axon guidance, and refinement of neuronal connectivity, we summarize herein the recent advances in understanding the features of cAMP signals and their dynamic interactions with calcium and cGMP involved in shaping the nervous system.

Keywords: cAMP, cGMP, calcium, subcellular compartmentalization, kinetics, axon outgrowth, axon guidance, topographic maps

INTRODUCTION

The development of nervous system connectivity is a multistage process that requires neuron specification and polarization, axon guidance and targeting, as well as refinement of synaptic connections. All stages require second messenger cascades involving cAMP. This cyclic nucleotide is required for the control of transcription (Pham et al., 2001; Root et al., 2008), involved in polarizing immature neurons (Shelly et al., 2010), promotes axon outgrowth (Roisen et al., 1972; Cai et al., 2001; Shewan et al., 2002; Corredor et al., 2012), and regulates the response of growing axons to guidance molecules (Song et al., 1997; Höpker et al., 1999; Nishiyama et al., 2003; Nicol et al., 2006b). Later during development, cAMP is crucial for the refinement of neuronal connectivity and the precise choice of synaptic partners (Welker et al., 1996; Ravary et al., 2003). It is also involved in a wide range of cellular processes that are not related to the development of neuronal connectivity including sugar and lipid metabolism. However, we still have a very partial understanding of how this second messenger can achieve specificity for each of its downstream pathways.

Although the influence of cAMP on the developing nervous system has been identified decades ago, the shape, duration or subcellular localization of its variations in living neurons is still elusive. The spatiotemporal attributes of cAMP signals might provide the bases of a code explaining the specificity of a given cAMP modulation for its proper downstream pathway. cAMP signaling is tightly related to two other second messengers, cGMP and calcium, and their intricate regulation contributes to enlarge the coding strategies leading to the activation of unique signaling pathways (Borodinsky and Spitzer, 2006; Zaccolo and Movsesian, 2007). A recent and expanding set of tools now enables a precise study of the features of cAMP signals. This includes a growing number of genetically-encoded FRET-based biosensors that have been improved over time (Zhang et al., 2001; Nikolaev et al., 2004; Ponsioen et al., 2004; Polito et al., 2013) and allow the monitoring of cAMP signals in living neurons. This toolbox is complemented with recently implemented optogenetic adenylyl cyclases (ACs—the cAMP-synthesizing enzyme), providing full spatio-temporal control of cAMP concentration in living neurons (Schröder-Lang et al., 2007; Ryu et al., 2010; Hong et al., 2011; Stierl et al., 2011). Said utilities have recently been applied to the study of nervous system connectivity, revealing some of the cAMP coding strategies in developing neurons.

MECHANISMS UNDERLYING THE GENERATION AND CONTROL OF SPATIOTEMPORAL cAMP SIGNALS

The biological significance of cAMP signals during different steps of neuronal development relies on a tight control of both, their temporal and spatial features. Synthesis of cAMP is dependent on ACs, whereas the hydrolysis of cyclic nucleotides and

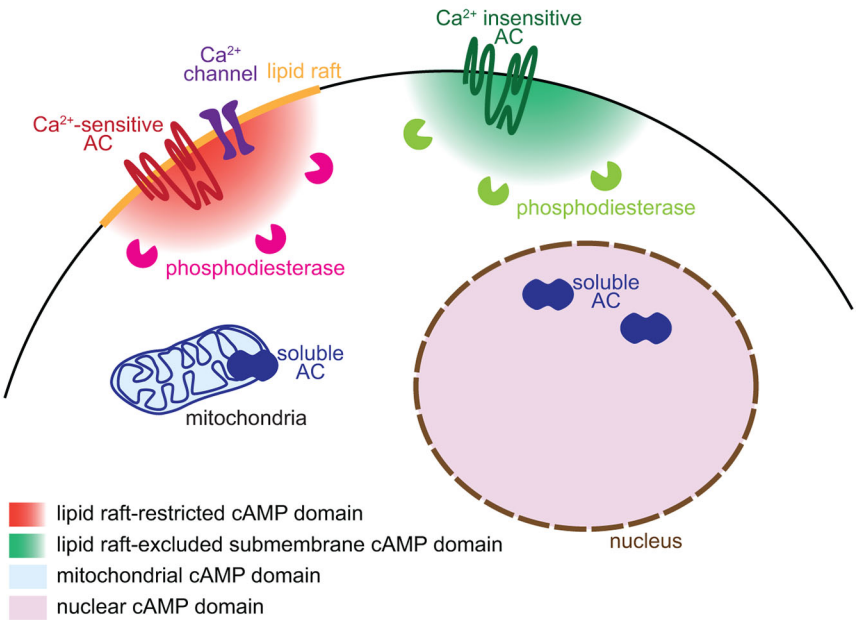

FIGURE 1 | Mechanisms underlying the generation of subcellular domains of cAMP. Distinct subcellular localizations of adenylyl cyclases and phosphodiesterases enable the generation of subcellular domains of cAMP. Ca^{2+}-sensitive transmembrane ACs and their regulating Ca^{2+} channels are restricted to lipid rafts whereas the Ca^{2+}-independent ACs are excluded from this plasma membrane territory. Phosphodiesterases degrade cAMP close to its site of synthesis and limit the diffusion of the signal. The soluble AC is responsible of cAMP synthesis in discrete locations of the cell including the mitochondria and the nucleus.

extinction of the signal relies on phosphodiesterases (PDEs). The diversity of regulation and localization of ACs (10 isoforms) and PDEs (more than 40 isoforms) offers a wide range of combination to shape specific signals in response to distinct stimuli (Omori and Kotera, 2007; Willoughby and Cooper, 2007; Kleppisch, 2009). The cooperation between ACs and PDEs is crucial to control the time of onset of cAMP elevation and to limit the spatial and temporal expansion of the signal, forming the relevant coding strategies controlling specific activation of cAMP downstream effectors (**Figure 1**).

Different AC isoforms are targeted to distinct cellular microdomains, providing the basis of locally generated cAMP signals. sAC/AC10 is associated with intracellular compartments including mitochondria, centrosome and nucleus (Zippin et al., 2003; Valsecchi et al., 2014). The calcium-sensitive transmembrane ACs (AC1, 3, 5, 6 and 8) are tethered to lipid rafts, a cholesterol- and sphyngolipid-enriched compartment of the plasma membrane. In contrast, the calcium-independent ACs (AC2, 4, 7 and 9) are targeted to the plasma membrane but excluded from lipid rafts (Willoughby and Cooper, 2007; **Figure 1**). Targeting or exclusion of specific AC isoforms from lipid rafts might be the crucial molecular correlate of distinct cAMP concentrations and signaling in compartments of the plasma membrane (Depry et al., 2011). Lipid rafts compartmentalize cAMP signals induced by beta adrenergic receptors in cardiomyocytes (Agarwal et al., 2011). In platelets, compartmentalized cAMP signals are created by lipid rafts and the cytoskeleton (Raslan and Naseem, 2014). This plasma membrane compartment is of particular interest to understand the development of neuronal connectivity. Its integrity is crucial for BDNF-, netrin-1- and Sema3A-induced, but not glutamate-dependent turning of *X. laevis* axons (Guirland et al., 2004). Evaluating whether lipid raft-restricted cAMP signals are required for axon pathfinding presents a promising approach to deciphering the second-messenger codes involved in axon guidance. Precise localization of ACs is also crucial for the coordination between second messengers. Interaction between AC8 and the pore component of the store operated calcium channels ensures a dynamic and coordinated relation between cAMP and calcium (Willoughby et al., 2012).

The cAMP turnover, balanced by synthesis and degradation, requires a tight regulation. Like ACs, PDEs are crucial for the spatio-temporal control of cAMP signaling. Their distinct intracellular localization, kinetics and regulatory mechanisms enable to shape a wide range of signals that differ in their spatiotemporal features and upstream regulators. Compartmentalization of PDEs is responsible for simultaneously generating multiple and contiguous cAMP domains, even far from the site of synthesis (Terrin et al., 2006). According to this model, synthesized cAMP is free to diffuse. The

specific activation of only a subset of its downstream pathways relies on the restricted subcellular localization of PDEs, acting locally as a cAMP sink to prevent the activation of downstream effectors (**Figure 1**). The cAMP-specific PDE4 family is crucial for this process in a wide number of cell types. In cardiomyocytes, the activation of PDE4D spatially limits the diffusion of cAMP, modulating cAMP-dependent protein kinase A (PKA) activation and the subsequent increase in calcium cycling required for contractile responses in the heart (Liu et al., 2012). In fibroblasts, PDE4B and PDE4D modulates cAMP concentration in discrete domains near the plasma membrane and are involved in distinct signaling pathways (Blackman et al., 2011). In neurons, the PDE4 family is involved in the functional compartmentation of cAMP, modulating the propagation of PKA activation from the plasma membrane to the nucleus (Castro et al., 2010; Vincent et al., 2012).

For ACs and PDEs to properly control the localization of cAMP signals, the targeting of these enzymes is tightly regulated. A-kinase anchoring proteins (AKAPs) are critical for this process. AKAP isoforms are targeted to distinct subcellular compartments and modulate the spatial spread of cAMP, binding at least some isoform of PDEs and ACs (Piggott et al., 2008; Willoughby et al., 2010; Delint-Ramirez et al., 2011; Terrin et al., 2012). In addition, AKAPs bind downstream effectors of cAMP including PKA and the cAMP-stimulated GDP exchange factors (Epacs), segregating distinct cAMP downstream pathways (Wong and Scott, 2004; McConnachie et al., 2006). Although to date there are only a few studies focusing on the spatial restriction of cAMP signals by AKAPs in developing neurons, these anchoring proteins have been extensively studied in other cell types. For instance, in airway smooth muscle cells, AKAPs modulates cAMP accumulation in response to β2-adrenergic agonists. PKA activation in turn phosphorylates PDE4, increasing its activity and reducing cAMP concentration in specific domains where AKAP proteins are localized (Horvat et al., 2012). In the nucleus, AKAPs have been proposed to control a PKA/PDE modulated cAMP signal different from that in the cytosol microdomain (Sample et al., 2012). Indeed, cAMP signaling at the plasma membrane followed by slow diffusion into the nucleus results into slow kinetics of PKA activity likely to be limited by the translocation of the catalytic domain of PKA from the cytosol to the nucleus. Indeed, PDEs keep the cAMP concentration in the nucleus too low to activate PKA. However, a direct activation of cAMP synthesis in the nucleus would result into fast kinetics of the nuclear PKA response. In this case, the spatio-temporal modulation of cAMP is responsible for a kinetically distinct activation of PKA, and the local negative regulator PDE4 contributes to establishing a local signaling threshold to convert spatial second messenger signals to temporal control of kinase activity. Finally, a dynamic and delicate control of cAMP signals has also been identified in the centrosome, a key subcellular structure for migration and cell cycle progression. In this subcellular domain, cAMP concentration is independent on cAMP levels in the cytosol and relies on PDE4D3 and PKA anchoring to AKAP 450 (Terrin et al., 2012).

EARLY EVENTS: NEURONAL POLARIZATION AND NEUROTRANSMITTER SPECIFICATION

The polarization of postmitotic neurons leads to the segregation of two distinct subcellular compartments: a single axon and a somato-dendritic compartment including multiple dendrites (Arimura and Kaibuchi, 2007; Barnes et al., 2008). Axon/dendrite specification of undifferentiated neurites involves cyclic nucleotide signaling aiming at the development of a single axon in each neuron. The use of cAMP and cGMP reporters enabled the identification of local cyclic nucleotide signals regulating axon/dendrite specification. cAMP initiates a positive feedback involving phosphorylation of the serine/threonine kinase LKB1 (Liver Kinase B1) and its interactor STRAD (STE20-related adapter protein), leading to differentiation and stabilization of the axon (Shelly et al., 2007). In contrast, cGMP favors the differentiation of immature neurites into mature dentrites (Shelly et al., 2010). Local and distal interactions between these two second messengers create two subcellular compartments that define the polarity of the neuron. Local cAMP elevation at the tip of a neurite leads to a local reduction of cGMP concentration, and a distal cAMP suppression and cGMP elevation in the other neurites and vice versa (Shelly et al., 2010; **Figure 2**). This local modulation of cyclic nucleotide levels is observed in maturing neurons in response to extracellular cues that favor either axon or dendrite initiation like BDNF or Semaphorin3A respectively (Shelly et al., 2011), or by activation of $GABA_B$ receptors (Bony et al., 2013). These observations emphasize the influence of local cyclic nucleotide signaling for axono- and dendritogenesis.

A second feature of neuronal differentiation is the specification of neurotransmitters. This is a crucial step in the development of the nervous system to ensure appropriate connectivity and to finely tune the balance between excitation and inhibition. In developing neurons, spontaneous calcium spikes play a critical role in the choice of neurotransmitter. The frequency of these calcium transients dictates the expression of an inhibitory or excitatory neurotransmitter. Expression of the hyperpolarizing potassium channel Kir2.1 suppresses calcium spikes in spinal *X. laevis* neurons and triggers the expression of the excitatory neurotransmitters machinery, including the glutamate vesicular transporter (VGluT) and choline acetyltransferase transporters (ChAT). In contrast, overexpression of the voltage gated sodium channel $Na_v1.2$ increases calcium spike frequency and the number of the inhibitory GABAergic and glycinergic spinal neurons at the expense of VGluT and ChAT-expressing neurons, demonstrating that pattern calcium activity affects neuronal differentiation (Borodinsky et al., 2004). Metabotropic $GABA_B$ receptors and group III metabotropic glutamate receptors regulate PKA activity, one of the main cAMP effectors, and modulate the generation of calcium spikes (Root et al., 2008). Interestingly, cAMP transients, rather than sustained elevation of this second messenger, are generated in *X. laevis* spinal neurons at the same developmental stage than calcium spikes that regulate neurotransmitter specification (Gorbunova and Spitzer, 2002). cAMP transients and calcium spikes are interdependent. Bursts of calcium spikes induce slow cAMP transients (3–7 min in young and older neurons respectively) and increasing cAMP

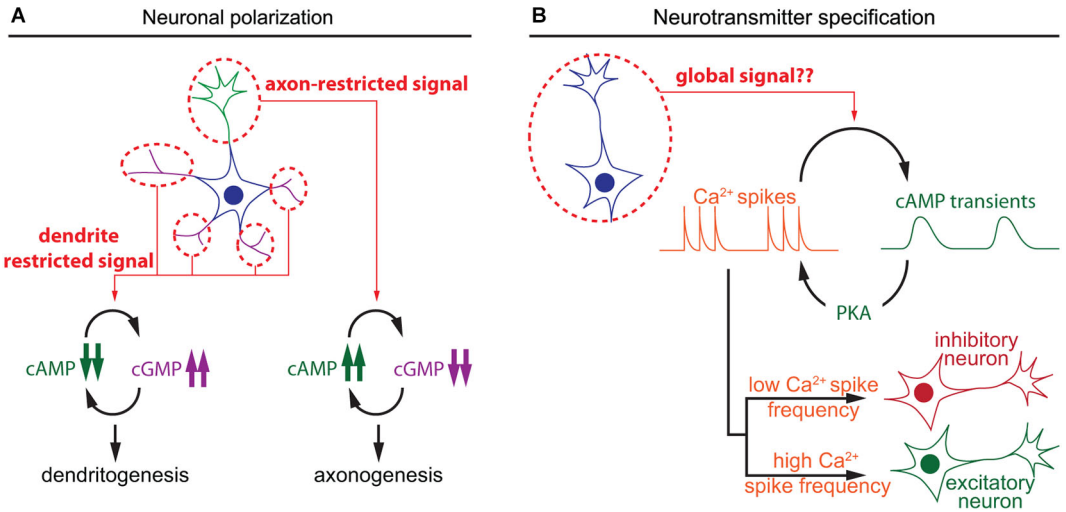

FIGURE 2 | Spatiotemporal dynamics of cAMP during neuronal polarization and neurotransmitter specification. **(A)** Local interactions between cAMP and cGMP determine neurite maturation into axon or dendrite. High cAMP and low cGMP concentrations promote axonogenesis, whereas low cAMP and high cGMP lead to dentritogenesis. **(B)** In developing neurons, cAMP transients and calcium spikes are interdependent. The choice of expression of excitatory or an inhibitory neurotransmitter is modulated by the frequency of calcium spikes, which is regulated by the activity of a set of kinases including the cAMP effector PKA.

concentration concomitantly increases the frequency of calcium spikes (Gorbunova and Spitzer, 2002; **Figure 2**). This reciprocal interaction between calcium and cAMP signal dynamics has been observed in a wide range of non-neuronal cell types (Landa et al., 2005; Borodinsky and Spitzer, 2006; Dyachok et al., 2006; Willoughby and Cooper, 2006). However, a possible direct relationship between cAMP transients and neurotransmitter specification has not been investigated. It would be of interest to evaluate if the frequency of cAMP transients influences neurotransmitter specification in developing neurons, like the frequency of calcium spikes.

AXON OUTGROWTH

Once neurons are polarized, axons grow over long distances to reach their synaptic partners. Axon elongation is dependent on cAMP signaling and high concentration of this second messenger favors axon outgrowth (Roisen et al., 1972; Cai et al., 2001; Shewan et al., 2002; Corredor et al., 2012). In this process as well, cAMP signaling is tightly linked to calcium to regulate axon outgrowth. Transient calcium elevations, termed calcium waves, have been visualized in the growth cone of extending axons. Calcium waves cover the entire growth cone at once and their kinetics is relatively slow. The frequency is inversely proportional to the speed of axon outgrowth in a wide range of models: lower frequency of calcium transients correlates with a high rate of axonal growth, while a high frequency is observed in slow growing axons (Gomez et al., 1995; Gomez and Spitzer, 1999; Tang et al., 2003). For instance in the developing spinal cord of *X. laevis*, Rohon-Beard neurons, ventral motor neurons and ascending interneurons exhibit a low frequency of calcium transients and a rapid outgrowth. In contrast, the frequency of calcium transients is higher in the slow growing dorso-lateral ascending interneurons (Gomez and Spitzer, 1999). A direct link between cAMP signals modulating axon outgrowth and calcium waves in growth cones has not been investigated so far. However, cAMP transients have been detected in axonal growth cones exposed to netrin-1, a guidance molecule that modulates both, the direction and the speed of axon elongation. cAMP transients require extracellular calcium influx and coincide with an increased frequency of calcium waves, that are not dependent on transmembrane AC activity (Nicol et al., 2011; **Figure 3**). The transient change in cAMP suggests that a temporal control might contribute to the coding strategy of cAMP signals regulating axon outgrowth.

Only cAMP signals from a subset of ACs are able to modulate axon outgrowth. The synthesis of cAMP by soluble AC (sAC/AC10) but not transmembrane ACs (AC1 to 9) is required for the intrinsic ability of axons to grow (Corredor et al., 2012). sAC/AC10 is also critical for netrin-1-induced outgrowth (Wu et al., 2006), but does not contribute to the cAMP-dependent modulation of axon pathfinding by netrin-1 (Moore et al., 2008). This suggests that cAMP signals generated by different ACs are not identical, although the features allowing the distinction between diverse cAMP signals have not been identified. A likely hypothesis is that subcellular localization of signals would provide a code to link each cAMP signal to its appropriate downstream pathway. Indeed sAC/AC10 is restricted to intracellular compartments in non-neuronal cells (Zippin et al., 2003; Feng et al., 2006), whereas the other ACs are transmembrane proteins.

AXON GUIDANCE

To reach their synaptic partners, axons follow stereotypic paths, guided by attractive and repulsive cues, which they encounter

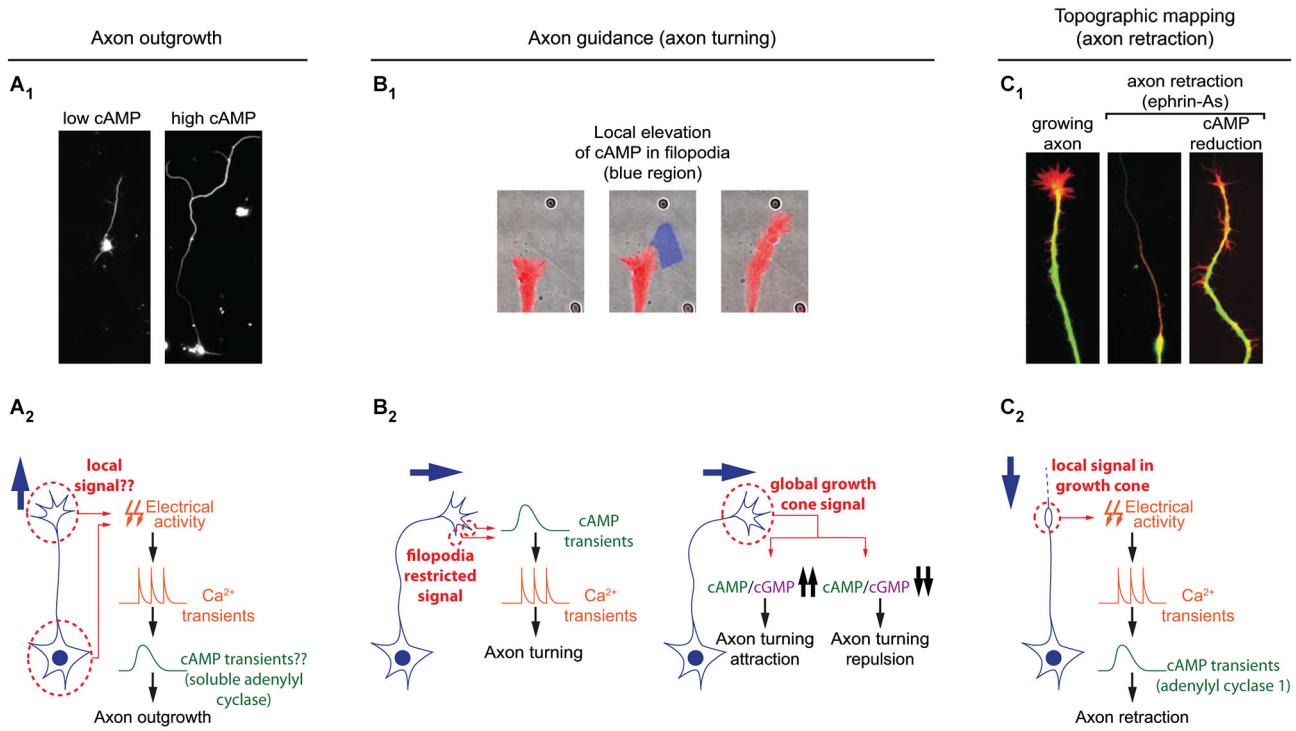

FIGURE 3 | Spatiotemporal dynamics of cAMP during axon outgrowth, axon guidance and topographic maps development. **(A_1)** Axon elongation is enhanced in cultured retinal ganglion cell with an increased cAMP concentration. **(A_2)** Electrical activity and calcium transients modulates cAMP synthesis by the soluble adenylyl cyclase (sAC/AC10). Both signals cooperate to regulate axon outgrowth. It is still unclear whether or not this signal transduction pathway is spatiotemporally restricted. **(B_1)** Transient and local cAMP synthesis by light-mediated activation of an optogenetic AC (within the blue region) is sufficient to induce axon turning. **(B_2)** Brief cAMP signal in filopodia induces an increase in the frequency of filopodia-restricted Ca^{2+} transients and a change of direction in axon outgrowth. cAMP/cGMP ratio sets the polarity of netrin-1-induced axon guidance. A high cAMP/cGMP ratio leads to attraction whereas a low ratio converts attraction into repulsion. **(C_1)** cAMP signaling perturbation (lack of AC1, pharmacological blockade of ACs, or PKA blockade) prevents the axon repellents ephrin-As to induce axon retraction. **(C_2)** Transient electrical activity- and calcium-dependent modulation of cAMP is required in growth cones for the backward movement of axons when exposed to ephrin-As.

on the way to their final targets. cAMP signaling is a crucial modulator of axonal response to guidance molecules and enables the conversion of attractive cues into repulsive ones and vice versa (Ming et al., 1997; Song et al., 1997; Höpker et al., 1999; Murray et al., 2009). However, the spatio-temporal dynamics of cAMP signals regulating axon guidance have been investigated only recently. As during neurotransmitter specification and axon outgrowth, cAMP signaling involved in axon pathfinding is linked to calcium. Calcium signaling is critical for axonal response to guidance molecules (Hong et al., 2000; Nishiyama et al., 2003; Li et al., 2009). In addition to slow calcium waves regulating axon outgrowth, fast calcium transients restricted to filopodia have been visualized in developing axons (Gomez et al., 2001). An asymmetric frequency of calcium transients in filopodia from both sides of the growth cone is able to orient axon outgrowth (Gomez et al., 2001; Robles et al., 2003). Guidance molecules such as netrin-1 modulate the frequency of filopodial calcium transients. Transient elevations of cAMP precede and are required for the increase in frequency of local filopodial calcium transients (Nicol et al., 2011), making cAMP crucial to orient netrin-1-induced axon outgrowth. Although netrin-1 exposure also drives an increase in cAMP concentration in the central domain of the growth cone, this signal is not involved in the regulation of axon growth direction (Nicol et al., 2011). This suggests that axon guidance molecules can induce cAMP synthesis in a restricted area of the growth cone for a limited duration. This idea is supported by observations of axon turning generated by exogenous spatially- and temporally-restricted cAMP signals *in vitro* (Munck et al., 2004; Nicol et al., 2011). *In vivo*, transient cAMP elevations are sufficient to restore outgrowth of commissural axons towards the ventral midline of the spinal cord when DCC-dependent netrin-1 signaling is blocked. In contrast, sustained increase or decrease of cAMP concentration leads to abnormal trajectories of spinal commissural axons in *X. laevis* (Nicol et al., 2011), suggesting that spatio-temporal features of cAMP signals are crucial for the modulation of axonal pathfinding (**Figure 3**).

The regulation of axon pathfinding by cAMP signaling tightly controlled in space and time is most likely not the only cAMP-dependent process regulating axon guidance. Axon turning can be modulated by sustained and global manipulations of PKA activity that are sufficient to modify the amplitude of imposed fast and local calcium transients dependent on ryanodine receptors (Ooashi et al., 2005). The resting cAMP concentration is tuned

by adhesion molecules such as laminin that also regulate axon guidance (Höpker et al., 1999; Ooashi et al., 2005). In addition, cAMP interacts with cGMP signaling, often counteracting its effects. Whereas high cAMP concentration favors attraction, cGMP is associated with axonal repulsion. A high cAMP/cGMP ratio in spinal axons leads to attraction by netrin-1, whereas a low ratio converts this attraction into repulsion. This highlights the relevance of relative cAMP levels compared to cGMP rather than an absolute concentration of one or the other cyclic nucleotide (Nishiyama et al., 2003; **Figure 3**). The antagonizing effect of cAMP and cGMP might be due to their opposite regulation of common downstream effectors. Both second messengers modulate the amplitude of the ryanodine receptor-dependent local calcium transient. The cAMP/PKA pathway promotes ryanodine receptor-mediated calcium induced calcium release, whereas cGMP and its downstream effector protein kinase G (PKG) reduces the ryanodine receptor-dependent mobilization of internal calcium stores (Ooashi et al., 2005; Tojima et al., 2009). Simultaneous imaging of cAMP and cGMP in growing axons emphasized a temporally correlated regulation of cAMP and cGMP in growth cones. As during axonogenesis, an increase of cAMP correlates with a reduction in cGMP concentration (Kobayashi et al., 2013). The mechanisms underlying these opposite modulations are unclear. In other systems, inverse regulation of both cyclic nucleotides are related to PDE activity (Shelly et al., 2010; Polito et al., 2013). So far, not much attention has been attributed to evaluating the impact of these cAMP/cGMP degrading enzymes, which might be crucial players in cyclic nucleotide oscillations in axon guidance.

AXON BRANCHING AND TARGETING (TOPOGRAPHIC MAPS)

Once axons have reached their targets, dense terminal axonal arbors develop. The precise positioning of this termination zone is tightly controlled and crucial for appropriate wiring of the nervous system. This process has been extensively studied in sensory systems, in which projections are topographically organized. Axonal arbors are organized in their target regions in correlation with the information they carry. For instance, axons originating from neighboring retinal ganglion cells arborize in neighboring areas in their targets. Similarly, olfactory neurons expressing the same olfactory receptor target the same region of the olfactory bulb. cAMP signaling is crucial for the development of topographic maps. Among the ACs tested, only two are required for topographic map formation: AC1 in the visual and somatosensory systems (Welker et al., 1996; Ravary et al., 2003; Nicol et al., 2006a), and AC3 in the olfactory projections (Wong et al., 2000; Col et al., 2007; Zou et al., 2007). In AC1 and AC3 knock-out mice, ectopic axonal branches fail to be pruned during development resulting in larger termination zones. In contrast, AC1 and AC3 are not involved in axon outgrowth, a process requiring sAC/AC10 (Wu et al., 2006; Corredor et al., 2012). The distinct roles of each AC suggest that they generate cAMP signals with unique features.

AC1-dependent cAMP signaling involved in the development of topographic maps requires calcium. Retinal axons lacking this calcium-activated AC (Fagan et al., 2000) or exposed to calcium-free extracellular medium show the same phenotype when exposed to the axon repellent ephrin-As: in both conditions axons fail to retract (Nicol et al., 2006b, 2007). This reduced retraction is likely to contribute to the impaired axonal pruning seen in $AC1^{-/-}$ mice since ephrin-As are crucial for the development of retinal topography (Frisén et al., 1998; Feldheim et al., 2000). Ephrin-A-induced retraction also requires electrical activity. In absence of electrical activity, short and repeated cAMP pulses in growth cones are sufficient to rescue axonal retraction. In contrast, global and sustained elevation of cAMP does not rescue axon retraction. Sustained high or low cAMP concentration is sufficient to prevent ephrin-A-induced repulsion, suggesting that the temporal features of cAMP signaling is crucial for axonal retraction and the development of topographic maps (Nicol et al., 2007; **Figure 3**).

AC3 is required for the correct antero-posterior position in terminal zones of olfactory projections and for the convergence of olfactory axons expressing the same olfactory receptor into the same glomerulus (Wong et al., 2000; Col et al., 2007; Zou et al., 2007). The cAMP-dependent signaling pathways involved differ in these two developmental processes, only one of them interacting with calcium signaling. AC3-dependent cAMP signaling regulates the expression of the axon guidance molecule semaphorin-3A and its receptor neuropilin-1 to modulate the position of axonal arbors along the antero-posterior axis in a CREB-dependent mechanism (Imai et al., 2006). In contrast, AC3-dependent activation of the cyclic nucleotide gated calcium channel α2 is required for the development of glomeruli receiving axons expressing the same olfactory receptor (Serizawa et al., 2006). The spatiotemporal analysis of cAMP modulation in developing olfactory neurons revealed that activation of olfactory receptors at axonal growth cones induces a local increase of cAMP and calcium, followed by the nuclear translocation of the catalytic subunit of PKA (Maritan et al., 2009). Exposure of olfactory axon terminals to odorants also leads to a local cAMP- and calcium-dependent increase of cGMP (Pietrobon et al., 2011). Activation of downstream cGMP signaling is sufficient but not necessary to induce CREB phosphorylation in the nucleus of olfactory neurons (Pietrobon et al., 2011), suggesting that cGMP might be involved in the modulation of gene expression during olfactory map development.

ACTIVITY-DEPENDENT AXONAL AND SYNAPTIC COMPETITION

Once axonal branches are positioned in their targets, they carefully choose their synaptic partners, often through an axonal or synaptic competition process. cAMP has a crucial role in modulating this competition that represents a critical process for the development of a properly organized neuronal connectivity (Luo and O'Leary, 2005; Luo and Flanagan, 2007). Competition is dependent on electrical activity, and its regulation by cAMP often relates to spontaneous activity generated during development (Penn et al., 1998; Stellwagen and Shatz, 2002; Zhang et al., 2012; Furman et al., 2013). In the developing retina, spontaneous calcium waves appear prior to vision. The frequency and propagation of these calcium waves are modulated by cAMP, with a higher

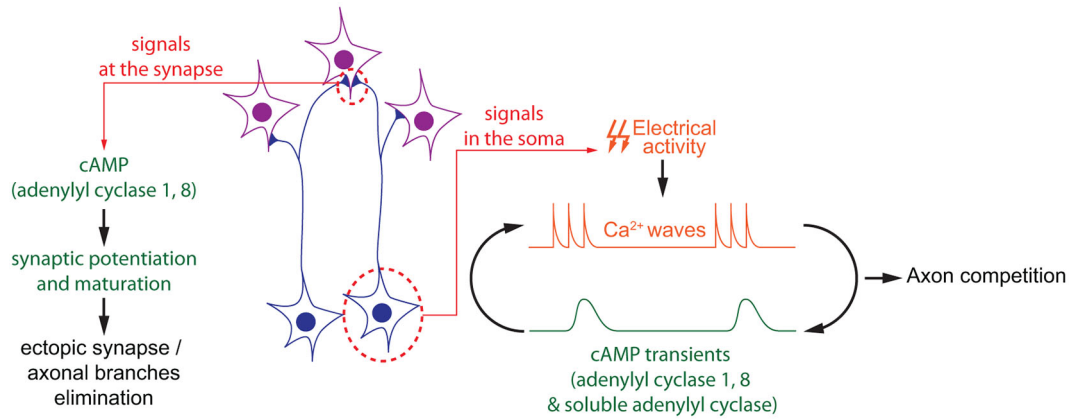

FIGURE 4 | Spatiotemporal dynamics of cAMP during developmental pruning of ectopic axonal branches, and synaptic competition. cAMP is required in two subcellular compartments during the synaptic refinement of neuronal projections. In the soma of retinal ganglion cells, cAMP oscillations and spontaneous calcium waves are interdependent. Spontaneous calcium waves are required for competition between axons in their targets. In the synapses, cAMP signaling mediated by adenylyl cyclases 1 and 8 is involved in synaptic potentiation and hebbian mechanisms, which are crucial to eliminate misplaced synapses.

frequency and a propagation over longer distances when cAMP is increased (Stellwagen et al., 1999; Stellwagen and Shatz, 2002). Interactions between cAMP and calcium waves in the developing retina are bidirectional: depolarization-induced calcium influx is sufficient to produce brief cAMP elevation, and cAMP transients are spontaneously generated in post-natal retinal ganglion cells (Dunn et al., 2006; **Figure 4**). Like the cAMP elevations observed in *X. laevis* spinal neurons, spontaneous cAMP / PKA activity transients in the developing retina are observed upon long but not short bursts of electrical activity (Gorbunova and Spitzer, 2002; Dunn et al., 2006). Surprisingly, the genetic removal of AC1, the main calcium-stimulated AC expressed in retinal ganglion cells, is not sufficient to perturb depolarization-induced cAMP elevations. In AC1/AC8 double knock-out mice, cAMP transients only exhibit a reduced amplitude and are abolished only with pharmacological blockade of both, transmembrane (AC1 to 9) and soluble (sAC/AC10) ACs, suggesting that several ACs cooperate to generate brief cAMP / PKA activity transients in the retina (Dunn et al., 2009).

During development, cAMP-dependent spontaneous electrical activity in the retina is crucial for the precise organization of retinal axons in their targets. Retinal axons from each eye arborize in non-overlapping regions of their targets in a competition-dependent mechanism. When retinal calcium waves are perturbed, the normally well segregated territories occupied by axons from each eye overlap (Rossi et al., 2001; Muir-Robinson et al., 2002). Although AC1 is not required for the generation of cAMP transients or calcium waves in the developing retina (Dunn et al., 2009; Dhande et al., 2012), its genetic removal prevents the segregation of retinal projections in eye-specific territories in the dorso-lateral geniculate nucleus and the superior colliculus (Ravary et al., 2003; Nicol et al., 2006a), revealing that other cAMP signals are dependent on this particular AC. The stimulation of AC1 by calcium influx (Fagan et al., 2000), and the phenotypic similarity between $AC1^{-/-}$ mice and models displaying altered spontaneous retinal waves or impaired electrical activity suggests that AC1 and calcium waves are part of the same signaling pathway regulating the development of eye-specific territories (Rossi et al., 2001; Muir-Robinson et al., 2002; Dhande et al., 2011). Converging evidence indicates that the deficit in the segregation of eye-specific territories in $AC1^{-/-}$ mice is dependent on AC activity in retinal ganglion cells but not their targets (Nicol et al., 2006b; Dhande et al., 2012). Since cAMP signaling is not affected in the soma of retinal ganglion cells in AC1-deficient mice, it is probable that cAMP signaling restricted to the axonal/synaptic compartment plays a role in the competition leading to segregation of eye-specific territories. AC1 is required for synaptic maturation and potentiation, a process required for the refinement of retinal connections (Lu et al., 2006; Iwasato et al., 2008; **Figure 4**). However, the features of cAMP signaling required for synaptic competition need to be characterized in more detail to improve our understanding of the signaling code involved in synaptic competition.

CONCLUSION

cAMP is involved in a wide range of processes influencing the development of nervous system connectivity. We summarize the recent progress in investigating the specific modulation of these multiple processes by spatio-temporally distinct cAMP signals. Temporal control of cAMP signals in subcellular compartments is a potential coding strategy to translate distinct cAMP signals into activation of specific downstream pathways in developing neurons. Crosstalk with other second messenger systems (cGMP and calcium) are of special importance to gain new insight into the spatiotemporal control of cAMP signals. Pursuing the analysis of these coding strategies will provide a better understanding of the regulatory second messenger networks shaping neuronal connectivity.

ACKNOWLEDGMENTS

We thank Heike Blockus for helpful critical reading of the manuscript. The research in our laboratory is supported by Fondation de France, and by the French National Agency for Research (ANR) in the frame of the PDOC program (ANR-11-PDOC-0004), and of the LABEX LIFESENSES (ANR-10-LABX-65) within the Investissements d'Avenir program (ANR-11-IDEX-0004-02).

REFERENCES

Agarwal, S. R., MacDougall, D. A., Tyser, R., Pugh, S. D., Calaghan, S. C., and Harvey, R. D. (2011). Effects of cholesterol depletion on compartmentalized cAMP responses in adult cardiac myocytes. *J. Mol. Cell. Cardiol.* 50, 500–509. doi: 10.1016/j.yjmcc.2010.11.015

Arimura, N., and Kaibuchi, K. (2007). Neuronal polarity: from extracellular signals to intracellular mechanisms. *Nat. Rev. Neurosci.* 8, 194–205. doi: 10.1038/nrn2056

Barnes, A. P., Solecki, D., and Polleux, F. (2008). New insights into the molecular mechanisms specifying neuronal polarity in vivo. *Curr. Opin. Neurobiol.* 18, 44–52. doi: 10.1016/j.conb.2008.05.003

Blackman, B. E., Horner, K., Heidmann, J., Wang, D., Richter, W., Rich, T. C., et al. (2011). PDE4D and PDE4B function in distinct subcellular compartments in mouse embryonic fibroblasts. *J. Biol. Chem.* 286, 12590–12601. doi: 10.1074/jbc.m110.203604

Bony, G., Szczurkowska, J., Tamagno, I., Shelly, M., Contestabile, A., and Cancedda, L. (2013). Non-hyperpolarizing GABAB receptor activation regulates neuronal migration and neurite growth and specification by cAMP/LKB1. *Nat. Commun.* 4:1800. doi: 10.1038/ncomms2820

Borodinsky, L. N., Root, C. M., Cronin, J. A., Sann, S. B., Gu, X., and Spitzer, N. C. (2004). Activity-dependent homeostatic specification of transmitter expression in embryonic neurons. *Nature* 429, 523–530. doi: 10.1038/nature02518

Borodinsky, L. N., and Spitzer, N. C. (2006). Second messenger pas de deux: the coordinated dance between calcium and cAMP. *Sci. STKE* 2006:pe22. doi: 10.1126/stke.3362006pe22

Cai, D., Qiu, J., Cao, Z., McAtee, M., Bregman, B. S., and Filbin, M. T. (2001). Neuronal cyclic AMP controls the developmental loss in ability of axons to regenerate. *J. Neurosci.* 21, 4731–4739.

Castro, L. R. V., Gervasi, N., Guiot, E., Cavellini, L., Nikolaev, V. O., Paupardin-Tritsch, D., et al. (2010). Type 4 phosphodiesterase plays different integrating roles in different cellular domains in pyramidal cortical neurons. *J. Neurosci.* 30, 6143–6151. doi: 10.1523/jneurosci.5851-09.2010

Col, J. A. D., Matsuo, T., Storm, D. R., and Rodriguez, I. (2007). Adenylyl cyclase-dependent axonal targeting in the olfactory system. *Development* 134, 2481–2489. doi: 10.1242/dev.006346

Corredor, R. G., Trakhtenberg, E. F., Pita-Thomas, W., Jin, X., Hu, Y., and Goldberg, J. L. (2012). Soluble adenylyl cyclase activity is necessary for retinal ganglion cell survival and axon growth. *J. Neurosci.* 32, 7734–7744. doi: 10.1523/jneurosci.5288-11.2012

Delint-Ramirez, I., Willoughby, D., Hammond, G. V. R., Ayling, L. J., and Cooper, D. M. F. (2011). Palmitoylation targets AKAP79 protein to lipid rafts and promotes its regulation of calcium-sensitive adenylyl cyclase type 8. *J. Biol. Chem.* 286, 32962–32975. doi: 10.1074/jbc.m111.243899

Depry, C., Allen, M. D., and Zhang, J. (2011). Visualization of PKA activity in plasma membrane microdomains. *Mol. Biosyst.* 7, 52–58. doi: 10.1039/c0mb00079e

Dhande, O. S., Bhatt, S., Anishchenko, A., Elstrott, J., Iwasato, T., Swindell, E. C., et al. (2012). Role of adenylate cyclase 1 in retinofugal map development. *J. Comp. Neurol.* 520, 1562–1583. doi: 10.1002/cne.23000

Dhande, O. S., Hua, E. W., Guh, E., Yeh, J., Bhatt, S., Zhang, Y., et al. (2011). Development of single retinofugal axon arbors in normal and β2 knock-out mice. *J. Neurosci.* 31, 3384–3399. doi: 10.1523/JNEUROSCI.4899-10.2011

Dunn, T. A., Storm, D. R., and Feller, M. B. (2009). Calcium-dependent increases in protein kinase-A activity in mouse retinal ganglion cells are mediated by multiple adenylate cyclases. *PLoS One* 4:e7877. doi: 10.1371/journal.pone.0007877

Dunn, T. A., Wang, C.-T., Colicos, M. A., Zaccolo, M., DiPilato, L. M., Zhang, J., et al. (2006). Imaging of cAMP levels and protein kinase A activity reveals that retinal waves drive oscillations in second-messenger cascades. *J. Neurosci.* 26, 12807–12815. doi: 10.1523/jneurosci.3238-06.2006

Dyachok, O., Isakov, Y., Sågetorp, J., and Tengholm, A. (2006). Oscillations of cyclic AMP in hormone-stimulated insulin-secreting beta-cells. *Nature* 439, 349–352. doi: 10.1038/nature04410

Fagan, K. A., Graf, R. A., Tolman, S., Schaack, J., and Cooper, D. M. (2000). Regulation of a Ca2+-sensitive adenylyl cyclase in an excitable cell. Role of voltage-gated versus capacitative Ca2+ entry. *J. Biol. Chem.* 275, 40187–40194. doi: 10.1074/jbc.m006606200

Feldheim, D. A., Kim, Y. I., Bergemann, A. D., Frisén, J., Barbacid, M., and Flanagan, J. G. (2000). Genetic analysis of ephrin-A2 and ephrin-A5 shows their requirement in multiple aspects of retinocollicular mapping. *Neuron* 25, 563–574. doi: 10.1016/s0896-6273(00)81060-0

Feng, Q., Zhang, Y., Li, Y., Liu, Z., Zuo, J., and Fang, F. (2006). Two domains are critical for the nuclear localization of soluble adenylyl cyclase. *Biochimie* 88, 319–328. doi: 10.1016/j.biochi.2005.09.003

Frisén, J., Yates, P. A., McLaughlin, T., Friedman, G. C., O'Leary, D. D., and Barbacid, M. (1998). Ephrin-A5 (AL-1/RAGS) is essential for proper retinal axon guidance and topographic mapping in the mammalian visual system. *Neuron* 20, 235–243. doi: 10.1016/s0896-6273(00)80452-3

Furman, M., Xu, H.-P., and Crair, M. C. (2013). Competition driven by retinal waves promotes morphological and functional synaptic development of neurons in the superior colliculus. *J. Neurophysiol.* 110, 1441–1454. doi: 10.1152/jn.01066.2012

Gomez, T. M., Robles, E., Poo, M., and Spitzer, N. C. (2001). Filopodial calcium transients promote substrate-dependent growth cone turning. *Science* 291, 1983–1987. doi: 10.1126/science.1056490

Gomez, T. M., Snow, D. M., and Letourneau, P. C. (1995). Characterization of spontaneous calcium transients in nerve growth cones and their effect on growth cone migration. *Neuron* 14, 1233–1246. doi: 10.1016/0896-6273(95)90270-8

Gomez, T. M., and Spitzer, N. C. (1999). In vivo regulation of axon extension and pathfinding by growth-cone calcium transients. *Nature* 397, 350–355. doi: 10.1038/16927

Gorbunova, Y. V., and Spitzer, N. C. (2002). Dynamic interactions of cyclic AMP transients and spontaneous Ca2+ spikes. *Nature* 418, 93–96. doi: 10.1038/nature00835

Guirland, C., Suzuki, S., Kojima, M., Lu, B., and Zheng, J. Q. (2004). Lipid rafts mediate chemotropic guidance of nerve growth cones. *Neuron* 42, 51–62. doi: 10.1016/s0896-6273(04)00157-6

Hong, K., Nishiyama, M., Henley, J., Tessier-Lavigne, M., and Poo, M. (2000). Calcium signalling in the guidance of nerve growth by netrin-1. *Nature* 403, 93–98. doi: 10.1038/47507

Hong, K. P., Spitzer, N. C., and Nicol, X. (2011). Improved molecular toolkit for cAMP studies in live cells. *BMC Res. Notes* 4:241. doi: 10.1186/1756-0500-4-241

Höpker, V. H., Shewan, D., Tessier-Lavigne, M., Poo, M., and Holt, C. (1999). Growth-cone attraction to netrin-1 is converted to repulsion by laminin-1. *Nature* 401, 69–73. doi: 10.1038/43441

Horvat, S. J., Deshpande, D. A., Yan, H., Panettieri, R. A., Codina, J., DuBose, T. D. Jr., et al. (2012). A-kinase anchoring proteins regulate compartmentalized cAMP signaling in airway smooth muscle. *FASEB J.* 26, 3670–3679. doi: 10.1096/fj.11-201020

Imai, T., Suzuki, M., and Sakano, H. (2006). Odorant receptor-derived cAMP signals direct axonal targeting. *Science* 314, 657–661. doi: 10.1126/science.1131794

Iwasato, T., Inan, M., Kanki, H., Erzurumlu, R. S., Itohara, S., and Crair, M. C. (2008). Cortical adenylyl cyclase 1 is required for thalamocortical synapse maturation and aspects of layer IV barrel development. *J. Neurosci.* 28, 5931–5943. doi: 10.1523/JNEUROSCI.0815-08.2008

Kleppisch, T. (2009). Phosphodiesterases in the central nervous system. *Handb. Exp. Pharmacol.* 191, 71–92. doi: 10.1007/978-3-540-68964-5_5

Kobayashi, T., Nagase, F., Hotta, K., and Oka, K. (2013). Crosstalk between second messengers predicts the motility of the growth cone. *Sci. Rep.* 3:3118. doi: 10.1038/srep03118

Landa, L. R. Jr., Harbeck, M., Kaihara, K., Chepurny, O., Kitiphongspattana, K., Graf, O., et al. (2005). Interplay of Ca2+ and cAMP signaling in the insulin-secreting MIN6 beta-cell line. *J. Biol. Chem.* 280, 31294–31302. doi: 10.1074/jbc.m505657200

Li, L., Hutchins, B. I., and Kalil, K. (2009). Wnt5a induces simultaneous cortical axon outgrowth and repulsive axon guidance through distinct signaling mechanisms. *J. Neurosci.* 29, 5873–5883. doi: 10.1523/jneurosci.0183-09.2009

Liu, S., Li, Y., Kim, S., Fu, Q., Parikh, D., Sridhar, B., et al. (2012). Phosphodiesterases coordinate cAMP propagation induced by two stimulatory G protein-coupled receptors in hearts. *Proc. Natl. Acad. Sci. U S A* 109, 6578–6583. doi: 10.1073/pnas.1117862109

Lu, H.-C., Butts, D. A., Kaeser, P. S., She, W.-C., Janz, R., and Crair, M. C. (2006). Role of efficient neurotransmitter release in barrel map development. *J. Neurosci.* 26, 2692–2703. doi: 10.1523/jneurosci.3956-05.2006

Luo, L., and Flanagan, J. G. (2007). Development of continuous and discrete neural maps. *Neuron* 56, 284–300. doi: 10.1016/j.neuron.2007.10.014

Luo, L., and O'Leary, D. D. M. (2005). Axon retraction and degeneration in development and disease. *Annu. Rev. Neurosci.* 28, 127–156. doi: 10.1146/annurev.neuro.28.061604.135632

Maritan, M., Monaco, G., Zamparo, I., Zaccolo, M., Pozzan, T., and Lodovichi, C. (2009). Odorant receptors at the growth cone are coupled to localized cAMP and Ca2+ increases. *Proc. Natl. Acad. Sci. U S A* 106, 3537–3542. doi: 10.1073/pnas.0813224106

McConnachie, G., Langeberg, L. K., and Scott, J. D. (2006). AKAP signaling complexes: getting to the heart of the matter. *Trends Mol. Med.* 12, 317–323. doi: 10.1016/j.molmed.2006.05.008

Ming, G. L., Song, H. J., Berninger, B., Holt, C. E., Tessier-Lavigne, M., and Poo, M. M. (1997). cAMP-dependent growth cone guidance by netrin-1. *Neuron* 19, 1225–1235. doi: 10.1016/s0896-6273(00)80414-6

Moore, S. W., Lai Wing Sun, K., Xie, F., Barker, P. A., Conti, M., and Kennedy, T. E. (2008). Soluble adenylyl cyclase is not required for axon guidance to netrin-1. *J. Neurosci.* 28, 3920–3924. doi: 10.1523/jneurosci.0547-08.2008

Muir-Robinson, G., Hwang, B. J., and Feller, M. B. (2002). Retinogeniculate axons undergo eye-specific segregation in the absence of eye-specific layers. *J. Neurosci.* 22, 5259–5264.

Munck, S., Bedner, P., Bottaro, T., and Harz, H. (2004). Spatiotemporal properties of cytoplasmic cyclic AMP gradients can alter the turning behaviour of neuronal growth cones. *Eur. J. Neurosci.* 19, 791–797. doi: 10.1111/j.0953-816x.2004.03118.x

Murray, A. J., Tucker, S. J., and Shewan, D. A. (2009). cAMP-dependent axon guidance is distinctly regulated by Epac and protein kinase A. *J. Neurosci.* 29, 15434–15444. doi: 10.1523/jneurosci.3071-09.2009

Nicol, X., Bennis, M., Ishikawa, Y., Chan, G. C.-K., Repérant, J., Storm, D. R., et al. (2006a). Role of the calcium modulated cyclases in the development of the retinal projections. *Eur. J. Neurosci.* 24, 3401–3414. doi: 10.1111/j.1460-9568.2006.05227.x

Nicol, X., Hong, K. P., and Spitzer, N. C. (2011). Spatial and temporal second messenger codes for growth cone turning. *Proc. Natl. Acad. Sci. U S A* 108, 13776–13781. doi: 10.1073/pnas.1100247108

Nicol, X., Muzerelle, A., Rio, J. P., Métin, C., and Gaspar, P. (2006b). Requirement of adenylate cyclase 1 for the ephrin-A5-dependent retraction of exuberant retinal axons. *J. Neurosci.* 26, 862–872. doi: 10.1523/jneurosci.3385-05.2006

Nicol, X., Voyatzis, S., Muzerelle, A., Narboux-Nême, N., Südhof, T. C., Miles, R., et al. (2007). cAMP oscillations and retinal activity are permissive for ephrin signaling during the establishment of the retinotopic map. *Nat. Neurosci.* 10, 340–347. doi: 10.1038/nn1842

Nikolaev, V. O., Bünemann, M., Hein, L., Hannawacker, A., and Lohse, M. J. (2004). Novel single chain cAMP sensors for receptor-induced signal propagation. *J. Biol. Chem.* 279, 37215–37218. doi: 10.1074/jbc.C400302200

Nishiyama, M., Hoshino, A., Tsai, L., Henley, J. R., Goshima, Y., Tessier-Lavigne, M., et al. (2003). Cyclic AMP/GMP-dependent modulation of Ca2+ channels sets the polarity of nerve growth-cone turning. *Nature* 423, 990–995. doi: 10.1038/nature01751

Omori, K., and Kotera, J. (2007). Overview of PDEs and their regulation. *Circ. Res.* 100, 309–327. doi: 10.1161/01.res.0000256354.95791.f1

Ooashi, N., Futatsugi, A., Yoshihara, F., Mikoshiba, K., and Kamiguchi, H. (2005). Cell adhesion molecules regulate Ca2+-mediated steering of growth cones via cyclic AMP and ryanodine receptor type 3. *J. Cell Biol.* 170, 1159–1167. doi: 10.1083/jcb.200503157

Penn, A. A., Riquelme, P. A., Feller, M. B., and Shatz, C. J. (1998). Competition in retinogeniculate patterning driven by spontaneous activity. *Science* 279, 2108–2112. doi: 10.1126/science.279.5359.2108

Pham, T. A., Rubenstein, J. L., Silva, A. J., Storm, D. R., and Stryker, M. P. (2001). The CRE/CREB pathway is transiently expressed in thalamic circuit development and contributes to refinement of retinogeniculate axons. *Neuron* 31, 409–420. doi: 10.1016/s0896-6273(01)00381-6

Pietrobon, M., Zamparo, I., Maritan, M., Franchi, S. A., Pozzan, T., and Lodovichi, C. (2011). Interplay among cGMP, cAMP and Ca2+ in living olfactory sensory neurons in vitro and in vivo. *J. Neurosci.* 31, 8395–8405. doi: 10.1523/jneurosci.6722-10.2011

Piggott, L. A., Bauman, A. L., Scott, J. D., and Dessauer, C. W. (2008). The A-kinase anchoring protein Yotiao binds and regulates adenylyl cyclase in brain. *Proc. Natl. Acad. Sci. U S A* 105, 13835–13840. doi: 10.1073/pnas.0712100105

Polito, M., Klarenbeek, J., Jalink, K., Paupardin-Tritsch, D., Vincent, P., and Castro, L. R. V. (2013). The NO/cGMP pathway inhibits transient cAMP signals through the activation of PDE2 in striatal neurons. *Front. Cell. Neurosci.* 7:211. doi: 10.3389/fncel.2013.00211

Ponsioen, B., Zhao, J., Riedl, J., Zwartkruis, F., van der Krogt, G., Zaccolo, M., et al. (2004). Detecting cAMP-induced Epac activation by fluorescence resonance energy transfer: Epac as a novel cAMP indicator. *EMBO Rep.* 5, 1176–1180. doi: 10.1038/sj.embor.7400290

Raslan, Z., and Naseem, K. M. (2014). Compartmentalisation of cAMP-dependent signalling in blood platelets: the role of lipid rafts and actin polymerisation. *Platelets*, 1–9. doi: 10.3109/09537104.2014.916792. [Epub ahead of print].

Ravary, A., Muzerelle, A., Hervé, D., Pascoli, V., Ba-Charvet, K. N., Girault, J.-A., et al. (2003). Adenylate cyclase 1 as a key actor in the refinement of retinal projection maps. *J. Neurosci.* 23, 2228–2238.

Robles, E., Huttenlocher, A., and Gomez, T. M. (2003). Filopodial calcium transients regulate growth cone motility and guidance through local activation of calpain. *Neuron* 38, 597–609. doi: 10.1016/s0896-6273(03)00260-5

Roisen, F. J., Murphy, R. A., Pichichero, M. E., and Braden, W. G. (1972). Cyclic adenosine monophosphate stimulation of axonal elongation. *Science* 175, 73–74. doi: 10.1126/science.175.4017.73

Root, C. M., Velázquez-Ulloa, N. A., Monsalve, G. C., Minakova, E., and Spitzer, N. C. (2008). Embryonically expressed GABA and glutamate drive electrical activity regulating neurotransmitter specification. *J. Neurosci.* 28, 4777–4784. doi: 10.1523/jneurosci.4873-07.2008

Rossi, F. M., Pizzorusso, T., Porciatti, V., Marubio, L. M., Maffei, L., and Changeux, J.-P. (2001). Requirement of the nicotinic acetylcholine receptor $\beta 2$ subunit for the anatomical and functional development of the visual system. *Proc. Natl. Acad. Sci. U S A* 98, 6453–6458. doi: 10.1073/pnas.101120998

Ryu, M.-H., Moskvin, O. V., Siltberg-Liberles, J., and Gomelsky, M. (2010). Natural and engineered photoactivated nucleotidyl cyclases for optogenetic applications. *J. Biol. Chem.* 285, 41501–41508. doi: 10.1074/jbc.M110.177600

Sample, V., DiPilato, L. M., Yang, J. H., Ni, Q., Saucerman, J. J., and Zhang, J. (2012). Regulation of nuclear PKA revealed by spatiotemporal manipulation of cyclic AMP. *Nat. Chem. Biol.* 8, 375–382. doi: 10.1038/nchembio.799

Schröder-Lang, S., Schwärzel, M., Seifert, R., Strünker, T., Kateriya, S., Looser, J., et al. (2007). Fast manipulation of cellular cAMP level by light in vivo. *Nat. Methods* 4, 39–42. doi: 10.1038/nmeth975

Serizawa, S., Miyamichi, K., Takeuchi, H., Yamagishi, Y., Suzuki, M., and Sakano, H. (2006). A neuronal identity code for the odorant receptor-specific and activity-dependent axon sorting. *Cell* 127, 1057–1069. doi: 10.1016/j.cell.2006.10.031

Shelly, M., Cancedda, L., Heilshorn, S., Sumbre, G., and Poo, M.-M. (2007). LKB1/STRAD promotes axon initiation during neuronal polarization. *Cell* 129, 565–577. doi: 10.1016/j.cell.2007.04.012

Shelly, M., Cancedda, L., Lim, B. K., Popescu, A. T., Cheng, P., Gao, H., et al. (2011). Semaphorin3A regulates neuronal polarization by suppressing axon formation and promoting dendrite growth. *Neuron* 71, 433–446. doi: 10.1016/j.neuron.2011.06.041

Shelly, M., Lim, B. K., Cancedda, L., Heilshorn, S. C., Gao, H., and Poo, M. (2010). Local and long-range reciprocal regulation of cAMP and cGMP in axon/dendrite formation. *Science* 327, 547–552. doi: 10.1126/science.1179735

Shewan, D., Dwivedy, A., Anderson, R., and Holt, C. E. (2002). Age-related changes underlie switch in netrin-1 responsiveness as growth cones advance along visual pathway. *Nat. Neurosci.* 5, 955–962. doi: 10.1038/nn919

Song, H. J., Ming, G. L., and Poo, M. M. (1997). cAMP-induced switching in turning direction of nerve growth cones. *Nature* 388, 275–279. doi: 10.1038/40864

Stellwagen, D., and Shatz, C. J. (2002). An instructive role for retinal waves in the development of retinogeniculate connectivity. *Neuron* 33, 357–367. doi: 10.1016/s0896-6273(02)00577-9

Stellwagen, D., Shatz, C. J., and Feller, M. B. (1999). Dynamics of retinal waves are controlled by cyclic AMP. *Neuron* 24, 673–685. doi: 10.1016/s0896-6273(00)81121-6

Stierl, M., Stumpf, P., Udwari, D., Gueta, R., Hagedorn, R., Losi, A., et al. (2011). Light modulation of cellular cAMP by a small bacterial photoactivated adenylyl cyclase, bPAC, of the soil bacterium Beggiatoa. *J. Biol. Chem.* 286, 1181–1188. doi: 10.1074/jbc.M110.185496

Tang, F., Dent, E. W., and Kalil, K. (2003). Spontaneous calcium transients in developing cortical neurons regulate axon outgrowth. *J. Neurosci.* 23, 927–936.

Terrin, A., Di Benedetto, G., Pertegato, V., Cheung, Y.-F., Baillie, G., Lynch, M. J., et al. (2006). PGE(1) stimulation of HEK293 cells generates multiple contiguous domains with different [cAMP]: role of compartmentalized phosphodiesterases. *J. Cell Biol.* 175, 441–451. doi: 10.1083/jcb.200605050

Terrin, A., Monterisi, S., Stangherlin, A., Zoccarato, A., Koschinski, A., Surdo, N. C., et al. (2012). PKA and PDE4D3 anchoring to AKAP9 provides distinct regulation of cAMP signals at the centrosome. *J. Cell Biol.* 198, 607–621. doi: 10.1083/jcb.201201059

Tojima, T., Itofusa, R., and Kamiguchi, H. (2009). The nitric oxide-cGMP pathway controls the directional polarity of growth cone guidance via modulating cytosolic Ca2+ signals. *J. Neurosci.* 29, 7886–7897. doi: 10.1523/jneurosci.0087-09.2009

Valsecchi, F., Konrad, C., and Manfredi, G. (2014). Role of soluble adenylyl cyclase in mitochondria. *Biochim. Biophys. Acta* doi: 10.1016/j.bbadis.2014.05.035. [Epub ahead of print].

Vincent, P., Castro, L. R. V., Gervasi, N., Guiot, E., Brito, M., and Paupardin-Tritsch, D. (2012). PDE4 control on cAMP/PKA compartmentation revealed by biosensor imaging in neurons. *Horm. Metab. Res.* 44, 786–789. doi: 10.1055/s-0032-1311631

Welker, E., Armstrong-James, M., Bronchti, G., Ourednik, W., Gheorghita-Baechler, F., Dubois, R., et al. (1996). Altered sensory processing in the somatosensory cortex of the mouse mutant barrelless. *Science* 271, 1864–1867. doi: 10.1126/science.271.5257.1864

Willoughby, D., and Cooper, D. M. F. (2006). Ca2+ stimulation of adenylyl cyclase generates dynamic oscillations in cyclic AMP. *J. Cell Sci.* 119, 828–836. doi: 10.1242/jcs.02812

Willoughby, D., and Cooper, D. M. F. (2007). Organization and Ca2+ regulation of adenylyl cyclases in cAMP microdomains. *Physiol. Rev.* 87, 965–1010. doi: 10.1152/physrev.00049.2006

Willoughby, D., Everett, K. L., Halls, M. L., Pacheco, J., Skroblin, P., Vaca, L., et al. (2012). Direct binding between Orai1 and AC8 mediates dynamic interplay between Ca2+ and cAMP signaling. *Sci. Signal.* 5:ra29. doi: 10.1126/scisignal.2002299

Willoughby, D., Masada, N., Wachten, S., Pagano, M., Halls, M. L., Everett, K. L., et al. (2010). AKAP79/150 interacts with AC8 and regulates Ca2+-dependent cAMP synthesis in pancreatic and neuronal systems. *J. Biol. Chem.* 285, 20328–20342. doi: 10.1074/jbc.m110.120725

Wong, W., and Scott, J. D. (2004). AKAP signalling complexes: focal points in space and time. *Nat. Rev. Mol. Cell Biol.* 5, 959–970. doi: 10.1038/nrm1527

Wong, S. T., Trinh, K., Hacker, B., Chan, G. C., Lowe, G., Gaggar, A., et al. (2000). Disruption of the type III adenylyl cyclase gene leads to peripheral and behavioral anosmia in transgenic mice. *Neuron* 27, 487–497. doi: 10.1016/s0896-6273(00)00060-x

Wu, K. Y., Zippin, J. H., Huron, D. R., Kamenetsky, M., Hengst, U., Buck, J., et al. (2006). Soluble adenylyl cyclase is required for netrin-1 signaling in nerve growth cones. *Nat. Neurosci.* 9, 1257–1264. doi: 10.1038/nn1767

Zaccolo, M., and Movsesian, M. A. (2007). cAMP and cGMP signaling cross-talk: role of phosphodiesterases and implications for cardiac pathophysiology. *Circ. Res.* 100, 1569–1578. doi: 10.1161/circresaha.106.144501

Zhang, J., Ackman, J. B., Xu, H.-P., and Crair, M. C. (2012). Visual map development depends on the temporal pattern of binocular activity in mice. *Nat. Neurosci.* 15, 298–307. doi: 10.1038/nn.3007

Zhang, J., Ma, Y., Taylor, S. S., and Tsien, R. Y. (2001). Genetically encoded reporters of protein kinase A activity reveal impact of substrate tethering. *Proc. Natl. Acad. Sci. U S A* 98, 14997–15002. doi: 10.1073/pnas.211566798

Zippin, J. H., Chen, Y., Nahirney, P., Kamenetsky, M., Wuttke, M. S., Fischman, D. A., et al. (2003). Compartmentalization of bicarbonate-sensitive adenylyl cyclase in distinct signaling microdomains. *FASEB J.* 17, 82–84. doi: 10.1096/fj.02-0598fje

Zou, D.-J., Chesler, A. T., Le Pichon, C. E., Kuznetsov, A., Pei, X., Hwang, E. L., et al. (2007). Absence of adenylyl cyclase 3 perturbs peripheral olfactory projections in mice. *J. Neurosci.* 27, 6675–6683. doi: 10.1523/jneurosci.0699-07.2007

Conflict of Interest Statement: The authors declare that the research was conducted in the absence of any commercial or financial relationships that could be construed as a potential conflict of interest.

Received: 10 September 2014; paper pending published: 05 October 2014; accepted: 21 October 2014; published online: 13 November 2014.

*Citation: Averaimo S and Nicol X (2014) Intermingled cAMP, cGMP and calcium spatiotemporal dynamics in developing neuronal circuits. Front. Cell. Neurosci. **8**:376. doi: 10.3389/fncel.2014.00376*

This article was submitted to the journal Frontiers in Cellular Neuroscience.

frontiers in
MOLECULAR NEUROSCIENCE

REVIEW ARTICLE
published: 04 March 2015
doi: 10.3389/fnmol.2015.00006

cGMP in mouse rods: the spatiotemporal dynamics underlying single photon responses

Owen P. Gross[1†], Edward N. Pugh Jr.[2,3,4] and Marie E. Burns[1,2,4]*

[1] *Center for Neuroscience, University of California Davis, Davis, CA, USA*
[2] *Departments of Ophthalmology and Vision Science, University of California Davis, Davis, CA, USA*
[3] *Physiology and Membrane Biology, University of California Davis, Davis, CA, USA*
[4] *Cell Biology and Human Anatomy, University of California Davis, Davis, CA, USA*

Edited by:
Hans-Georg Breitinger, German University in Cairo, Egypt

Reviewed by:
Florentina Soto, Washington University in St. Louis, USA
Karl-Wilhelm Koch, Carl von Ossietzky University Oldenburg, Germany

***Correspondence:**
Marie E. Burns, Center for Neuroscience, University of California Davis, 1544 Newton Court, Davis, CA 95618, USA
e-mail: meburns@ucdavis.edu

†Present address:
Owen P. Gross, Vollum Institute, Oregon Health and Science University, Portland, OR 97239, USA

Vertebrate vision begins when retinal photoreceptors transduce photons into electrical signals that are then relayed to other neurons in the eye, and ultimately to the brain. In rod photoreceptors, transduction of single photons is achieved by a well-understood G-protein cascade that modulates cGMP levels, and in turn, cGMP-sensitive inward current. The spatial extent and depth of the decline in cGMP during the single photon response (SPR) have been major issues in phototransduction research since the discovery that single photons elicit substantial and reproducible changes in membrane current. The spatial profile of cGMP decline during the SPR affects signal gain, and thus may contribute to reduction of trial-to-trial fluctuations in the SPR. Here we summarize the general principles of rod phototransduction, emphasizing recent advances in resolving the spatiotemporal dynamics of cGMP during the SPR.

Keywords: phototransduction, photoreceptor, rod, vision, rhodopsin

OVERVIEW OF ROD PHOTOTRANSDUCTION

The conversion of light energy into electrical signals in rod and cone photoreceptor cells of the retina is the first step in vision. When photoreceptors die, as in diseases such as retinitis pigmentosa or age-related macular degeneration, the otherwise intact visual system loses its normal input, and vision is lost. Fundamental properties of rods and cones, including photon capture efficiency, amplification, kinetics, and spectral sensitivity, strongly constrain the information relayed to the rest of the visual system and ultimately experienced as brightness, form, color, motion, etc.

Night vision under the almost 1000-fold illumination range from starlight to full moonlight operates on a diet literally starved for photons (Burns and Pugh, 2014). All aspects of vision under such nighttime conditions are governed exclusively by signals arising from rods, which generate highly reliable changes in membrane current in response to the absorption of single photons (Baylor et al., 1979b) These single photon responses (SPRs) are driven by a chain of biochemical reactions ("phototransduction") that transduce photon absorption into changes in the intracellular concentration of cGMP, which through its actions on cGMP-sensitive ion channels enables this exquisite sensitivity to light.

The proteins and signaling pathways underlying rod phototransduction are highly conserved across vertebrates, and in many species the key proteins involved are amenable to efficient biochemical purification and *in vitro* assays. From decades of biochemical work, we know much about the identity, stoichiometries, binding interactions, and even the structure of most of the proteins required for signaling. For example, we know that a photon of appropriate energy excites the G-protein coupled receptor, rhodopsin, which in turn activates many copies of the G-protein transducin ($G\alpha_t\beta_1\gamma_1$). Each activated $G\alpha_t$ stoichiometrically activates cGMP phosphodiesterase (PDE6), leading to the fall in cGMP concentration. This fall in cGMP causes cyclic nucleotide-gated (CNG) channels on the plasma membrane to close, leading to the reduction of inward cation current (and intracellular free Ca^{2+} levels) and ultimately, membrane hyperpolarization that reduces the synaptic release of glutamate. Timely restoration of the current requires synthesis of cGMP by guanylate cyclases and deactivation of rhodopsin and G-protein/PDE molecules.

The rates of many of these steps can be investigated physiologically in intact rods using suction electrode recording (Baylor et al., 1979a), where the enzymes and substrates are present in their natural concentrations and the membrane current reflects the concentration of cGMP with millisecond precision. With the wide availability of genetically manipulated phototransduction proteins (Fu and Yau, 2007; Burns and Pugh, 2010), mouse rods have become a particularly valuable preparation for investigating the spatiotemporal dynamics of cGMP signaling.

STRUCTURAL AND BIOCHEMICAL CONSTRAINTS ON cGMP SIGNALING IN RODS

THE SPATIAL SPREAD OF cGMP SIGNALING IS RESTRICTED BY THE INTRACELLULAR DISKS

The nature of the disk stack

Phototransduction occurs within a specialized cylindrical subcellular compartment, the outer segment, which is exclusively devoted to absorbing and transducing photons (**Figure 1A**).

The outer segment is filled with a dense stack of protein-rich lipid membranes called disks (**Figure 1B**). The disks house the membrane-associated enzymes of the cascade, including rhodopsin, transducin, phosphodiesterase (PDE), guanylate cyclase as well as regulatory proteins like rhodopsin kinase (GRK1) and the RGS9 complex (below). The abundance of rhodopsin in the disk membranes (25,000–30,000 μm^{-2}) and the large number of densely stacked disks (30 μm^{-1}) create a high axial absorbance, insuring that a large proportion of incident photons are captured. The density of transducin and PDE is sufficient to insure high diffusional encounter rates, allowing transduction of a single photon to be rapid and strongly amplified (Pugh and Lamb, 1993).

While the primary cascade enzymes – photoexcited rhodopsin (R*), and transducin-activated PDE (E*) – are confined to the disk membrane surface where a photon has been captured, the second messengers cGMP and Ca^{2+} are cytosolic, and can diffuse both radially and axially in the outer segment. Cytosolic diffusion in rods equilibrates much more rapidly in the radial direction than in the axial or longitudinal dimension (Lamb et al., 1981; Olson and Pugh, 1993). As a consequence, diffusion of cGMP in the rod can be characterized by an effective

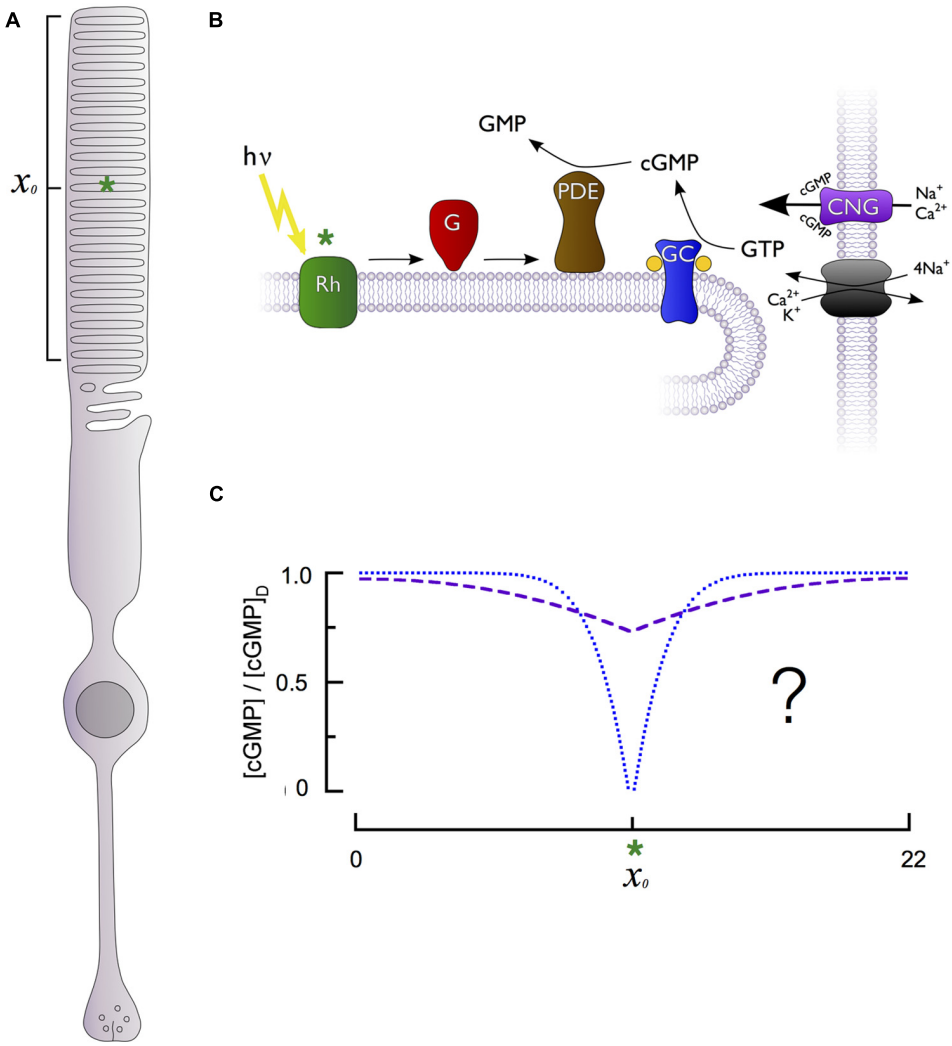

FIGURE 1 | Generation of cGMP spatiotemporal dynamics by the phototransduction cascade of retinal rods. (A) Schematic of a rod photoreceptor, highlighting the light-sensitive outer segment compartment (bracket) containing stacks of intracellular membranous disks and a hypothetical photon absorption (green asterisk) occurring in the middle of the outer segment's length (x_0). **(B)** The primary enzymes responsible for generation of cGMP dynamics are located on the intracellular disk membranes, separated from the cGMP-sensitive channel (CNG) and Na^+/Ca^{2+}, K^+ exchanger located on the plasma membrane. Photon absorption (green asterisk) by a rhodopsin molecule (Rh) activates multiple G-proteins (G) and cGMP phosphodiesterases (PDE), which are unable to diffuse longitudinally within the rod due to their tight association with the disk membrane. PDE activation in effect produces a point sink for decline in cytoplasmic cGMP along the rod longitudinal axis. The cGMP level is restored by guanylate cyclase activity (GC). **(C)** The fall in cGMP [relative to the dark level, $(cGMP)_D$] as a function of distance from the site of photon absorption (x_0, green asterisk) could be either shallow and broad (dashed purple curve) or deep and narrow (dotted blue curve), with markedly different consequences for signal reproducibility and linearity (see text).

longitudinal diffusion coefficient (D_{cG}). Because the disks occupy more than 95% of the cross-section of the outer segment, they retard axial diffusion 20-fold or more below its value in unobstructed cytosol (Lamb et al., 1981; Cameron and Pugh, 1990; Olson and Pugh, 1993; Holcman and Korenbrot, 2004). Whether the fall in cGMP is relatively shallow but spatially widespread or deep and spatially restricted (**Figure 1C**) fundamentally affects rod signaling, including the degree to which fluctuations in biochemical processes elicit electrical fluctuations and the range over which rods can linearly sum concurrently absorbed photons. This question has been addressed many times experimentally and theoretically, and the results are summarized below.

Variations in ultrastructure cause D_{cG} to vary between the rods of different species. Outer segments of toads and salamanders have far larger diameters (6–15 μm) than those of their mammalian counterparts (1–2 μm). In addition, rod disks have narrow radial gaps called "incisures" that tend to be aligned axially (Cohen, 1963) and greatly facilitate longitudinal diffusion. The length and number of incisures vary across species, ranging from 1 in mouse and human peripheral rods, to 18 or more in tiger salamander rods (Olson and Pugh, 1993).

Estimates of D_{cG} have been made from optical measurements of the diffusion of fluorescent compounds, including fluorescein-cGMP (Olson and Pugh, 1993; Holcman and Korenbrot, 2004), and from electrical measurements of cGMP-activated current in dialyzed rods (Cameron and Pugh, 1990; Koutalos et al., 1995a,c; Wu et al., 2006). For the largest diameter rods (salamander), D_{cG} was found to be 5–10 $\mu m^2\ s^{-1}$ (Cameron and Pugh, 1990; Olson and Pugh, 1993), while for narrow mouse rods, ∼40 $\mu m^2\ s^{-1}$ (Holcman and Korenbrot, 2004; Gross et al., 2012b). D_{cG} is, however, only one of several factors governing the spatial profile of cGMP depletion during the SPR, as we now discuss.

THE SPATIAL EXTENT AND DEPTH OF LOCAL cGMP DEPLETION DURING THE SINGLE PHOTON RESPONSE

Direct measurement of the axial spread of cGMP or Ca^{2+} during the SPR is challenging, because most light used for imaging strongly activates phototransduction. As a consequence, measurements based on the analysis of electrophysiological data have provided the primary body of evidence. Though such measurements are indirect, they are simplified by the lack of voltage-dependence of the rod cGMP channels and the absence of other significant outer segment currents. One experimental approach involves using slits or small spots to deliver light stimuli to different locations in the outer segment while recording the membrane current. Such experiments have yielded conflicting results, with some authors concluding that during the SPR cGMP falls only slightly from its resting level over a large spatial extent (Hemilä and Reuter, 1981; Field and Rieke, 2002), while others concluded that the change is highly localized (Lamb et al., 1981; Gray-Keller et al., 1999). Discrepancies between experiments might be expected because they were performed on rods of different species with distinct outer segment morphology and cGMP diffusion coefficients (see above).

A steady-state measure of the spatial spread of cGMP signaling in mouse rods

A recent investigation (Gross et al., 2012b) determined the spatial spread of the cGMP signal initiated by naturally occurring very long-lived "rogue" R*'s, which produce SPRs that are step-like in shape (Baylor et al., 1984). For such SPRs, the spatial profile of cGMP is in steady-state. The cGMP concentration declines as a function of distance from the "point sink" of PDE activity and is predicted by a straightforward analytic expression:

$$\frac{cG(x)}{cG_{dark}} = \frac{1 - e^{-|x-x_0|/\lambda}}{1 + C} \quad (1)$$

Here $cG(x)$ represents the cGMP concentration at axial position x along the outer segment, cG_{dark} the uniform concentration in the rod in darkness, x_0 the location of photon absorption, $\lambda = \sqrt{D_{cG}/\beta_{dark}}$ the space constant of the cGMP profile, and C a constant that depends on known parameters of rod geometry and the measured lifetime of E*. The parameter β_{dark} is the rate constant of spontaneous cGMP hydrolysis in the outer segment in the dark, determined to be 4.1 s^{-1} in mouse rods (Gross et al., 2012b). This mathematical description of the cGMP spatial profile can be converted into the expected change in outer segment current by substituting the well-established relationship between cGMP and channel gating (see Eqs 2 and 3, below) into Eq. 1, and performing spatial integration over the length of the outer segment. Gross et al. (2012b) determined λ and C from experimentally measured, steady-state rogue SPR amplitudes, obtaining $\lambda = 3.1$ μm for the space constant and $[1/(1+C)] = 0.61$ for the depth of cGMP decline at x_0. From the same analysis, D_{cG} was estimated to be 40 $\mu m^2\ s^{-1}$, remarkably close to the value 36 $\mu m^2\ s^{-1}$ estimated for rodent rods by Holcman and Korenbrot (2004) solely from geometric considerations. While this analysis of the spatial profile of cGMP during the SPR was based on the steady-state SPR amplitudes driven by "rogue" rhodopsins, the analysis provides a rigorous lower bound on the depth of the cGMP profile and an upper bound on the spatial extent. It also provides reasonable and consistent estimates of D_{cG} and the composite transduction gain (Leskov et al., 2000; Heck and Hofmann, 2001). Most importantly, the resulting values of the parameters β_{dark} and D_{cG} are valid generally, and are essential for constraining a spatiotemporal model that incorporates the normal lifetimes of R* and E*, as well as the effects of calcium feedback regulation to cGMP synthesis, as discussed in the following sections.

PDE CONTRIBUTES AMPLIFICATION TO THE SPR BUT ALSO SPEEDS SIGNALING AND LIMITS ITS RELIABILITY

R* is normally active for only a short time (∼40 ms; Gross and Burns, 2010). However, during its brief lifetime R* activates transducins (G_t) at a high rate, ∼350 s^{-1} per R* in mammalian rods at body temperature (Heck and Hofmann, 2001). In turn, each G_t activates a PDE, with the result that at the peak of the SPR, ∼10 E* are active (Gross et al., 2012b). Despite this small number of E*, a sizable change in cGMP concentration is ensured because E* act upon cGMP in the relatively small volume of the interdiscal space, and each E* is a highly efficient enzyme. Thus, the PDE catalytic efficiency is $k_{cat}/K_m = 4.4 \times 10^8\ M^{-1}\ s^{-1}$ (Leskov et al.,

2000), which is close to the rate limit ($\sim 10^9$ M^{-1} s^{-1}) set by cGMP diffusion to the PDE catalytic site (Reingruber et al., 2013).

Phosphodiesterase activity affects signaling in other ways, particularly in the dark-adapted rod, because PDE molecules occasionally become spontaneously active. First, this spontaneous or basal "dark" activity sets a threshold that must be overcome by the light-activated PDE activity generated by a single R*. Second, the reciprocal of the basal rate of PDE hydrolysis ($1/\beta_{dark}$) corresponds to the average lifetime of a cGMP molecule in the dark, and contributes to the speed of SPR recovery (Nikonov et al., 2000; Gross et al., 2012b; Reingruber et al., 2013). Third, the basal hydrolysis rate determines the space constant of the cGMP spatial profile (see above. Eq. 1). Fourth, spontaneous PDE activity produces sizable fluctuations in the membrane current, termed "continuous noise" (Baylor et al., 1980; Rieke and Baylor, 1996), which varies with the membrane density of the PDE in a manner that may compensate for differences in outer segment diameter (Reingruber et al., 2013).

THE FALL IN cGMP IS SUFFICIENTLY SMALL TO MAXIMIZE THE GAIN CONFERRED BY COOPERATIVE CHANNEL GATING

CNG channel properties

Light-stimulated PDE activity decreases the cytoplasmic cGMP concentration, leading to closure of cGMP-gated (CNG) channels in the plasma membrane and reduction of the inward current they carry. The rod CNG channel is a heterotetramer comprising three α- and one β-subunit (Shuart et al., 2011), and is permeable to Na^+, K^+, and Ca^{2+} (Craven and Zagotta, 2006). The α-subunit of the channel binds to the Na^+/Ca^{2+}-K^+ exchanger in the plasma membrane (Schwarzer et al., 2000) via glutamic acid rich protein-like (GARP) domains, likely contributing to the spatiotemporal dynamics of internal calcium. Cytosolic GARP proteins (GARP-1 and GARP-2) are also of fundamental importance in the assembly of the outer segment structure and in stabilizing the disk rims (Korschen et al., 1999; Poetsch et al., 2001; Ritter et al., 2011).

The conductance of CNG channels equilibrates with cGMP concentration within milliseconds (Cobbs and Pugh, 1987; Karpen et al., 1988), so that the time course of the SPR is not limited by the response time of the channel, but rather tracks the changing local cGMP concentration. The cGMP concentration in the dark is 3–4 μM, low relative to the $K_{1/2}$ (~20 μM) of the channels, so that most CNG channels are closed even in complete darkness. These features of the channel, as well as its relative insensitivity to voltage in the physiological range of membrane potentials (Bodoia and Detwiler, 1985; Baylor and Nunn, 1986), have enabled investigation of phototransduction biochemistry via the electrical response. The gating of the CNG channel by cGMP is cooperative, as captured in the Hill relation that describes the dependence on cGMP of CNG current in a patch of outer segment membrane:

$$\frac{J_{cG}}{J_{max}} = \frac{cG^n}{cG^n + K_{1/2}{}^n} \quad (2)$$

where J is current, cG is the concentration of cGMP, n the Hill coefficient and $K_{1/2}$ the half-saturating concentration. Early estimates of the Hill coefficient for the channel ranged between 1 and 3 (e.g., Fesenko et al., 1985; Haynes et al., 1986). However, Ruiz et al. (1999) showed that the lower Hill coefficients were likely due to heterogeneity in sensitivity to cGMP ($K_{1/2}$) across the population of channels in any given patch. This heterogeneity leads to a more shallow dose response curve, resulting in underestimation of the true Hill coefficient. In single channel experiments, the Hill coefficient consistently was measured to be three, a value now widely accepted.

Contribution of cooperative gating to gain

In the living rod $cG << K_{1/2}$ and so from Eq. 2 the CNG channel current density $J_{cG}(x)$at any point x along the outer segment satisfies

$$\frac{J_{cG}(x)}{J_{dark}} = \left[\frac{cG(x)}{cG_{dark}}\right]^n \quad (3)$$

where J_{dark} is the axial current density in darkness. Thus, the contribution of the cGMP channel's cooperative gating to the gain of phototransduction is determined by the extent to which the local cGMP level falls during the SPR. If the fractional decline in cGMP is less than about 20%, the change in current will be amplified threefold relative to the fractional change in cGMP concentration. On the other hand, if the local fractional decrease in cGMP exceeds ~20%, the proportionality between the response amplitude and the overall decline in cGMP will fall short of three, effectively causing "saturation" of the local cGMP-mediated signal. The question of whether or not local saturation contributes to reduction of the trial-to-trial variability of SPRs has been addressed by experiments in toad (Rieke and Baylor, 1998), guinea pig and monkey rods (Field and Rieke, 2002), which concluded that complete local closure of channels is not a major factor limiting variability. In mouse rods, the local fall in cGMP at the peak of the SPR is normally less than 15% of the dark concentration (Gross et al., 2012b) primarily because of the rapid increase in cGMP synthesis, which we now describe.

CALCIUM FEEDBACK TO cGMP SYNTHESIS

Balance between cGMP synthesis and hydrolysis

In darkness there is a balance between cGMP synthesis and hydrolysis, leading to a steady level of cGMP (cG_{dark} in Eq. 3). With the rate of synthesis identified as α_{dark} and the rate constant of hydrolysis as β_{dark} (see above), the steady-state cGMP concentration in darkness must satisfy

$$cG_{dark} = \alpha_{dark}/\beta_{dark} \quad (4)$$

The basal rate of cGMP synthesis has been estimated from biochemical assays to be between 9 and 24 μM s^{-1} in dark-adapted mouse rod outer segments (Makino et al., 2008). Given $\beta_{dark} = 4.1$ s^{-1} (Gross et al., 2012b), a synthesis rate of 9 μM s^{-1} corresponds to cG_{dark} = 2.4 μM, while that of 24 μM s^{-1} corresponds to 6.6 μM. The former of these values is close to that (3.2 μM) estimated from experiments in salamander rods (Cameron and Pugh, 1990).

Activation of guanylate cyclase by declining calcium

Activation of rhodopsin by light adjusts the equilibrium level of cGMP by stimulating not only cGMP hydrolysis, but also synthesis in an intricate feedback involving Ca^{2+}. In darkness about 15% of the inward current through the CNG channels is carried

by Ca^{2+}, which is homeostatically pumped out by the Na/Ca-K exchanger (NCKX): closure of channels rapidly causes internal Ca^{2+} to decline as its influx decreases and extrusion by NCKX exchange continues. Following light stimulation, recovery to the dark-adapted state requires not only deactivation of R* and E*, but also restoration of the dark concentration of cGMP, which is synthesized from GTP by retinal guanylate cyclase 1 and 2 (RetGC-1 and RetGC-2, "GC"; for review see Sharma, 2010). The rate of cGMP synthesis depends strongly on intracellular calcium concentration (Koch and Stryer, 1988; Koutalos et al., 1995b). This calcium dependence is conferred by guanylate cyclase activating proteins (GCAP-1 and GCAP-2), which are inhibited by calcium binding (Palczewski et al., 1994; Dizhoor and Hurley, 1996, 1999; Ames et al., 1999) but disinhibited as calcium declines during the light response.

The calcium dependence of cyclase activation by GCAPs follows a Hill relation with a Hill coefficient of ~2 and an effective $K_{1/2}$ between 60 and 130 nM (Dizhoor and Hurley, 1996; Ames et al., 1999; Palczewski et al., 2000; Makino et al., 2008; Peshenko et al., 2011). Mechanistically, calcium sensitivity is conferred by three functional EF-hands, while a fourth EF-hand does not bind calcium. In the dark-adapted outer segment when Ca^{2+} is at its highest level, metal binding sites are occupied by calcium, and GCAPs are inhibited from activating GC. As Ca^{2+} falls during the light response, these binding sites become occupied instead by Mg^{2+}, which facilitates GC activation (Peshenko and Dizhoor, 2004). The Ca^{2+}/Mg^{2+} sensor properties exhibit slightly different sensitivities for GCAP-1 and GCAP-2, likely contributing to their differential effects on the light response (Dizhoor et al., 2010).

Cyclase activation in living rods

The time course with which Ca^{2+} declines when channels close depends on the rate and $K_{1/2}$ of the Na^+/Ca^{2+}-K^+ exchanger (NCKX), the volume the outer segment, the calcium buffering capacity and the diffusion coefficient (Lagnado et al., 1992). In large amphibian rods the decrease in calcium estimated from the exchange current has a principal time constant of ~2 s (Cobbs and Pugh, 1987; Hodgkin et al., 1987), while in small mammalian rods the decline is more than 10-fold faster (Makino et al., 2004). Measurements of the concentration of calcium of the outer segment in the dark in rods of different species range from to 250 nM (mouse, Woodruff et al., 2002), to 273 nM (toad, Korenbrot and Miller, 1989), to 670 nM (salamander, Sampath et al., 1998).

Strong cyclase activation occurs even during the SPR, restricting its amplitude and speeding its recovery: in mouse rods lacking calcium feedback activation of cyclase ($GCAPs^{-/-}$) the SPR has an approximately three- to fourfold greater amplitude than that of WT rods, reaching its peak amplitude and recovering much more slowly (**Figure 2A**; Mendez et al., 2001; Burns et al., 2002). While the increased amplitude of SPRs of $GCAPs^{-/-}$ rods results primarily from the absence of calcium feedback to cyclase, the slowed recovery is determined by the time constant of cGMP turnover ($1/\beta_{dark}$ = 245 ms), which becomes the rate-limiting step of recovery (see above; Nikonov et al., 2000; Gross et al., 2012b).

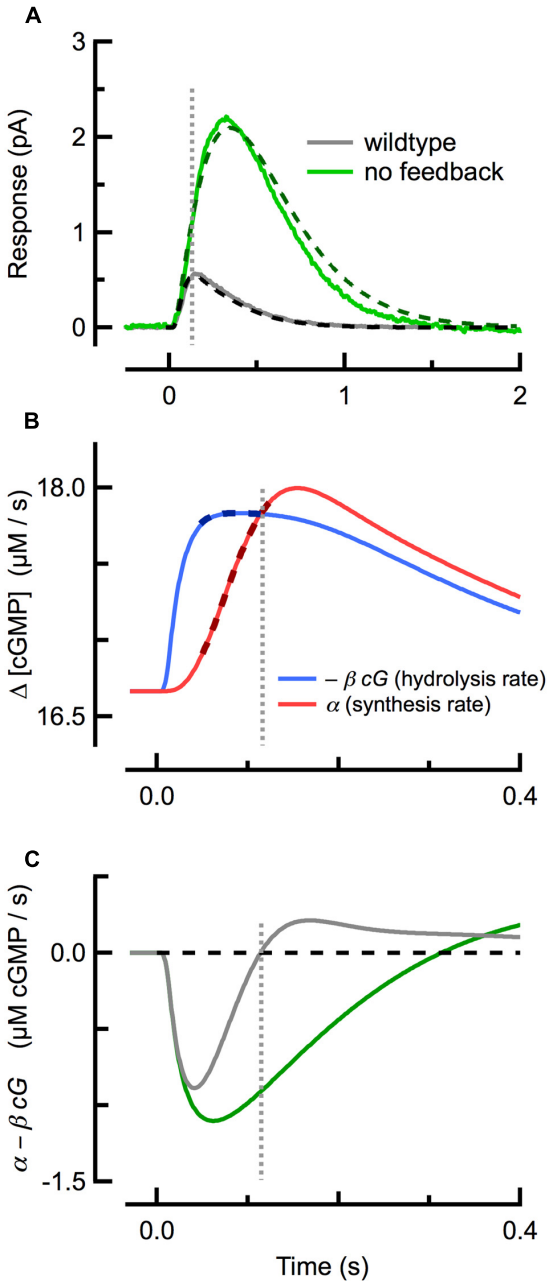

FIGURE 2 | Delayed, ramping cGMP synthesis contributes to the temporal precision and reproducible amplitude of the SPR. **(A)** Measured (solid) and simulated (dashed) SPRs for WT (gray) and $GCAPs^{-/-}$ (green; no calcium feedback) rods originally published in Gross et al. (2012b). **(B)** Spatially integrated rates of cGMP hydrolysis (blue trace) and synthesis (red) during during the WT SPR, as computed with the spatiotemporal model fitting the WT trace in **(A)**. The rate of cGMP hydrolysis plateaus quickly, while the rate of cGMP synthesis exhibits a brief delay followed by a slower, ramping climb to its maximum. Thick dashed lines indicate the coincident plateau and ramping phases of hydrolysis and synthesis, respectively. **(C)** The difference between the cGMP synthesis and hydrolysis rates for WT and $GCAPs^{-/-}$ rods. The rate of cGMP synthesis in $GCAPs^{-/-}$ rods remains constant (not shown) due to the absence of calcium feedback. Note that the zero-crossings of the traces in **(C)** correspond to the SPR peaks in **(A)**. Vertical dashed line indicates time of WT SPR peak in all panels.

INSIGHTS FROM A SPATIOTEMPORAL MODEL OF cGMP AND Ca^{2+} DYNAMICS

VALUE OF MATHEMATICAL MODELS OF THE SINGLE PHOTON RESPONSE

Mathematical models can contribute much to the understanding of cellular dynamics by compactly embodying current molecular knowledge, by yielding quantitative insight into key biological functions such signal gain and reliability, and by providing explanations of malfunction in disease or molecularly manipulated states (e.g., Boyett et al., 2000; Tao et al., 2011). Models of phototransduction have contributed, for example, to the understanding of the molecular mechanisms of amplification of the light response (Pugh and Lamb, 1993). For many years it has been understood and generally accepted that the entire time course of the rod light response should be describable in terms of a pair of coupled partial differential equations governing cytoplasmic cGMP and Ca^{2+} with initial and boundary conditions, and with an appropriate kinetic model of R* and E* activation and inactivation (Lamb and Pugh, 1992; Andreucci et al., 2003). The SPR has been an important target of this modeling, and perhaps no feature of the SPR has been more celebrated and yet more difficult to understand in molecular terms than its stereotypic amplitude: specifically, the measured coefficient of variation of the amplitude (SD/mean) is 0.2–0.4 (Baylor et al., 1979b; Rieke and Baylor, 1998; Whitlock and Lamb, 1999; Field and Rieke, 2002; Hamer et al., 2003; Gross et al., 2012a), much lower than that (1.0) that would occur were the single R* underlying it to deactivate in a single stochastic step. Several models of the SPR have been published that address this issue (Rieke and Baylor, 1998; Field and Rieke, 2002; Hamer et al., 2003), including several spatiotemporal models, i.e., models that include the diffusion of cGMP and Ca^{2+} (e.g., Andreucci et al., 2003; Bisegna et al., 2008; Reingruber and Holcman, 2008; Caruso et al., 2010, 2011; Gross et al., 2012a; Reingruber et al., 2013). In the following paragraphs we summarize some novel results that have come from developing and applying a "fully constrained" spatiotemporal model of phototransduction to the SPR of mouse rods with specific molecular perturbations to the phototransduction machinery (Gross et al., 2012a,b), including fresh insight into the molecular mechanisms underlying its stereotypic amplitude. First, we state the principles, briefly explaining what is meant by "fully constrained."

GROUNDING THE MODEL IN BIOCHEMICAL AND BIOPHYSICAL MEASUREMENTS AND CONSTRAINTS

Given that solutions to the governing equations can be produced that adequately fit rod photoresponses, a critical question to be addressed before valid inferences can be drawn is "Are the parameters of the model well constrained?" Ill-constrained models, even if they accurately describe aspects of the data, can lead to ambiguous and even false inferences. Thus, every potential constraint from structure, biochemistry and experiment independent of the fitting process should be incorporated, such that in the ideal there are no truly "free parameters," i.e., parameters whose values are determined solely by fitting.

As described above, the key spatial parameter D_{cG}, rate parameter β_{dark}, and the composite transduction gain were determined from independent measurements (Gross et al., 2012b). The *in situ* lifetimes of the transduction amplifiers (R* and E*) were incorporated from previous electrophysiological measurements of bright flash responses in genetically targeted mice (Krispel et al., 2006; Gross and Burns, 2010), and kinetic parameters relating to Ca^{2+}-dependent activation of NCKX and GCAPs were taken directly from biochemical studies. Dark and maximal cyclase activation levels were determined from experiments and analysis independent of fitting the shape of the SPR. The average lifetimes *in situ* of the amplifying enzymes R* and the PDE active complex (E*) were determined from independent measurements from bright flash responses of genetically targeted mice.

The rods of molecularly targeted mice provide a rich body of individual constraints on model parameters. One of the most important such constraints came from rods lacking GCAPs: the absence of GCAPs completely eliminates calcium feedback to GC and thus uncouples parameters governing calcium dynamics from the rest of the phototransduction equations. Requiring the model of WT SPRs to employ precisely the same parameters as used to describe $GCAPs^{-/-}$ SPRs is highly constraining and informative (Gross et al., 2012b), as the values for a only few parameters involved in calcium fluxes and buffering could then be constrained within biochemically determined limits, and then optimized by the fitting process.

CALCIUM-FEEDBACK ACTIVATED cGMP SYNTHESIS CONFERS TEMPORAL PRECISION AND AMPLITUDE STABILITY TO THE SPR

Several studies had previously concluded that calcium feedback to cGMP synthesis does not play a role in the reproducibility of the SPR (Rieke and Baylor, 1998; Whitlock and Lamb, 1999), but this conclusion has proven to be inconsistent with work showing that reproducibility is degraded in $GCAPs^{-/-}$ rods (Gross et al., 2012a). Investigation of the underlying cGMP dynamics using a spatiotemporal model revealed that a delay in cyclase activation relative to cGMP hydrolysis plays a critical role. At the beginning of the SPR (**Figure 2A**), the rate of light-driven cGMP hydrolysis increases rapidly (**Figure 2B**; blue), after which it begins to plateau as Ca^{2+} declines steadily and the rate of calcium-sensitive cGMP synthesis rises along a ramp (**Figure 2B**; red). The steepness of the synthesis ramp is roughly proportional to the plateau of the hydrolysis rate, so that the ramp overtakes the plateau of hydrolysis at nearly the same time, almost independent of the R* lifetime (Gross et al., 2012a). This equilibrium between cGMP hydrolysis and synthesis corresponds to a net rate of change of cGMP of zero (**Figure 2C**) and so to the peak of the SPR. Thus, delayed, ramping calcium feedback activation of cyclase confers invariance to the SPR time-to-peak in mice with altered R* and E* lifetimes, and a result, to their SPR amplitudes.

CALCIUM FEEDBACK CONTRIBUTES SUBSTANTIALLY TO THE REPRODUCIBILITY OF THE SPR

It has long been hypothesized that late steps in biochemically feasible R* deactivation would greatly decrease SPR reliability "at late times," and that the only possible explanation for the observed high reliability would be a large number of small deactivation steps (Rieke and Baylor, 1998). However, more recent work showed that a broad distribution of R* lifetimes ("noisy" rhodopsin) can be overcome by calcium feedback and generate reproducible SPRs.

The very mechanism that explains "amplitude stability" of the SPR across genotypes also explains why late-stage R* deactivation steps do not decrease SPR reproducibility: specifically, when R* activity to be prolonged due to stochastic deactivation, delayed calcium feedback to cyclase ramps up to overcome the prolonged activity, stabilizing the WT SPR peak timing and amplitude. Modeling further reveals that, due to low-pass filtering of R* activity by the slow deactivation of E*, trial-to-trial fluctuations in the brief lifetime of R* (~40 ms) can account for the full degree of "late-stage" variability observed beyond the peak of the SPR (>130 ms; Gross et al., 2012a).

MEMBRANE FLUX TRUMPS INTRACELLULAR DIFFUSION FOR INTRACELLULAR CALCIUM DYNAMICS

For mouse rods with normal Ca^{2+} feedback to cyclase, theoretical calculations suggest that the spatial extent of the fall in calcium concentration largely mirrors that of cGMP (**Figure 3A**). Interestingly, this similarity in spatial profiles is largely independent of the value of the axial diffusion coefficient for calcium (D_{Ca}) over the full range (0.1–10 $\mu m^2\ s^{-1}$) of physiologically plausible values, given relatively strong intracellular calcium buffering (**Figure 3B**). While the maximal depth of the calcium decline is slightly altered when D_{Ca} is varied, the amplitude and time course of the simulated outer segment current response are not. The calcium profile is insensitive to D_{Ca} because the local net flux of Ca^{2+} through CNG channels and NCKX, which depends on the concentration gradient of calcium across the cell membrane, is much larger than what can be achieved through passive diffusion, given the relatively modest intracellular concentration gradient. To a first approximation, the magnitude of the exchange current is comparable to that of the Ca^{2+} component of the CNG channel current after a brief delay (Lagnado et al., 1992). Because

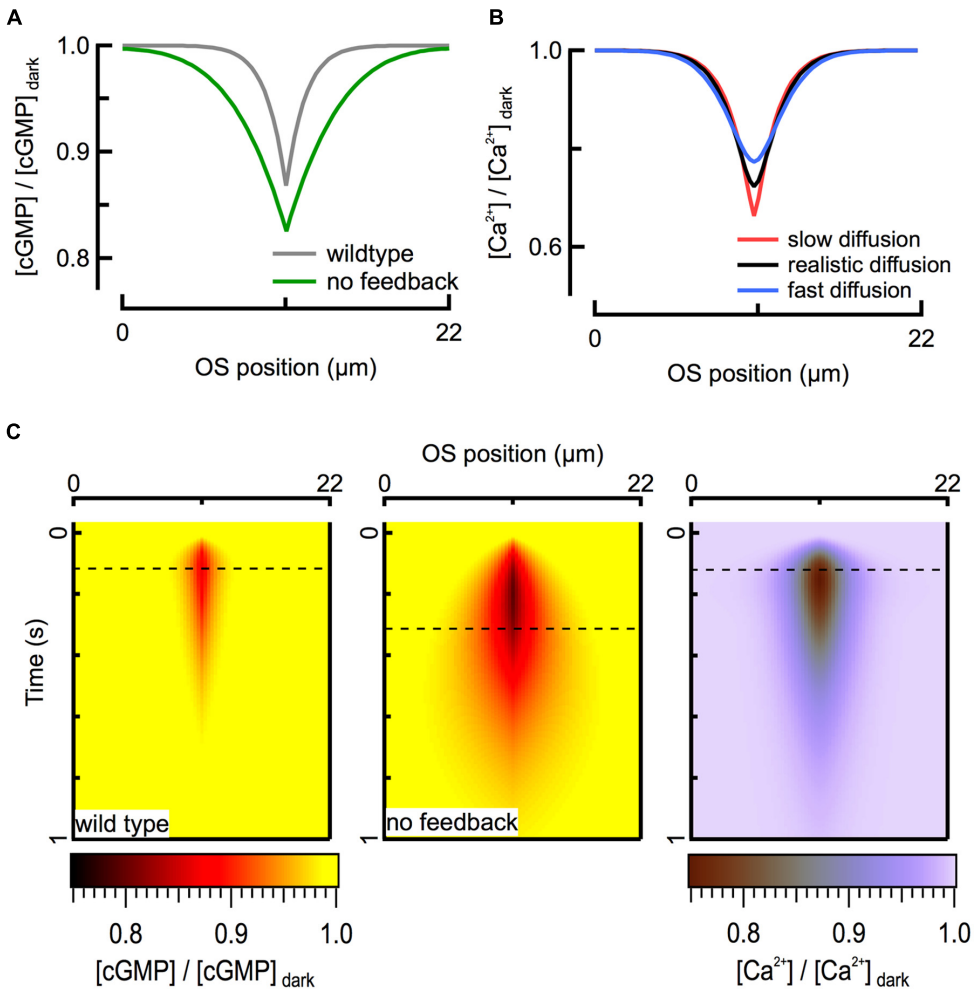

FIGURE 3 | Ca^{2+} feedback to cGMP synthesis restricts the spread of second messenger signals. (A) Calculated spatial profiles of cGMP decline at the time of the peak of the WT (125 ms; gray) and GCAPs$^{-/-}$ (320 ms; green) SPRs for an R* located in the middle of the rod (x = 11 μm). **(B)** The fall in intracellular Ca^{2+} is largely determined by the flux through CNG channels and is therefore insensitive to the value of the diffusion coefficient over the range 0.1 (red) – 10 (blue) $\mu m^2\ s^{-1}$. Black profile represents D_{Ca} = 2 $\mu m^2\ s^{-1}$. All traces correspond to the peak of the WT SPR. **(C)** Heat map representation of calculated cGMP spatiotemporal profiles during WT (*left*) and GCAPs$^{-/-}$ (*center*) SPRs. The corresponding Ca^{2+} profile (*right*) is shown for the WT SPR. Dashed lines indicate time of peak response amplitudes.

the CNG channel current is determined exclusively by cGMP concentration, calcium concentration is also determined by the cGMP concentration (**Figure 3C**). Thus the diffusion barriers present in the outer segment directly influence only the spatio-temporal dynamics of cGMP, and the spatio-temporal dynamics of cGMP determine the distribution of calcium during a light response. Apparently, the calcium feedback system provides a form of self-restriction for the intracellular spread of the second messenger signal, contributing to linearity of the response by limiting overlap of signaling domains originating from multiple rhodopsin isomerizations.

SUMMARY

Application of biochemical, electrophysiological, and computational approaches to understanding the spatio-temporal dynamics of cGMP signaling in vertebrate rods has yielded very good general agreement about the biochemical rates and local diffusional constraints underlying the amplitude, time course, and reproducibility of the SPR. The unification of our understanding across different genetic perturbations in mice (e.g., Gross et al., 2012a) and across vertebrate species (e.g., Reingruber et al., 2013) is encouraging, but there is still a great deal of work to be done. It is important to note that the single photon detection regime of rods constitutes only about three of the six orders of magnitude of intensities over which rods contribute to vision (e.g., Naarendorp et al., 2010). With higher light intensities come fundamental changes in biochemical parameters, cGMP and Ca^{2+} buffering, feedback mechanisms and cGMP dynamics. Future work will aim to build upon our understanding of spatiotemporal dynamics of cGMP signaling in dark-adapted rods by extending existing models to encompass known and new mechanisms of adaptation.

REFERENCES

Ames, J. B., Dizhoor, A. M., Ikura, M., Palczewski, K., and Stryer, L. (1999). Three-dimensional structure of guanylyl cyclase activating protein-2, a calcium-sensitive modulator of photoreceptor guanylyl cyclases. *J. Biol. Chem.* 274, 19329–19337. doi: 10.1074/jbc.274.27.19329

Andreucci, D., Bisegna, P., Caruso, G., Hamm, H. E., and Dibenedetto, E. (2003). Mathematical model of the spatio-temporal dynamics of second messengers in visual transduction. *Biophys. J.* 85, 1358–1376. doi: 10.1016/S0006-3495(03)74570-6

Baylor, D. A., Lamb, T. D., and Yau, K. W. (1979a). The membrane current of single rod outer segments. *J. Physiol.* 288, 589–611.

Baylor, D. A., Lamb, T. D., and Yau, K. W. (1979b). Responses of retinal rods to single photons. *J. Physiol.* 288, 613–634.

Baylor, D. A., Matthews, G., and Yau, K. W. (1980). Two components of electrical dark noise in toad retinal rod outer segments. *J. Physiol.* 309, 591–621. doi: 10.1113/jphysiol.1980.sp013529

Baylor, D. A., and Nunn, B. J. (1986). Electrical properties of the light-sensitive conductance of rods of the salamander *Ambystoma tigrinum*. *J. Physiol.* 371, 115–145. doi: 10.1113/jphysiol.1986.sp015964

Baylor, D. A., Nunn, B. J., and Schnapf, J. L. (1984). The photocurrent, noise and spectral sensitivity of rods of the monkey *Macaca fascicularis*. *J. Physiol.* 357, 575–607. doi: 10.1113/jphysiol.1984.sp015518

Bisegna, P., Caruso, G., Andreucci, D., Shen, L., Gurevich, V. V., Hamm, H. E., et al. (2008). Diffusion of the second messengers in the cytoplasm acts as a variability suppressor of the single photon response in vertebrate phototransduction. *Biophys. J.* 94, 3363–3383. doi: 10.1529/biophysj.107.114058

Bodoia, R. D., and Detwiler, P. B. (1985). Patch-clamp recordings of the light-sensitive dark noise in retinal rods from the lizard and frog. *J. Physiol.* 367, 183–216. doi: 10.1113/jphysiol.1985.sp015820

Boyett, M. R., Honjo, H., and Kodama, I. (2000). The sinoatrial node, a heterogeneous pacemaker structure. *Cardiovasc. Res.* 47, 658–687. doi: 10.1016/S0008-6363(00)00135-8

Burns, M. E., Mendez, A., Chen, J., and Baylor, D. A. (2002). Dynamics of cyclic GMP synthesis in retinal rods. *Neuron* 36, 81–91. doi: 10.1016/S0896-6273(02)00911-X

Burns, M. E., and Pugh, E. N. Jr. (2010). Lessons from photoreceptors: turning off g-protein signaling in living cells. *Physiology (Bethesda)* 25, 72–84. doi: 10.1152/physiol.00001.2010

Burns, M. E., and Pugh, E. N. Jr. (2014). "Visual transduction by rod and cone photoreceptors," in *The New Visual Neurosciences*, eds J. S. Werner and L. M. Chalupa (Cambridge, MA: The MIT Press), 7–18.

Cameron, D. A., and Pugh, E. N. Jr. (1990). The magnitude, time course and spatial distribution of current induced in salamander rods by cyclic guanine nucleotides. *J. Physiol.* 430, 419–439. doi: 10.1113/jphysiol.1990.sp018299

Caruso, G., Bisegna, P., Andreucci, D., Lenoci, L., Gurevich, V. V., Hamm, H. E., et al. (2011). Identification of key factors that reduce the variability of the single photon response. *Proc. Natl. Acad. Sci. U.S.A.* 108, 7804–7807. doi: 10.1073/pnas.1018960108

Caruso, G., Bisegna, P., Lenoci, L., Andreucci, D., Gurevich, V. V., Hamm, H. E., et al. (2010). Kinetics of rhodopsin deactivation and its role in regulating recovery and reproducibility of rod photoresponse. *PLoS Comput. Biol.* 6:e1001031. doi: 10.1371/journal.pcbi.1001031

Cobbs, W. H., and Pugh, E. N. Jr. (1987). Kinetics and components of the flash photocurrent of isolated retinal rods of the larval salamander, *Ambystoma tigrinum*. *J. Physiol.* 394, 529–572. doi: 10.1113/jphysiol.1987.sp016884

Cohen, A. I. (1963). Vertebrate retinal cells and their organization. *Biol. Rev.* 38, 427–459. doi: 10.1111/j.1469-185X.1963.tb00789.x

Craven, K. B., and Zagotta, W. N. (2006). CNG and HCN channels: two peas, one pod. *Annu. Rev. Physiol.* 68, 375–401. doi: 10.1146/annurev.physiol.68.040104.134728

Dizhoor, A. M., and Hurley, J. B. (1996). Inactivation of EF-hands makes GCAP-2 (p24) a constitutive activator of photoreceptor guanylyl cyclase by preventing a Ca^{2+}-induced "activator-to-inhibitor" transition. *J. Biol. Chem.* 271, 19346–19350. doi: 10.1074/jbc.271.32.19346

Dizhoor, A. M., and Hurley, J. B. (1999). Regulation of photoreceptor membrane guanylyl cyclases by guanylyl cyclase activator proteins. *Methods* 19, 521–531. doi: 10.1006/meth.1999.0894

Dizhoor, A. M., Olshevskaya, E. V., and Peshenko, I. V. (2010). Mg^{2+}/Ca^{2+} cation binding cycle of guanylyl cyclase activating proteins (GCAPs): role in regulation of photoreceptor guanylyl cyclase. *Mol. Cell. Biochem.* 334, 117–124. doi: 10.1007/s11010-009-0328-6

Fesenko, E. E., Kolesnikov, S. S., and Lyubarsky, A. L. (1985). Induction by cyclic GMP of cationic conductance in plasma membrane of retinal rod outer segment. *Nature* 313, 310–313. doi: 10.1038/313310a0

Field, G. D., and Rieke, F. (2002). Mechanisms regulating variability of the single photon responses of mammalian rod photoreceptors. *Neuron* 35, 733–747. doi: 10.1016/S0896-6273(02)00822-X

Fu, Y., and Yau, K. W. (2007). Phototransduction in mouse rods and cones. *Pflugers. Arch.* 454, 805–819. doi: 10.1007/s00424-006-0194-y

Gray-Keller, M., Denk, W., Shraiman, B., and Detwiler, P. B. (1999). Longitudinal spread of second messenger signals in isolated rod outer segments of lizards. *J. Physiol.* 519(Pt 3), 679–692. doi: 10.1111/j.1469-7793.1999.0679n.x

Gross, O. P., and Burns, M. E. (2010). Control of rhodopsin's active lifetime by arrestin-1 expression in mammalian rods. *J. Neurosci.* 30, 3450–3457. doi: 10.1523/JNEUROSCI.5391-09.2010

Gross, O. P., Pugh, E. N. Jr., and Burns, M. E. (2012a). Calcium feedback to cGMP synthesis strongly attenuates single-photon responses driven by long rhodopsin lifetimes. *Neuron* 76, 370–382. doi: 10.1016/j.neuron.2012.07.029

Gross, O. P., Pugh, E. N. Jr., and Burns, M. E. (2012b). Spatiotemporal cGMP dynamics in living mouse rods. *Biophys. J.* 102, 1775–1784. doi: 10.1016/j.bpj.2012.03.035

Hamer, R. D., Nicholas, S. C., Tranchina, D., Liebman, P. A., and Lamb, T. D. (2003). Multiple steps of phosphorylation of activated rhodopsin can account for the

reproducibility of vertebrate rod single-photon responses. *J. Gen. Physiol.* 122, 419–444. doi: 10.1085/jgp.200308832

Haynes, L. W., Kay, A. R., and Yau, K. W. (1986). Single cyclic GMP-activated channel activity in excised patches of rod outer segment membrane. *Nature* 321, 66–70. doi: 10.1038/321066a0

Heck, M., and Hofmann, K. P. (2001). Maximal rate and nucleotide dependence of rhodopsin-catalyzed transducin activation: initial rate analysis based on a double displacement mechanism. *J. Biol. Chem.* 276, 10000–10009. doi: 10.1074/jbc.M009475200

Hemilä, S., and Reuter, T. (1981). Longitudinal spread of adaptation in the rods of the frog's retina. *J. Physiol.* 310, 501–528. doi: 10.1113/jphysiol.1981.sp013564

Hodgkin, A. L., Mcnaughton, P. A., and Nunn, B. J. (1987). Measurement of sodium-calcium exchange in salamander rods. *J. Physiol.* 391, 347–370. doi: 10.1113/jphysiol.1987.sp016742

Holcman, D., and Korenbrot, J. I. (2004). Longitudinal diffusion in retinal rod and cone outer segment cytoplasm: the consequence of cell structure. *Biophys. J.* 86, 2566–2582. doi: 10.1016/S0006-3495(04)74312-X

Karpen, J. W., Zimmerman, A. L., Stryer, L., and Baylor, D. A. (1988). Gating kinetics of the cyclic-GMP-activated channel of retinal rods: flash photolysis and voltage-jump studies. *Proc. Natl. Acad. Sci. U.S.A.* 85, 1287–1291. doi: 10.1073/pnas.85.4.1287

Koch, K. W., and Stryer, L. (1988). Highly cooperative feedback control of retinal rod guanylate cyclase by calcium ions. *Nature* 334, 64–66. doi: 10.1038/334064a0

Korenbrot, J. I., and Miller, D. L. (1989). Cytoplasmic free calcium concentration in dark-adapted retinal rod outer segments. *Vision Res.* 29, 939–948. doi: 10.1016/0042-6989(89)90108-9

Korschen, H. G., Beyermann, M., Muller, F., Heck, M., Vantler, M., Koch, K. W., et al. (1999). Interaction of glutamic-acid-rich proteins with the cGMP signalling pathway in rod photoreceptors. *Nature* 400, 761–766. doi: 10.1038/23468

Koutalos, Y., Brown, R. L., Karpen, J. W., and Yau, K.-W. (1995a). Diffusion coefficient of the cyclic GMP analog 8-(fluoresceinyl)thioguanosine 3′,5′ cyclic monophosphate in the salamander rod outer segment. *Biophys. J.* 69, 2163–2167. doi: 10.1016/S0006-3495(95)80090-1

Koutalos, Y., Nakatani, K., Tamura, T., and Yau, K. W. (1995b). Characterization of guanylate cyclase activity in single retinal rod outer segments. *J. Gen. Physiol.* 106, 863–890. doi: 10.1085/jgp.106.5.863

Koutalos, Y., Nakatani, K., and Yau, K.-W. (1995c). Cyclic GMP diffusion coefficient in rod photoreceptor outer segments. *Biophys. J.* 68, 373–382. doi: 10.1016/S0006-3495(95)80198-0

Krispel, C. M., Chen, D., Melling, N., Chen, Y. J., Martemyanov, K. A., Quillinan, N., et al. (2006). RGS expression rate-limits recovery of rod photoresponses. *Neuron* 51, 409–416. doi: 10.1016/j.neuron.2006.07.010

Lagnado, L., Cervetto, L., and Mcnaughton, P. A. (1992). Calcium homeostasis in the outer segments of retinal rods from the tiger salamander. *J. Physiol.* 455, 111–142. doi: 10.1113/jphysiol.1992.sp019293

Lamb, T. D., Mcnaughton, P. A., and Yau, K. W. (1981). Spatial spread of activation and background desensitization in toad rod outer segments. *J. Physiol.* 319, 463–496. doi: 10.1113/jphysiol.1981.sp013921

Lamb, T. D., and Pugh, E. N. Jr. (1992). A quantitative account of the activation steps involved in phototransduction in amphibian photoreceptors. *J. Physiol.* 449, 719–758. doi: 10.1113/jphysiol.1992.sp019111

Leskov, I. B., Klenchin, V. A., Handy, J. W., Whitlock, G. G., Govardovskii, V. I., Bownds, M. D., et al. (2000). The gain of rod phototransduction: reconciliation of biochemical and electrophysiological measurements. *Neuron* 27, 525–537. doi: 10.1016/S0896-6273(00)00063-5

Makino, C. L., Dodd, R. L., Chen, J., Burns, M. E., Roca, A., Simon, M. I., et al. (2004). Recoverin regulates light-dependent phosphodiesterase activity in retinal rods. *J. Gen. Physiol.* 123, 729–741. doi: 10.1085/jgp.200308994

Makino, C. L., Peshenko, I. V., Wen, X. H., Olshevskaya, E. V., Barrett, R., and Dizhoor, A. M. (2008). A role for GCAP2 in regulating the photoresponse. Guanylyl cyclase activation and rod electrophysiology in GUCA1B knock-out mice. *J. Biol. Chem.* 283, 29135–29143. doi: 10.1074/jbc.M804445200

Mendez, A., Burns, M. E., Sokal, I., Dizhoor, A. M., Baehr, W., Palczewski, K., et al. (2001). Role of guanylate cyclase-activating proteins (GCAPs) in setting the flash sensitivity of rod photoreceptors. *Proc. Natl. Acad. Sci. U.S.A.* 98, 9948–9953. doi: 10.1073/pnas.171308998

Naarendorp, F., Esdaille, T. M., Banden, S. M., Andrews-Labenski, J., Gross, O. P., and Pugh, E. N. Jr. (2010). Dark light, rod saturation, and the absolute and incremental sensitivity of mouse cone vision. *J. Neurosci.* 30, 12495–12507. doi: 10.1523/JNEUROSCI.2186-10.2010

Nikonov, S., Lamb, T. D., and Pugh, E. N. Jr. (2000). The role of steady phosphodiesterase activity in the kinetics and sensitivity of the light-adapted salamander rod photoresponse. *J. Gen. Physiol.* 116, 795–824. doi: 10.1085/jgp.116.6.795

Olson, A., and Pugh, E. N. Jr. (1993). Diffusion coefficient of cyclic GMP in salamander rod outer segments estimated with two fluorescent probes. *Biophys. J.* 65, 1335–1352. doi: 10.1016/S0006-3495(93)81177-9

Palczewski, K., Polans, A. S., Baehr, W., and Ames, J. B. (2000). Ca(2+)-binding proteins in the retina: structure, function, and the etiology of human visual diseases. *Bioessays* 22, 337–350. doi: 10.1002/(SICI)1521-1878(200004)22:4<337::AID-BIES4>3.0.CO;2-Z

Palczewski, K., Subbaraya, I., Gorczyca, W. A., Helekar, B. S., Ruiz, C. C., Ohguro, H., et al. (1994). Molecular cloning and characterization of retinal photoreceptor guanylyl cyclase-activating protein. *Neuron* 13, 395–404. doi: 10.1016/0896-6273(94)90355-7

Peshenko, I. V., and Dizhoor, A. M. (2004). Guanylyl cyclase-activating proteins (GCAPs) are Ca^{2+}/Mg^{2+} sensors: implications for photoreceptor guanylyl cyclase (RetGC) regulation in mammalian photoreceptors. *J. Biol. Chem.* 279, 16903–16906. doi: 10.1074/jbc.C400065200

Peshenko, I. V., Olshevskaya, E. V., Savchenko, A. B., Karan, S., Palczewski, K., Baehr, W., et al. (2011). Enzymatic properties and regulation of the native isozymes of retinal membrane guanylyl cyclase (RetGC) from mouse photoreceptors. *Biochemistry* 50, 5590–5600. doi: 10.1021/bi200491b

Poetsch, A., Molday, L. L., and Molday, R. S. (2001). The cGMP-gated channel and related glutamic acid-rich proteins interact with peripherin-2 at the rim region of rod photoreceptor disc membranes. *J. Biol. Chem.* 276, 48009–48016.

Pugh, E. N. Jr., and Lamb, T. D. (1993). Amplification and kinetics of the activation steps in phototransduction. *Biochim. Biophys. Acta* 1141, 111–149. doi: 10.1016/0005-2728(93)90038-H

Reingruber, J., and Holcman, D. (2008). Estimating the rate constant of cyclic GMP hydrolysis by activated phosphodiesterase in photoreceptors. *J. Chem. Phys.* 129:145102. doi: 10.1063/1.2991174

Reingruber, J. R., Pahlberg, J., Woodruff, M. L., Sampath, A. P., Fain, G. L., and Holcman, D. (2013). Detection of single photons by toad and mouse rods. *Proc. Natl. Acad. Sci. U.S.A.* 110, 19378–19383. doi: 10.1073/pnas.1314030110

Rieke, F., and Baylor, D. A. (1996). Molecular origin of continuous dark noise in rod photoreceptors. *Biophys. J.* 71, 2553–2572. doi: 10.1016/S0006-3495(96)79448-1

Rieke, F., and Baylor, D. A. (1998). Origin of reproducibility in the responses of retinal rods to single photons. *Biophys. J.* 75, 1836–1857. doi: 10.1016/S0006-3495(98)77625-8

Ritter, L. M., Khattree, N., Tam, B., Moritz, O. L., Schmitz, F., and Goldberg, A. F. (2011). In situ visualization of protein interactions in sensory neurons: glutamic acid-rich proteins (GARPs) play differential roles for photoreceptor outer segment scaffolding. *J. Neurosci.* 31, 11231–11243. doi: 10.1523/JNEUROSCI.2875-11.2011

Ruiz, M., Brown, R. L., He, Y., Haley, T. L., and Karpen, J. W. (1999). The single-channel dose-response relation is consistently steep for rod cyclic nucleotide-gated channels: implications for the interpretation of macroscopic dose-response relations. *Biochemistry* 38, 10642–10648. doi: 10.1021/bi990532w

Sampath, A. P., Matthews, H. R., Cornwall, M. C., and Fain, G. L. (1998). Bleached pigment produces a maintained decrease in outer segment Ca^{2+} in salamander rods. *J. Gen. Physiol.* 111, 53–64. doi: 10.1085/jgp.111.1.53

Schwarzer, A., Schauf, H., and Bauer, P. J. (2000). Binding of the cGMP-gated channel to the Na/Ca-K exchanger in rod photoreceptors. *J. Biol. Chem.* 275, 13448–13454. doi: 10.1074/jbc.275.18.13448

Sharma, R. K. (2010). Membrane guanylate cyclase is a beautiful signal transduction machine: overview. *Mol. Cell. Biochem.* 334, 3–36. doi: 10.1007/s11010-009-0336-6

Shuart, N. G., Haitin, Y., Camp, S. S., Black, K. D., and Zagotta, W. N. (2011). Molecular mechanism for 3:1 subunit stoichiometry of rod cyclic nucleotide-gated ion channels. *Nat. Commun.* 2, 457–457. doi: 10.1038/ncomms1466

Tao, T., Paterson, D. J., and Smith, N. P. (2011). A model of cellular cardiac-neural coupling that captures the sympathetic control of sinoatrial node excitability in normotensive and hypertensive rats. *Biophys. J.* 101, 594–602. doi: 10.1016/j.bpj.2011.05.069

Whitlock, G. G., and Lamb, T. D. (1999). Variability in the time course of single photon responses from toad rods: termination of rhodopsin's activity. *Neuron* 23, 337–351. doi: 10.1016/S0896-6273(00)80784-9

Woodruff, M. L., Sampath, A. P., Matthews, H. R., Krasnoperova, N. V., Lem, J., and Fain, G. L. (2002). Measurement of cytoplasmic calcium concentration in the rods of wild-type and transducin knock-out mice. *J. Physiol.* 542, 843–854. doi: 10.1113/jphysiol.2001.013987

Wu, Q., Chen, C., and Koutalos, Y. (2006). Longitudinal diffusion of a polar tracer in the outer segments of rod photoreceptors from different species. *Photochem. Photobiol.* 82, 1447–1451. doi: 10.1562/2006-02-22-RA-807

Conflict of Interest Statement: The authors declare that the research was conducted in the absence of any commercial or financial relationships that could be construed as a potential conflict of interest.

Received: 28 December 2014; accepted: 12 February 2015; published online: 04 March 2015.

Citation: Gross OP, Pugh EN Jr. and Burns ME (2015) cGMP in mouse rods: the spatiotemporal dynamics underlying single photon responses. Front. Mol. Neurosci. ***8****:6. doi: 10.3389/fnmol.2015.00006*

This article was submitted to the journal Frontiers in Molecular Neuroscience.

frontiers in
CELLULAR NEUROSCIENCE

REVIEW ARTICLE
published: 28 October 2014
doi: 10.3389/fncel.2014.00350

cAMP signaling microdomains and their observation by optical methods

Davide Calebiro [1,2] **** and Isabella Maiellaro*** [1,2]

[1] *Institute of Pharmacology and Toxicology, University of Würzburg, Würzburg, Germany*
[2] *Bio-Imaging Center/Rudolf Virchow Center for Experimental Biomedicine, University of Würzburg, Würzburg, Germany*

Edited by:
Pierre Vincent, Centre National de la Recherche Scientifique, France

Reviewed by:
Thomas Rich, University of South Alabama College of Medicine, USA
Nicolas Gervasi, Institut National de la Santé et de la Recherche Médicale, France

****Correspondence:***
Davide Calebiro, Institute of Pharmacology and Toxicology, University of Würzburg, Versbacherstr. 9, 97078 Würzburg, Germany
e-mail: davide.calebiro@toxi.uni-wuerzburg.de

The second messenger cyclic AMP (cAMP) is a major intracellular mediator of many hormones and neurotransmitters and regulates a myriad of cell functions, including synaptic plasticity in neurons. Whereas cAMP can freely diffuse in the cytosol, a growing body of evidence suggests the formation of cAMP gradients and microdomains near the sites of cAMP production, where cAMP signals remain apparently confined. The mechanisms responsible for the formation of such microdomains are subject of intensive investigation. The development of optical methods based on fluorescence resonance energy transfer (FRET), which allow a direct observation of cAMP signaling with high temporal and spatial resolution, is playing a fundamental role in elucidating the nature of such microdomains. Here, we will review the optical methods used for monitoring cAMP and protein kinase A (PKA) signaling in living cells, providing some examples of their application in neurons, and will discuss the major hypotheses on the formation of cAMP/PKA microdomains.

Keywords: G protein-coupled receptor, cyclic AMP, signaling microdomain, fluorescence resonance energy transfer, neurons

INTRODUCTION

The concept of second messenger made its first appearance nearly 60 years ago after the identification of cyclic AMP (cAMP) as the heat-stable and dialyzable molecule that mediated the intracellular actions of the hormones glucagon and epinephrine in the liver (Rall and Sutherland, 1958). Subsequently, cAMP has been shown to regulate a myriad of cellular processes such as gene expression, proliferation, apoptosis, exocytosis or migration as well as a wide range of physiological functions including immune responses, cardiac contractility and memory formation (Beavo and Brunton, 2002).

The events triggering the production of cAMP have long been believed to begin exclusively at the plasma membrane, where a variety of ligands are capable of binding to and activating several members of the large family of G protein-coupled receptors (GPCRs; Pierce et al., 2002; Lefkowitz, 2013). Subsequently, active GPCRs induce the exchange of GTP for GDP on the α-subunit of the Gs protein, which in turn activates adenylyl cyclases (AC). These enzymes, which exist in different isoforms, convert ATP to cAMP, which ultimately stimulates different effector proteins, namely cyclic-nucleotide-gated (CNG) channels, guanine-nucleotide exchanging proteins activated by cAMP (Epac) and protein kinase A (PKA). A group of phosphodiesterases (PDEs), which degrade cAMP to AMP, are finally responsible for bringing the concentration of cAMP back to the basal level, so that the cell can respond to a new stimulus (Beavo and Brunton, 2002).

For many years after the discovery of cAMP, its intracellular concentration has been thought to increase uniformly after stimulation of a receptor located on the plasma membrane. This view was based on at least two important observations: first, cAMP is a small soluble molecule with a high diffusion coefficient in solution; second, dissimilarly from Ca^{2+} ions, which are buffered by binding proteins in the cytosol, cAMP remains largely free in the cytoplasm. However, this view has been challenged by an increasing number of experimental observations, which provide convincing evidence that cAMP may remain confined in microdomains near the sites of its synthesis, thus leading to the selective activation of a subset of effectors located in their proximity.

First indirect evidence for such compartmentation in cAMP/PKA signaling was provided by Corbin et al. (1977) working on heart lysates. Few years later, it was reported that prostaglandin E1 (PGE_1) and the β-adrenergic agonist isoproterenol caused similar elevations of cAMP in heart tissue, but only isoproterenol was able to activate glycogen phosphorylase (Brunton et al., 1979, 1981; Hayes et al., 1979, 1980). Interestingly, it was subsequently found that PGE_1 activated PKA only in a soluble fraction, whereas isoproterenol could also activate PKA in a particulate fraction, which was apparently required for its effects on glycogen phosphorylase (Buxton and Brunton, 1983). A number of analogous observations of hormones inducing dissimilar effects in the same tissue have been reported by several groups (Steinberg and Brunton, 2001; Zaccolo, 2011; Lefkimmiatis and Zaccolo, 2014). Moreover, Jurevicius and Fischmeister performed an elegant experiment in which they used a set-up that allowed perfusing the two halves of a frog cardiomyocyte with two different solutions and at the same time record L-type calcium currents

induced by β-adrenergic stimulation. Based on their results, they concluded that β-adrenergic receptors (β-AR) induced local cAMP elevations, which caused the preferential activation of nearby Ca^{2+} channels (Jurevicius and Fischmeister, 1996).

However, it was only later, thanks to the introduction of optical methods for monitoring cAMP/PKA signaling in living cells, that a direct observation and investigation of cAMP microdomains became possible. This review will focus on the currently available tools for monitoring cAMP levels and PKA activation in living cells, providing some illustrative examples of their application in neurons. Moreover, we will discuss the major hypotheses on the mechanisms responsible for the formation of such microdomains, which have emerged from these studies.

FLUORESCENCE RESONANCE ENERGY TRANSFER (FRET) SENSOR FOR MONITORING cAMP SIGNALING IN LIVING CELLS

The currently available optical methods for monitoring cAMP signaling in living cells are largely based on fluorescence resonance energy transfer (FRET; Förster, 1948). FRET is a physical phenomenon that occurs between two fluorophores located in close proximity: if the distance between two fluorophores is less than approximately 10 nm and there is a certain overlap between their fluorescence spectra, the energy in the excited state of the first fluorophore (donor) can be transferred without emission of a photon to the second fluorophore (acceptor), which will in turn emit a photon of a lower energy. The resulting red-shift of the emitted light, or, alternatively, the shortening of the time the donor resides in the excited state can be used to monitor FRET. Such measurements can be performed in living cells with the spatial and temporal resolution of fluorescence microscopy. This approach has been exploited to follow all the major steps of GPCR signaling, including the generation of cAMP and the activation of PKA (Adams et al., 1991; Zaccolo et al., 2000; Zhang et al., 2001; DiPilato et al., 2004; Nikolaev et al., 2004; Ponsioen et al., 2004)—for a comprehensive review on sensors for monitoring other steps in GPCR signaling see Lohse et al. (2008) and Lohse et al. (2012). Here we will focus on the sensors used for monitoring cAMP concentrations and PKA activation.

The first FRET sensor used to monitor cAMP was based on PKA. This sensor consisted of two PKA catalytic (C) subunits labeled with fluorescein as FRET donor and two PKA regulatory (R) subunits labeled with rhodamine as FRET acceptor—hence the name FICRhR (fluorescein-labeled catalytic subunit and rhodamine-labeled regulatory subunit, pronounced "flicker"). In the presence of low cAMP concentrations, the R and C subunits are associated and FRET can occur between the two nearby fluorophores. When cAMP concentrations increase, cAMP binds to the R subunits causing dissociation of the C subunits and a concomitant loss of FRET. This sensor was used to monitor cAMP signaling in different neuronal preparations, such as invertebrate neurons (Bacskai et al., 1993; Hempel et al., 1996), *Xenopus* embryonic spinal neurons (Gorbunova and Spitzer, 2002) or murine thalamic neurons (Goaillard and Vincent, 2002), as well as in oocytes (Webb et al., 2002; Takeda et al., 2006) and frog ventricular myocytes (Goaillard et al., 2001). A drawback of this sensor was that it had to be injected into the cytoplasm, which was a challenging task, particularly for cells of small size. Moreover, it has been suggested that the injection pipette might work as a "cAMP sink", artificially reducing the cAMP concentration inside the cell (Vincent and Brusciano, 2001).

These problems were later overcome by Manuela Zaccolo and Tullio Pozzan with the introduction of a genetically-encoded PKA-based sensor (Zaccolo et al., 2000). In this sensor, the PKA R and C subunits were fused with two color variants of GFP—BFP and GFP, later replaced by CFP and YFP, respectively (Zaccolo and Pozzan, 2002). This sensor could now be introduced into cells by co-transfection of two plasmids, each coding for one of the two fluorescently labeled PKA subunit. Although this represented a major advancement, some limitations and possible drawbacks remained. Most importantly, this sensor retained PKA catalytic activity, which can alter intracellular signaling and various cellular functions. Moreover, both labeled subunits had to be overexpressed and present in comparable amounts in order to associate into a functional sensor, which complicated the use of this sensor and increased the chances that it might interfere with the functions of the cell (Rich and Karpen, 2002; Haugh, 2012; Saucerman et al., 2013; Rich et al., 2014).

In an attempt to circumvent the remaining limitations of PKA-based sensors, the group of Martin Lohse in Würzburg developed a new type of cAMP sensor that was single-chain and catalytically inactive. The first version of this sensor was based on a cAMP-binding domain derived from Epac1, a GTP exchange factor for Rap1 activated by cAMP, which was fused on either side to CFP and YFP (Nikolaev et al., 2004)—binding of cAMP to this sensor causes a decrease of FRET between CFP and YFP. In parallel, two other groups generated similar types of sensors that were based on full-length or partially truncated version of Epac proteins (DiPilato et al., 2004; Ponsioen et al., 2004; Dunn et al., 2006). A whole range of single-chain cAMP sensors with improved characteristics have been developed by utilizing cAMP binding domains derived from other proteins, deleting functional domains of Epac proteins, introducing point mutations in the cAMP binding domains and/or using improved donor:acceptor pairs (Nikolaev et al., 2005, 2006; Violin et al., 2006, 2008; Norris et al., 2009; Klarenbeek et al., 2011; Polito et al., 2013).

In addition, endogenous PKA signaling can be monitored by FRET sensors known as AKARs, standing for A-kinase activity reporters (Zhang et al., 2001). This family of biosensors has been generated by sandwiching a PKA substrate sequence and a phosphoamino acid binding domain between a FRET donor (e.g., CFP) and a FRET acceptor (e.g., YFP or Venus). Once phosphorylated by PKA, the PKA substrate contained in the sensor interacts with the phosphoamino acid binding domain, leading to an increase in FRET between the two fluorophores. Like for cAMP sensors, several generations of AKAR sensors with progressively improved characteristics have been produced by replacing the initial fluorophores with brighter and more photostable ones (Zhang et al., 2005; Allen and Zhang, 2006; Depry et al., 2011; Erard et al., 2013; Chen et al., 2014) or

introducing a long flexible linker between the PKA substrate and the phosphoamino acid binding domain (Komatsu et al., 2011). It should be noted that, since the phosphorylation of AKAR sensors and the accompanying FRET changes are rapidly reversed by the action of endogenous phosphatases, these sensors measure the equilibrium between phosphorylation and dephosphorylation and not just PKA activity.

Although FRET-based methods for monitoring cAMP/PKA signaling offer several advantages compared to other approaches, there are still some limitations and potential pitfalls that deserve careful consideration—for a detailed review see Rich and Karpen (2002), Haugh (2012) and Rich et al. (2014). One is the already mentioned catalytic activity of some sensors. In addition, all sensors have the potential of interacting with other proteins present in the cell. This risk should be particularly low with the use of small sensors that contain no specific interacting domains. Finally, all sensors have the potential of buffering intracellular cAMP. Performing measurements at different levels of expression of the sensor (Castro et al., 2013) appears to be a good strategy for evaluating the presence of such an unwanted effect.

VISUALIZATION OF cAMP/PKA MICRODOMAINS BY FRET MICROSCOPY

One of the first applications of the new method was to study cAMP signaling in the giant sensory neurons of the see snail *Aplysia californica*, a model organism that had been extensively used by the group of Eric Kandel to demonstrate the importance of cAMP in synaptic plasticity (Kandel, 2009; Kandel et al., 2014). In this model, serotonin released by interneurons activates a Gs-coupled receptor located on pre-synaptic termini, where it induces both short-term and long-term facilitation. Since the latter requires phosphorylation of CREB as well as mRNA and protein synthesis, it was postulated that the cAMP signals produced in the periphery must reach the soma in order to induce long-term changes in synaptic transmission. Using *Aplysia* sensory neurons injected with FlCRhR, Bacskai et al. (1993) found that bath stimulation with saturating serotonin concentrations induced PKA activation in the distal processes but only a minimal PKA activation near the nucleus. Interestingly, such cAMP gradient between the periphery and the central compartment was observed also with forskolin stimulation and was not prevented by treatment with IBMX, a PDE inhibitor. At the same time, injected cAMP was found to be freely diffusible, with a diffusion coefficient of 780 $\mu m^2/s$. Based on these observations, the authors hypothesized that the observed gradient between the periphery and the soma was due to the higher surface-to-volume ratio of the fine processes compared to the cell body. However, it has been suggested that buffering by FICRhR might artificially favor the formation of cAMP gradients, an effect that could be bypassed if the concentration of injected cAMP should exceed the buffering capacity of the sensor (Rich et al., 2001). This factor may complicate the interpretation of the results of Bacskai et al. (Rich et al., 2001).

Subsequent experiments performed in neurons of the lobster stomatogastric ganglion injected with the same PKA sensor revealed that electric stimulation of afferent fibers, presumably through release of endogenous modulators, is capable of inducing local increases of cAMP in fine neurite branches (Hempel et al., 1996). Interestingly, after repeated electric stimulation for 2–3 min, a unidirectional propagation of cAMP signals from the fine neurites towards the soma was observed. The authors explained this as the intracellular diffusion of cAMP from its peripheral site of production towards the central compartment (Hempel et al., 1996). However, measurements of the time required for the axonal propagation of the cAMP signal gave values that are consistently lower than it would be expected for the free diffusion of cAMP and about 6–8 times lower than those experimentally observed after local cAMP microinjection (Bacskai et al., 1993). Moreover, the results obtained with lobster stomatogastric ganglion neurons were inconsistent with the simple hypothesis that differences in the surface-to-volume ratio might be the major cause for the formation of cAMP gradients between fine peripheral structures and the soma.

Subsequently, optical measurements of cAMP levels and PKA activation in neurons have been performed in various mammalian preparations (Nikolaev et al., 2004; Gervasi et al., 2007; Dunn and Feller, 2008; Neves et al., 2008; Mironov et al., 2009; Castro et al., 2010, 2013; Shelly et al., 2010; Hu et al., 2011; Nicol et al., 2011). Some of these studies provided further evidence for the existence of cAMP/PKA microdomains. For instance, Nikolaev et al. (2004) followed the formation of transient cAMP gradients in hippocampal neurons transfected with the Epac1-camps sensor and locally stimulated with the β-adrenergic agonist isoproterenol. They measured a very rapid diffusion of cAMP inside neurons (diffusion coefficient ∼500 $\mu m^2/s$), which was ∼20-fold slower if measured with a PKA-based sensor (Nikolaev et al., 2004). These data confirmed the high diffusibility of cAMP in neurons.

In an elegant study, Neves et al. (2008) performed a series of spatial simulations of the propagation of cAMP signals in hippocampal CA1 neurons, which they subsequently validated in rat hippocampal slices transfected with the Epac1-camps sensor. This study confirmed the possible generation of cAMP gradients between fine processes and the cell body as a consequence of different surface-to-volume ratios, despite a homogenous distribution of receptors and AC on the entire plasma membrane (Neves et al., 2008). In agreement with these findings, a study by Castro et al. (2010) in pyramidal cortical neurons imaged by two-photon microscopy revealed higher cAMP and PKA responses to isoproterenol stimulation in small distal dendrites compared to the bulk cytosol.

Another emerging model to study the spatiotemporal dynamics of cAMP/PKA signaling in neurons is represented by *Drosophila melanogaster*, in which several genetic studies have revealed the importance of cAMP/PKA signaling for memory formation and synaptic plasticity (Kandel, 2009). Interestingly, a number of studies have employed FRET sensors to directly monitor cAMP/PKA signaling in semi-intact larval and adult preparations as well as in intact flies (Shafer et al., 2008; Tomchik and Davis, 2009; Gervasi et al., 2010; Duvall and Taghert, 2012; Boto et al., 2014). For example, flies expressing the Epac1-camps sensor

have been used to investigate cAMP signaling in the pacemaker neurons of the central nervous system that are involved in circadian rhythms (Shafer et al., 2008; Duvall and Taghert, 2012). These studies provide evidence that the response to the neuropeptide Pigment Dispersing Factor (PDF) in the pacemaker M cells requires the presence of AC3 and the A-kinase anchoring protein (AKAP) Nervy. Interestingly, signaling by other GPCRs in M cells or by the PDF receptor in other pacemaker cells was not affected by depletion of either AC3 or Nervy. These findings suggest a high degree of compartmentation of PDF signaling in M cells.

Another interesting line of research in *Drosophila* focuses on the involvement of cAMP/PKA signaling in olfactory memory, which is processed in specialized brain regions called Mushroom Bodies (MBs). In an interesting study, Tomchik and Davis (2009) used a FRET sensor to monitor cAMP signaling in two regions of the MBs called α-lobe and calix. They found that the responses to dopamine and octopamine differed substantially in the two regions, with the calyx being particularly sensitive to octopamine while dopamine inducing the largest response in the α-lobe. In a subsequent study, Gervasi et al. (2010) analyzed PKA signaling in the different regions of MBs using an AKAR sensor. They suggested that, whereas octopamine can induce a generalized PKA response in MBs, dopamine induces a localized PKA activation in the α-lobe. Interestingly, the selective localization of PKA signals in α-lobes in response to dopamine was lost in mutant flies that carried an inactive Dunce PDE (Gervasi et al., 2010). These studies are consistent with the hypothesis that cAMP/PKA signals might be spatially restricted in MB neurons.

Furthermore, targeting of cAMP or PKA sensors to different signaling complexes by fusion with one of their components, such as type-I and type-II PKA regulatory subunits (Di Benedetto et al., 2008), PDEs (Herget et al., 2008) and ACs (Wachten et al., 2010), has provided additional evidence for the existence of cAMP microdomains in different types of non-neuronal cells. The application of similar approaches to neurons might allow to further investigate the organization of cAMP microdomains in these cells. For instance, Herbst et al. (2011) used an AKAR sensor targeted to the plasma membrane via a K-ras domain to show the existence of a distinct sub-membrane compartment for cAMP signaling in PC12 cells.

MECHANISMS RESPONSIBLE FOR SIGNAL COMPARTMENTATION

This topic has been thoroughly discussed elsewhere (Willoughby and Cooper, 2007; Conti et al., 2014; Lefkimmiatis and Zaccolo, 2014; Saucerman et al., 2013; Rich et al., 2014). Here we will highlight some general aspects and provide a few selected examples.

Different mechanisms have been put forward to explain the compartmentation of cAMP/PKA signaling in spite of the high diffusibility of cAMP in solution. These include the formation of cAMP gradients due to reaction-diffusion mechanisms, a different subcellular localization of signaling molecules (receptors, ACs, PDEs, etc.), factors (e.g., fiscal barriers, buffering, higher viscosity) capable of hindering the diffusion of cAMP, and the association of signaling molecules into supramolecular complexes, often through the intervention of scaffolding proteins (**Figure 1**). Indeed, all these mechanisms could cause local variations in cAMP concentrations, ultimately leading to activation of PKA and downstream targets in a spatially restricted manner.

The formation of cAMP gradients from the plasma membrane to the cell interior has been predicted on the basis of the spatial segregation of ACs on the plasma membrane and PDEs in the cytosol long before the advent of optical methods (Fell, 1980; Kholodenko, 2006; Kholodenko and Kolch, 2008). In addition, differences in the surface-to-volume ratio among different parts of a cell, for instance between the fine neurites and the soma of a neuron, have been claimed for similar reasons to generate a gradient, with cAMP being higher in the finer structures (Kholodenko and Kolch, 2008; Neves et al., 2008). Such gradients have been directly visualized by FRET microscopy in cardiomyocytes (Zaccolo and Pozzan, 2002; Nikolaev et al., 2006, 2010) and in neurons (Bacskai et al., 1993; Neves et al., 2008; Castro et al., 2010; Gervasi et al., 2010).

Another mechanism that has been advocated for the formation of cAMP microdomains involves the non-uniform localization of the proteins implicated in cAMP/PKA signaling in different subcellular structures and/or microdomains. For instance, in cardiomyocytes β_1-adrenergic receptors (β_1-ARs) have been suggested to be localized in both caveolar and non-caveolar membrane fractions, whereas β_2-ARs appear to be prevalently localized in caveolae and to exit caveolae upon activation (Rybin et al., 2000). Interestingly, pharmacological disruption of caveolae enhances and prolongs β_2-AR-mediated cAMP accumulation (DiPilato and Zhang, 2009). Moreover, combining FRET and scanning ion conductance microscopy, it was shown that functional β_2-ARs are localized selectively in transverse tubules of cardiomyocytes, whereas β_1-ARs are distributed across the entire cell surface (Nikolaev et al., 2010). Such selective localization on the surface of cardiomyoctes might explain why stimulation of β_1- and β_2-ARs produce different effects although both receptors activate the cAMP signaling pathway. More recently, we and another group have independently found that GPCRs can not only activate ACs once located at the cell surface, but can continue stimulating cAMP production after internalization to an endosomal compartment that contains G-proteins and ACs (Calebiro et al., 2009, 2010; Ferrandon et al., 2009). Very recently, such a phenomenon has also been described for the β_2-AR (Irannejad et al., 2013). Interestingly, the authors of this study were able to directly visualize active β_2-ARs and $G\alpha_s$-subunits on endosomal membranes by taking advantage of fluorescently labeled nanobodies that bind to these proteins only when they are in an active state (Irannejad et al., 2013). Similarly, there is increasing evidence for a functional role of GPCRs located on the nuclear membrane (for a review see Tadevosyan et al., 2012). These findings provide a new basis to explain compartmentation in GPCR signaling, and could allow reconciling the notion of spatially confined cAMP/PKA signaling with the known phosphorylation by PKA of targets located deep inside the cell or distant from the site of receptor activation, as might occur in neurons.

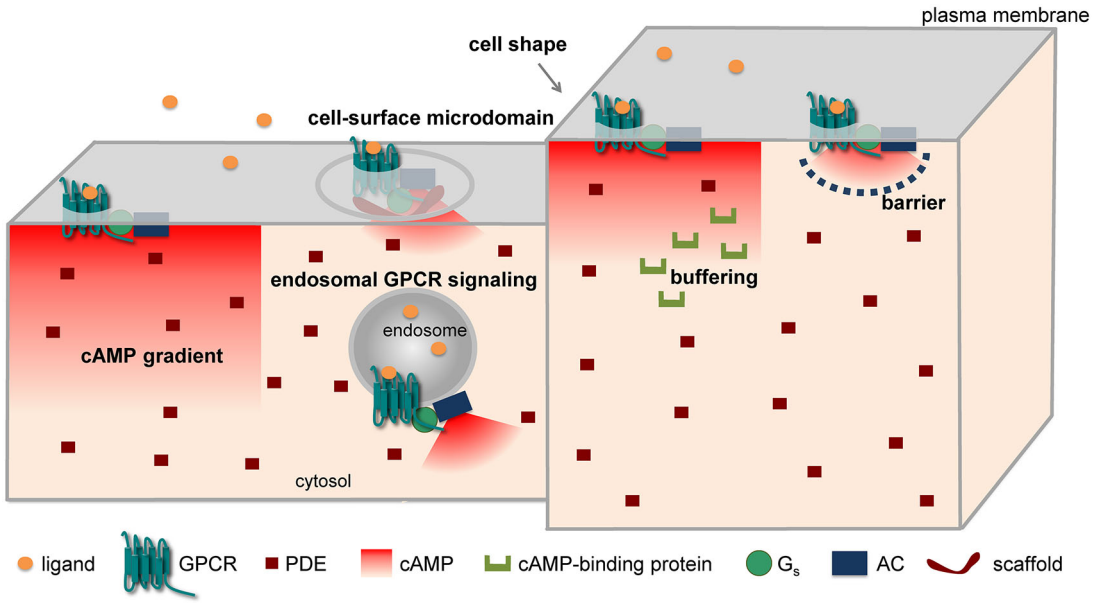

FIGURE 1 | Major mechanisms implicated in cAMP compartmentation.

A hindered diffusion of cAMP has been advocated by Rich et al. (2000) to explain the results of whole-cell patch clamp experiments in which cAMP concentrations near the plasma membrane were measured using CNG channels. Since they found a low exchange of cAMP between the cytoplasm immediately below the plasma membrane and the bulk cytosol, they hypothesized the presence of a 3D barrier, possibly involving the endoplasmic reticulum, which would limit diffusion of cAMP between these two compartments.

Finally, a number of studies have revealed that different components of GPCR signaling cascades can assemble into functional molecular complexes, thus allowing the formation of signaling domains of the size of a few nanometers (for a detailed review see Lefkimmiatis and Zaccolo, 2014). An illustrative example of such concept is represented by the reported formation of a signaling complex involving the β_2-AR, heterotrimeric G-proteins, AC, PKA and its target, the L-type Ca^{2+} channel Ca_V 1.2 (Davare et al., 2001). Such compartmentalization could explain electrophysiological data obtained in frog ventricular cardiomyocytes that support the preferential functional coupling of β-ARs to nearby L-type Ca^{2+} channels (Jurevicius and Fischmeister, 1996). An important role in this context is played by AKAPs. The over 50 AKAPs identified so far are capable of localizing PKA to multiple subcellular structures via interaction with a specific domain localized at the N-terminus of PKA regulatory subunits. Interestingly, AKAPs do not only interact with both PKA-I and II isoforms, but can bind several other proteins involved in GPCR signaling, such as receptors, ACs, PDEs and phosphatases (Esseltine and Scott, 2013). Thus, these scaffolding proteins appear to play a fundamental role in assembling focal cAMP/PKA signaling complexes. An elegant demonstration of this concept comes from a study by Di Benedetto et al. (2008) in cardiomyocytes. In this study, a FRET sensor for cAMP was fused to either RI- or RII-derived AKAP-binding domains, thus allowing its targeted localization to different compartments. Interestingly, it was found that isoproterenol stimulation causes a larger cAMP elevation at the level of the RII-tethered sensor. In contrast, the RI-tethered sensor was preferentially responding to PGE_1. Moreover, the two PKA pools had a different sensitivity to different isoform-selective PDE inhibitors and were coupled to different downstream targets (Di Benedetto et al., 2008). This study provided a possible molecular explanation for the observations made by Buxton and Brunton (1983) nearly 25 years before.

Although all these studies have provided fundamental insights into the possible mechanisms of cAMP compartmentation, putting all the pieces of the puzzle together is not trivial. Moreover, some hypotheses on the formation of cAMP gradients are difficult to verify, due to the lack of adequate tools. Here, an important help may come from mathematical models and simulations capable of predicting the behavior of signaling cascades (Kholodenko, 2006; Kholodenko and Kolch, 2008) and, thus, of verifying, in a systematic way, the possible contribution of different mechanisms to cAMP compartmentation. Indeed, several groups have built a series of mathematical models of GPCR/cAMP signaling pathways and performed different types of simulations (e.g., single/multiple compartment vs. spatial, or deterministic vs. stochastic), a topic that has been recently reviewed by Saucerman et al. (2013).

Most of these simulations confirm the importance of having differentially localized AC and PDE activities for the generation of cAMP gradients. Some simulations have suggested that the presence of ACs on the plasma membrane and a higher PDE

activity in the cytosol is sufficient to produce a cAMP gradient in the cell. For instance, Oliveira et al. (2010) performed a stochastic simulation of cAMP production and degradation in HEK293 cells, which they validated with previous cAMP FRET measurements. They concluded that the formation of cAMP gradients requires a pool of PDE4D anchored in the cytosol as well as PDE4D phosphorylation by PKA. In a subsequent paper, the same group simulated dopamine D1 signaling in a segment of a spiny projection neuron dendrite, and evaluated the effect of anchoring the receptor/AC and/or PKA in the spine heads *vs*. the dendrite. The results indicated that when receptors and ACs were located on the spine heads, cAMP was significantly higher there than in the dendrite. In addition, PKA activation was predicted to be more efficient when PKA was located together with AC in the same compartment (Oliveira et al., 2012). However, it has been pointed out that these simulations utilized rather high AC and PDE activities, which may not reflect the physiological ones (Saucerman et al., 2013; Conti et al., 2014). On the other hand, simulations by other groups suggest that the formation of a cAMP gradient requires the presence of additional factors capable of reducing the effective cAMP diffusion. Proposed factors include the presence of physical barriers, buffering of cAMP and local changes in the viscosity of the cytoplasm (Saucerman et al., 2013). For instance, Feinstein et al. (2012) applied a mathematical model to study the contribution of all the major mechanisms proposed for the formation of cAMP microdomains in pulmonary microvascular endothelia cells. They concluded that, with experimentally measured PDE and AC activities in these cells, the formation of a gradient could be observed only using a diffusion coefficient for cAMP of 3 $\mu m^2/s$ or less, i.e., at least 100-fold lower than experimentally measured in the bulk cytoplasm. However, it should be mentioned that, while mathematical simulations are a very powerful tool for interpreting experimental results and formulating new hypotheses, they also have a number of limitations. First, they are based on simplified models of cellular biochemistry. Second, they also have spatial and temporal limits. In particular, since the size of signaling complexes is in the range of tens to hundreds of nanometers, it would be important to be able to predict the behavior of signaling molecules at such short distances. Third, the results of simulations are largely dependent on the kinetics parameters and initial concentrations used. Unfortunately, for several of these parameters we possess only rough estimations, which are mostly based on *in vitro* measurements, and therefore do not necessarily reflect the values in intact cells. Further efforts to better estimate these parameters would help improving the reliability and predictive power of such simulations.

CONCLUSIONS AND FUTURE PERSPECTIVES

The development of optical methods that allow monitoring cAMP/PKA signaling in living cells played a fundamental role in revealing an unexpected level of organization in GPCR signaling cascades. On the one hand, receptors and downstream signaling molecules appear to be highly organized in micro- or nanodomains on biological membranes. Contrary to what originally thought, such high degree of compartmentation appears to also involve a rapidly diffusing molecule such as cAMP. On the other hand, the finding of receptor signaling on endosomes and possibly other intracellular compartments adds another level of organization, which could help explaining why receptors coupled to the same downstream signaling pathway can induce dissimilar biological effects. It is likely that new technological developments, as is often the case, will play a fundamental role in further elucidating the organization of signaling microdomains located on the cell surface and on other intracellular membranes. Indeed, optical methods with higher temporal and spatial resolution would permit to better dissect the nature of such microdomains. In this context, methods based on single molecule microscopy, which have been recently applied by us and other groups to GPCRs (Hern et al., 2010; Kasai et al., 2011; Calebiro et al., 2013), appear particularly indicated to analyze the composition of protein complexes on the surface of living cells and to capture dynamic events such as protein-protein interactions with high temporal and spatial resolution. Furthermore, new models such as *Drosophila* and new methods such as two-photon microscopy are hopefully going to permit a direct observation of these phenomena *in vivo*, thus allowing to address the role of cAMP compartmentation under highly physiological conditions. After all, almost six decades after the discovery of cAMP, there are still many good reasons to expect novel and exciting discoveries in this field.

ACKNOWLEDGMENTS

This work was supported by the Deutsche Forschungsgemeinschaft (DFG grant CA 1014/1-1 to Davide Calebiro).

REFERENCES

Adams, S. R., Harootunian, A. T., Buechler, Y. J., Taylor, S. S., and Tsien, R. Y. (1991). Fluorescence ratio imaging of cyclic AMP in single cells. *Nature* 349, 694–697. doi: 10.1038/349694a0

Allen, M. D., and Zhang, J. (2006). Subcellular dynamics of protein kinase A activity visualized by FRET-based reporters. *Biochem. Biophys. Res. Commun.* 348, 716–721. doi: 10.1016/j.bbrc.2006.07.136

Bacskai, B. J., Hochner, B., Mahaut-Smith, M., Adams, S. R., Kaang, B. K., Kandel, E. R., et al. (1993). Spatially resolved dynamics of cAMP and protein kinase A subunits in *Aplysia* sensory neurons. *Science* 260, 222–226. doi: 10.1126/science.7682336

Beavo, J. A., and Brunton, L. L. (2002). Cyclic nucleotide research—still expanding after half a century. *Nat. Rev. Mol. Cell Biol.* 3, 710–718. doi: 10.1038/nrm911

Boto, T., Louis, T., Jindachomthong, K., Jalink, K., and Tomchik, S. M. (2014). Dopaminergic modulation of cAMP drives nonlinear plasticity across the *Drosophila* mushroom body lobes. *Curr. Biol.* 24, 822–831. doi: 10.1016/j.cub.2014.03.021

Brunton, L. L., Hayes, J. S., and Mayer, S. E. (1979). Hormonally specific phosphorylation of cardiac troponin I and activation of glycogen phosphorylase. *Nature* 280, 78–80. doi: 10.1038/280078a0

Brunton, L. L., Hayes, J. S., and Mayer, S. E. (1981). Functional compartmentation of cyclic AMP and protein kinase in heart. *Adv. Cyclic Nucleotide Res.* 14, 391–397.

Buxton, I. L., and Brunton, L. L. (1983). Compartments of cyclic AMP and protein kinase in mammalian cardiomyocytes. *J. Biol. Chem.* 258, 10233–10239.

Calebiro, D., Nikolaev, V. O., Gagliani, M. C., de Filippis, T., Dees, C., Tacchetti, C., et al. (2009). Persistent cAMP-signals triggered by internalized G-protein-coupled receptors. *PLoS Biol.* 7:e1000172. doi: 10.1371/journal.pbio.1000172

Calebiro, D., Nikolaev, V. O., Persani, L., and Lohse, M. J. (2010). Signaling by internalized G-protein-coupled receptors. *Trends Pharmacol. Sci.* 31, 221–228. doi: 10.1016/j.tips.2010.02.002

Calebiro, D., Rieken, F., Wagner, J., Sungkaworn, T., Zabel, U., Borzi, A., et al. (2013). Single-molecule analysis of fluorescently labeled G-protein-coupled

receptors reveals complexes with distinct dynamics and organization. *Proc. Natl. Acad. Sci. U S A* 110, 743–748. doi: 10.1073/pnas.1205798110

Castro, L. R., Brito, M., Guiot, E., Polito, M., Korn, C. W., Hervé, D., et al. (2013). Striatal neurones have a specific ability to respond to phasic dopamine release. *J. Physiol.* 591, 3197–3214. doi: 10.1113/jphysiol.2013.252197

Castro, L. R., Gervasi, N., Guiot, E., Cavellini, L., Nikolaev, V. O., Paupardin-Tritsch, D., et al. (2010). Type 4 phosphodiesterase plays different integrating roles in different cellular domains in pyramidal cortical neurons. *J. Neurosci.* 30, 6143–6151. doi: 10.1523/JNEUROSCI.5851-09.2010

Chen, Y., Saulnier, J. L., Yellen, G., and Sabatini, B. L. (2014). A PKA activity sensor for quantitative analysis of endogenous GPCR signaling via 2-photon FRET-FLIM imaging. *Front. Pharmacol.* 5:56. doi: 10.3389/fphar.2014.00056

Conti, M., Mika, D., and Richter, W. (2014). Cyclic AMP compartments and signaling specificity: role of cyclic nucleotide phosphodiesterases. *J. Gen. Physiol.* 143, 29–38. doi: 10.1085/jgp.201311083

Corbin, J. D., Sugden, P. H., Lincoln, T. M., and Keely, S. L. (1977). Compartmentalization of adenosine 3′,5′-monophosphate and adenosine 3′,5′-monophosphate-dependent protein kinase in heart tissue. *J. Biol. Chem.* 252, 3854–3861.

Davare, M. A., Avdonin, V., Hall, D. D., Peden, E. M., Burette, A., Weinberg, R. J., et al. (2001). A β_2 adrenergic receptor signaling complex assembled with the Ca^{2+} channel Cav1.2. *Science* 293, 98–101. doi: 10.1126/science.293.5527.98

Depry, C., Allen, M. D., and Zhang, J. (2011). Visualization of PKA activity in plasma membrane microdomains. *Mol. Biosyst.* 7, 52–58. doi: 10.1039/c0mb00079e

Di Benedetto, G., Zoccarato, A., Lissandron, V., Terrin, A., Li, X., Houslay, M. D., et al. (2008). Protein kinase A type I and type II define distinct intracellular signaling compartments. *Circ. Res.* 103, 836–844. doi: 10.1161/CIRCRESAHA.108.174813

DiPilato, L. M., Cheng, X., and Zhang, J. (2004). Fluorescent indicators of cAMP and Epac activation reveal differential dynamics of cAMP signaling within discrete subcellular compartments. *Proc. Natl. Acad. Sci. U S A* 101, 16513–16518. doi: 10.1073/pnas.0405973101

DiPilato, L. M., and Zhang, J. (2009). The role of membrane microdomains in shaping β_2-adrenergic receptor-mediated cAMP dynamics. *Mol. Biosyst.* 5, 832–837. doi: 10.1039/b823243a

Dunn, T. A., and Feller, M. B. (2008). Imaging second messenger dynamics in developing neural circuits. *Dev. Neurobiol.* 68, 835–844. doi: 10.1002/dneu.20619

Dunn, T. A., Wang, C. T., Colicos, M. A., Zaccolo, M., Dipilato, L. M., Zhang, J., et al. (2006). Imaging of cAMP levels and protein kinase A activity reveals that retinal waves drive oscillations in second-messenger cascades. *J. Neurosci.* 26, 12807–12815. doi: 10.1523/jneurosci.3238-06.2006

Duvall, L. B., and Taghert, P. H. (2012). The circadian neuropeptide PDF signals preferentially through a specific adenylate cyclase isoform AC3 in M pacemakers of *Drosophila*. *PLoS Biol.* 10:e1001337. doi: 10.1371/journal.pbio.1001337

Erard, M., Fredj, A., Pasquier, H., Beltolngar, D. B., Bousmah, Y., Derrien, V., et al. (2013). Minimum set of mutations needed to optimize cyan fluorescent proteins for live cell imaging. *Mol. Biosyst.* 9, 258–267. doi: 10.1039/c2mb25303h

Esseltine, J. L., and Scott, J. D. (2013). AKAP signaling complexes: pointing towards the next generation of therapeutic targets? *Trends Pharmacol. Sci.* 34, 648–655. doi: 10.1016/j.tips.2013.10.005

Feinstein, W. P., Zhu, B., Leavesley, S. J., Sayner, S. L., and Rich, T. C. (2012). Assessment of cellular mechanisms contributing to cAMP compartmentalization in pulmonary microvascular endothelial cells. *Am. J. Physiol. Cell Physiol.* 302, C839–C852. doi: 10.1152/ajpcell.00361.2011

Fell, D. A. (1980). Theoretical analyses of the functioning of the high- and low-Km cyclic nucleotide phosphodiesterases in the regulation of the concentration of adenosine 3′,5′-cyclic monophosphate in animal cells. *J. Theor. Biol.* 84, 361–385. doi: 10.1016/s0022-5193(80)80011-7

Ferrandon, S., Feinstein, T. N., Castro, M., Wang, B., Bouley, R., Potts, J. T., et al. (2009). Sustained cyclic AMP production by parathyroid hormone receptor endocytosis. *Nat. Chem. Biol.* 5, 734–742. doi: 10.1038/nchembio.206

Förster, T. (1948). Zwischenmolekulare Energiewanderung und Fluoreszenz. *Ann. Phys.* 437, 55–75. doi: 10.1002/andp.19484370105

Gervasi, N., Hepp, R., Tricoire, L., Zhang, J., Lambolez, B., Paupardin-Tritsch, D., et al. (2007). Dynamics of protein kinase A signaling at the membrane, in the cytosol and in the nucleus of neurons in mouse brain slices. *J. Neurosci.* 27, 2744–2750. doi: 10.1523/jneurosci.5352-06.2007

Gervasi, N., Tchénio, P., and Preat, T. (2010). PKA dynamics in a *Drosophila* learning center: coincidence detection by rutabaga adenylyl cyclase and spatial regulation by dunce phosphodiesterase. *Neuron* 65, 516–529. doi: 10.1016/j.neuron.2010.01.014

Goaillard, J. M., and Vincent, P. (2002). Serotonin suppresses the slow afterhyperpolarization in rat intralaminar and midline thalamic neurones by activating 5-HT_7 receptors. *J. Physiol.* 541, 453–465. doi: 10.1113/jphysiol.2001.013896

Goaillard, J. M., Vincent, P. V., and Fischmeister, R. (2001). Simultaneous measurements of intracellular cAMP and L-type Ca^{2+} current in single frog ventricular myocytes. *J. Physiol.* 530, 79–91. doi: 10.1111/j.1469-7793.2001.0079m.x

Gorbunova, Y. V., and Spitzer, N. C. (2002). Dynamic interactions of cyclic AMP transients and spontaneous Ca^{2+} spikes. *Nature* 418, 93–96. doi: 10.1038/nature00835

Haugh, J. M. (2012). Live-cell fluorescence microscopy with molecular biosensors: what are we really measuring? *Biophys. J.* 102, 2003–2011. doi: 10.1016/j.bpj.2012.03.055

Hayes, J. S., Brunton, L. L., Brown, J. H., Reese, J. B., and Mayer, S. E. (1979). Hormonally specific expression of cardiac protein kinase activity. *Proc. Natl. Acad. Sci. U S A* 76, 1570–1574. doi: 10.1073/pnas.76.4.1570

Hayes, J. S., Brunton, L. L., and Mayer, S. E. (1980). Selective activation of particulate cAMP-dependent protein kinase by isoproterenol and prostaglandin E_1. *J. Biol. Chem.* 255, 5113–5119.

Hempel, C. M., Vincent, P., Adams, S. R., Tsien, R. Y., and Selverston, A. I. (1996). Spatio-temporal dynamics of cyclic AMP signals in an intact neural circuit. *Nature* 384, 166–169. doi: 10.1038/384166a0

Herbst, K. J., Allen, M. D., and Zhang, J. (2011). Spatiotemporally regulated protein kinase A activity is a critical regulator of growth factor-stimulated extracellular signal-regulated kinase signaling in PC12 cells. *Mol. Cell Biol.* 31, 4063–4075. doi: 10.1128/MCB.05459-11

Herget, S., Lohse, M. J., and Nikolaev, V. O. (2008). Real-time monitoring of phosphodiesterase inhibition in intact cells. *Cell. Signal.* 20, 1423–1431. doi: 10.1016/j.cellsig.2008.03.011

Hern, J. A., Baig, A. H., Mashanov, G. I., Birdsall, B., Corrie, J. E., Lazareno, S., et al. (2010). Formation and dissociation of M_1 muscarinic receptor dimers seen by total internal reflection fluorescence imaging of single molecules. *Proc. Natl. Acad. Sci. U S A* 107, 2693–2698. doi: 10.1073/pnas.0907915107

Hu, E., Demmou, L., Cauli, B., Gallopin, T., Geoffroy, H., Harris-Warrick, R. M., et al. (2011). VIP, CRF and PACAP act at distinct receptors to elicit different cAMP/PKA dynamics in the neocortex. *Cereb. Cortex* 21, 708–718. doi: 10.1093/cercor/bhq143

Irannejad, R., Tomshine, J. C., Tomshine, J. R., Chevalier, M., Mahoney, J. P., Steyaert, J., et al. (2013). Conformational biosensors reveal GPCR signalling from endosomes. *Nature* 495, 534–538. doi: 10.1038/nature12000

Jurevicius, J., and Fischmeister, R. (1996). cAMP compartmentation is responsible for a local activation of cardiac Ca^{2+} channels by β-adrenergic agonists. *Proc. Natl. Acad. Sci. U S A* 93, 295–299. doi: 10.1073/pnas.93.1.295

Kandel, E. R. (2009). The biology of memory: a forty-year perspective. *J. Neurosci.* 29, 12748–12756. doi: 10.1523/JNEUROSCI.3958-09.2009

Kandel, E. R., Dudai, Y., and Mayford, M. R. (2014). The molecular and systems biology of memory. *Cell* 157, 163–186. doi: 10.1016/j.cell.2014.03.001

Kasai, R. S., Suzuki, K. G., Prossnitz, E. R., Koyama-Honda, I., Nakada, C., Fujiwara, T. K., et al. (2011). Full characterization of GPCR monomer-dimer dynamic equilibrium by single molecule imaging. *J. Cell Biol.* 192, 463–480. doi: 10.1083/jcb.201009128

Kholodenko, B. N. (2006). Cell-signalling dynamics in time and space. *Nat. Rev. Mol. Cell Biol.* 7, 165–176. doi: 10.1038/nrm1838

Kholodenko, B. N., and Kolch, W. (2008). Giving space to cell signaling. *Cell* 133, 566–567. doi: 10.1016/j.cell.2008.04.033

Klarenbeek, J. B., Goedhart, J., Hink, M. A., Gadella, T. W., and Jalink, K. (2011). A mTurquoise-based cAMP sensor for both FLIM and ratiometric read-out has improved dynamic range. *PLoS One* 6:e19170. doi: 10.1371/journal.pone.0019170

Komatsu, N., Aoki, K., Yamada, M., Yukinaga, H., Fujita, Y., Kamioka, Y., et al. (2011). Development of an optimized backbone of FRET biosensors for kinases and GTPases. *Mol. Biol. Cell* 22, 4647–4656. doi: 10.1091/mbc.E11-01-0072

Lefkimmiatis, K., and Zaccolo, M. (2014). cAMP signaling in subcellular compartments. *Pharmacol. Ther.* 143, 295–304. doi: 10.1016/j.pharmthera.2014.03.008

Lefkowitz, R. J. (2013). A brief history of G-protein coupled receptors (Nobel Lecture). *Angew. Chem. Int. Ed. Engl.* 52, 6366–6378. doi: 10.1002/anie.201301924

Lohse, M. J., Nikolaev, V. O., Hein, P., Hoffmann, C., Vilardaga, J. P., and Bünemann, M. (2008). Optical techniques to analyze real-time activation and signaling of G-protein-coupled receptors. *Trends Pharmacol. Sci.* 29, 159–165. doi: 10.1016/j.tips.2007.12.002

Lohse, M. J., Nuber, S., and Hoffmann, C. (2012). Fluorescence/bioluminescence resonance energy transfer techniques to study G-protein-coupled receptor activation and signaling. *Pharmacol. Rev.* 64, 299–336. doi: 10.1124/pr.110.004309

Mironov, S. L., Skorova, E., Taschenberger, G., Hartelt, N., Nikolaev, V. O., Lohse, M. J., et al. (2009). Imaging cytoplasmic cAMP in mouse brainstem neurons. *BMC Neurosci.* 10:29. doi: 10.1186/1471-2202-10-29

Neves, S. R., Tsokas, P., Sarkar, A., Grace, E. A., Rangamani, P., Taubenfeld, S. M., et al. (2008). Cell shape and negative links in regulatory motifs together control spatial information flow in signaling networks. *Cell* 133, 666–680. doi: 10.1016/j.cell.2008.04.025

Nicol, X., Hong, K. P., and Spitzer, N. C. (2011). Spatial and temporal second messenger codes for growth cone turning. *Proc. Natl. Acad. Sci. U S A* 108, 13776–13781. doi: 10.1073/pnas.1100247108

Nikolaev, V. O., Bünemann, M., Hein, L., Hannawacker, A., and Lohse, M. J. (2004). Novel single chain cAMP sensors for receptor-induced signal propagation. *J. Biol. Chem.* 279, 37215–37218. doi: 10.1074/jbc.c400302200

Nikolaev, V. O., Bünemann, M., Schmitteckert, E., Lohse, M. J., and Engelhardt, S. (2006). Cyclic AMP imaging in adult cardiac myocytes reveals far-reaching β_1-adrenergic but locally confined β_2-adrenergic receptor-mediated signaling. *Circ. Res.* 99, 1084–1091. doi: 10.1161/01.res.0000250046.69918.d5

Nikolaev, V. O., Gambaryan, S., Engelhardt, S., Walter, U., and Lohse, M. J. (2005). Real-time monitoring of the PDE2 activity of live cells: hormone-stimulated cAMP hydrolysis is faster than hormone-stimulated cAMP synthesis. *J. Biol. Chem.* 280, 1716–1719. doi: 10.1074/jbc.c400505200

Nikolaev, V. O., Moshkov, A., Lyon, A. R., Miragoli, M., Novak, P., Paur, H., et al. (2010). β_2-adrenergic receptor redistribution in heart failure changes cAMP compartmentation. *Science* 327, 1653–1657. doi: 10.1126/science.1185988

Norris, R. P., Ratzan, W. J., Freudzon, M., Mehlmann, L. M., Krall, J., Movsesian, M. A., et al. (2009). Cyclic GMP from the surrounding somatic cells regulates cyclic AMP and meiosis in the mouse oocyte. *Development* 136, 1869–1878. doi: 10.1242/dev.035238

Oliveira, R. F., Kim, M., and Blackwell, K. T. (2012). Subcellular location of PKA controls striatal plasticity: stochastic simulations in spiny dendrites. *PLoS Comput. Biol.* 8:e1002383. doi: 10.1371/journal.pcbi.1002383

Oliveira, R. F., Terrin, A., Di Benedetto, G., Cannon, R. C., Koh, W., Kim, M., et al. (2010). The role of type 4 phosphodiesterases in generating microdomains of cAMP: large scale stochastic simulations. *PLoS One* 5:e11725. doi: 10.1371/journal.pone.0011725

Pierce, K. L., Premont, R. T., and Lefkowitz, R. J. (2002). Seven-transmembrane receptors. *Nat. Rev. Mol. Cell Biol.* 3, 639–650. doi: 10.1038/nrm908

Polito, M., Klarenbeek, J., Jalink, K., Paupardin-Tritsch, D., Vincent, P., and Castro, L. R. (2013). The NO/cGMP pathway inhibits transient cAMP signals through the activation of PDE2 in striatal neurons. *Front. Cell. Neurosci.* 7:211. doi: 10.3389/fncel.2013.00211

Ponsioen, B., Zhao, J., Riedl, J., Zwartkruis, F., van der Krogt, G., Zaccolo, M., et al. (2004). Detecting cAMP-induced Epac activation by fluorescence resonance energy transfer: Epac as a novel cAMP indicator. *EMBO Rep.* 5, 1176–1180. doi: 10.1038/sj.embor.7400290

Rall, T. W., and Sutherland, E. W. (1958). Formation of a cyclic adenine ribonucleotide by tissue particles. *J. Biol. Chem.* 232, 1065–1076.

Rich, T. C., Fagan, K. A., Nakata, H., Schaack, J., Cooper, D. M., and Karpen, J. W. (2000). Cyclic nucleotide-gated channels colocalize with adenylyl cyclase in regions of restricted cAMP diffusion. *J. Gen. Physiol.* 116, 147–161. doi: 10.1085/jgp.116.2.147

Rich, T. C., and Karpen, J. W. (2002). Review article: cyclic AMP sensors in living cells: what signals can they actually measure? *Ann. Biomed. Eng.* 30, 1088–1099. doi: 10.1114/1.1511242

Rich, T. C., Tse, T. E., Rohan, J. G., Schaack, J., and Karpen, J. W. (2001). *In vivo* assessment of local phosphodiesterase activity using tailored cyclic nucleotide-gated channels as cAMP sensors. *J. Gen. Physiol.* 118, 63–78. doi: 10.1085/jgp.118.1.63

Rich, T. C., Webb, K. J., and Leavesley, S. J. (2014). Can we decipher the information content contained within cyclic nucleotide signals? *J. Gen. Physiol.* 143, 17–27. doi: 10.1085/jgp.201311095

Rybin, V. O., Xu, X., Lisanti, M. P., and Steinberg, S. F. (2000). Differential targeting of β-adrenergic receptor subtypes and adenylyl cyclase to cardiomyocyte caveolae. A mechanism to functionally regulate the cAMP signaling pathway. *J. Biol. Chem.* 275, 41447–41457. doi: 10.1074/jbc.m006951200

Saucerman, J. J., Greenwald, E. C., and Polanowska-Grabowska, R. (2013). Perspectives on: cyclic nucleotide microdomains and signaling specificity: mechanisms of cyclic amp compartmentation revealed by computational models. *J. Gen. Physiol.* 143, 39–48. doi: 10.1085/jgp.201311044

Shafer, O. T., Kim, D. J., Dunbar-Yaffe, R., Nikolaev, V. O., Lohse, M. J., and Taghert, P. H. (2008). Widespread receptivity to neuropeptide PDF throughout the neuronal circadian clock network of *Drosophila* revealed by real-time cyclic AMP imaging. *Neuron* 58, 223–237. doi: 10.1016/j.neuron.2008.02.018

Shelly, M., Lim, B. K., Cancedda, L., Heilshorn, S. C., Gao, H., and Poo, M. M. (2010). Local and long-range reciprocal regulation of cAMP and cGMP in axon/dendrite formation. *Science* 327, 547–552. doi: 10.1126/science.1179735

Steinberg, S. F., and Brunton, L. L. (2001). Compartmentation of G protein-coupled signaling pathways in cardiac myocytes. *Annu. Rev. Pharmacol. Toxicol.* 41, 751–773. doi: 10.1146/annurev.pharmtox.41.1.751

Tadevosyan, A., Vaniotis, G., Allen, B. G., Hebert, T. E., and Nattel, S. (2012). G protein-coupled receptor signalling in the cardiac nuclear membrane: evidence and possible roles in physiological and pathophysiological function. *J. Physiol.* 590, 1313–1330. doi: 10.1113/jphysiol.2011.222794

Takeda, N., Kyozuka, K., and Deguchi, R. (2006). Increase in intracellular cAMP is a prerequisite signal for initiation of physiological oocyte meiotic maturation in the hydrozoan *Cytaeis uchidae*. *Dev. Biol.* 298, 248–258. doi: 10.1016/j.ydbio.2006.06.034

Tomchik, S. M., and Davis, R. L. (2009). Dynamics of learning-related cAMP signaling and stimulus integration in the *Drosophila* olfactory pathway. *Neuron* 64, 510–521. doi: 10.1016/j.neuron.2009.09.029

Vincent, P., and Brusciano, D. (2001). Cyclic AMP imaging in neurones in brain slice preparations. *J. Neurosci. Methods* 108, 189–198. doi: 10.1016/s0165-0270(01)00393-4

Violin, J. D., Dewire, S. M., Barnes, W. G., and Lefkowitz, R. J. (2006). G protein-coupled receptor kinase and β-arrestin-mediated desensitization of the angiotensin II type 1A receptor elucidated by diacylglycerol dynamics. *J. Biol. Chem.* 281, 36411–36419. doi: 10.1074/jbc.m607956200

Violin, J. D., Dipilato, L. M., Yildirim, N., Elston, T. C., Zhang, J., and Lefkowitz, R. J. (2008). β_2-adrenergic receptor signaling and desensitization elucidated by quantitative modeling of real time cAMP dynamics. *J. Biol. Chem.* 283, 2949–2961. doi: 10.1074/jbc.m707009200

Wachten, S., Masada, N., Ayling, L. J., Ciruela, A., Nikolaev, V. O., Lohse, M. J., et al. (2010). Distinct pools of cAMP centre on different isoforms of adenylyl cyclase in pituitary-derived GH3B6 cells. *J. Cell Sci.* 123, 95–106. doi: 10.1242/jcs.058594

Webb, R. J., Marshall, F., Swann, K., and Carroll, J. (2002). Follicle-stimulating hormone induces a gap junction-dependent dynamic change in [cAMP] and protein kinase A in mammalian oocytes. *Dev. Biol.* 246, 441–454. doi: 10.1006/dbio.2002.0630

Willoughby, D., and Cooper, D. M. (2007). Organization and Ca^{2+} regulation of adenylyl cyclases in cAMP microdomains. *Physiol. Rev.* 87, 965–1010. doi: 10.1152/physrev.00049.2006

Zaccolo, M. (2011). Spatial control of cAMP signalling in health and disease. *Curr. Opin. Pharmacol.* 11, 649–655. doi: 10.1016/j.coph.2011.09.014

Zaccolo, M., De Giorgi, F., Cho, C. Y., Feng, L., Knapp, T., Negulescu, P. A., et al. (2000). A genetically encoded, fluorescent indicator for cyclic AMP in living cells. *Nat. Cell Biol.* 2, 25–29. doi: 10.1038/71345

Zaccolo, M., and Pozzan, T. (2002). Discrete microdomains with high concentration of cAMP in stimulated rat neonatal cardiac myocytes. *Science* 295, 1711–1715. doi: 10.1126/science.1069982

Zhang, J., Hupfeld, C. J., Taylor, S. S., Olefsky, J. M., and Tsien, R. Y. (2005). Insulin disrupts β-adrenergic signalling to protein kinase A in adipocytes. *Nature* 437, 569–573. doi: 10.1038/nature04140

Zhang, J., Ma, Y., Taylor, S. S., and Tsien, R. Y. (2001). Genetically encoded reporters of protein kinase A activity reveal impact of substrate tethering. *Proc. Natl. Acad. Sci. U S A* 98, 14997–15002. doi: 10.1073/pnas.211566798

Conflict of Interest Statement: The authors declare that the research was conducted in the absence of any commercial or financial relationships that could be construed as a potential conflict of interest.

Received: 28 July 2014; accepted: 07 October 2014; published online: 28 October 2014.
Citation: Calebiro D and Maiellaro I (2014) cAMP signaling microdomains and their observation by optical methods. Front. Cell. Neurosci. ***8****:350. doi: 10.3389/fncel.2014.00350*
This article was submitted to the journal Frontiers in Cellular Neuroscience.

frontiers in
CELLULAR NEUROSCIENCE

REVIEW ARTICLE
published: 04 December 2014
doi: 10.3389/fncel.2014.00395

Visualization of cyclic nucleotide dynamics in neurons

Kirill Gorshkov and Jin Zhang*

Laboratory of Dr. Jin Zhang, Department of Pharmacology and Molecular Sciences, Johns Hopkins University School of Medicine, Baltimore, Maryland, USA

Edited by:
Pierre Vincent, Centre National de la Recherche Scientifique, France

Reviewed by:
Bernd Kuhn, Okinawa Institute of Science and Technology Graduate University, Japan
Liliana Ribeiro Vivas Castro, Université Pierre et Marie Curie, France
Viacheslav Nikolaev, University of Goettingen, Germany

****Correspondence:***
Jin Zhang, Laboratory of Dr. Jin Zhang, Department of Pharmacology and Molecular Sciences, Johns Hopkins University School of Medicine, 725 North Wolfe Street, Baltimore, Maryland, 21205, USA
e-mail: jzhang32@jhmi.edu

The second messengers cyclic adenosine monophosphate (cAMP) and cyclic guanosine monophosphate (cGMP) transduce many neuromodulatory signals from hormones and neurotransmitters into specific functional outputs. Their production, degradation and signaling are spatiotemporally regulated to achieve high specificity in signal transduction. The development of genetically encodable fluorescent biosensors has provided researchers with useful tools to study these versatile second messengers and their downstream effectors with unparalleled spatial and temporal resolution in cultured cells and living animals. In this review, we introduce the general design of these fluorescent biosensors and describe several of them in more detail. Then we discuss a few examples of using cyclic nucleotide fluorescent biosensors to study regulation of neuronal function and finish with a discussion of advances in the field. Although there has been significant progress made in understanding how the specific signaling of cyclic nucleotide second messengers is achieved, the mechanistic details in complex cell types like neurons are only just beginning to surface. Current and future fluorescent protein reporters will be essential to elucidate the role of cyclic nucleotide signaling dynamics in the functions of individual neurons and their networks.

Keywords: biosensor, neuron, FRET, fluorescence, signaling, cyclic nucleotide, cAMP, cGMP

INTRODUCTION

The cyclic nucleotides cyclic adenosine monophosphate (cAMP) and cyclic guanosine monophosphate (cGMP) are ubiquitous second messengers present in most cell types. Within the brain, cyclic nucleotides transduce neuromodulatory signals into functional outputs for individual neurons leading to changes in neural networks themselves or their function. The importance of cyclic nucleotide signaling pathways is well appreciated in the field of clinical neuroscience and psychiatry, with many drugs targeting the G-protein coupled receptors to modulate neuronal activity (Lim, 2007; Taly, 2013). The effects of cAMP and cGMP signaling range from regulating neuronal differentiation and growth to axonal guidance and modulation of neuronal excitability. To accomplish this, cyclic nucleotides are coupled to many downstream effectors (Antoni, 2000). cAMP, the prototypical cyclic nucleotide, transduces G-protein signals to activate protein kinase A (PKA) and exchange protein activated by cAMP (Epac). cGMP, on the other hand, relays signals from nitric oxide to activate protein kinase G (PKG). Phosphodiesterase (PDE), the enzyme that degrades cGMP, can be a cGMP effector with its activity modulated by cGMP binding to regulatory domains forming feedback loops (Conti and Richter, 2014). Both cyclic nucleotides also activate cyclic nucleotide gated ion channels (Rich et al., 2014).

The idea of compartmentalized signaling is an essential component to the cyclic nucleotide signaling model. To elicit their diverse functional effects in a highly specific manner, cAMP and cGMP signaling is thought to be spatially compartmentalized (Zaccolo and Stangherlin, 2014). The levels of cyclic nucleotides and the activities of downstream effectors are not uniform throughout the cell, but instead form specific nanodomains or microdomains inside the cell. The spatial compartmentation is achieved, at least partially, by strict regulation of cyclic nucleotide production and degradation. cAMP is produced by adenylyl cyclase (AC) and cGMP is produced by guanylyl cyclase (GC). These enzymes are located within the plasma membrane as transmembrane proteins, or within the cytoplasm or organelles as soluble forms of the enzyme. The degradation of cAMP and cGMP is carried out by PDEs which have specificity for cAMP, cGMP, or both. PDEs have been shown to function as cAMP and cGMP sinks to help maintain these microdomains (Terrin et al., 2006; Biswas et al., 2008). The tight spatiotemporal regulation of cAMP signaling is achieved with the help of the A-kinase anchoring protein (Esseltine and Scott, 2013), which assembles signaling complexes consisting of members of the cAMP/PKA signaling pathway like ACs, PDEs, PKA and its substrate, and other effectors. These signalosomes, which can be found throughout various compartments including the plasma membrane, the cytosol and the nucleus, have been shown to play important roles in achieving functional specificity of the cAMP/PKA pathway. In addition to biochemical regulation, the structural properties of cells can also affect the signaling dynamics of second messengers (Castro et al., 2010; Neves, 2012).

Relatively recent advances in fluorescent biosensor technology allow researchers to track the dynamics of cyclic nucleotides and

Abbreviations: cyclic nucleotide binding domain, CNBD; Dopamine 1 receptor, D1R; light-oxygen-voltage, LOV; sensors of blue light using FAD, BLUF.

their effectors in living neurons and brain tissue. Here we will describe several genetically encoded fluorescent biosensors for monitoring cyclic nucleotide dynamics. Then we will focus on a few studies that demonstrate their implementation in living neurons for the purpose of understanding how cyclic nucleotides impact neuronal function. We will end with a discussion of novel tools and modeling efforts that help us understand neuronal cyclic nucleotide dynamics.

GENETICALLY ENCODED FLUORESCENT BIOSENSORS

The genetically encoded fluorescent biosensors described in the following sections allow for the continuous monitoring of free cyclic nucleotides with high spatiotemporal resolution. These biosensors are engineered based on a general design: a sensing unit to detect the change in free cyclic nucleotide concentration and a reporting unit to convert the biochemical change into a fluorescent readout. The sensing unit for cyclic nucleotide biosensors is one or more cyclic nucleotide binding domains (CNBD). The reporting unit can be made up of two fluorescent proteins flanking the sensing unit as is the typical arrangement for fluorescence resonance energy transfer (FRET)-based biosensors. In FRET, energy is transferred non-radiatively from an excited donor molecule to an acceptor molecule. For a fixed FRET donor-acceptor pair, the efficiency of FRET is dependent on the distance and orientation of the two fluorophores. In a FRET-based biosensor, cyclic nucleotide binding induces conformational changes of the CNBD sensing unit, which acts as a molecular switch to change the physical separation or orientation between the fluorescent protein pair resulting in a change in FRET (**Figure 1A**). In intensity-based biosensors, on the other hand, the reporting unit can be a single fluorescent protein. In this case, conformational changes in the sensing unit are translated into changes in fluorescence intensity (**Figure 1B**). Different sensors vary in their CNBD sensing units and fluorescent protein reporting units. For a thorough overview of fluorescence and fluorescent proteins used in many different types of biosensors, please refer to the reviews by Sample et al. (2009); Newman et al. (2011). The following subsections describe the various designs of many cAMP and cGMP reporters. Please refer to **Table 1** for a detailed list of the biosensors described here.

FLUORESCENT INDICATORS OF cAMP

cAMP reporter based on dissociation of PKA holoenzyme

For the purposes of tracking cAMP, researchers have been developing molecular biosensors for the past several decades. The first of such biosensors called FlCRhR (**Fl**uorescein-labeled PKA **C**atalytic subunit and **Rh**odamine-labeled **R**egulatory subunit) was based on chemically labeled regulatory and catalytic subunits of the PKA holoenzyme (Adams et al., 1991). Upon cAMP binding the catalytic and regulatory subunits dissociate producing a change in FRET. This labeled holoenzyme was microinjected into living cells and imaged under wide-field microscopy. A genetically encodable version was generated allowing for expression in a wide array of cell types, thereby expanding the scope of the application (Zaccolo et al., 2000). The fusion protein contained an 11 amino acid linker between the PKA regulatory subunit and the fluorescent proteins (RII-EBFP; C-GFP^{S65T}). A newer version was generated using CFP fused to the RII regulatory domain and YFP fused to the catalytic domain (Zaccolo and Pozzan, 2002; Mongillo et al., 2004). By using molecular dynamics simulations, this design was further improved with the introduction of a longer, more rigid 20 amino acid linker (Lissandron et al., 2005). Live-cell fluorescent lifetime and acceptor sensitized measurements of this sensor showed a doubling of the dynamic range.

Single-chain FRET-based cAMP indicators

Multimeric biosensors like RII-CFP/C-YFP require equal expression of both subunits to form the PKA tetramer. In addition, there can be interactions with endogenous PKA subunits which do not make contributions to the FRET response. On the other hand, single chain biosensors offer ease of use and targeting to subcellular locations, increasing the spatial resolution offered by FRET-based biosensors. In 2004, three groups independently developed single-chain cAMP FRET sensors using the CNBD from Epac, a Rap1 guanine nucleotide exchange factor, or PKA. The reported affinities for cAMP range from ∼0.3 to 50 μM. However, we note that experimental variations such as biosensor concentrations when determining EC_{50}s could largely affect the resulting values. We include the experimentally determined EC_{50}s in **Table 1** but these values may not accurately reflect the differences in biosensor affinities.

In Epac1-camps, the cAMP binding domain of the Epac1 protein (Epac1$^{157-316}$) was flanked by an N-terminal CFP and a C-terminal YFP (Nikolaev et al., 2004). Epac2-camps used the cAMP binding domain B from Epac2 (Epac2B$^{284-443}$) instead. Both biosensors generated a decrease in the yellow to cyan emission ratio upon binding cAMP, indicating a decrease in FRET. In an attempt to generate a more sensitive cAMP probe called Epac2-camps300, Norris et al. introduced a K405E mutation into Epac2-camps that decreased the EC_{50} from ∼0.9 μM to ∼0.3 μM (Norris et al., 2009). Nikolaev et al. also generated a single chain PKA-camps using a portion the PKA regulatory βII subunit (RIIβ) sandwiched between ECFP and EYFP (Nikolaev et al., 2004). PKA-camps incorporated the cAMP binding domain B from amino acids 264–403 of RIIβ as the sensing unit. Upon binding cAMP, RIIβ undergoes a conformational change conducive to a change in FRET. These single CNBD containing biosensors are the smallest cAMP probes currently available.

A series of Epac based reporters called ICUE (**I**ndicator of **c**AMP **U**sing **E**pac) have been developed in parallel. First in the series, ICUE1 contained full-length Epac1 sandwiched between ECFP and the YFP variant Citrine (DiPilato et al., 2004). Like Epac1-camps and Epac2-camps, ICUE also responds to cAMP with a decrease in the yellow to cyan emission ratio. ICUE2, an improved version of ICUE1, has an EC_{50} of ∼12.5 μM and contains a N-terminally truncated Epac1 protein (Epac1$^{149-881}$) (Violin et al., 2008). This biosensor showed improvement in localization over ICUE1 due to removal of a membrane and mitochondria targeting sequence located at the N-terminus. More recently, we developed ICUE3 with an increased dynamic

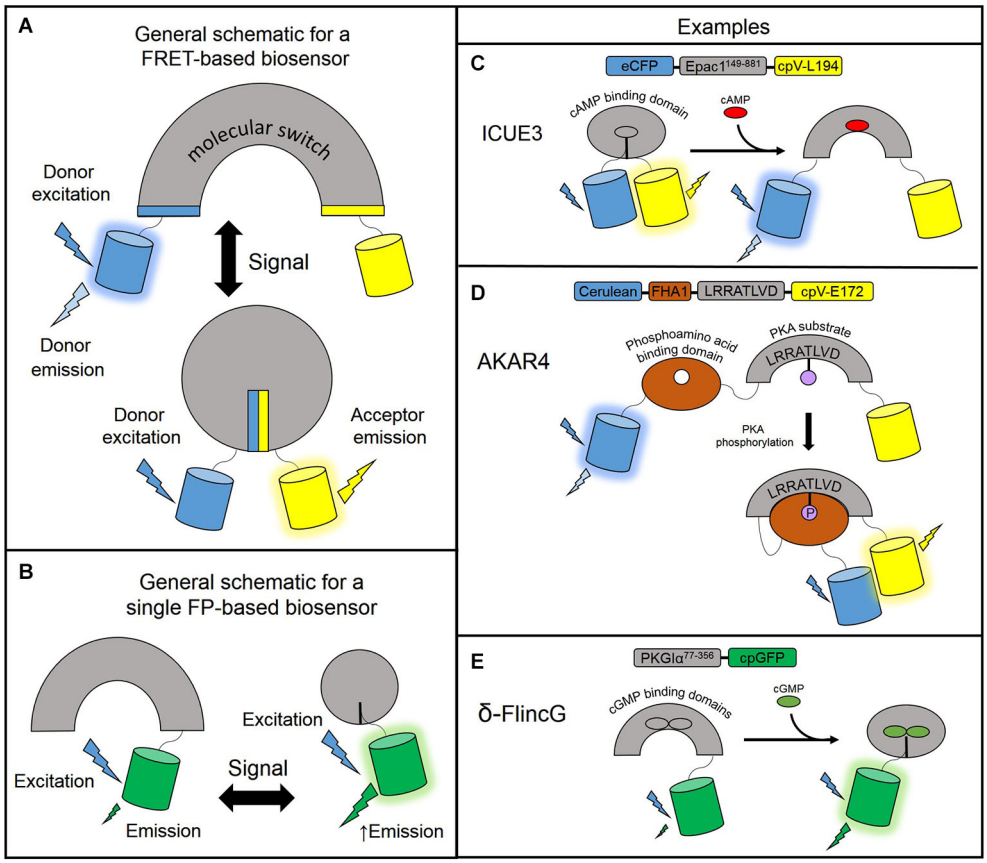

FIGURE 1 | Designs of genetically encodable biosensors. **(A)** General design of a FRET-based biosensor consisting of a sensing unit which acts as a molecular switch to change the distance or orientation of the fluorescent protein reporting unit. In a low FRET situation, the donor fluorescent protein is excited and emits light at its own wavelength. In the high FRET situation, donor excitation allows for resonance energy transfer to the acceptor fluorescent protein which emits light at its own wavelength. **(B)** General design of a single fluorescent protein-based biosensor. The sensing unit transduces a signal via a conformational change to the linked fluorescent protein reporting unit which undergoes its own conformational change and modulates fluorescence intensity. A circularly permuted GFP is often used to enhance the change in fluorescence. **(C)** ICUE3 consists of an Epac1$^{149-881}$ sensing unit flanked by an ECFP donor and a cpV-L194 acceptor reporting unit. Upon binding cAMP, the sensor switches from a high FRET to a low FRET conformation. **(D)** AKAR4 contains a sensing unit consisting of a FHA1 phosphoamino acid binding domain and a substrate peptide. The reporting unit is comprised of a Cerulean donor and cpV-E172 acceptor reporting unit. When PKA activity is high, the substrate peptide is phosphorylated and binds the FHA1 domain to induce FRET. **(E)** δ-FlincG utilizes a PKG1α$^{77-356}$ sensing unit linked to a single cpGFP reporting unit. Upon binding cGMP, the fluorescence intensity of cpGFP increases.

range by changing the FRET acceptor Citrine to a circularly permuted Venus at lysine 194 (cpV-L194; DiPilato and Zhang, 2009; **Figure 1C**). The large dynamic range of ICUE3 (∼100% emission ratio change) makes it suitable for subcellular targeting for detecting local cAMP changes (e.g., plasma membrane and nucleus (Sample et al., 2012), sarcoplasmic reticulum (Liu et al., 2012), primary cilia (Marley et al., 2013)) as addition of subcellular localization tags sometimes leads to decreased response amplitudes.

The Jalink lab developed a similar biosensor CFP-Epac(δDEP-CD)-YFP using Epac1$^{149-881}$ flanked by an amino-terminal CFP and carboxy-terminal YFP (Ponsioen et al., 2004). Mutations T781A and F782A were introduced to generate a catalytically dead (CD) Epac1. The lab has recently developed newer versions, some of which are useful for fluorescence lifetime imaging FRET (FLIM-FRET) measurements (Klarenbeek et al., 2011; Polito et al., 2013). Named Epac-S^{H150}, the newest version in this series incorporated the Q270E mutation (Dao et al., 2006) to increase the affinity for cAMP (EC_{50} 4 μM) and used mTurquoise2 as the FRET donor and a single circularly-permuted Citrine as the FRET acceptor (Polito et al., 2013).

In some cases, the concentration of cAMP in a cell can saturate a highly sensitive reporter. To accommodate large fluctuations in signaling, Nikolaev et al. used the hyperpolarization-sensitive cyclic nucleotide gated channel 2 (HCN2) to generate HCN2-camps and image large changes in cAMP concentration in cardiomyocytes (Nikolaev et al., 2006a). In the context of probes like PKA-camps, Epac-camps, and CFP-RII/C-YFP, this probe exhibited a lower affinity for cAMP (EC_{50} ∼6 μM) and provides another tool to monitor cAMP in cells with larger basal or fluctuating concentrations.

Table 1 | A detailed list of biosensors currently available for cAMP, PKA, and cGMP.

Sensor name	Sensing domain	Design	EC_{50} (cAMP)	Response	Comments	Reference
cAMP						
FICRhR	PKA catalytic and RIIβ subunits	Multimeric	0.09 μM	FRET ↓	Chemically labeled, high affinity	Adams et al. (1991)
			Genetically encoded sensors			
RII-CFP; C-YFP	As above	Multimeric	∼0.3 μM	FRET ↓	Original version contained EBFP/EGFP, newest version has a 20 aa linker between CFP and RII	Zaccolo and Pozzan (2002), Mongillo et al. (2004), Lissandron et al. (2005)
PKA-camps	PKA RIIβ subunit	Single Chain	1.9 μM	FRET ↓	Less robust response than Epac-camps	Nikolaev et al. (2004)
Epac-camps family	Epac 1/2 CNBD	Single Chain	Epac1-camps—2.4 μM, Epac2-camps—0.9 μM, Epac2-camps300—∼0.3 μM	FRET ↓	Epac2-camps300 has K405E mutation, range of relatively high affinities	Nikolaev et al. (2004), Norris et al. (2009)
ICUE Family	Full length or truncated Epac	Single Chain	ICUE2/3—∼12.5 μM	FRET ↓	cpV-L194 replaces Citrine in ICUE3, doubles the dynamic range	DiPilato et al. (2004), Violin et al. (2008), DiPilato and Zhang (2009)
$^{T}Epac^{VV}$	Epac Δ DEP, catalytically dead (CD)	Single Chain	∼14 μM for CFP-YFP version	FRET ↓	Lower affinity, T781A and F782A catalytically dead mutations, mTurquoiseΔ and tandem cpV-E173-Venus reporting unit	Ponsioen et al. (2004), Klarenbeek et al. (2011)
Epac-S^{H150}	EpacI Δ (DEP, CD) Q270E	Single Chain	4.0 μM	FRET ↓	Higher affinity, mTurquoise2 and cpCitrine, large dynamic range	Polito et al. (2013)
HCN2-camps	HCN2 CNBD	Single Chain	6.0 μM	FRET ↓	Based on CNGC	Nikolaev et al. (2006a)
Nanolantem-camps	Epac $1^{170–327}$, Q270E	Single Chain	1.6 μM	Luminescence ↑	Uses VenusΔC10 and split Rluc8ΔN3, no excitation light reguired, low absolute intensity	Saito et al. (2012)

(Continued)

Table 1 | Continued

Sensor name	Sensing domain	Design	EC_{50} (cAMP)	Response	Comments	Reference
PKA						
AKAR family	FHA1 PAABD and PKA substrate	Single Chain	NA	FRET ↑	Cerulean and cpV-E172 in AKAR4, very bright, fast kinetics, amplifies cAMP signal through kinase activity	Zhang et al. (2001), Allen and Zhang (2006), Depry et al. (2011)
^{Aq}AKAR^{Cit}	Same as AKAR	Single Chain	NA	FRET ↑	Uses Aquamarine and cpCitrine, stable to environmental pH	Erard et al. (2013)
GAkdY family	Same as AKAR	Single Chain	NA	Fluorescence ↑	Conformationally senstive GFP variant incorporated into AKAR, single wavelength probe, two-photon imaging of dendrites and spines	Bonnot et al. (2014)
Dual Specificity Probe						
ICUEPID	As above plus Epac 1	Single Chain	NA	For PKA (CFP-RFP) FRET ↑ For cAMP (RFP-YFP) FRET↓	Dual specificity for cAMP/PKA for co-imaging using single construct	Ni et al. (2011)
Epac						
CFP-Epac2-YFP	Full length Epac	Single Chain	NA	FRET ↓	Reports on [cAMP] as well as Epac dynamics	Zhang et al. (2009), Herbst et al. (2011)

(Continued)

Table 1 | Continued

Sensor Name	Sensing Domain	Design	EC_{50} (cAMP)	Response	Comments	Reference
cGMP						
CGY-Del1	PKG1α CNBD	Single Chain	20 nM	FRET ↑	cGMP/cAMP selectivity = 7.6	Sato et al. (2000), Nikolaev et al. (2006b)
Cygnet family	PKG1α CNBD	Single Chain	cygnet-1 = 1.5 μM, cygnet-2 = 1.9 μM	FRET ↓	cGMP/cAMP selectivity cygnet-2.1 >600	Honda et al. (2001)
cGES family	PDE2/5 GAF CNBD	Single Chain	cGES-DE2 = 0.9 μM, cGES-DE5 = 1.5 μM. redcGES-DE5 = 40 nM	FRET ↑	cGMP/cAMP selectivity cGES-DE5 = 420	Nikolaev et al. (2006b), Niino et al. (2009)
cGi family	tandem PKGIα CNBD	Single Chain	cGi500 = 0.5 μM, cGi3000 = 3.0 μM, cGi6000 = 6.0 μM	FRET ↑	fast kinetics with high selectivity	Russwurm et al. (2007)
FlincG family	truncated PKG1α	Single Chain	δ-FlincG = 0.15 μM	Intensity ↑	cGMP/cAMP selectivity = 1140, 30, 280 for α, β, δ, respectively	Nausch et al. (2008)
Cygnus	PDE5 GAF-A CNBD	Single Chain	1.0 μM	Intensity ↑	Uses mTagBFP and dark YFP sREACH, cGMP/cAMP selectivity >400, useful for multi-parameter imaging	Niino et al. (2010)

Indicators of downstream cAMP effectors

Neuromodulatory signals can be transduced by cAMP and cGMP through their downstream target kinases PKA and PKG, respectively (Giese and Mizuno, 2013). Although there are no biosensors yet available for PKG activity, the A-kinase activity reporter (AKAR) can report on the kinase activity of PKA (Zhang et al., 2001). AKAR uses a molecular switch consisting of a phosphoamino acid binding domain linked to a PKA-specific substrate sequence, flanked by CFP and YFP. PKA phosphorylation of its substrate induces binding of the phosphorylated substrate to the phosphoamino acid binding domain, leading to an increase in FRET. AKAR1 displayed an irreversible FRET response which prevented continuous monitoring of PKA dynamics. This was presumably due to the high affinity of the 14-3-3 binding domain for the substrate as tight binding may prevent phosphatases from dephosphorylating the substrate and reversing the FRET response. This was overcome by the generation of AKAR2 which utilized the lower binding affinity forkhead-associated domain 1 (FHA1) and exhibited a reversible FRET response (Zhang et al., 2005). The kinetics of AKAR2 were improved in AKAR2.2 by replacing the dimeric forms of ECFP and Citrine with versions that resist dimerization. The dynamic range was doubled in AKAR3 by replacing the YFP acceptor in AKAR2 with cpV-E172 (Allen and Zhang, 2006). The dynamic range of AKAR was further enhanced with latest version, AKAR4, by replacing ECFP with Cerulean (Depry et al., 2011; **Figure 1D**). Due to the amplification of the cAMP signal by PKA phosphorylation activity, PKA activity reporters may be able to detect signals not picked up by cAMP binding probes. Recently, a modified AKAR probe named ^{Aq}AKAR^{Cit}, was generated by replacing Cerulean with Aquamarine, a newly engineered CFP variant, which has mutations T65S and H148G (Erard et al., 2013). These modifications to ECFP increased its photophysical properties and reduced its environmental sensitivity to low pH.

The modular design of FRET-based biosensors allows researchers to couple the same sensing unit to different reporting units. For example, red fluorescent protein (RFP) can act as an acceptor for both CFP and YFP. ICUE2 was redesigned as a YFP-RFP FRET sensor (YR-ICUE) and co-imaged with a CFP-RFP-AKAR (CR-AKAR) to analyze the temporal relationship between cAMP and PKA signaling following receptor activation in HEK-293 cells (Aye-Han et al., 2012). Utilizing the CFP-RFP and YFP-RFP based biosensors for co-imaging is a simple technique to monitor two biochemical events in parallel and only requires the addition of an RFP emission filter to the imaging setup. With the shared RFP receptor, these two biosensors were further combined to generate the single-chain dual-specificity probe ICUEPID which can sense both cAMP and PKA simultaneously (Ni et al., 2011). It utilizes CFP and YFP donors and a single RFP acceptor. The PKA activity sensing unit is flanked by CFP and RFP while the cAMP sensing unit is flanked by RFP and YFP. This sensor proved useful in Min6 pancreatic β-cells to detect synchronized oscillations of cAMP and PKA within the same subcellular location.

A single-wavelength PKA activity sensor was designed by utilizing a conformation sensitive GFP variant and combining it with the sensing unit of AKAR2 to generate GAkdY (Bonnot et al., 2014). PKA phosphorylation of the substrate changes the conformation of the probe and modulates GFP fluorescence intensity and lifetime. Single color activity sensors such as this probe provide a way to image multiple kinase activities with single excitation wavelengths for each sensor. Three of these sensors were incorporated into Sindbis viral vectors and expressed in brain slices to visualize PKA dynamics in pyramidal cell bodies, thin dendrites, and dendritic spines using two-photon microscopy.

Indicators of enzyme activation typically have sensing domains comprised of the full length endogenous protein. Epac1 and Epac2 share similar activation mechanisms whereby cAMP binding relieves the steric block of the regulatory domain on the Rap1 binding catalytic site by inducing a conformational change in the regulatory domain hinge helix (Selvaratnam et al., 2012). In this context, ICUE1 is also an Epac1 activation probe. A FRET reporter for Epac2 activation was generated by sandwiching full length Epac2 between ECFP and EYFP (Zhang et al., 2009). A brighter Epac2 activation reporter is also available containing Cerulean and Venus, variants of CFP and YFP, respectively (Herbst et al., 2011).

FLUORESCENT INDICTORS OF cGMP

Cyclic guanosine monophosphate probes, like cAMP probes, report the presence of cGMP by using a CNBD derived from PKG or cGMP-specific PDEs. Because the concentration of cGMP in neurons is lower than cAMP, the probes must be highly sensitive and specific in order to provide a high signal to noise ratio and large dynamic range.

Single-chain FRET-based indicators of cGMP

The cygnet series of cGMP reporters was developed by the Dostmann lab and utilized both CNBDs from PKG1α as a sensing unit that responds to cGMP (Honda et al., 2001). Therefore, each molecule of cygnet binds two molecules of cGMP. In cygnet-1 (**cy**clic **G**MP i**n**dicator using **e**nergy **t**ransfer), the first 77 amino acids of PKG1α (PKG1α$^{\Delta 1-77}$) were truncated. PKG1α$^{\Delta 1-77}$ was flanked by a reporting unit comprised of ECFP and EYFP at the N- and C- termini, respectively. Cygnet-2, the catalytically inactive version of cygnet-1, was generated by introducing mutation T516A to PKG1α$^{\Delta 1-77}$. The pH-insensitive EYFP variant Citrine was used to replace YFP in cygnet-2 to generate cygnet-2.1. cGMP binding to the cygnet reporters induces a decrease in FRET. Cygnet-1 and cygnet-2 have an affinity of 1.5 μM and 1.9 μM for cGMP, respectively, although endogenous PKG1α has a cGMP affinity of ∼100 nM. It is conceivable that fusion of the fluorescent proteins or the Δ1–77 N-terminal truncation and catalytic site mutations affected their cGMP binding affinity. Around the same time, Sato et al. generated a similar PKG1α based probe called CGY-Del1 which had an N-terminal truncation of the first 47 amino acids (Sato et al., 2000). cGMP binding induces an increase in FRET in this probe.

Nikolaev et al. developed smaller probes utilizing a single CNBD from PKG1α$^{231-350}$, PDE2$^{392-525}$ and PDE5$^{154-308}$ (Nikolaev et al., 2006b). Their efforts culminated in the generation of three sensors, cGES-GKIB (for cGMP energy transfer sensor derived from GKI-B (PKGI) site), cGES-DE2 (derived from PDE2A), and cGES-DE5 (derived from PDE5A). All three

FRET sensors had reporting units consisting of EYFP and ECFP at the N- and C- termini, respectively. Interestingly, cGES-GKIB exhibited a cGMP-dependent decrease in FRET whereas cGES-DE2/5 exhibited a cGMP-dependent increase in FRET. These three probes all exhibited strong FRET responses, but cGES-DE5 containing the GAF-A domain of PDE5A had a ∼400–600 fold greater selectivity for cGMP:cAMP making it the preferred cGMP sensor for live-cell applications. More recently, a red version of cGES-DE5 was generated for co-imaging experiments with CFP-YFP sensors by using the GFP variant T-SapphireCΔ11 and RFP dimer2 (Niino et al., 2009). Surprisingly, switching the CFP-YFP to GFP-RFP variants increased the affinity of cGES-DE5. The large enhancement in the probe affinity (EC_{50} ∼ 40 nM) makes it potentially suitable for detecting low cGMP concentrations but may also be confounded by variations in experimental conditions when determining the EC_{50}. The probe was used to develop a method for simultaneous measurements of signaling activities by using a single excitation light that excites both T-sapphire and CFP, four channel detection and linear unmixing.

Russwurm and colleagues generated a series of FRET based cGMP sensors in order to achieve faster kinetics and provide an array of probes with a range of affinities (Russwurm et al., 2007). These sensors used the tandem CNBD domains from PKGIα as their sensing unit. Beginning with the indicator construct CFP-PKGIα$^{79-336}$-YFP, they elongated the N- and C- termini of PKGIα$^{79-336}$ and screened for constructs based on cGMP affinity and the FRET response amplitude. Using this approach, they generated a series of cGMP biosensors cGi-500 (EC_{50} = 500 nM), cGi-3000 (EC_{50} = 3.0 μM), and cGi-6000 (EC_{50} = 6.0 μM).

Single-FP based cGMP sensors

Nausch et al. generated a line of biosensors called fluorescent indicators of cGMP (FlincG; Nausch et al., 2008). The reporting unit of FlincG contains a single circularly-permuted EGFP (cpEGFP) molecule. In this series, complete or truncated cGMP binding regulatory domains from PKG1 were used to construct the sensing unit. First in line, α-FlincG used the complete regulatory domain of PKG1α$^{1-356}$. Second, β-FlincG contained the complete regulatory domain from PKG1β, which has an activation constant of 1.0–1.8 μM compared to 75 nM for PKG1α, fused to the N-terminus of cpEGFP. PKGIβ has a completely different N-terminus than PKG1α, which highlights the importance of the N-terminus for cGMP binding affinity. Lastly, the researchers removed the entire N-terminal domain, the first 77 amino acids of PKG1α, to generate δ-FlincG (**Figure 1E**). This decreases the K_D of PKG1α$^{\Delta 1-77}$ to ∼170 nM. Because δ-FlincG had a superior dynamic range and retained nanomolar affinity for cGMP in living cells, it was chosen as the preferred single-GFP linked cGMP biosensor for further characterization and application. Single-color sensors with adequate spectral separation allow for multi-parameter imaging of interacting molecules in complex signal transduction networks. In addition to the green cGMP sensor described above, a blue single-color cGMP sensor named Cygnus was developed by using a blue fluorescent protein (BFP) and a dark fluorescent protein acceptor (Niino et al., 2010). This biosensor was generated by sandwiching the GAF-A domain of PDE5 between mTagBFP and the quenching acceptor YFP sREACH. Cygnus was used to demonstrate cGMP imaging in rat hippocampal neurons and triple parameter imaging of Ca^{2+}, cAMP, and cGMP in HEK-293T cells.

APPLICATION OF CYCLIC NUCLEOTIDE BIOSENSORS TO STUDY NEURONAL SYSTEMS

The following section highlights a few studies that utilize cyclic nucleotide biosensors in investigating neuronal polarization, axon guidance and growth, signaling, and plasticity.

POLARIZATION

Cyclic adenosine monophosphate and PKA are one of the few bona fide axon determinants that play a critical role in axon polarization (Cheng and Poo, 2012). In a recent study, Shelly et al. investigated the contributions of cAMP and cGMP to the process of axon and dendrite formation of early stage hippocampal neurons in isolated cultures. Given that cAMP and cGMP exerted opposing actions in other cell systems, it was possible that they played some role in the differentiation of neuronal processes to form distinct compartments. It was discovered that neurites exposed to cAMP have a high probability of differentiating into axons and those exposed to cGMP become dendrites (Shelly et al., 2010). But how are these processes coordinated in a single cell to ensure that only one neurite becomes the axon? Using the fluorescent biosensors ICUE and cGES-DE5 the researchers examined the effects of locally stimulating a single neurite with a glass bead soaked in cAMP agonist or cGMP analog. Local elevation of cAMP in one of the neurites resulted in a decrease of cAMP and increase of cGMP at the other neurites. Locally elevating cGMP only decreased cAMP at the stimulated neurite and did not exhibit long range inhibition of cGMP. They concluded that local and long range reciprocal regulation of cAMP and cGMP ensures the development of a single axon and multiple dendrites, although the exact mechanism of long range inhibition remains to be elucidated.

The question still stands as to which endogenous factors act through cAMP and cGMP to induce a single neurite to become an axon. In a follow-up study, Shelly et al. examined the effects of Semaphorin3A (Sema3A), a secreted molecule that guides axon/dendrites growth and neuronal migration (Shelly et al., 2011). Here, the researchers utilized the biosensors cGES-DE5, ICUE, and AKAR to monitor the effects of Sema3a and BDNF on cAMP and cGMP. Bath application of Sema3A led to a decrease in the levels of cAMP and PKA activity and an increase in cGMP. Bath application of BDNF led to the opposite changes in cAMP, PKA, and cGMP. Furthermore, blocking soluble guanylyl cyclase (sGC) and PKG with small molecule inhibitors prevented the increase in cGMP by Sema3A, indicating that Sema3A exerts its effects via PKG regulation of sGC. The same compounds prevented the Sema3A induced decrease in cAMP. These results suggest that Sema3A and BDNF exert opposing actions on axon-dendrite differentiation mediated through reciprocal regulation of cyclic nucleotides, consistent with their previously reported findings (Shelly et al., 2010). This study revealed Sema3a's role as a polarizing factor which favors the differentiation of neurites to dendrites while suppressing axon formation in cultured hippocampal neurons.

GROWTH

Cyclic adenosine monophosphate probes can be used to dissect the specific contributions of cAMP modulating GPCRs to physiological changes like axon growth. ICUE3 was recently used to investigate the impact of ionotropic and metabotropic purinergic receptor signaling on axon elongation (del Puerto et al., 2012). Metabotropic P2Y receptors are activated by ADP, whereas the ionotropic P2X receptors are activated by ATP. By modulating purinergic signaling pathways in cultured hippocampal neurons, the authors found that P2Y1 enhances axonal elongation while P2Y13 and P2X7 halt axonal elongation. Addition of ADP or a P2X7 antagonist increased cAMP levels in the distal region of the axon as reported by ICUE3. Concurrent application of an AC5 inhibitor prevented the cAMP increase. Therefore, the purinergic receptors regulate cAMP levels through AC5 and regulate axonal elongation triggered by neurotrophic factors.

GUIDANCE

Cyclic adenosine monophosphate is a second messenger that has long been appreciated in guiding axon elongation as the first step in neural circuit formation. The high spatial and temporal resolution of FRET based biosensors allows researchers to study transient cAMP signals in restricted areas of the neuron such as the growth cone, a structure at the tip of the growing axon that regulates axonal growth and pathfinding. Epac2-camps was used extensively in a study that investigated the spatial and temporal dynamic interactions between cAMP and calcium within the axonal growth cone and its filopodia (Nicol et al., 2011). By fusing the sensor to an N-terminal plasma membrane localization signal (pm-Epac2-camps), the researchers were able to reduce differences in fluorescence intensity between the filopodia and growth cone center allowing for direct comparison of FRET signals. First, the authors showed that bath application of the axon guidance molecule Netrin-1 induces cAMP and calcium transients with similar kinetics. Next, by modulating AC, they were able to show that Netrin-1 induced calcium transients in growth cone filopodia are driven by transient elevation of cAMP. The growth cone center, on the other hand, was shown to have a delayed and prolonged calcium driven cAMP increase as compared to the filopodia. Therefore, the cAMP in the growth cone center is downstream of calcium, opposite that of the filopodia.

SIGNALING AND EXCITABILITY

Genetically encoded biosensors have provided direct evidence for signaling compartmentalization in neurons. For example, the AKAR biosensor targeted to nuclear and cytosolic compartments revealed that PKA signaling within the nucleus of thalamic intralaminar neurons is delayed four-fold as compared to the cytosol (Gervasi et al., 2007). This data is consistent with the view that PKA signals propagate slowly to the nucleus via diffusion of the PKA catalytic subunit (Harootunian et al., 1993). Additionally, the thin dendrites of mouse cortical neurons exhibit larger cAMP and PKA responses than the bulk cytosol (Castro et al., 2010). This data corresponds well to modeling predictions of stronger cAMP and PKA signals in regions which have higher surface area to volume ratios (Neves, 2012). Castro et al. further compared cAMP/PKA responses in mouse brain slices triggered by dopamine D1 receptors in the cortex and the striatum (Castro et al., 2013). Biosensor imaging in pyramidal cortical neurons and striatal medium spiny neurons (MSNs) showed that cAMP/PKA response was stronger, faster, and longer lasting in the striatum than the cortex. They attributed this to more active PDE4 in the cortex, stronger AC activity in the striatum, and the phosphatase inhibitor DARPP-32 in the striatum which prolong the effects of PKA substrate phosphorylation. Thus, the PKA signaling cascade exhibits differential integration of upstream modulators within different brain areas and cell types.

Signaling crosstalks can also be dissected using fluorescent biosensors. Polito et al. used Cygnet2 and Epac-S^{H150} to monitor cGMP and cAMP, respectively in medium spiny neurons of the striatum (Polito et al., 2013). They studied the NO response in striatonigral and striatopallidal MSNs and found that it was partially controlled by PDE2. D1 and D2 MSNs were found to have different transient cAMP responses to brief Fsk stimulation. PDE2 activation by cGMP prevented these cAMP responses and was magnified at the level of PKA activity as visualized by the AKAR3 biosensor. Therefore, PDE2 is a critical effector of NO and modulates the post-synaptic response of MSNs to dopaminergic transmission.

The application of fluorescent biosensors has also provided new insights into signaling mechanisms. It is known that dopamine D1 receptors undergo rapid endocytosis following agonist induced activation. In another recent study, researchers from the von Zastrow lab set out to investigate the functional significance of dopamine receptor endocytosis using the Epac1-camps biosensor in cultured striatal neurons (Kotowski et al., 2011). In this study, internalization of a pH-sensitive fluorescently tagged D1R was tightly coupled (<1 min.) to an increase in cAMP upon stimulation with the D1R agonist SKF81297. The researchers then showed there was a causal relationship between internalization and cAMP accumulation by treating cultured striatal neurons with dynasore, a dynamin inhibitor to block endocytosis. Dynasore reduced the effect of dopamine mediated cAMP elevation indicating that D1R activation and endocytosis is responsible for cellular cAMP accumulation. This study showed that D1R endocytosis supports rapid dopaminergic neurotransmission through the early endocytic pathway.

PLASTICITY

The use of fluorescent biosensors in the field of neuroscience can lead to discoveries of previously undefined roles for signal transduction pathways. The synapse is the primary site of neurotransmission which undergoes a great deal of remodeling known as synaptic plasticity. The cAMP/PKA pathway regulates changes at the pre- and post-synapse through PKA phosphorylation of synaptic membrane components as well as cAMP responsive element binding protein (CREB) mediated gene transcription (Kandel, 2012). Modulation of normal synaptic processes leads to changes in cognition and behavior such as aggression, fear, anxiety, and learning and memory (Wallace et al., 2009; Liu et al., 2014). In 1991, a WD repeat actin binding protein called coronin 1 was identified in D. *discoideum* (de Hostos et al., 1991). Absence of coronin 1 in transgenic mice lead to defects in synaptic plasticity and behavior. Recently,

Jayachandran et al. investigated the mechanism by which coronin 1 exerts its effects on the nervous system (Jayachandran et al., 2014). Investigation into the cellular localization of coronin 1 found that it localizes to excitatory synapses and not inhibitory synapses. Furthermore, PKA-dependent pre-synaptic LTP was absent in coronin 1 null mice indicating a defect in PKA signaling. Other experiments examining PKA phosphorylation of CREB and cAMP related physiological changes further suggested a change in cAMP/PKA signaling in coronin 1 null mice. To directly measure how cAMP is affected by coronin 1, the researchers used ICUE3 to monitor cAMP production in the coronin 1 deficient cell line Mel JuSo. Treatment with isoproterenol led to a minimal increase in cAMP whereas co-transfection of ICUE3 with a coronin 1 expression plasmid produced a robust increase in the cyan to yellow emission ratio. By combining the above data and data from protein-protein interaction experiments, the researchers concluded that coronin 1 potentiates cAMP/PKA signaling by positively interacting with the G-protein subunit Gαs.

ADVANCES IN THE FIELD

BRAIN SLICE AND LIVE-ANIMAL IMAGING

From shedding light on the kinetics of neuromodulatory signaling events to uncovering new aspects of signal transduction, fluorescent biosensors have been an invaluable tool for neuroscience research. Over the past decade, FRET-based biosensors have been used to dissect the intricacies of cyclic nucleotide signaling in the nervous system with unprecedented detail. Second messenger signaling is now being studied in more physiologically relevant samples like brain slices and transgenic animals with FRET-based biosensors (Calebiro et al., 2009; Thunemann et al., 2013). Polito and colleagues recently published a thorough protocol for imaging biosensors like AKAR in brain slices (Polito et al., 2014). These techniques are more demanding as they require intensive sample preparation and advanced equipment to preserve the spatial resolution afforded by single cell imaging experiments. The development of far-red and infrared biosensors will give researchers the ability to probe the biochemistry of cyclic nucleotides in deep tissues difficult to reach with current imaging methods (Shcherbakova and Verkhusha, 2013). Advances in microscopy tools are also an integral part of live brain imaging research. One such tool is fibered fluorescence microscopy that allows for a tissue imaging depth of up to 6 mm (Vincent et al., 2006). Using this technique, Vincent et al. were able to image peripheral nerve regeneration and calcium dynamics in central nervous nuclei of an anesthetized mouse. Although it has not yet been demonstrated, it is likely that the next wave of *in vivo* brain imaging will include studies of cyclic nucleotide signaling dynamics in live animals.

PERTURBATION OF CYCLIC NUCLEOTIDE SIGNALING IN LIVING CELLS

In addition to monitoring the biochemistry underlying neuronal activity, researchers are constantly developing innovative tools to perturb signaling molecules. One of these tools has been developed over the past decade in order to control the activity of neurons with light (Boyden et al., 2005). The technique is based on the light-driven ion channel called channelrhodopsin which can be genetically encoded, expressed and manipulated with light to depolarize or silence individual or groups of neurons. Optogenetics was a great leap forward in neuroscience allowing researchers to map circuits in brain slices and control the neural activity of transgenic animals. Similar tools have been developed to perturb cyclic nucleotide signaling. Light driven modulation of cyclic nucleotides began with the development of caged molecules that are activated through a photolysis reaction (Nargeot et al., 1983). Dimethoxy nitrobenzyl caged-cAMP was used in combination with AKAR in several different studies (Castro et al., 2013). Coumarinylmethyl caged cNMP derivatives developed over the past decade are more efficiently released under nondamaging light conditions (>360 nm wavelength). (Hagen et al., 2001; Geißler et al., 2003). New bis-carboxymethyl variants can allow for one and two-photon flash uncaging and could provide cyclic nucleotide release within deep tissue preparations (Hagen et al., 2005).

Neuronal cyclic nucleotide research has benefited from the implementation of genetically encodable photoactivatable adenylyl cyclase enzymes (PAC). This valuable addition to the toolbox allows for active user-controlled manipulation of cAMP and cGMP levels in specific locations within the cell. These blue-light (450 nm wavelength) sensitive nucleotidyl cyclases respond to light via conformational changes in the light-oxygen-voltage (LOV) or sensors of blue light using FAD (BLUF) photoreceptor protein domains. EuPAC from *Euglena gracilis* was the first to have a demonstrated PAC activity. It was used to show for example that focal stimulation of intracellular cAMP can steer the growth of *Xenopus* spinal commissural axons (Nicol et al., 2011). However, it suffered from high dark activity and poor heterologous cell expression due to its large size (Iseki et al., 2002). bPAC, also known as BlaC, was discovered in *Beggiatoa* sp. It was significantly smaller than EuPAC with low dark state activity which could be tuned by manipulating the level of expression (Ryu et al., 2010; Stierl et al., 2011). Stierl et al. used bPAC to successfully induce activity in cultured hippocampal neurons co-transfected with cyclic nucleotide gated ion channel. Ryu et al. further engineered it into a photoactivatable guanylyl cyclase, BlaG, by introducing three mutations into the region responsible for substrate binding. BlaG is the first photoactivatable guanylyl cyclase. More recently, mPAC was discovered in *Microcoleus chthonoplastes* (Raffelberg et al., 2013). This enzyme uses a LOV domain rather than the BLUF domain as in EuPAC and bPAC and has a greater AC activity in both the dark and light-activated state. The *in vivo* application of the aforementioned PACs is limited by the low tissue penetrance of the blue light needed to activate them. To increase tissue penetration, researchers developed a near-infrared adenylyl cyclase (IlaC) by fusing a bacteriophytochrome BphG1 to a bacterial adenylate cyclase CyaB1. IlaC was expressed in *Caenorhabditis elegans* cholinergic neurons and was shown to induce locomotion with exposure to red light (650 nm) as measured by the number of body bends per minute (Ryu et al., 2014). Given the spectral separation, IlaC opens up the possibility for PACs to be combined with biosensors for real-time manipulation and monitoring of cAMP and cGMP signaling pathways.

COMPUTATIONAL MODELING AND SIMULATION

A fundamental question in cyclic nucleotide research is the maintenance of specific signaling in the midst of multiple inputs and outputs. For example, within neurons there is substantial cross-regulation of cAMP, cGMP and Ca^{2+}. How do multiple signaling pathways interact to form a coherent output instead of chaos? Despite the advances in monitoring and manipulating cyclic nucleotides, we still do not have a clear understanding and additional tools such as mathematic modeling are needed to understand the intricacies of second messenger crosstalk and compartmentation (Saucerman et al., 2014). Significant efforts by different laboratories have been directed towards building mechanistic models to drive research hypotheses. One such study has started to reveal how a neuron's cell shape, topological distribution of biological components, and enzyme kinetics allows a cAMP/PKA microdomain to translate into a gradient of MAPK activity (Neves et al., 2008). The use of genetically encoded biosensors for imaging cyclic nucleotide signaling dynamics, either one at a time or better yet, in a co-imaging mode for multiple parameters, can help obtain more quantitative information, thereby facilitating model development and testing (Ni et al., 2011). Computational modeling efforts are aided by modeling software such as NeuroRD. These programs allow integration and simulation of structural data, enzyme kinetics, and diffusion rates for signaling networks. A guide to using NeuroRD is available with detailed information on developing and analyzing computational models of neuronal signaling networks (Blackwell et al., 2013). This tool has been used to demonstrate the role of PDE4D in maintaining subcellular cAMP microdomains with the requirements of PDE4D being anchored in the bulk cytosol and regulated by PKA phosphorylation (Oliveira et al., 2010). Similarly, stochastic reaction-diffusion models of dopamine signaling in the dendrites have demonstrated the importance of subcellular PKA colocalization with other components of the pathway to determine spatial signaling specificity (Oliveira et al., 2012).

With the multitude of neuromodulatory inputs affecting cyclic nucleotide levels, signaling information needs to be encoded specifically to produce specific cellular responses. Encoding can occur on spatial, temporal, and digital levels using molecular distribution, enzyme kinetics, and signal thresholding to elicit various physiological outputs from cAMP and cGMP signal transduction (Rich et al., 2014). Our understanding of cyclic nucleotide signaling within the context of neuromodulation continues to grow, facilitated by advances in biosensor and imaging technology. An interdisciplinary approach combining experimental and computational strategies may pave the way for future discoveries.

ACKNOWLEDGMENTS

This work is supported by funding from the NSF GRFP (1232825) to Kirill Gorshkov and NIH (R01DK073368) to Jin Zhang. We also thank Jessica Yang for critical reading of this manuscript, as well as the other members of the Zhang Lab and the Johns Hopkins School of Medicine Department of Pharmacology and Molecular Sciences for support.

REFERENCES

Adams, S. R., Harootunian, A. T., Buechler, Y. J., Taylor, S. S., and Tsien, R. Y. (1991). Fluorescence ratio imaging of cyclic AMP in single cells. *Nature* 349, 694–697. doi: 10.1038/349694a0

Allen, M. D., and Zhang, J. (2006). Subcellular dynamics of protein kinase A activity visualized by FRET-based reporters. *Biochem. Biophys. Res. Commun.* 348, 716–721. doi: 10.1016/j.bbrc.2006.07.136

Antoni, F. A. (2000). Molecular diversity of cyclic AMP signalling. *Front. Neuroendocrinol.* 21, 103–132. doi: 10.1006/frne.1999.0193

Aye-Han, N.-N., Allen, M. D., Ni, Q., and Zhang, J. (2012). Parallel tracking of cAMP and PKA signaling dynamics in living cells with FRET-based fluorescent biosensors. *Mol. Biosyst.* 8, 1435–1440. doi: 10.1039/c2mb05514g

Biswas, K. H., Sopory, S., and Visweswariah, S. S. (2008). The GAF domain of the cGMP-binding, cGMP-specific phosphodiesterase (PDE5) is a sensor and a sink for cGMP. *Biochemistry* 47, 3534–3543. doi: 10.1021/bi702025w

Blackwell, K. T., Wallace, L. J., Kim, B., Oliveira, R. F., and Koh, W. (2013). Modeling spatial aspects of intracellular dopamine signaling. *Methods Mol. Biol.* 964, 61–75. doi: 10.1007/978-1-62703-251-3_5

Bonnot, A., Guiot, E., Hepp, R., Cavellini, L., Tricoire, L., and Lambolez, B. (2014). Single-fluorophore biosensors based on conformation-sensitive GFP variants. *FASEB J.* 28, 1375–1385. doi: 10.1096/fj.13-240507

Boyden, E. S., Zhang, F., Bamberg, E., Nagel, G., and Deisseroth, K. (2005). Millisecond-timescale, genetically targeted optical control of neural activity. *Nat. Neurosci.* 8, 1263–1268. doi: 10.1038/nn1525

Calebiro, D., Nikolaev, V. O., Gagliani, M. C., de Filippis, T., Dees, C., Tacchetti, C., et al. (2009). Persistent cAMP-signals triggered by internalized G-protein-coupled receptors. *PLoS Biol.* 7:e1000172. doi: 10.1371/journal.pbio.1000172

Castro, L. R., Brito, M., Guiot, E., Polito, M., Korn, C. W., Hervé, D., et al. (2013). Striatal neurones have a specific ability to respond to phasic dopamine release. *J. Physiol.* 591, 3197–3214. doi: 10.1113/jphysiol.2013.252197

Castro, L. R., Gervasi, N., Guiot, E., Cavellini, L., Nikolaev, V. O., Paupardin-Tritsch, D., et al. (2010). Type 4 phosphodiesterase plays different integrating roles in different cellular domains in pyramidal cortical neurons. *J. Neurosci.* 30, 6143–6151. doi: 10.1523/JNEUROSCI.5851-09.2010

Cheng, P.-L., and Poo, M.-M. (2012). Early events in Axon/Dendrite polarization. *Annu. Rev. Neurosci.* 35, 181–201. doi: 10.1146/annurev-neuro-061010-113618

Conti, M., and Richter, W. (2014). "Phosphodiesterases and cyclic nucleotide signaling in the CNS," in *Cyclic-Nucleotide Phosphodiesterases in the Central Nervous System*, eds N. J. Brandon and A. R. West (John Wiley and Sons, Inc.), 1–46.

Dao, K. K., Teigen, K., Kopperud, R., Hodneland, E., Schwede, F., Christensen, A. E., et al. (2006). Epac1 and cAMP-dependent protein kinase holoenzyme have similar cAMP affinity, but their cAMP domains have distinct structural features and cyclic nucleotide recognition. *J. Biol. Chem.* 281, 21500–21511. doi: 10.1074/jbc.m603116200

de Hostos, E. L., Bradtke, B., Lottspeich, F., Guggenheim, R., and Gerisch, G. (1991). Coronin, an actin binding protein of Dictyostelium discoideum localized to cell surface projections, has sequence similarities to G protein beta subunits. *EMBO J.* 10, 4097–4104.

del Puerto, A., Díaz-Hernández, J.-I., Tapia, M., Gomez-Villafuertes, R., Benitez, M. J., Zhang, J., et al. (2012). Adenylate cyclase 5 coordinates the action of ADP, P2Y1, P2Y13 and ATP-gated P2X7 receptors on axonal elongation. *J. Cell Sci.* 125, 176–188. doi: 10.1242/jcs.091736

Depry, C., Allen, M. D., and Zhang, J. (2011). Visualization of PKA activity in plasma membrane microdomains. *Mol. Biosyst.* 7, 52–58. doi: 10.1039/c0mb00079e

DiPilato, L. M., Cheng, X., and Zhang, J. (2004). Fluorescent indicators of cAMP and Epac activation reveal differential dynamics of cAMP signaling within discrete subcellular compartments. *Proc. Natl. Acad. Sci. U S A* 101, 16513–16518. doi: 10.1073/pnas.0405973101

DiPilato, L. M., and Zhang, J. (2009). The role of membrane microdomains in shaping [small beta]2-adrenergic receptor-mediated cAMP dynamics. *Mol. Biosyst.* 5, 832–837. doi: 10.1039/b823243a

Erard, M., Fredj, A., Pasquier, H., Beltolngar, D.-B., Bousmah, Y., Derrien, V., et al. (2013). Minimum set of mutations needed to optimize cyan fluorescent proteins for live cell imaging. *Mol. Biosyst.* 9, 258–267. doi: 10.1039/c2mb25303h

Esseltine, J. L., and Scott, J. D. (2013). AKAP signaling complexes: pointing towards the next generation of therapeutic targets? *Trends Pharmacol. Sci.* 34, 648–655. doi: 10.1016/j.tips.2013.10.005

Geißler, D., Kresse, W., Wiesner, B., Bendig, J., Kettenmann, H., and Hagen, V. (2003). DMACM-caged adenosine nucleotides: ultrafast phototriggers for ATP, ADP and AMP activated by long-wavelength irradiation. *Chembiochem* 4, 162–170. doi: 10.1002/cbic.200390027

Gervasi, N., Hepp, R., Tricoire, L., Zhang, J., Lambolez, B., Paupardin-Tritsch, D., et al. (2007). Dynamics of protein kinase A signaling at the membrane, in the cytosol and in the nucleus of neurons in mouse brain slices. *J. Neurosci.* 27, 2744–2750. doi: 10.1523/jneurosci.5352-06.2007

Giese, K. P., and Mizuno, K. (2013). The roles of protein kinases in learning and memory. *Learn. Mem.* 20, 540–552. doi: 10.1101/lm.028449.112

Hagen, V., Bendig, J., Frings, S., Eckardt, T., Helm, S., Reuter, D., et al. (2001). Highly efficient and Ultrafast Phototriggers for cAMP and cGMP by using long-wavelength UV/Vis-activation. *Angew. Chem. Int. Ed Engl.* 40, 1045–1048. doi: 10.1002/1521-3773(20010316)40:6<1045::aid-anie10450>3.0.co;2-f

Hagen, V., Dekowski, B., Nache, V., Schmidt, R., Geißler, D., Lorenz, D., et al. (2005). Coumarinylmethyl esters for ultrafast release of high concentrations of cyclic nucleotides upon one- and two-photon photolysis. *Angew. Chem. Int. Ed Engl.* 44, 7887–7891. doi: 10.1002/anie.200502411

Harootunian, A. T., Adams, S. R., Wen, W., Meinkoth, J. L., Taylor, S. S., and Tsien, R. Y. (1993). Movement of the free catalytic subunit of cAMP-dependent protein kinase into and out of the nucleus can be explained by diffusion. *Mol. Biol. Cell* 4, 993–1002. doi: 10.1091/mbc.4.10.993

Herbst, K. J., Coltharp, C., Amzel, L. M., and Zhang, J. (2011). Direct activation of Epac by sulfonylurea is isoform selective. *Chem. Biol.* 18, 243–251. doi: 10.1016/j.chembiol.2010.12.007

Honda, A., Adams, S. R., Sawyer, C. L., Lev-Ram, V., Tsien, R. Y., and Dostmann, W. R. (2001). Spatiotemporal dynamics of guanosine 3′,5′-cyclic monophosphate revealed by a genetically encoded, fluorescent indicator. *Proc. Natl. Acad. Sci. U S A* 98, 2437–2442. doi: 10.1073/pnas.051631298

Iseki, M., Matsunaga, S., Murakami, A., Ohno, K., Shiga, K., Yoshida, K., et al. (2002). A blue-light-activated adenylyl cyclase mediates photoavoidance in Euglena gracilis. *Nature* 415, 1047–1051. doi: 10.1038/4151047a

Jayachandran, R., Liu, X., Bosedasgupta, S., Müller, P., Zhang, C. L., Moshous, D., et al. (2014). Coronin 1 regulates cognition and behavior through modulation of cAMP/protein kinase A signaling. *PLoS Biol.* 12:e1001820. doi: 10.1371/journal.pbio.1001820

Kandel, E. R. (2012). The molecular biology of memory: cAMP, PKA, CRE, CREB-1, CREB-2 and CPEB. *Mol. Brain* 5:14. doi: 10.1186/1756-6606-5-14

Klarenbeek, J. B., Goedhart, J., Hink, M. A., Gadella, T. W., and Jalink, K. (2011). A mTurquoise-based cAMP sensor for both FLIM and ratiometric read-out has improved dynamic range. *PLoS One* 6:e19170. doi: 10.1371/journal.pone.0019170

Kotowski, S. J., Hopf, F. W., Seif, T., Bonci, A., and von Zastrow, M. (2011). Endocytosis promotes rapid dopaminergic signaling. *Neuron* 71, 278–290. doi: 10.1016/j.neuron.2011.05.036

Lim, W. K. (2007). GPCR drug discovery: novel ligands for CNS receptors. *Recent Pat. CNS Drug Discov.* 2, 107–112. doi: 10.2174/157488907780832689

Lissandron, V., Terrin, A., Collini, M., D'alfonso, L., Chirico, G., Pantano, S., et al. (2005). Improvement of a FRET-based Indicator for cAMP by linker design and stabilization of donor-acceptor interaction. *J. Mol. Biol.* 354, 546–555. doi: 10.1016/j.jmb.2005.09.089

Liu, X., Gu, Q. H., Duan, K., and Li, Z. (2014). NMDA receptor-dependent LTD is required for consolidation but not acquisition of fear memory. *J. Neurosci.* 34, 8741–8748. doi: 10.1523/JNEUROSCI.2752-13.2014

Liu, S., Li, Y., Kim, S., Fu, Q., Parikh, D., Sridhar, B., et al. (2012). Phosphodiesterases coordinate cAMP propagation induced by two stimulatory G protein-coupled receptors in hearts. *Proc. Natl. Acad. Sci. U S A* 109, 6578–6583. doi: 10.1073/pnas.1117862109

Marley, A., Choy, R. W., and von Zastrow, M. (2013). GPR88 reveals a discrete function of primary cilia as selective insulators of GPCR cross-talk. *PLoS One* 8:e70857. doi: 10.1371/journal.pone.0070857

Mongillo, M., Mcsorley, T., Evellin, S., Sood, A., Lissandron, V., Terrin, A., et al. (2004). Fluorescence resonance energy transfer-based analysis of cAMP dynamics in live neonatal rat cardiac myocytes reveals distinct functions of compartmentalized phosphodiesterases. *Circ. Res.* 95, 67–75. doi: 10.1161/01.res.0000134629.84732.11

Nargeot, J., Nerbonne, J. M., Engels, J., and Lester, H. A. (1983). Time course of the increase in the myocardial slow inward current after a photochemically generated concentration jump of intracellular cAMP. *Proc. Natl. Acad. Sci. U S A* 80, 2395–2399. doi: 10.1073/pnas.80.8.2395

Nausch, L. W., Ledoux, J., Bonev, A. D., Nelson, M. T., and Dostmann, W. R. (2008). Differential patterning of cGMP in vascular smooth muscle cells revealed by single GFP-linked biosensors. *Proc. Natl. Acad. Sci. U S A* 105, 365–370. doi: 10.1073/pnas.0710387105

Neves, S. R. (2012). Modeling of spatially-restricted intracellular signaling. *Wiley Interdiscip. Rev. Syst. Biol. Med.* 4, 103–115. doi: 10.1002/wsbm.155

Neves, S. R., Tsokas, P., Sarkar, A., Grace, E. A., Rangamani, P., Taubenfeld, S. M., et al. (2008). Cell shape and negative links in regulatory motifs together control spatial information flow in signaling networks. *Cell* 133, 666–680. doi: 10.1016/j.cell.2008.04.025

Newman, R. H., Fosbrink, M. D., and Zhang, J. (2011). Genetically encodable fluorescent biosensors for tracking signaling dynamics in living cells. *Chem. Rev.* 111, 3614–3666. doi: 10.1021/cr100002u

Ni, Q., Ganesan, A., Aye-Han, N. N., Gao, X., Allen, M. D., Levchenko, A., et al. (2011). Signaling diversity of PKA achieved via a Ca2+-cAMP-PKA oscillatory circuit. *Nat. Chem. Biol.* 7, 34–40. doi: 10.1038/nchembio.478

Nicol, X., Hong, K. P., and Spitzer, N. C. (2011). Spatial and temporal second messenger codes for growth cone turning. *Proc. Natl. Acad. Sci. U S A* 108, 13776–13781. doi: 10.1073/pnas.1100247108

Niino, Y., Hotta, K., and Oka, K. (2009). Simultaneous live cell imaging using dual FRET sensors with a single excitation light. *PLoS One* 4:e6036. doi: 10.1371/journal.pone.0006036

Niino, Y., Hotta, K., and Oka, K. (2010). Blue fluorescent cGMP sensor for multiparameter fluorescence imaging. *PLoS One* 5:e9164. doi: 10.1371/journal.pone.0009164

Nikolaev, V. O., Bünemann, M., Hein, L., Hannawacker, A., and Lohse, M. J. (2004). Novel single chain cAMP sensors for receptor-induced signal propagation. *J. Biol. Chem.* 279, 37215–37218. doi: 10.1074/jbc.c400302200

Nikolaev, V. O., Bünemann, M., Schmitteckert, E., Lohse, M. J., and Engelhardt, S. (2006a). Cyclic AMP imaging in adult cardiac myocytes reveals far-reaching β1-adrenergic but locally confined β2-adrenergic receptor-mediated signaling. *Circ. Res.* 99, 1084–1091. doi: 10.1161/01.res.0000250046.69918.d5

Nikolaev, V. O., Gambaryan, S., and Lohse, M. J. (2006b). Fluorescent sensors for rapid monitoring of intracellular cGMP. *Nat. Methods* 3, 23–25. doi: 10.1038/nmeth816

Norris, R. P., Ratzan, W. J., Freudzon, M., Mehlmann, L. M., Krall, J., Movsesian, M. A., et al. (2009). Cyclic GMP from the surrounding somatic cells regulates cyclic AMP and meiosis in the mouse oocyte. *Development* 136, 1869–1878. doi: 10.1242/dev.035238

Oliveira, R. F., Kim, M., and Blackwell, K. T. (2012). Subcellular location of PKA controls striatal plasticity: stochastic simulations in spiny dendrites. *PLoS Comput. Biol.* 8:e1002383. doi: 10.1371/journal.pcbi.1002383

Oliveira, R. F., Terrin, A., Di Benedetto, G., Cannon, R. C., Koh, W., Kim, M., et al. (2010). The role of type 4 phosphodiesterases in generating microdomains of cAMP: large scale stochastic simulations. *PLoS One* 5:e11725. doi: 10.1371/journal.pone.0011725

Polito, M., Klarenbeek, J., Jalink, K., Paupardin-Tritsch, D., Vincent, P., and Castro, L. R. (2013). The NO/cGMP pathway inhibits transient cAMP signals through the activation of PDE2 in striatal neurons. *Front. Cell. Neurosci.* 7:211. doi: 10.3389/fncel.2013.00211

Polito, M., Vincent, P., and Guiot, E. (2014). Biosensor imaging in brain slice preparations. *Methods Mol. Biol.* 1071, 175–194. doi: 10.1007/978-1-62703-622-1_14

Ponsioen, B., Zhao, J., Riedl, J., Zwartkruis, F., van der Krogt, G., Zaccolo, M., et al. (2004). Detecting cAMP-induced Epac activation by fluorescence resonance energy transfer: Epac as a novel cAMP indicator. *EMBO Rep.* 5, 1176–1180. doi: 10.1038/sj.embor.7400290

Raffelberg, S., Wang, L., Gao, S., Losi, A., Gärtner, W., and Nagel, G. (2013). A LOV-domain-mediated blue-light-activated adenylate (adenylyl) cyclase from the cyanobacterium Microcoleus chthonoplastes PCC 7420. *Biochem. J.* 455, 359–365. doi: 10.1042/BJ20130637

Rich, T. C., Webb, K. J., and Leavesley, S. J. (2014). Can we decipher the information content contained within cyclic nucleotide signals? *J. Gen. Physiol.* 143, 17–27. doi: 10.1085/jgp.201311095

Russwurm, M., Mullershausen, F., Friebe, A., Jäger, R., Russwurm, C., and Koesling, D. (2007). Design of fluorescence resonance energy transfer (FRET)-based cGMP indicators: a systematic approach. *Biochem. J.* 407, 69–77. doi: 10.1042/bj20070348

Ryu, M. H., Kang, I. H., Nelson, M. D., Jensen, T. M., Lyuksyutova, A. I., Siltberg-Liberles, J., et al. (2014). Engineering adenylate cyclases regulated by near-infrared window light. *Proc. Natl. Acad. Sci. U S A* 111, 10167–10172. doi: 10.1073/pnas.1324301111

Ryu, M. H., Moskvin, O. V., Siltberg-Liberles, J., and Gomelsky, M. (2010). Natural and engineered photoactivated nucleotidyl cyclases for optogenetic applications. *J. Biol. Chem.* 285, 41501–41508. doi: 10.1074/jbc.M110.177600

Saito, K., Chang, Y. F., Horikawa, K., Hatsugai, N., Higuchi, Y., Hashida, M., et al. (2012). Luminescent proteins for high-speed single-cell and whole-body imaging. *Nat. Commun.* 3:1262. doi: 10.1038/ncomms2248

Sample, V., DiPilato, L. M., Yang, J. H., Ni, Q., Saucerman, J. J., and Zhang, J. (2012). Regulation of nuclear PKA revealed by spatiotemporal manipulation of cyclic AMP. *Nat. Chem. Biol.* 8, 375–382. doi: 10.1038/nchembio.799

Sample, V., Newman, R. H., and Zhang, J. (2009). The structure and function of fluorescent proteins. *Chem. Soc. Rev.* 38, 2852–2864. doi: 10.1039/b913033k

Sato, M., Hida, N., Ozawa, T., and Umezawa, Y. (2000). Fluorescent indicators for cyclic GMP based on cyclic GMP-dependent protein kinase Ialpha and green fluorescent proteins. *Anal. Chem.* 72, 5918–5924. doi: 10.1021/ac0006167

Saucerman, J. J., Greenwald, E. C., and Polanowska-Grabowska, R. (2014). Mechanisms of cyclic AMP compartmentation revealed by computational models. *J. Gen. Physiol.* 143, 39–48. doi: 10.1085/jgp.201311044

Selvaratnam, R., Mazhab-Jafari, M. T., Das, R., and Melacini, G. (2012). The auto-inhibitory role of the EPAC hinge helix as mapped by NMR. *PLoS One* 7:e48707. doi: 10.1371/journal.pone.0048707

Shcherbakova, D. M., and Verkhusha, V. V. (2013). Near-infrared fluorescent proteins for multicolor in vivo imaging. *Nat. Methods* 10, 751–754. doi: 10.1038/nmeth.2521

Shelly, M., Cancedda, L., Lim, B. K., Popescu, A. T., Cheng, P.-L., Gao, H., et al. (2011). Semaphorin3A regulates neuronal polarization by suppressing axon formation and promoting dendrite growth. *Neuron* 71, 433–446. doi: 10.1016/j.neuron.2011.06.041

Shelly, M., Lim, B. K., Cancedda, L., Heilshorn, S. C., Gao, H., and Poo, M.-M. (2010). Local and long-range reciprocal regulation of cAMP and cGMP in Axon/Dendrite formation. *Science* 327, 547–552. doi: 10.1126/science.1179735

Stierl, M., Stumpf, P., Udwari, D., Gueta, R., Hagedorn, R., Losi, A., et al. (2011). Light modulation of cellular cAMP by a small bacterial photoactivated adenylyl cyclase, bPAC, of the soil bacterium Beggiatoa. *J. Biol. Chem.* 286, 1181–1188. doi: 10.1074/jbc.M110.185496

Taly, A. (2013). Novel approaches to drug design for the treatment of schizophrenia. *Expert Opin. Drug Discov.* 8, 1285–1296. doi: 10.1517/17460441.2013.821108

Terrin, A., Di Benedetto, G., Pertegato, V., Cheung, Y.-F., Baillie, G., Lynch, M. J., et al. (2006). PGE1 stimulation of HEK293 cells generates multiple contiguous domains with different [cAMP]: role of compartmentalized phosphodiesterases. *J. Cell Biol.* 175, 441–451. doi: 10.1083/jcb.200605050

Thunemann, M., Wen, L., Hillenbrand, M., Vachaviolos, A., Feil, S., Ott, T., et al. (2013). Transgenic mice for cGMP imaging. *Circ. Res.* 113, 365–371. doi: 10.1161/CIRCRESAHA.113.301063

Vincent, P., Maskos, U., Charvet, I., Bourgeais, L., Stoppini, L., Leresche, N., et al. (2006). Live imaging of neural structure and function by fibred fluorescence microscopy. *EMBO Rep.* 7, 1154–1161. doi: 10.1038/sj.embor.7400801

Violin, J. D., DiPilato, L. M., Yildirim, N., Elston, T. C., Zhang, J., and Lefkowitz, R. J. (2008). β2-adrenergic receptor signaling and desensitization elucidated by quantitative modeling of real time cAMP dynamics. *J. Biol. Chem.* 283, 2949–2961. doi: 10.1074/jbc.m707009200

Wallace, D. L., Han, M. H., Graham, D. L., Green, T. A., Vialou, V., Iñiguez, S. D., et al. (2009). CREB regulation of nucleus accumbens excitability mediates social isolation-induced behavioral deficits. *Nat. Neurosci.* 12, 200–209. doi: 10.1038/nn.2257

Zaccolo, M., De Giorgi, F., Cho, C. Y., Feng, L., Knapp, T., Negulescu, P. A., et al. (2000). A genetically encoded, fluorescent indicator for cyclic AMP in living cells. *Nat. Cell Biol.* 2, 25–29. doi: 10.1038/71345

Zaccolo, M., and Pozzan, T. (2002). Discrete Microdomains with high concentration of cAMP in stimulated rat neonatal cardiac myocytes. *Science* 295, 1711–1715. doi: 10.1126/science.1069982

Zaccolo, M., and Stangherlin, A. (2014). "Compartmentalization and regulation of cyclic nucleotide signaling in the CNS," in *Cyclic-Nucleotide Phosphodiesterases in the Central Nervous System*, eds N. J. Brandon and A. R. West (John Wiley and Sons, Inc.), 59–76.

Zhang, J., Hupfeld, C. J., Taylor, S. S., Olefsky, J. M., and Tsien, R. Y. (2005). Insulin disrupts beta-adrenergic signalling to protein kinase A in adipocytes. *Nature* 437, 569–573. doi: 10.1038/nature04140

Zhang, C. L., Katoh, M., Shibasaki, T., Minami, K., Sunaga, Y., Takahashi, H., et al. (2009). The cAMP sensor Epac2 is a direct target of antidiabetic sulfonylurea drugs. *Science* 325, 607–610. doi: 10.1126/science.1172256

Zhang, J., Ma, Y., Taylor, S. S., and Tsien, R. Y. (2001). Genetically encoded reporters of protein kinase a activity reveal impact of substrate tethering. *Proc. Natl. Acad. Sci. U S A* 98, 14997–15002. doi: 10.1073/pnas.211566798

Conflict of Interest Statement: The authors declare that the research was conducted in the absence of any commercial or financial relationships that could be construed as a potential conflict of interest.

Received: 27 August 2014; accepted: 04 November 2014; published online: 04 December 2014.

*Citation: Gorshkov K and Zhang J (2014) Visualization of cyclic nucleotide dynamics in neurons. Front. Cell. Neurosci. **8**:395. doi: 10.3389/fncel.2014.00395*

This article was submitted to the journal Frontiers in Cellular Neuroscience.